THE IMPACT OF GENETIC AND EPIGENETIC INTERACTIONS ON PROPAGATION OF THE [*PSI*$^{+}$] PRION

by

MARTINA STRBUNCELJ

B.S., University of Connecticut, 2002

A DISSERTATION SUBMITTED IN PARTIAL FULFILLMENT OF THE REQUIREMENTS FOR THE DEGREE OF DOCTOR OF PHILOSOPHY IN THE DEPARTMENT OF MOLECULAR BIOLOGY, CELL BIOLOGY, AND BIOCHEMISTRY AT BROWN UNIVERSITY

Providence, Rhode Island

May 2009

This dissertation by Martina Strbuncelj is accepted in its present form by the Department of Molecular Biology, Cell Biology, and Biochemistry, as satisfying the dissertation requirements for the degree of Doctor of Philosophy.

Date_____ _____
Tricia Serio, Advisor

Recommended to the Graduate Council

Date_____ _____
Albert Dahlberg, Reader

Date_____ _____
Richard Freiman, Reader

Date_____ _____
Mark Zervas, Reader

Date_____ _____
Irina Derkatch, External Reader
(NYU School of Medicine)

Recommended to the Graduate Council

Date_____ _____
Sheila Bonde
Dean of the Graduate School

Martina Strbuncelj

Curriculum Vitae

EDUCATION

Brown University, Providence, Rhode Island 2002 – 2008

- Ph. D., Molecular Biology, Cell Biology, and Biochemistry, May 2009
- Award**:** Ruth L. Kirschstein National Research Service Award from the National Institutes of Health, full academic scholarship with stipend, research and travel funds, 2006-2007

University of Connecticut, Storrs, Connecticut 1998 – 2002

- B. S., Molecular and Cell Biology; Art History Minor
- Honors**:** Graduated *Magna cum laude* and Honors Scholar; Phi Beta Kappa
- Awards**:** (1) Full tuition Presidential Scholarship, 1998 – 2002; (2) Summer Undergraduate Research Fund Scholarship, 2001; (3) New England Scholar, 2000 (> 3.7 GPA for two consecutive semesters)

TEACHING EXPERIENCE

Laboratory Mentor, **Brown University** 2006 – 2008

- Supervised an undergraduate student working on a senior thesis.
- Trained students and colleagues in lab techniques and use of research software.

Teaching Consultant, **The Sheridan Center for Teaching and Learning** 2005 – 2008

- Improved graduate students' teaching skills.
- Provided critique and feedback after observing clients' teaching methods.

Graduate Teaching Assistant, Molecular Biology, Cell Biology, and Biochemistry 2003 – 2004

- Taught two undergraduate laboratory classes with discussion sections.
- Trained students in laboratory techniques, taught theoretical background, prepared laboratory exercises and quizzes, held office hours for additional instruction, graded exams and laboratory reports.

PEDAGOGICAL TRAINING

The Sheridan Center for Teaching and Learning, Brown University 2005 – 2007

- Teaching Certificates: (I) Teaching Seminar and (II) Professional Development Seminar
- Completed lectures and workshops on classroom teaching, teaching to different learning styles, syllabus construction, assessment, and communication.
- Certification attained through assessment of a departmental micro-teaching session and a formal lecture presentation to the MCB graduate student body.

RESEARCH EXPERIENCE

Graduate Research Assistant, **Brown University** 2002 – 2008

- Investigated the properties of prion proteins.

Undergraduate Research Assistant, **University of Connecticut** 2000 – 2002

- Collaborated with two teams to explore oxidative damage to red blood cells and chromosome evolution.

Summer Intern, **University of Connecticut Health Center** 2000

- Award: Summer research scholarship from the graduate school to study the cell's response to damaged DNA.

SKILLS

Languages: Native English and Croatian

Computer: Adobe Photoshop, Acrobat, Illustrator, MS Office, Pages, Gene Construction Kit, NCBI BLAST, Windows and Mac OS X

Laboratory: Set up and manage a microbiology lab, yeast genetics, molecular biology and biochemistry techniques

PUBLICATIONS

Brown JD, Strbuncelj M, Giardina C, O'Neill RJ. Interspecific hybridization induced amplification of Mdm2 on double minutes in a Mus hybrid. *Cytogenetic and Genome Research* 2002; 98(2-3): 184-8.

CONFERENCE ABSTRACTS AND PRESENTATIONS

Strbuncelj M, Kusmierczyk A, and Serio TR. The prefoldin chaperone complex mediates the stable propagation of Sup35 forms *in vivo.* MCB Department Data Club, Brown University, September 2006.

Strbuncelj M, Kusmierczyk A, and Serio TR. The prefoldin chaperone complex mediates the stable propagation of Sup35 forms *in vivo.* Cold Spring Harbor Laboratory Meeting, Molecular Chaperones and the Heat Shock Response, May 2006.

Strbuncelj M, Kusmierczyk A, and Serio TR. The prefoldin chaperone complex mediates the stable propagation of Sup35 forms *in vivo.* Wellcome Trust Genome Campus, Hinxton, UK, Prion Biology Meeting, September 2005.

Strbuncelj M, Kusmierczyk A, and Serio TR. The prefoldin chaperone complex mediates the stable propagation of Sup35 forms *in vivo.* Cold Spring Harbor Laboratory Meeting, Molecular Chaperones and the Heat Shock Response, May 2004.

Acknowledgements

There are many people who have helped me during my six years at Brown. I would like to thank my family for all their encouragement and support. I want to thank my husband, Mauro, my parents, Nevenka and Zlatko, and my sister Maja, for encouraging me and for helping me in every way they could.

I want to thank my advisor, Tricia Serio, for her enthusiasm and creativity, which motivated me and helped me realize this project. I feel lucky that I have had the pleasure to work with an amazing group of people, so I want to thank everyone in the Laney and Serio labs for making our lab a great, fun place to work. I also want to thank all my friends in Providence outside of the lab for all the fun times. My colleagues, friends, and family were my base of support while in graduate school, and I want to thank all of them for helping me to realize this goal.

Table of Contents

List of Tables

Chapter 3

List of Illustrations

Chapter 1

Chapter 2

Chapter 3

Chapter 1: Introduction

I. Transmissible spongiform encephalopathy (TSE) diseases in mammals

Transmissible spongiform encephalopathies (TSEs) form a group of mammalian neurodegenerative diseases associated with a self-perpetuating change in the physical state of the mammalian prion protein PrP [1, 2]. About two decades ago, experimental studies began to reveal that TSEs are based on a proteinaceous infectious (prion) disease agent, but TSE diseases have existed and have been documented for much longer. Scrapie in sheep is the first documented prion disease, but other ruminants also suffer from TSEs: mad cow disease in cattle and chronic wasting disease (CWD) in deer and elk [3]. These fatal diseases share several features. Brain cross-sections of diseased animals show an accumulation of holes (vacuolation), and clinical symptoms include gradual loss of motor function and dementia, though the specifics of each symptom and the timing of their onset can vary between diseases as well as within each particular disease [3]. Human prion diseases are similar in symptoms to TSEs in animals, and they are Creutzfeldt-Jakob disease (CJD), kuru, fatal familial insomnia (FFI), and Gerstmann-Straussler-Scheinker syndrome [3]. One unusual feature of prion diseases is that they can be genetic, transmissible, and sporadic in nature [3]. No other known diseases can be attributed to all three mechanisms, so an uncommon disease agent must underlie TSE etiology.

TSEs are infectious and transmissible

Our understanding of TSEs began with D. Carleton Gajdusek's study of kuru, a disease unique to the Fore people of New Guinea. Kuru puzzled scientists because the disease seemed to be infectious and could spread between persons, yet infected individuals showed no classic signs of infection such as fever or inflammation [4]. At the same time that

Gajdusek was studying kuru, Hadlow was investigating the well-known sheep disease scrapie. Hadlow (1959) was the first to point out similarities between kuru and scrapie. Specifically, kuru and scrapie-infected individuals showed the formation of plaques and holes in the brain [5]. Gajdusek had not yet proven that kuru can be transmitted when Hadlow made the connection between kuru and scrapie, but Gajdusek noted that its presentation resembled that of a slow virus infection of the nervous system, first hypothesized by Bjorn Sigurdsson, and he strongly felt that this new class of slow viruses was the culprit behind kuru [6, 7]. Gajdusek's group also noted similarities in neuronal changes between kuru and CJD, a sporadic or familial human disease [8], thus drawing another parallel between previously unrelated diseases. Gajdusek also reported that kuru and Gerstmann-Straussler-Scheinker syndrome are similar because both diseases show the presence of plaques in the brain [4].

After drawing connections between previously unrelated brain diseases of humans and animals, Gajdusek's group demonstrated that kuru, scrapie, and CJD can all be transmitted to primates by inoculation [9-12]. Their subsequent work showed that CJD could be passaged through monkeys and retain its infectivity to cause disease in a second monkey [13]. Though Gajdusek's group was successful in drawing connections between neurological human and animal diseases, and then showing that these diseases can be infectious and transmissible, all of the group's attempts to isolate the causative slow virus responsible for kuru, CJD, and scrapie were unsuccessful. The suspected slow virus was unusual because it showed resistance to gamma radiation at doses that inactivate typical viruses and bacteria, suggesting that it is either protein- or polysaccharide-based [14-17]. This inspired Griffith to propose that a protein can be infectious [18].

TSE disease agents are protein-based: formulation of the prion hypothesis

Further work on scrapie from Stanley Prusiner's group showed that denaturing detergents and chaotropic ions inactivate the scrapie agent, further pointing to the importance of the disease agent's protein component for infectivity [19, 20]. Work from Tikvah Alper's group showed that the scrapie agent is resistant to germicidal levels of exposure to ultraviolet light, arguing that the agent is perhaps lipid-based [16, 17, 21, 22]. Follow-up studies from Prusiner showed that chemical modification of the scrapie agent's amino acids and proteinase K digestion of scrapie preparations destroy 99.9% of scrapie infectivity [23]. All of Prusiner's scrapie studies culminated in the proposal of the prion hypothesis, suggesting that scrapie is caused by a proteinaceous infectious (prion) particle distinct from viruses, plasmids, and virions [24]. Prusiner argued that the scrapie agent is protein-based because of evidence that the agent is inactivated by protein-specific treatments (proteinase K digestion, inactivation by diethyl pyrocarbonate, SDS, chaotropic salts, phenol, and urea), and resistant to treatments that destroy nucleic acids (nuclease, UV irradiation, psoralens) [19, 20, 23, 25]. However, the proteinaceous agent behind scrapie was still unknown.

Linking the scrapie prion to the PrP protein

Subsequent work from the Prusiner group linked the scrapie agent to the mammalian PrP protein [1, 24-27]. The initial discovery that the scrapie disease agent is associated with PrP was surprising because the PrP protein is host-encoded and expressed in both sick and healthy individuals, suggesting that differences between the normal (PrP^{c} for PrP-cellular) and the disease associated form of PrP (PrP^{sc} for PrP-scrapie) are post-translational [1, 27]. Another added perplexity was the discovery that PrP is highly conserved in mammals and birds [27, 28], and even found in zebrafish [29], suggesting that PrP serves an important

function in many organisms. Further studies of PrP function revealed that it is localized primarily to cell membranes, and expressed most highly in the central nervous system [27, 30]. All of these findings describe PrP as an evolutionarily conserved, benign cellular protein, so it was difficult to reconcile these data with the discovery that PrP is associated directly with the scrapie disease agent.

The first evidence linking scrapie prion infectivity to PrP was that PrP co-purified with the scrapie prion and showed partial proteinase K resistance in scrapie-infected hamster brain tissue, compared to proteinase K sensitivity of similarly sized proteins in brain tissue from healthy individuals [25]. A follow-up study showed that PrP concentration correlates directly with the scrapie prion titer, and that extended proteinase K digestion of PrP directly overlays scrapie prion inactivation kinetics [26]. Though in many ways PrP resembles an ordinary cellular protein, these studies make it clear that PrP is endowed with some special property that enables it to function as a benign protein in healthy individuals, and also to alter its form and become a more proteinase-resistant, crucial component of the scrapie agent in sick animals.

The most convincing proof that PrP may be the causative agent of scrapie came from Charles Weissmann's group when they demonstrated that PrP-null mice are resistant to scrapie [31]. This study demonstrated that PrP is necessary for scrapie infection, but it did not prove that PrP alone is sufficient to cause scrapie. The discovery that PrP is necessary for scrapie infection can be explained alternatively by its being intimately associated with another disease agent, instead of PrP itself being the disease agent. It is possible that the disease-associated PrP^{sc} envelops the disease agent in sick animals, so that extended

proteinase K digestion eventually degrades PrP^{sc} and leaves the disease agent sensitive to inactivation by other cellular factors. Such an intimate association between PrP^{sc} and the scrapie causative factor would explain the observation that scrapie inactivation kinetics directly overlay PrP^{sc} proteinase degradation kinetics [26].

The true way to demonstrate that PrP alone is sufficient to cause scrapie would be to express a recombinant PrP protein, purify it, inoculate it into animals, and then show the onset of disease. Stanley Prusiner's group tried this experiment. They expressed recombinant PrP fragments in *E. coli*, demonstrated that the recombinant protein can form fibrils *in vitro*, and showed that these fibrils cause neurological disease when inoculated into mice [32]. Furthermore, tissues from mice infected with these synthetic prions can transmit the disease to a second set of mice. Though this set of experiments aims to prove that PrP alone is sufficient to cause scrapie, there are problems with the approach. In order for the recombinant PrP to be infectious, inoculated mice have to express about 16-fold higher than normal levels of PrP^{c} [33]. Animals that express such high levels of PrP show increased spontaneous rates of spongiform encephalopathies, so it is possible that the mice used in the study would have developed scrapie on their own, and that inoculation with recombinant PrP merely precipitates or speeds up the onset of disease instead of causing the disease. Another problem with the study is that there is a long period before disease onset in mice that are inoculated with recombinant PrP, but subsequent mouse-to-mouse transmission produces a fast onset of disease symptoms. This prolonged incubation before the appearance of disease caused by recombinant PrP but not by the subsequent infection with diseased mouse tissue can again be explained by the fact that the inoculated mice are poised

to develop the disease spontaneously because of abnormally high PrP expression, and once they develop the disease, it is easy to transmit it to other animals.

Another approach to validating the prion hypothesis in mammals has been developed by Claudio Soto's group. Soto's group created an *in vitro* PrP^{sc} amplification system, where a minute amount of the disease-associated PrP^{sc} protein is mixed with purified PrP^{c} so that aggregates can form, followed by sonication of aggregates to break them up and generate more surfaces for conversion of PrP^{c} to PrP^{sc}, and then the cycle is repeated multiple times, analogous to PCR amplification [34-36]. If this cyclic misfolding amplification process is continued for very long periods of time, such that there is no original inoculum brain tissue remaining because it has been diluted out by rounds of amplification, the *in vitro* generated PrP^{sc} can still cause disease in hamsters with identical symptoms as inoculation with the original, unamplified PrP^{sc} [36]. Though these studies come close to validating the prion hypothesis in mammals, it can be argued that the *in vitro* protein misfolding amplification system can still harbor some minute amounts of the original disease agent despite repeated rounds of dilution, or that the disease agent lies dormant in association with purified PrP^{c} samples that are used as substrates for conversion in the amplification system. Despite its weak points, this set of experiments is the closest proof of the prion hypothesis in mammals to date.

The prion hypothesis stipulates that a protein agent is required for infection. The protein-only hypothesis predicts that a change in protein conformation can cause disease, so one of the conditions of the hypothesis is that the disease will not be able to be established in the absence of the protein. This stipulation of the protein-only hypothesis was proven by the

resistance to scrapie in PrP-null mice. Another stipulation of the protein-only hypothesis is that the prion should not be able to replicate in the absence of PrP. This was also proven by the Prusiner and Weissmann groups when they showed that PrP-null mice do not replicate the scrapie agent, and do not show any signs of disease even 300 days after inoculation [37, 38]. However, these experiments only show that PrP is necessary for scrapie, and not that PrP alone is sufficient, so it is still possible that PrP is a necessary incubator for another disease agent. In order for a prion protein to be infectious, it must be able to convert PrP^{c} into the disease-associated form PrP^{sc}. No final proof of such direct, protein-only conversion has been shown in the mammalian prion system; the best evidence for this point is the cyclic misfolding PrP^{sc} amplification system, but since the system uses purified PrP^{c} from healthy animals as the substrate for conversion into the PrP^{sc} form, some form of contamination with another agent is still possible [34-36]. Clearly, some points of the protein-only prion hypothesis still remain to be proven in the mammalian system, but work with prions in yeast has shown that protein alone is necessary and sufficient for prion infection, and that post-translational conversion into the prion form is possible [39-41].

II. Prions also exist in lower eukaryotes

Though initial prion research was centered around mammalian TSEs, we now know that prions are found in many eukaryotes, from unicellular organisms to mammals [42]. Several fungal prion proteins have been described. Unlike their mammalian counterparts, prion proteins in lower eukaryotes do not cause disease but rather regulate protein function in a heritable way, conferring phenotypic plasticity upon their hosts. The prions [*PSI*$^{+}$], [*URE3*],

[*PIN*$^+$], [*NU*$^+$], [*SWI*$^+$], and the putative prion [*ISP*$^+$] are found in *Saccharomyces cerevisiae* [43-49]. [Het-S] and the prion-like phenotype [*C*$^+$] are found in the filamentous fungus *Podospora anserina*, the prion-like phenotype Cin is found in *Schizosaccharomyces pombe*, and some bacteria express prion-like protein fibers named curli that are associated with biofilms [50-53]. Most of these epigenetic traits have been studied for years, but it was not until 1994 that it was proposed that inheritance of these traits could be explained by a prion mechanism [45].

The most extensively studied yeast prions [*PSI*$^+$], [*URE3*], and [*PIN*$^+$] have all been shown to be protein-based epigenetic elements by transforming yeast with recombinant proteins, and inducing appearance of the prion phenotype [39, 40, 54, 55]. Protein-only transmission of [*PSI*$^+$] was demonstrated simultaneously by two independent groups [39, 40]. Both groups expressed a recombinant version of Sup35, the prion protein determinant for [*PSI*$^+$], induced the purified recombinant protein to form fibers *in vitro*, and then transformed these fibers into yeast and demonstrated that the recombinant Sup35 fibers alone are sufficient to induce appearance of the [*PSI*$^+$] prion [39, 40]. The same approach was next applied to the [*URE3*] prion, and transformation of yeast with recombinant fibers of the Ure2 prion protein was shown to result in the appearance of the [*URE3*] prion [55]. Most recently, this experimental set-up demonstrated that the yeast [*PIN*$^+$] prion can also be induced by transforming cells with *in vitro* polymerized fibers of Rnq1, the protein determinant of the [*PIN*$^+$] prion [54]. The fact that three unrelated yeast prion phenotypes can be transmitted solely through protein has provided a great proof-of-principle that strengthens the prion hypothesis proposal that a change in protein state can be self-propagating and alter cellular phenotype.

Most yeast prions share the following characteristics. The yeast prion phenotype resembles a loss-of-function mutation in the corresponding protein (true for [*PSI*$^+$] and [*URE3*], but not for [Het-s] and unknown for [*PIN*$^+$]), increased expression of the corresponding protein increases the rate of *de novo* prion appearance presumably by increasing the number of misfolded prion proteins, and the prion phenotype depends upon continual prion protein expression [45]. Additionally, fungal prions are associated with the *in vivo* formation of prion protein aggregates that can be detected by GFP fusions and by differential centrifugation of cell lysates [43, 44, 56-61]. Yeast prions display non-Mendelian inheritance because they are dominant in cell crosses with non-prion cells, and the prion phenotype is not inherited in a 2:2 ratio by meiotic progeny, in contrast to 2:2 Mendelian meiotic inheritance. Non-Mendelian inheritance of yeast prions indicates that they are transmitted cytoplasmically, but cytoplasmic transmission can also be explained by mitochondrial traits. What separates mitochondrial from prion cytoplasmic inheritance is that the prion phenotype can be reversed by treatments that do not disrupt or alter nucleic acids, indicating an underlying epigenetic mechanism, and the prion phenotype can reappear after elimination [62]. Further evidence for the protein-based nature of yeast prions is that they can appear and disappear spontaneously without accompanying genetic changes, and that their *de novo* appearance can be induced by transient over-expression of the determinant prion protein [45, 63-66].

Prions in *S. cerevisiae*

[*PSI*$^+$]

The [*PSI*$^+$] prion determinant is Sup35 [43, 44, 64, 66]. Sup35 is part of the eukaryotic release complex and functions in translation termination [67]. In its non-prion form ([*psi*$^-$]), Sup35 is soluble and ensures faithful translational termination. In its prion form ([*PSI*$^+$]),

Sup35 is aggregated and its function is compromised, resulting in translational termination read-through (fig. 1) [43, 44]. When in the prion form, Sup35 is folded into one of multiple conformations, and each of these forms compromises its function to varying degrees [40, 66, 68, 69]. Despite Sup35's conformational flexibility, [*PSI*$^+$] variants (*i.e.* the distinct Sup35 functional states) are largely stable once they appear in the cell [63].

The King and Weissman labs proved independently that [*PSI*$^+$] is a true prion that depends solely on Sup35 protein state [39, 40]. Each lab purified recombinant Sup35, induced it to form fibers *in vitro*, and then transformed these fibers into yeast [39, 40]. Transformation with recombinant Sup35 fibers caused the appearance of [*PSI*$^+$], but proteinase K treatment of the fibers before transformation into yeast abolished their infectivity, so these control transformants remained non-prion [*psi*$^-$] cells [39, 40]. Transformation with soluble recombinant Sup35 did not cause the appearance of [*PSI*$^+$], but RNase-treated recombinant Sup35 fibers could induce [*PSI*$^+$] [39, 40]. These parallel studies demonstrated that the [*PSI*$^+$] phenotype is protein-based and related to an aggregated form of Sup35, providing support for the protein-only prion hypothesis. The sensitivity of Sup35 fibers to agents that affect proteins and their resistance to agents that affect nucleic acids shows that infection with Sup35 fibers is based on the physical state of a protein-based agent, supporting the prion hypothesis and demonstrating the protein-only nature of [*PSI*$^+$].

The physical state of Sup35 can be monitored directly at the cellular level with a Sup35-GFP fusion protein, or biochemically by monitoring differences in the level of aggregated Sup35 protein (fig. 1) [43] [44]. Indirectly, Sup35 state can be gleaned at colony level by the growth of *ade 1-14* (UGA) mutants on rich media or on media lacking adenine (fig. 1). The *ade1-14*

allele is a nonsense mutation that allows for a colony color read-out of Sup35 function. Non-prion [*psi*] cells contain soluble, functional Sup35, so they recognize the premature stop codon in *ade1-14*, the Ade1 protein is not made, and an adenine biosynthetic intermediate builds up in the cells, causing red colonies on rich medium [43, 44, 70]. [*psi*] cells cannot grow in the absence of adenine. When Sup35 is in its prion [*PSI*$^{+}$] form, it is mostly aggregated and unavailable to act as a translation termination factor, leading to read-through of *ade1-14*, allowing cells to grow in the absence of adenine, and causing cells grow into white colonies on rich medium because there is no build-up of the red adenine metabolic intermediate. Variants of [*PSI*$^{+}$] have been isolated that produce pink colonies on rich medium, and they are referred to as [*PSI*$^{+}$]^{weak} [66, 68]. These [*PSI*$^{+}$]^{weak} variants contain higher levels of soluble Sup35 than the white colony producing [*PSI*$^{+}$]^{strong} variants. Increased levels of soluble, functional Sup35 in [*PSI*$^{+}$]^{weak} cells result in an intermediate level of *ade1-14* translational read-through, leading to pink rather than white colonies on rich medium.

[*PSI*$^{+}$] is a metastable epigenetic factor. Interconversions between [*PSI*$^{+}$] and [*psi*] states occur spontaneously about once in a million cells [47]. It is possible to direct or induce a change in Sup35's protein state. [*PSI*$^{+}$] can be induced by transient overexpression of Sup35's prion domain or full-length protein [64] [66] [65]. It is believed that overexpression of Sup35 increases the chances of misfolding, an otherwise stochastic event, thereby resulting in the appearance of the prion form. Switches from the [*PSI*$^{+}$] to the [*psi*] state are also possible; [*PSI*$^{+}$] can be eliminated (or "cured") by chemical treatment, most commonly with guanidine hydrochloride (GdnHCl) [71] [62]. GdnHCl cures [*PSI*$^{+}$] by inactivating the Hsp104 chaperone [72]. The Hsp104 chaperone is a molecular disaggregase that helps to

resolubilize heat-aggregated proteins [73]. Hsp104 expression level is crucial for [*PSI*$^+$]; overexpression of Hsp104 eliminates [*PSI*$^+$] by an unknown mechanism, while deletion of Hsp104 is thought to eliminate [*PSI*$^+$] by disrupting transmission of Sup35 particles to daughter cells [74] [70].

The Sup35 sequence can be divided into three regions, N, M and C, each starting with a methionine (fig. 2) [75, 76]. The C-terminal region of Sup35 encodes the essential translation termination factor [65]. The M region is non-essential, highly charged, and thus far of unknown function, though it is important in the propagation of specific [*PSI*$^+$] variants [77, 78]. The non-essential N-terminal region of Sup35 is referred to as the prion domain, and it gives Sup35 the ability to modulate its physical state [65]. The N region alone is sufficient to propagate [*PSI*$^+$] [44, 66]. Sup35's N-terminal prion domain contains a QN-rich region and oligopeptide repeats that play crucial roles in its conformational flexibility and prion properties [79-81]. Sup35's oligopeptide repeats (PQGGYQQYN) are very similar to oligopeptide repeats found in the mammalian prion protein PrP (PHGGGWGQ) [80]. Though Sup35-N is not necessary for viability, it seems to be important because it is conserved among 21 strains of *S. cerevisiae* suggesting that it is useful to the cell, perhaps because its prion nature allows a cell quick phenotypic changes by modulating Sup35 termination function [82]. Specifically, what is highly conserved in the Sup35 N-terminal prion region is its bias for glutamine and asparagines residues across distantly related fungi, and its conservation of the prion-associated oligopeptide repeats [83]. Both of these characteristics are believed to be important for prions because they are linked to the formation of β-sheets, which allow some prion proteins to form fibrils *in vitro* [83].

[*URE3*]

Another well-studied yeast prion is [*URE3*]. The protein determinant of [*URE3*] is Ure2, a regulator of nitrogen catabolism [84, 85]. In its non-prion [*ure-o*] form, Ure2 inhibits the uptake of poor nitrogen sources. [*URE3*] shares characteristics of other prions. Ure2 extracted from [*URE3*] yeast shows resistance to limited proteinase K digestion, while Ure2 from wildtype cells is susceptible to proteinase degradation [86]. [*URE3*] is solely dependent on the Ure2 protein: recombinant Ure2 can form fibers *in vitro*, and transformation of these fibers into yeast can induce appearance of the [*URE3*] prion [55].

[*PIN*$^+$] / [*RNQ*$^+$]

The [*PIN*$^+$] prion is necessary for [*PSI*$^+$] induction [87]. The [*PIN*$^+$] phenotype can be conferred by multiple proteins, but its most common protein determinant is Rnq1, so the prion phenotype can also be called [*RNQ*$^+$] [61] [88]. The cellular function of the non-prion form of Rnq1 is currently unknown and an *rnq1* deletion has no known phenotype during vegetative growth [60]. While [*PSI*$^+$] and [*URE3*] mimic a loss-of-function mutation in their protein determinants, [*PIN*$^+$] is more accurately described as a gain-of-function prion phenotype because it enables cells to establish [*PSI*$^+$].

[*NU*$^+$]

Another protein that can confer the [*PIN*$^+$] phenotype is called New1 [61]. Like Sup35 and Ure2, New1 contains a QN-rich region that is found in many prion proteins. By fusing the prion domain of New1 with the C-terminal translation termination catalytic domain of Sup35, Osherovich *et al.* created the [*NU*$^+$] prion [88]. The [*NU*$^+$] prion and [*nu*$^-$] non-prion phenotypes can be distinguished *via* Sup35C's translation termination activity or a GFP

fusion protein, just as for [*PSI*$^+$]. New1's function is not yet known, but its *Candida albicans* homologue is a member of the ATP-binding cassette (ABC) transporter proteins, whose family members are involved in trans-membrane transport and translation [89].

[*ISP*$^+$]

[*ISP*$^+$] is a prion-like phenotype in yeast associated with control of translational fidelity [49]. [*ISP*$^+$] can be transferred to non-prion cells by cytoplasmic mixing in the absence of nuclear DNA transfer, and is dependent on certain *sup35* alleles. However, the protein determinant for [*ISP*$^+$] is unknown.

[*SWI*$^+$]

The newest prion discovered in yeast is [*SWI*$^+$], the prion form of the chromatin remodeling factor Swi1 [48]. [*SWI*$^+$] shows all the classic yeast prion characteristics outlined earlier, such as a Swi1 partial loss-of-function phenotype, sensitivity to Hsp104 inactivation or deletion, a dependence on continual Swi1 expression, dominant cytoplasmic inheritance, and aggregation when in the prion form.

Prions in *P. anserina*

[Het-s]

The HET-s prion protein of the filamentous fungus *Podospora anserina* is involved in cellular recognition, ensuring that genetically distinct *P. anserina* colonies do not fuse through a programmed cell death phenomenon known as heterokaryon incompatibility [50, 90]. Recombinant HET-s protein aggregates can be bombarded into cells on tungsten particles and induce the [Het-s] prion phenotype, proving that [Het-s] is a *bona fide* protein-only prion

phenotype [91]. [Het-s] is the only fungal prion that can propagate in the absence of the molecular disaggregase Hsp104 [92].

[*C*$^+$]

[*C*$^+$] is a prion-like phenomenon found in *P. anserina* [51]. [*C*$^+$] is associated with the Crippled Growth (CG) phenotype and is present in the cytoplasm. Like many fungal prions, [*C*$^+$] can be eliminated by a variety of cellular stresses, but it is lost during meiosis. [*C*$^+$] is linked to translational fidelity: *P. anserina* strains carrying mutations that decrease translation termination accuracy do not propagate [*C*$^+$], while strains with mutations that increase translational accuracy are compatible with [*C*$^+$] [51]. The [*C*$^+$] determinant is not yet known.

The Cin prion-like element in *Schizosaccharomyces pombe*

Calnexin is an essential molecular chaperone in *S. pombe* that aids in the folding of secreted and membrane-bound proteins [52]. Unexpectedly, a calnexin mutant that is deleted for a highly conserved region of the protein allows cells to grow in the absence of calnexin function [52]. This novel phenotype was named Cin for calnexin independent. Cin can be maintained in the presence and absence of the wildtype calnexin *cnx1* allele, it is dominant in cell crosses and transmitted to all four meiotic progeny, and it can be introduced into non-Cin cells by transformation of cell extract [52]. Treatment of Cin cell extracts with DNase, RNase, and UV at levels that destroy control plasmids does not reduce the infectivity of Cin extracts, but proteinase K treatment of Cin cell extract greatly reduces, though not completely abolishes, Cin transmissibility. These experiments show that a crucial component of the Cin phenotype is protein-based, and this novel non-chromosomal element is named [*cif*] [52].

Curli in Eubacteria

Though so far there are no know *bona fide* prions in prokaryotes, the curli fibers that are expressed by some strains of *E. coli* and *Salmonella* exhibit a few prion-like characteristics [53]. Curli fibers form the major proteinaceous component of the bacterial extracellular matrix that is produced when bacteria exist as biofilm communities [53]. Curli fibers and some prion proteins share the characteristic that they can form β-sheet rich amyloid fibers *in vitro*, and curli expressing bacteria can be assayed by the growth of red colonies on medium supplemeted with Congo Red, a dye that binds amyloid fibers *in vitro* [53]. Though curli fibers are not prions and are only similar to some prion proteins because they can both form β-sheet rich amyloid fibers, this similarity suggests that the self-assembly of proteins into amyloid fibers may be an important mechanism of protein regulation that operates both in eukaryotes and prokaryotes.

Amyloids

Amyloids are *in vitro* polymerized protein fibers with a cross β-strand structure [93, 94]. Amyloid fibers are composed of β-sheets that are stacked parallel to the fiber axis, with individual β-strands being perpendicular to the fiber axis [93, 94]. Both yeast and mammalian prion proteins form amyloids *in vitro* [91, 95-97]. Amyloids can be distinguished from other protein fibers by their ability to bind the dyes Congo Red, thioflavin S, and thioflavin T [98]. Another characteristic of amyloids is that they produce a "cross-β" x-ray diffraction pattern, most likely because amyloids are assembled from stacked β-sheets that are parallel to the fiber axis [93, 99, 100]. The exact relationship between prion structures *in vivo* and amyloid fibers *in vitro* is unclear, but some parallels exist between amyloid formation *in vitro* and prion propagation *in vivo*. Both processes are a result of template-driven, self-

perpetuating changes in protein conformation, and the amyloid fiber form of recombinant prion proteins is infectious [39, 40, 101]. For example, only the *in vitro* polymerized fibers of recombinant Sup35, but not soluble recombinant Sup35, can transmit prion infection to yeast cells [39, 40]. It is unclear if prion proteins assume an amyloid form *in vivo*, but since infection with *in vitro* formed amyloids leads to prion appearance and propagation *in vivo*, prions and amyloids probably share some common characteristics.

III. Prion variants exist and are analogous to bacterial and viral strains

Mammalian prion variants

Scrapie variants

Prions exist in multiple physical states (called variants) with distinct phenotypes. The earliest observation of prion variants occurred in studies of the sheep disease scrapie when the disease was experimentally transmitted to mice, long before the prion hypothesis was proposed [102]. In a 1973 study, Fraser and Dickinson inoculated two inbred strains of mice with five isolates of scrapie. The scrapie isolates could be distinguished by the degree of vacuole formation in nine regions of the brain, and by the variation in vacuole distribution across the nine possible regions, together forming a "lesion profile." Both inbred strains of mice, each with its own isogenic PrP gene, could propagate unique lesion profiles corresponding to the original scrapie agent inoculate, arguing that the variant scrapie disease phenotypes are encoded for and determined by each scrapie agent isolate, and not by the particular genetic make-up of the host.

Transmissible mink encephalopathy variants

Another study of transmissible mink encephalopathy (TME) variants termed drowsy (DY) and hyper (HY) linked the disease variants to unique PrP proteolytic profiles [103]. Hyper and drowsy TME variants differ in incubation times, brain histopathology, and clinical symptoms. The hyper variant causes overexcitability, body tremors, and a lack of coordination, while the drowsy variant produces a progressive lethargy [103]. Over a time course of digestion with proteinase K, brain PrP from TME-infected hamsters yielded unique peptide profiles for each TME variant. The amount of proteolytic degradation at each time point correlated with the degree of TME infectivity. The drowsy (DY) TME variant is much more susceptible to proteinase K degradation, so that by the end of the proteolysis time course infection by the DY TME variant could not be detected.

Bovine spongiform encephalopathy variants

Seven unrelated bovine spongiform encephalopathy (BSE) variants have been experimentally shown to retain unique characteristics after serial passage through different animals [104]. Brain lesion profiles show that directly infecting mice with BSE variants, or first passaging these BSE variants in six different species before infecting mice, both result in variant-specific mouse brain histopathology. From this it can be concluded that the donor species (cow or any animal through which the variant was passaged) has little influence on the characteristics of each BSE variant, and that the prion variant itself determines the resulting disease phenotype. These experiments had also revealed a species or transmission barrier to infection: cross-species infection by BSE or scrapie resulted in longer incubation times before the onset of symptoms, but subsequent mouse-to-mouse infections had much shorter

incubation times [104]. The authors' interpretation of the results is that it may be more difficult to establish cross-species prion infection because of sequence differences in the PrP proteins of different species, but that once the infection is established, it is easy to transmit the disease between like (same-species) PrP molecules.

Another line of evidence that points to the importance of primary amino acid structure and the range of accessible states that is dictated by a protein's amino acid sequence is that transgenic mice with a methionine to valine mutation at position 129 in their human PrP gene are largely immune to infection by BSE and variant CJD (vCJD), the BSE-derived human prion disease, even after BSE and vCJD were passaged through isogenic mice prior to inoculation [105]. Thus, a single amino acid change in PrP severely impairs the ability of BSE to propagate, probably because 129M and 129V PrP proteins cannot access a mutually compatible conformation that would allow them to interact to establish disease. In this study, very few homozygous 129VV mice were able to develop a subclinical infection from BSE, but the disease phenotype (clinical symptoms, proteolytic fragments, and brain section immnohistochemistry) changed upon transmission to 129VV mice, while the 129MM mice retained the original BSE variant characteristics. This observation suggests that PrP's primary structure dictates which variants can be propagated by each PrP allele. These data reinforce epidemiological studies of CJD in humans, where it has been noted that certain forms of CJD have only been found in patients homozygous for methionine 129, while other forms of CJD are predominantly found in individuals with at least one valine 129 allele [105].

Prion variants in lower eukaryotes

[*PSI*$^+$] variants

Yeast prions can also exist in multiple forms. Though [*PSI*$^+$] and [*psi*$^-$] are distinct states, it is misleading to think about Sup35 as adopting only a prion or a functional form. The [*PSI*$^+$] phenotype can vary in terms of levels of translational termination efficiency, which can be monitored by colony color of *ade1-14* strains on rich media (fig. 3A). White [*PSI*$^+$] variants result from high levels of read-through, while pink [*PSI*$^+$] variants result from lower levels of read-through [66, 68]. White [*PSI*$^+$] variants are therefore called [*PSI*$^+$]^{strong}, while pink variants are called [*PSI*$^+$]^{weak}. Another difference between these [*PSI*$^+$] variants is their mitotic and meiotic stability; [*PSI*$^+$]^{strong} variants are more stable than [*PSI*$^+$]^{weak}, because [*PSI*$^+$]^{weak} variants show higher rates of loss (reversion to [*psi*$^-$]) or conversion to strong [*PSI*$^+$] [66, 68] [47]. Correlations between [*PSI*$^+$] variants and Sup35 state can be established through biochemical assays. One biochemical method that detects Sup35 state is a centrifugation assay [43] [44] (fig. 3B). Upon high-speed centrifugation of [*psi*$^-$] cell lysates, Sup35 is found in the supernatant fraction. Under the same conditions, Sup35 from strong [*PSI*$^+$] variants is found exclusively in the pellet fraction, while Sup35 from weak [*PSI*$^+$] variants is found divided between the supernatant and the pellet fractions. Both [*PSI*$^+$] variants can be induced in isogenic yeast strains by overexpression of Sup35, but [*PSI*$^+$]^{strong} is more stable mitotically than [*PSI*$^+$]^{weak} [66, 68]. Because of these observations, Derkatch *et al.* (1996) suggested that these [*PSI*$^+$] variants are a result of different Sup35 conformations and are analogous to mammalian prion strains.

Another way to distinguish [*PSI*$^+$] variants is through their interaction with mutant Sup35 molecules. The *PNM2* Sup35 allele has a missense mutation in one of Sup35's oligopeptide repeats in the N-terminal prion domain [106]. *PNM2* overexpression has different effects on [*PSI*$^+$]^{strong} and [*PSI*$^+$]^{weak} [107]. [*PSI*$^+$]^{weak} is stabilized and its translational read-through increased, while [*PSI*$^+$]^{strong}'s read-through is diminished by *PNM2* overproduction. [*PSI*$^+$] variants also differ in their interactions with mutations in Sup35's C-terminal translation termination domain [108]. The [*PSI*$^+$]^{weak} variant also known as [*ETA*$^+$] is lethal in combination with some Sup35 C-terminal mutations, but such a lethal interaction with [*PSI*$^+$]^{strong} has not been described [68, 108].

In [*PSI*$^+$] cells, aggregated Sup35 molecules interact and direct the conversion of non-aggregated Sup35 into the prion state [41]. In the prion form, Sup35 molecules interact through their N-termini (*i.e.* the prion domain), and this region alone is sufficient to transmit and induce [*PSI*$^+$] [44] [66, 78]. The King lab has taken advantage of this prion domain interaction and created a series of full-length Sup35 clones containing single point mutations in the prion domain [109]. Each of these mutants is compromised in its interaction with Sup35 aggregates, and therefore the read-through phenotype is affected (fig. 4). Every [*PSI*$^+$] variant is able to incorporate Sup35 mutants into its prion aggregates to a different degree, so the inability to incorporate mutant Sup35 into aggregates increases the fraction of protein found in the soluble and functional state, leading to a lower level of read-through and a redder colony on rich media. The interaction between each [*PSI*$^+$] variant and a prion domain mutant is unique and produces a characteristic colony color. It is possible to distinguish [*PSI*$^+$] variants of the same colony color through their unique interaction with this series of point mutants.

S. Liebman's group showed that at least the first 14 amino acids of Sup35's M domain are required along with the N-terminal prion domain for the faithful propagation of [*PSI*$^{+}$] variants; the prion domain alone (aa 1-123) can transmit an undifferentiated prion state [78]. Another study from J. Weissman's group tested which parts of Sup35 interact with each other in [*PSI*$^{+}$]^{strong} and [*PSI*$^{+}$]^{weak} variants. They found that in [*PSI*$^{+}$]^{strong}, the first 40 N-terminal amino acids are highly protected from hydrogen/deuterium exchange, while in [*PSI*$^{+}$]^{weak}, the first 70 amino acids show protection from H/D exchange, suggesting that [*PSI*$^{+}$] variants differ at the tertiary or quaternary level, or possibly both [69, 110].

Two independent groups simultaneously showed that [*PSI*$^{+}$] variants can be transmitted solely through protein, without the involvement of any nucleic acids. King and Diaz-Avalos (2004) showed that [*PSI*$^{+}$] variant prion "seeds" can be purified from yeast *via* a tagged Sup35 prion domain construct, and then used in an *in vitro* reaction with recombinant Sup35 to generate Sup35 fibers from recombinant protein expressed in *E. coli* and purified, which produced variant-specific phenotypes when introduced into [*psi*] yeast [39]. Analysis of fibrils formed at different temperatures revealed unique morphologies, variations in mass per length single amyloid fibril ratios, as well as differences in appearance after elecron microscopy analysis (lanky, hunky, wavy and jaggy fibrils) [111].

At the same time as the first King and Diaz-Avalos study, J. Weissman's group used purified recombinant Sup35-NM fragments in *in vitro* fiber-forming reactions at varying temperatures. Sup35-NM amyloids formed at different temperatures showed unique characteristics, assayed by thermal stability of the fibers and electron paramagnetic resonance spectroscopy. Transfecting yeast with the different amyloids produced [*PSI*$^{+}$] variant phenotypes, each

phenotype associating uniquely with a particular Sup35-NM amyloid parent [40]. These parallel studies show that in the yeast prion system, protein alone is sufficient for the formation and transmission of prion variants. The capability of protein-only prion variant formation and transmission has not yet been shown in the mammalian PrP prion system.

Cis- and trans- factors required for maintenance of [*PSI*$^+$] variants

The *de novo* appearance of [*PSI*$^+$] variants is influenced by the evolutionarily conserved heat shock transcription factor (HSF) [112]. After Sup35NM-GFP overexpression, *hsf1* mutants tend to show the appearance of just one type of [*PSI*$^+$] variant, specifically linked to a particular *hsf1* mutant. However, all *hsf1* mutants can propagate a spectrum of [*PSI*$^+$] variants if the variants are introduced into the mutant by cytoduction, a form of cytoplasmic mixing without nuclear DNA transfer. This work points out that [*PSI*$^+$] variant induction and propagation involve different cellular factors.

Sup35's N-terminal oligopeptide repeats are also important for [*PSI*$^+$] variant propagation. Only the first 64 amino acids in Sup35's prion domain are necessary to propagate [*PSI*$^+$], but amino acids 1-83 are necessary to maintain [*PSI*$^+$]^{weak} [113]. Sup35 prion domain oligopeptide truncation mutants are capable of propagating [*PSI*$^+$], but they cause [*PSI*$^+$]^{strong} to form pink colonies on rich medium, and thereby resemble [*PSI*$^+$]^{weak}. Though the oligopeptide truncation mutants change the [*PSI*$^+$] phenotype, they do maintain the parental physical Sup35 state, and the original [*PSI*$^+$] phenotype is revealed once wildtype Sup35 is reintroduced and the plasmids that express the oligopeptide truncation mutants are lost.

The Liebman lab has shown that an undifferentiated form of [*PSI*$^+$] can be maintained by Sup35's prion domain alone, which is composed of amino acids 1-123 [78]. However, the undifferentiated [*PSI*$^+$] variants propagated by the prion domain alone are capable of transferring variant-specific [*PSI*$^+$] phenotypes to full-length Sup35. In order for [*PSI*$^+$]^{weak} and [*PSI*$^+$]^{strong} variants to be faithfully propagated, Sup35 truncation mutants must contain at least amino acids 1-137. This work points out that Sup35 amino acids 124-137 are necessary for the faithful propagation of [*PSI*$^+$] variants.

[*URE3*] variants

As is the case for [*PSI*$^+$], [*URE3*] variants with distinct phenotypes can be induced and propagated in isogenic yeast strains [114]. These variants differ in their ability to take up a poor nitrogen source; they display different susceptibilities to elimination by co-expression of a Ure2-GFP fusion protein; they form variant-specific cytoplasmic aggregate patterns as visualized *via* interaction with the same Ure2-GFP fusion protein, and their distinct phenotypes can be transferred to isogenic cells by cytoplasmic mixing.

[*PIN*$^+$] variants

Yeast [*PIN*$^+$] variants have been characterized based on their ability to support [*PSI*$^+$] induction with varying efficiencies. "Very high" [*PIN*$^+$] is the prion variant that most efficiently supports [*PSI*$^+$] induction, while high, medium and low [*PIN*$^+$] are named in decreasing order of [*PSI*$^+$] inducibility [115]. While [*PSI*$^+$] variants are associated with different levels of soluble functional Sup35, [*PIN*$^+$] variants also differ in the amount of soluble Rnq1, but the amount of soluble Rnq1 does not correlate with the strength of the [*PIN*$^+$] phenotype. Rather, [*PIN*$^+$] variants can be distinguished by the pattern of

fluorescence from an Rnq1-GFP fusion, giving either a single fluorescent focus or multiple foci in individual cells [116].

Prion variants and interspecies disease transmission

The existence of prion variants indicates that each prion protein can access a unique spectrum of conformational states. This range of accessible states is limited by the amino acid sequence of each prion protein. It was briefly mentioned earlier with the BSE example that one prion's limited range of accessible states manifests itself as a species barrier [42, 104]. The range of prion states accessible to one protein can either limit its infectivity to one or a few species, or render it capable of interacting with the prion protein of another species. Some prion variants are promiscuous and can infect more than one species, while other variants cannot cross the species barrier [42] [117].

Mammalian interspecies prion transmission

The first evidence that cross-species infection can occur with prion diseases came from studies showing that the same agent causes BSE and a new type of the human CJD disease, called variant CJD (vCJD) [118-120]. vCJD differs from three well-studied classic types of CJD (classic CJDs are sporadic or familial in nature, not related to BSE exposure) both in its proteolytic profile and in the proportions of PrP glycoforms associated with the disease [120]. These two parameters along with clinical symptoms and brain histology are used to "type" CJD variants. Experimental transmission of BSE to mice by intracerebral inoculation produced the same proteolytic profile as seen in vCJD [120]. Mice infected with vCJD and with BSE show very similar incubation times (around 310 days), along with an identical pattern of vacuole formation in the brain, suggesting that the causative agent of BSE and

vCDJ may be the same [119]. In contrast, when three other classic CJD types were inoculated into mice, even 600-800 days after inoculation none of the mice had shown any signs of disease [119]. Earlier work from the Bruce group had shown that the promiscuous BSE variant that causes vCJD in humans is also capable of infecting domestic cats and sheep [104, 121, 122]. This data argues that the BSE prion agent is a particularly promiscuous prion variant, easily able to cross the species barrier, while the classic CJD variants are constrained by a species barrier and cannot be transmitted from humans to mice.

Yeast interspecies prion transmission

While the concept of the species barrier was first established for mammalian prions, work from Jonathan Weissman's lab has shown that [*PSI*$^{+}$] variant phenotypes are dependent on Sup35 protein states, and that Sup35 amino acid sequence limits the spectrum of accessible conformations [40, 117, 123-125]. For example, a point mutation can render Sup35, once capable of generating a promiscuous variant, unable to cross the species barrier. The species barrier can be recapitulated *in vitro*. If prion domains from two different yeast species (*C. albicans* and *S. cerevisiae*) are allowed to form amyloid fibers in a mixed reaction, the two prion domains form amyloids exclusively of one species prion domain, without any heterologous fiber formation [123]. Though *C. albicans* and *S. cerevisiae* Sup35 prion domains cannot cross the species barrier to infect each other, making a chimera construct with parts of each species' prion domain enables the chimera construct to accept and pass on Sup35 prion state from each species [124, 125]. The species barrier can also be tested *via* interaction between peptides from these three constructs on a surface-bound array of prion peptides [126]. Even in this *in vitro* protein-only system, only the chimeric construct is able to interact with peptides from both species.

Work from Y. Chernoff's group has shown that Sup35 from different *Saccharomyces* species (*S. cerevisiae, S. paradoxus,* and *S. bayanus*) retains the ability to form prions on its own, but when two species' Sup35s are co-expressed in *S. cerevisiae* in a plasmid shuffle experiment, the Sup35s co-aggregate in a [*PSI*$^+$]-dependent manner, but they are not able to pass on the prion state between each other [127]. Earlier work from the group had shown that transient overproduction of *P. methanolica* Sup35 in *S. cerevisiae* can induce stable [*PSI*$^+$] that persists even when the inducing *P. methanolica* Sup35 plasmid is lost [128]. However, the rate of [*PSI*$^+$] induction by the heterologous Sup35 was much lower than in a control experiment where [*PSI*$^+$] was induced by *S. cerevisiase* Sup35 overproduction, arguing that crossing the species barrier is a rare event that depends both on the ability of the heterologous prion protein to adopt a form that is capable of interacting with the native prion protein, and that this protein-protein interaction alone is not enough but that it must result in protein state transmission between the two heterologous proteins.

IV. Interactions between prions and prion variants

Interactions between mammalian prion variants

Scrapie

The first evidence that mammalian prion strains or variants can compete came from work on scrapie [129]. When two scrapie agents were injected into mice, the incubation time for the more lethal scrapie variant increased, though the mechanism of interaction between the

two agents could not be deduced. In a follow up study, the same group showed that when mice were inoculated with two scrapie agents with a 100-300 day break between the two injections, the second scrapie variant was not able to cause infection, and all the animals died from disease caused by the first scrapie variant that they were exposed to, as assessed by brain lesion intensity and distribution [130]. Thus, infection with one scrapie variant can block subsequent infection by another variant.

Transmissible mink encephalopathy

Another study of mammalian prion variant competition looked at the drowsy (DY) and hyper (HY) variants of transmissible mink encephalopathy (TME) [131]. The DY variant causes disease in hamsters only when injected into the brain or the sciatic nerve, but not when injected intraperitoneally. However, intraperitoneal injection of DY prior to a subsequent intraperitoneal injection with the HY variant extended the incubation time of HY disease symptoms. Inoculation of the DY variant into the sciatic nerve did not affect the onset of HY disease when HY was given as a second intrasciatic injection. PrP^{sc} western blotting was used to determine which TME variant caused the disease. These results suggest that the DY and HY variants compete somewhere in the body before establishing an infection in the nervous system.

Creutzfeldt-Jakob disease

Though each prion variant tends to cause a specific disease phenotype in mammals, recently it was demonstrated that two CJD variants can co-exist in CJD patients [132]. Aguzzi's group generated two anti-PrP monoclonal antibodies specific for proteinase K cleavage sites that can distinguish between two PrP^{sc} variants. When PrP proteolytic profile blots were

probed with these antibodies, both types of PrP^{sc} variants were detected in many patients, suggesting that the current CJD classification system may need to be refined.

Interactions between prion variants in lower eukaryotes

Interactions between [*PSI*$^+$] variants

S. Liebman's group has shown that [*PSI*$^+$]^{strong} variants are phenotypically dominant over [*PSI*$^+$]^{weak} variants [115]. Diploids generated by a cell cross between these two [*PSI*$^+$] variants always show the dominant [*PSI*$^+$]^{strong} phenotype, and this dominant phenotype is also inherited by all four meiotic progeny. The conclusion of this study was that the recessive [*PSI*$^+$]^{weak} aggregates must be lost when exposed to [*PSI*$^+$]^{strong}. However, cell crossing experiments look at the colony-level phenotype, and since it takes about twenty generations of cell growth to form a visible colony, this set of experiments does not reveal what happens to Sup35 protein dynamics when two [*PSI*$^+$] variants are mixed in the same cytoplasm. Alternative interpretations of Bradley and Liebman's results include the possibility that [*PSI*$^+$]^{weak} aggregates are propagated cryptically in cells from crosses with [*PSI*$^+$]^{strong}, and that [*PSI*$^+$]^{weak} aggregates are invisible phenotypically because [*PSI*$^+$]^{strong} reduces the level of soluble Sup35 and thereby increases the read-through phenotype, resulting in white colonies on rich medium (fig. 5). A third possibility is that [*PSI*$^+$] variants have a dynamic interaction that results in the formation of a novel type of [*PSI*$^+$] variant with the colony level [*PSI*$^+$]^{strong} phenotype. The above possibilities (loss of [*PSI*$^+$]^{weak}, co-existence of variants, and formation of a new variant) are not mutually exclusive, and it is possible that more than one of these mechanisms is taking place when two [*PSI*$^+$] variants interact. Further experiments

are needed to distinguish between these possibilities, and the molecular basis of the interaction between [*PSI*$^+$] variants will be addressed in chapter 2.

Interactions between [*PIN*$^+$] variants

Like [*PSI*$^+$] variants, [*PIN*$^+$] variants also compete with each other. Bradley and Liebman (2002) crossed different [*PIN*$^+$] variants to each other and performed genetic analysis to determine the resulting phenotype. The results show that [*PIN*$^+$] variants with greater ability to support [*PSI*$^+$] induction outcompete [*PIN*$^+$] variants that are not as efficient at inducing [*PSI*$^+$], with one exception. The "very high" [*PIN*$^+$] variant with the greatest ability to promote [*PSI*$^+$] induction was recessive to all other [*PIN*$^+$] variants [115]. These results suggest that there is not necessarily a linear correlation between the ability of a [*PIN*$^+$] variant to induce [*PSI*$^+$] and its dominance over other [*PIN*$^+$] variants in cell crosses. As with [*PSI*$^+$] variants described above, all meiotic progeny from [*PIN*$^+$] variant cell crosses always inherit the dominant [*PIN*$^+$] phenotype, and the dominant phenotype can be passed on solely through the cytoplasm without the exchange of nuclear DNA (cytoduction studies), showing that heritable differences among [*PIN*$^+$] variants do not depend on DNA, but are most likely the result of different [*PIN*$^+$] prion conformations. In a follow-up study where [*PIN*$^+$] variants were distinguished by a pattern of a single versus multiple cytoplasmic Rnq1-GFP dots, it was determined that the multiple dot [*PIN*$^+$] variant always outcompetes the single dot variant in cytoplasmic mixing (cytoduction) experiments [116]. An interesting parallel between [*PSI*$^+$] and [*PIN*$^+$] variants is that diploids and meiotic progeny from crosses between different [*PSI*$^+$] or [*PIN*$^+$] variants always show the phenotype of the parent with the smallest amount of soluble prion protein, arguing that the yeast prion variant with the

greatest ability to recruit and convert soluble protein into a prion form is usually dominant [115].

Interactions between [*PSI*$^+$], [*PIN*$^+$], and [*URE3*]

As explained earlier, the [*PIN*$^+$] prion is necessary for [*PSI*$^+$] induction by full-length Sup35 overproduction, but [*PIN*$^+$] and [*PSI*$^+$] can be eliminated or lost independently of each other [46, 87]. Thus, [*PIN*$^+$] is required only for the *de novo* appearance of [*PSI*$^+$] but not for [*PSI*$^+$] propagation, suggesting that the interaction between the two prions is limited to a distinct step in the [*PSI*$^+$] prion cycle. It is unclear how [*PSI*$^+$] and [*PIN*$^+$] interact *in vivo*, but aggregates or fibers of Rnq1 and Sup35-NM can cross-seed each other's polymerization *in vitro* [133, 134]. [*PIN*$^+$] also promotes, but [*PSI*$^+$] inhibits, *de novo* appearance of [*URE3*] [115]. The single dot [*PIN*$^+$] variant described earlier destabilizes and leads to loss of [*PSI*$^+$]^{weak} but not of [*PSI*$^+$]^{strong}, and, perplexingly, [*PSI*$^+$]^{weak} can also lead to the loss of medium single dot and very high single dot [*PIN*$^+$] variants [116]. The same study also showed that [*PIN*$^+$] variants may differ in their tendency to lead to [*PSI*$^+$]^{strong} or [*PSI*$^+$]^{weak} variants after Sup35 overproduction: multiple dot [*PIN*$^+$] induced stable [*PSI*$^+$]^{weak} and stable [*PSI*$^+$]^{strong}, while single dot [*PIN*$^+$] produced unstable [*PSI*$^+$]^{weak} and stable [*PSI*$^+$]^{strong}. [*URE3*] and [*PSI*$^+$] can exist in the same cell, but co-existence destabilizes them and leads to an increase in the rate of loss for both prions [135]. Their destabilizing interaction also reduces the rate of *de novo* induction of one prion in a cell that is already propagating the other prion. All these observations point out that two yeast prions do not always affect each other in the same way, but that each prion variant has a specific positive or negative effect on other heterologous prion variants. There is a general difference in the interactions between different conformations of the same protein, and in the interactions between different

prions. Different prions can sometimes affect each other positively, as [*PIN*$^+$] enables the appearance of [*PSI*$^+$], but when two conformations of the same prion protein come into contact, one form of the prion dominates over the other, as discussed earlier for the case of [*PSI*$^+$] and [*PIN*$^+$] variants [46, 115, 116].

Two proposed models explain the interaction between heterologous prions

Two models exist that explain the observation that, in general, prions facilitate the appearance of other prions in yeast: the cross-seeding model and the titration model [61, 88]. The cross-seeding model suggests that one prion can act directly as a template for the *de novo* formation of another prion. The titration model proposes that prions sequester a prion-inhibitory factor, and thereby increase the chances for general *de novo* prion formation. The cross-seeding mechanism of prion interaction has been shown to occur *in vitro*, but so far there is no *in vitro* experimental evidence to disprove the titration model mechanism [133, 134]. It is possible that both mechanisms operate *in vivo*, and that one is more important for the biogenesis of certain prions while the other plays a key role in the induction and propagation of other prions. For example, it is not necessarily true that [*PIN*$^+$] directly seeds [*PSI*$^+$] because the [*PSI*$^+$] phenotype is unaffected by the presence or absence of [*PIN*$^+$], and if the two prions formed heterologous complexes, the loss of [*PIN*$^+$] should affect the [*PSI*$^+$] phenotype [46]. Somewhat indirect evidence in support of the titration model is that [*PIN*$^+$] is induced by extended incubation at 4^{o}C [46]. Such conditions may alter the balance of chaperone proteins in the cell, suggesting that chaperones may be the titratable factor involved in prion induction. However, cross-seeding between different prions may be an extremely low frequency event that is difficult to detect experimentally. For now, neither the cross-seeding nor the titration model of prion induction can be ruled out.

V. Effects of chaperone proteins on the yeast prion cycle

In order for the yeast prion phenotype to be faithfully propagated, several necessary steps can be envisioned (fig. 6). First, a prion protein molecule must misfold into a self-replicating state, capable of directing other like molecules to assume the prion form. Next, the growing prion nucleus must be fragmented into smaller particles for two purposes: the smaller prion aggregate particles will serve as additional surfaces for recruitment and conversion of like molecules into the prion form, and they will ensure that a sufficient number of prion aggregates is passed on to daughter cells so that the prion phenotype is propagated stably. Little is known about co-factors that act at various steps in the prion cycle, but several molecular chaperones have been shown to play important roles in yeast prion propagation.

Hsp104

Hsp104 is a molecular chaperone whose role in [*PSI*$^+$] propagation is well understood [70, 136, 137]. Hsp104 is the major disaggregase in yeast, necessary for acquired thermotolerance and the rescue of unfolded proteins after heat shock [138] [73]. The Hsp104 chaperone is necessary for [*PSI*$^+$] propagation [70]. Specifically, Hsp104 levels are crucial for faithful [*PSI*$^+$] propagation: overexpression of Hsp104, as well as its inactivation by a dominant negative mutant or the pharmacological agent guanidine hydrochloride (GdnHCl) eliminates or "cures" the [*PSI*$^+$] prion [43, 70, 139]. Hsp104 is not necessary for the conversion of Sup35 to the prion state because [*PSI*$^+$] can be induced in Δ*hsp104* cells if Sup35 is co-expressed with the prion proteins New1 or Rnq1 [88, 140]. This data demonstrates that Hsp104 is not necessary for the first step of yeast prion biogenesis, which is conversion of soluble Sup35 into the prion form (fig. 6). Instead, Hsp104 fragments Sup35 aggregates,

aiding in transmission of the prion form to daughter cells, as well as facilitating prion form conversion by generating more prion template surfaces [136]. When Hsp104 is inhibited, Sup35 aggregates become larger and are not efficiently transmitted to daughter cells, leading to a loss of the prion phenotype [136]. These observations show that Hsp104 acts at step two of the yeast prion cycle (fig. 6), fragmenting growing prion particles into smaller complexes, and by breaking up prion aggregates it also aids with step three of the prion cycle, which is transmission of prion complexes into daughter cells.

Co-translational chaperones of the Hsp70 family and the prefoldin complex

In addition to Hsp104, members of the Hsp70 family are also involved in the [*PSI*$^+$] cycle. Co-translationally acting Hsp70 chaperones Ssb1p and Ssb2p have been implicated in [*PSI*$^+$] regulation [141] [142] [143]. Cells lacking these two Hsp70 proteins spontaneously acquire the prion state at higher levels and they show some resistance to [*PSI*$^+$] curing by Hsp104 overexpression [141]. The first of these observations suggests that Ssb proteins negatively regulate *de novo* [*PSI*$^+$] appearance, so it is possible that they are a negative regulator at step one of prion biogenesis (fig. 6), which is conversion of soluble Sup35 into the prion form. It is unknown if the initial conversion of a single Sup35 molecule occurs co-translationally as the Sup35 peptide emerges from the ribosome, or if the initial conversion into prion form occurs post-translationally. Given the fact that Ssbs are ribosome-associated co-translational chaperones, and that in their absence *de novo* rates of [*PSI*$^+$] induction are increased, it seems likely that Ssbs act as quality control regulators of Sup35 folding, preventing Sup35 from misfolding into the prion form [144]. However, it is also possible that Ssbs act at another step in the prion cycle. Simultaneous overexpression of Hsp104 and Ssbs leads to an increase in the rate of [*PSI*$^+$] curing [141]. The mechanism of [*PSI*$^+$] curing by Hsp104

overexpression is not known, but under normal conditions Hsp104 fragments [*PSI*$^+$] aggregates [136]. It is possible that Ssbs act as helper proteins downstream of Hsp104 and refold Sup35 that comes out of [*PSI*$^+$] complexes as a result of Hsp104 fragmentation into its non-prion state. Alternatively, if Hsp104 overexpression actually inhibits Hsp104 activity and causes [*PSI*$^+$] aggregates to increase in size, Ssb overexpression could aid in the curing of [*PSI*$^+$] by acting as a quality control regulator of Sup35 folding, and preventing soluble Sup35 from joining the [*PSI*$^+$] aggregates [74]. It is most likely that Ssbs always act as a quality control regulator of Sup35 folding, but perhaps their overexpression alone is not enough to prevent Sup35 from joining [*PSI*$^+$] aggregates, and Hsp104 activity must be inhibited in parallel to Ssb overexpression in order for Ssbs' anti-prion properties to be revealed.

The other major eukaryotic co-translational chaperone in addition to Ssbs is the prefoldin complex, which shuffles its target proteins from the ribosome to the CCT chaperonin for folding [145, 146]. Though the effects of Ssbs on [*PSI*$^+$] have been addressed, nothing is known about the possible role of the prefoldin chaperone in [*PSI*$^+$] biogenesis. Chapter 3 aims to address the role of prefoldin in [*PSI*$^+$] regulation.

Post-translational chaperones of the Hsp70 family

In addition to Ssbs, the post-translationally acting chaperones Ssa1, Ssa2, Ssa3 and Ssa4 are members of the Hsp70 family. The deletion of all four Ssas is lethal, but any one of them is sufficient for viability [147]. The role of the Ssa proteins in the [*PSI*$^+$] cycle is not well defined and can be confusing due to conflicting reports about their [*PSI*$^+$]-specific activity [70, 148]. An early study found that Ssa1 overexpression antagonizes [*PSI*$^+$]-dependent read-through, while a follow-up reported that Ssa1 overexpression protects [*PSI*$^+$] from

elimination by Hsp104 overexpression. In general, Ssa proteins show a pro-[*PSI*$^+$] effect, and [*PSI*$^+$] formation is increased when Ssas are overexpressed [149]. Also, Ssa overexpression increases [*PSI*$^+$]-mediated nonsense suppression, perhaps by making conversion of Sup35 into the prion form extremely efficient and thereby depleting soluble Sup35 [148]. These observations suggest it is possible that Ssas act in step one of [*PSI*$^+$] biogenesis (fig. 6), helping Sup35 fold into its prion form. In agreement with this, Ssas preferentially bind to the prion, but not to the non-prion form of Sup35 [150]. This preferential interaction with the prion form of Sup35 may also be shared by the chaperones Sse1, Sis1, and Hsp104, but in their case it cannot be ruled out that they also interact with the non-prion form of Sup35 [150].

The dominant negative mutant *SSA1-21* destabilizes [*PSI*$^+$] and causes cells to be more sensitive to [*PSI*$^+$] elimination when Hsp104 is inhibited by treatment with guanidine hydrochloride [151]. It is possible that this dominant negative mutant has an increased activity in promoting the folding of Sup35 into its prion form. Such a pro-[*PSI*$^+$] formation effect could actually be detrimental to [*PSI*$^+$] if its causes Sup35 aggregates to grow too large to be transported into daughter cells (fig. 6, step 3). If [*PSI*$^+$] aggregates are larger in *SSA1-21* cells, this would explain why [*PSI*$^+$] is more readily lost in this mutant, and why its combined effect with Hsp104 inhibition would increase [*PSI*$^+$] curing by producing large, immobile [*PSI*$^+$] aggregates that cannot be transmitted into daughter cells. Surprisingly, *SSA 1-21* has no effect on [*URE3*] and can propagate [*URE3*] in the absence of Ssa2, a set of conditions that is incompatible with [*PSI*$^+$] propagation [151] [152]. Another *ssa* mutant called *ssa2-10* destabilizes and leads to loss of [*URE3*] but does not affect [*PSI*$^+$], while Δ*ssa2*

null mutants can barely support [*URE3*] [153]. This shows that Hsp70 Ssa proteins do not interact equally with all yeast prions, but that their interactions and effects are prion-specific.

Hsp110

The yeast Sse1 protein from the Hsp110 family is a nucleotide exchange factor for Hsp70s that is necessary for stable propagation of [*PSI*$^+$] variants [154]. Overexpression of Sse1 aids *de novo* [*PSI*$^+$] formation, while Sse1 deletion decreases it. Since Sse1 is the nucleotide exchange factor for Hsp70s like Ssa, and since Ssa seems to stabilize the prion form of Sup35 at step 1 of yeast prion biogenesis (fig. 6), it is likely that overexpression of Sse1 helps Ssa in stabilizing Sup35 folding into the prion form, and thereby increases *de novo* [*PSI*$^+$] formation. Δ*sse1* cells propagate an unstable and undifferentiated prion form of Sup35, while isogenic wildtype cells can faithfully propagate a range of [*PSI*$^+$] variants [154]. This observation implies that the initial folding of Sup35 into a prion form may already determine what type of [*PSI*$^+$] variant will be produced, and that Sse1 probably in concert with Ssa1 helps to stabilize this nascent Sup35 variant fold. Sse1 overexpression interferes with [*PSI*$^+$] elimination by Hsp104 overexpression, and enables a low level of *de novo* [*PSI*$^+$] induction in [*pin*$^-$] cells [155]. This effect is also in agreement with the idea that Sse1 helps to stabilize a the prion form of Sup35, which may block [*PSI*$^+$] elimination by Hsp104 overexpression, and which may stabilize the prion form of Sup35 enough to enable [*PSI*$^+$] to appear spontaneously without help from the [*PIN*$^+$] prion.

Prion variant-specific chaperone effects

Chaperone proteins have been shown to have prion variant-specific effects. Deletion of the Hsp110 protein *SSE1* causes [*PSI*$^{+}$]^{strong} aggregates to increase in size and the corresponding cellular phenotype resembles [*PSI*$^{+}$]^{weak} [154], but [*PSI*$^{+}$]^{weak} is lost in Δ*sse1* cells. This effect is not surprising, because [*PSI*$^{+}$]^{weak} aggregates appear larger than [*PSI*$^{+}$]^{strong} aggregates under normal conditions, so if Δ*sse1* causes all [*PSI*$^{+}$] aggregates to increase in size, the smaller [*PSI*$^{+}$]^{strong} aggregates might tolerate this, but the larger [*PSI*$^{+}$]^{weak} aggregates will be lost because they will be too large to transmit into daughter cells. [*PSI*$^{+}$]^{strong} in Δ*sse1* cells may resemble the pink colony color phenotype of [*PSI*$^{+}$]^{weak} because the increase in [*PSI*$^{+}$]^{strong} aggregate size could reduce the number of [*PSI*$^{+}$] surfaces that are available to convert Sup35 into the prion form, so soluble Sup35 will accumulate and lead to the formation of pink colonies on rich medium. Both Sse1 overproduction and deletion cure [*URE3*], but its effect on [*PSI*$^{+}$] is prion variant-specific as described above [156]. This observation suggests that Sse1 plays a role both in [*PSI*$^{+}$] and [*URE3*] regulation, but that [*PSI*$^{+}$] is more tolerant than [*URE3*] to alterations in Sse1 activity.

Hsp40

The Hsp40 family of chaperone proteins consists of Sis1 and Ydj1. Hsp40 proteins interact with Hsp70 class Ssa, but not Ssb1/2, proteins [157]. The two Hsp40 proteins can cooperate with Ssas to specify Hsp70-substrate interaction. Hsp40 and Hsp70 can work together *in vitro* to renature proteins, and they can also cooperate with Hsp104 to rescue aggregated proteins [157] [158]. There has been much work linking Hsp40 proteins with various yeast prions, but so far no unifying model has been proposed to explain their role in yeast prion biogenesis. The Hsp40 family protein Sis1 associates with Rnq1 and Ssa1 in a

[*PIN*$^+$]-specific manner, and certain Sis1 mutants cannot propagate [*PIN*$^+$] [159] [160]. This suggests that Sis1 may act to stabilize [*PIN*$^+$] with the help of Ssa1, and that [*PIN*$^+$] needs Sis1 stabilizing activity for its propagation. Sis1 overexpression also ameliorates Rnq1 overexpression-mediated toxicity generated by promoting the assembly of Rnq1 into [*PIN*$^+$] prion aggregates, again showing that Sis1 may act to stabilize the [*PIN*$^+$] prion [161]. The other member of the Hsp40 family, Ydj1, eliminates only some [*PIN*$^+$] variants when it is overexpressed, suggesting that [*PIN*$^+$] variants may have different needs for the stabilizing effect of Hsp40 Ydj1 chaperone, and that too much stabilization of [*PIN*$^+$] by the Hsp40 proteins may also lead to its loss [115].

Specific aims

This thesis strives to clarify the nature of the interaction between different prion variants, and to elucidate the role of the co-translational chaperone prefoldin in prion biogenesis and regulation. While the role of the co-translational Hsp70 Ssb chaperones in the [*PSI*$^+$] cycle has been examined, there has been no exploration of the effect of the other major eukaryotic chaperone prefoldin on [*PSI*$^+$] biogenesis. Work in both the mammalian and yeast prion systems has shown that prion variants interact in the host, and that the competition between two prion variants can be beneficial for one, but is often detrimental for the other. The nature of the interaction between prion variants in one host is largely undefined. Most often, one prion variant seems to disappear at the phenotypic level as a result of interaction with another variant, but it remains possible that two prion variants continue to co-exist in a host while one variant is masked by the presence of the other, and that two prion variants interact dynamically to produce a novel variant. The yeast prion system provides an excellent model to study these interactions within the context of single cells, eliminating the complications of parallel propagation of different variant forms within different cells in metazoans.

Specifically, in this work I will:

1) Assess how the interaction between two prion variants affects their inheritance.

2) Determine the effects of the co-translational chaperone prefoldin on prion propagation.

References:

1. Basler, K., et al., *Scrapie and cellular PrP isoforms are encoded by the same chromosomal gene.* Cell, 1986. **46**(3): p. 417-28.
2. Weissmann, C., *The state of the prion.* Nat Rev Microbiol, 2004. **2**(11): p. 861-71.
3. Aguzzi, A., M. Heikenwalder, and M. Polymenidou, *Insights into prion strains and neurotoxicity.* Nat Rev Mol Cell Biol, 2007. **8**(7): p. 552-61.
4. Liberski, P.P. and P. Brown, *Kuru: Its ramifications after fifty years.* Exp Gerontol, 2008.
5. Hadlow, W.J., *Scrapie and kuru.* Lancet, 1959. **2**: p. 289-290.
6. Gajdusek, D.C., *Kuru: an appraisal of five years of investigation.* Eugen Q, 1962. **9**: p. 69-74.
7. Gajdusek, D.C. and C.J. Gibbs, *Attempts to Demonstrate a Transmissible Agent in Kuru, Amyotrophic Lateral Sclerosis, and Other Sub-Acute and Chronic Nervous System Degenerations of Man.* Nature, 1964. **204**: p. 257-9.
8. Klatzo, I., D.C. Gajdusek, and V. Zigas, *Pathology of Kuru.* Lab Invest, 1959. **8**(4): p. 799-847.
9. Gajdusek, D.C., C.J. Gibbs, and M. Alpers, *Experimental transmission of a Kuru-like syndrome to chimpanzees.* Nature, 1966. **209**(5025): p. 794-6.
10. Gajdusek, D.C., C.J. Gibbs, Jr., and M. Alpers, *Transmission and passage of experimenal "kuru" to chimpanzees.* Science, 1967. **155**(759): p. 212-4.
11. Gibbs, C.J., Jr., et al., *Creutzfeldt-Jakob disease (spongiform encephalopathy): transmission to the chimpanzee.* Science, 1968. **161**(839): p. 388-9.
12. Gibbs, C.J., Jr. and D.C. Gajdusek, *Transmission of scrapie to the cynomolgus monkey (Macaca fascicularis).* Nature, 1972. **236**(5341): p. 73-4.
13. Gibbs, C.J., Jr. and D.C. Gajdusek, *Infection as the etiology of spongiform encephalopathy (Creutzfeldt-Jakob disease).* Science, 1969. **165**(897): p. 1023-5.
14. Rogers, N.G., et al., *Latent viruses in chimpanzees with experimental kuru.* Nature, 1967. **216**(5114): p. 446-9.
15. Gibbs, C.J., Jr., D.C. Gajdusek, and R. Latarjet, *Unusual resistance to ionizing radiation of the viruses of kuru, Creutzfeldt-Jakob disease, and scrapie.* Proc Natl Acad Sci U S A, 1978. **75**(12): p. 6268-70.
16. Alper, T., et al., *Does the agent of scrapie replicate without nucleic acid?* Nature, 1967. **214**(5090): p. 764-6.
17. Alper, T., D.A. Haig, and M.C. Clarke, *The exceptionally small size of the scrapie agent.* Biochem Biophys Res Commun, 1966. **22**(3): p. 278-84.
18. Griffith, J.S., *Self-replication and scrapie.* Nature, 1967. **215**(5105): p. 1043-4.
19. Prusiner, S.B., et al., *Molecular properties, partial purification, and assay by incubation period measurements of the hamster scrapie agent.* Biochemistry, 1980. **19**(21): p. 4883-91.
20. Prusiner, S.B., et al., *Thiocyanate and hydroxyl ions inactivate the scrapie agent.* Proc Natl Acad Sci U S A, 1981. **78**(7): p. 4606-10.
21. Alper, T., D.A. Haig, and M.C. Clarke, *The scrapie agent: evidence against its dependence for replication on intrinsic nucleic acid.* J Gen Virol, 1978. **41**(3): p. 503-16.
22. Alper, T., *Scrapie agent unlike viruses in size and susceptibility to inactivation by ionizing or ultraviolet radiation.* Nature, 1985. **317**(6039): p. 750.

23. Prusiner, S.B., et al., *Scrapie agent contains a hydrophobic protein.* Proc Natl Acad Sci U S A, 1981. **78**(11): p. 6675-9.
24. Prusiner, S.B., *Novel proteinaceous infectious particles cause scrapie.* Science, 1982. **216**(4542): p. 136-44.
25. Bolton, D.C., M.P. McKinley, and S.B. Prusiner, *Identification of a protein that purifies with the scrapie prion.* Science, 1982. **218**(4579): p. 1309-11.
26. McKinley, M.P., D.C. Bolton, and S.B. Prusiner, *A protease-resistant protein is a structural component of the scrapie prion.* Cell, 1983. **35**(1): p. 57-62.
27. Oesch, B., et al., *A cellular gene encodes scrapie PrP 27-30 protein.* Cell, 1985. **40**(4): p. 735-46.
28. Westaway, D. and S.B. Prusiner, *Conservation of the cellular gene encoding the scrapie prion protein.* Nucleic Acids Res, 1986. **14**(5): p. 2035-44.
29. Cotto, E., et al., *Molecular characterization, phylogenetic relationships, and developmental expression patterns of prion genes in zebrafish (Danio rerio).* FEBS J, 2005. **272**(2): p. 500-13.
30. Ford, M.J., et al., *Selective expression of prion protein in peripheral tissues of the adult mouse.* Neuroscience, 2002. **113**(1): p. 177-92.
31. Bueler, H., et al., *Mice devoid of PrP are resistant to scrapie.* Cell, 1993. **73**(7): p. 1339-47.
32. Legname, G., et al., *Synthetic mammalian prions.* Science, 2004. **305**(5684): p. 673-6.
33. Collinge, J. and A.R. Clarke, *A general model of prion strains and their pathogenicity.* Science, 2007. **318**(5852): p. 930-6.
34. Castilla, J., et al., *In vitro generation of infectious scrapie prions.* Cell, 2005. **121**(2): p. 195-206.
35. Soto, C., et al., *Pre-symptomatic detection of prions by cyclic amplification of protein misfolding.* FEBS Lett, 2005. **579**(3): p. 638-42.
36. Saa, P., J. Castilla, and C. Soto, *Ultra-efficient replication of infectious prions by automated protein misfolding cyclic amplification.* J Biol Chem, 2006. **281**(46): p. 35245-52.
37. Prusiner, S.B., et al., *Ablation of the prion protein (PrP) gene in mice prevents scrapie and facilitates production of anti-PrP antibodies.* Proc Natl Acad Sci U S A, 1993. **90**(22): p. 10608-12.
38. Sailer, A., et al., *No propagation of prions in mice devoid of PrP.* Cell, 1994. **77**(7): p. 967-8.
39. King, C.Y. and R. Diaz-Avalos, *Protein-only transmission of three yeast prion strains.* Nature, 2004. **428**(6980): p. 319-23.
40. Tanaka, M., et al., *Conformational variations in an infectious protein determine prion strain differences.* Nature, 2004. **428**(6980): p. 323-8.
41. Satpute-Krishnan, P. and T.R. Serio, *Prion protein remodelling confers an immediate phenotypic switch.* Nature, 2005. **437**(7056): p. 262-5.
42. Chien, P., J.S. Weissman, and A.H. DePace, *Emerging principles of conformation-based prion inheritance.* Annu Rev Biochem, 2004. **73**: p. 617-56.
43. Patino, M.M., et al., *Support for the prion hypothesis for inheritance of a phenotypic trait in yeast.* Science, 1996. **273**(5275): p. 622-6.

44. Paushkin, S.V., et al., *Propagation of the yeast prion-like [psi+] determinant is mediated by oligomerization of the SUP35-encoded polypeptide chain release factor.* Embo J, 1996. **15**(12): p. 3127-34.
45. Wickner, R.B., *[URE3] as an altered URE2 protein: evidence for a prion analog in Saccharomyces cerevisiae.* Science, 1994. **264**(5158): p. 566-9.
46. Derkatch, I.L., et al., *Dependence and independence of [PSI(+)] and [PIN(+)]: a two-prion system in yeast?* Embo J, 2000. **19**(9): p. 1942-52.
47. Osherovich, L.Z., et al., *Dissection and design of yeast prions.* PLoS Biol, 2004. **2**(4): p. E86.
48. Du, Z., et al., *Newly identified prion linked to the chromatin-remodeling factor Swi1 in Saccharomyces cerevisiae.* Nat Genet, 2008. **40**(4): p. 460-5.
49. Volkov, K.V., et al., *Novel non-Mendelian determinant involved in the control of translation accuracy in Saccharomyces cerevisiae.* Genetics, 2002. **160**(1): p. 25-36.
50. Coustou, V., et al., *The protein product of the het-s heterokaryon incompatibility gene of the fungus Podospora anserina behaves as a prion analog.* Proc Natl Acad Sci U S A, 1997. **94**(18): p. 9773-8.
51. Silar, P., et al., *Propagation of a novel cytoplasmic, infectious and deleterious determinant is controlled by translational accuracy in Podospora anserina.* Genetics, 1999. **151**(1): p. 87-95.
52. Collin, P., et al., *A non-chromosomal factor allows viability of Schizosaccharomyces pombe lacking the essential chaperone calnexin.* J Cell Sci, 2004. **117**(Pt 6): p. 907-18.
53. Barnhart, M.M. and M.R. Chapman, *Curli biogenesis and function.* Annu Rev Microbiol, 2006. **60**: p. 131-47.
54. Patel, B.K. and S.W. Liebman, *"Prion-proof" for [PIN+]: infection with in vitro-made amyloid aggregates of Rnq1p-(132-405) induces [PIN+].* J Mol Biol, 2007. **365**(3): p. 773-82.
55. Brachmann, A., U. Baxa, and R.B. Wickner, *Prion generation in vitro: amyloid of Ure2p is infectious.* EMBO J, 2005. **24**(17): p. 3082-92.
56. Edskes, H.K., V.T. Gray, and R.B. Wickner, *The [URE3] prion is an aggregated form of Ure2p that can be cured by overexpression of Ure2p fragments.* Proc Natl Acad Sci U S A, 1999. **96**(4): p. 1498-503.
57. Coustou-Linares, V., et al., *In vivo aggregation of the HET-s prion protein of the fungus Podospora anserina.* Mol Microbiol, 2001. **42**(5): p. 1325-35.
58. Dos Reis, S., et al., *The HET-s prion protein of the filamentous fungus Podospora anserina aggregates in vitro into amyloid-like fibrils.* J Biol Chem, 2002. **277**(8): p. 5703-6.
59. Vitrenko, Y.A., et al., *Propagation of the [PIN+] prion by fragments of Rnq1 fused to GFP.* Curr Genet, 2007. **51**(5): p. 309-19.
60. Sondheimer, N. and S. Lindquist, *Rnq1: an epigenetic modifier of protein function in yeast.* Mol Cell, 2000. **5**(1): p. 163-72.
61. Derkatch, I.L., et al., *Prions affect the appearance of other prions: the story of [PIN(+)].* Cell, 2001. **106**(2): p. 171-82.

62. Tuite, M.F., C.R. Mundy, and B.S. Cox, *Agents that cause a high frequency of genetic change from [psi+] to [psi-] in Saccharomyces cerevisiae.* Genetics, 1981. **98**(4): p. 691-711.
63. Cox, B.S., *Ψ. a cytoplasmic suppressor of super-suppressor in yeast.* Heredity, 1965. **20**: p. 505-521.
64. Chernoff, Y.O., I.L. Derkach, and S.G. Inge-Vechtomov, *Multicopy SUP35 gene induces de-novo appearance of psi-like factors in the yeast Saccharomyces cerevisiae.* Curr Genet, 1993. **24**(3): p. 268-70.
65. Ter-Avanesyan, M.D., et al., *Deletion analysis of the SUP35 gene of the yeast Saccharomyces cerevisiae reveals two non-overlapping functional regions in the encoded protein.* Mol Microbiol, 1993. **7**(5): p. 683-92.
66. Derkatch, I.L., et al., *Genesis and variability of [PSI] prion factors in Saccharomyces cerevisiae.* Genetics, 1996. **144**(4): p. 1375-86.
67. Serio, T.R. and S.L. Lindquist, *[PSI+]: an epigenetic modulator of translation termination efficiency.* Annu Rev Cell Dev Biol, 1999. **15**: p. 661-703.
68. Zhou, P., et al., *The yeast non-Mendelian factor [ETA+] is a variant of [PSI+], a prion-like form of release factor eRF3.* Embo J, 1999. **18**(5): p. 1182-91.
69. Toyama, B.H., et al., *The structural basis of yeast prion strain variants.* Nature, 2007. **449**(7159): p. 233-7.
70. Chernoff, Y.O., et al., *Role of the chaperone protein Hsp104 in propagation of the yeast prion-like factor [psi+].* Science, 1995. **268**(5212): p. 880-4.
71. Lund, P.M. and B.S. Cox, *Reversion analysis of [psi-] mutations in Saccharomyces cerevisiae.* Genet Res, 1981. **37**(2): p. 173-82.
72. Jung, G. and D.C. Masison, *Guanidine hydrochloride inhibits Hsp104 activity in vivo: a possible explanation for its effect in curing yeast prions.* Curr Microbiol, 2001. **43**(1): p. 7-10.
73. Parsell, D.A., et al., *Protein disaggregation mediated by heat-shock protein Hsp104.* Nature, 1994. **372**(6505): p. 475-8.
74. Kryndushkin, D.S., et al., *Yeast [PSI+] prion aggregates are formed by small Sup35 polymers fragmented by Hsp104.* J Biol Chem, 2003. **278**(49): p. 49636-43.
75. Kushnirov, V.V., et al., *Nucleotide sequence of the SUP2 (SUP35) gene of Saccharomyces cerevisiae.* Gene, 1988. **66**(1): p. 45-54.
76. Serio, T.R. and S.L. Lindquist, *Protein-only inheritance in yeast: something to get [PSI+]-ched about.* Trends Cell Biol, 2000. **10**(3): p. 98-105.
77. Liu, J.J., N. Sondheimer, and S.L. Lindquist, *Changes in the middle region of Sup35 profoundly alter the nature of epigenetic inheritance for the yeast prion [PSI+].* Proc Natl Acad Sci U S A, 2002. **99 Suppl 4**: p. 16446-53.
78. Bradley, M.E. and S.W. Liebman, *The Sup35 domains required for maintenance of weak, strong or undifferentiated yeast [PSI+] prions.* Mol Microbiol, 2004. **51**(6): p. 1649-59.
79. DePace, A.H., et al., *A critical role for amino-terminal glutamine/asparagine repeats in the formation and propagation of a yeast prion.* Cell, 1998. **93**(7): p. 1241-52.
80. Liu, J.J. and S. Lindquist, *Oligopeptide-repeat expansions modulate 'protein-only' inheritance in yeast.* Nature, 1999. **400**(6744): p. 573-6.

81. Parham, S.N., C.G. Resende, and M.F. Tuite, *Oligopeptide repeats in the yeast protein Sup35p stabilize intermolecular prion interactions.* EMBO J, 2001. **20**(9): p. 2111-9.
82. Jensen, M.A., et al., *Molecular population genetics and evolution of a prion-like protein in Saccharomyces cerevisiae.* Genetics, 2001. **159**(2): p. 527-35.
83. Harrison, L.B., et al., *Evolution of budding yeast prion-determinant sequences across diverse fungi.* J Mol Biol, 2007. **368**(1): p. 273-82.
84. Lacroute, F., *Non-Mendelian mutation allowing ureidosuccinic acid uptake in yeast.* J Bacteriol, 1971. **106**(2): p. 519-22.
85. Aigle, M. and F. Lacroute, *Genetical aspects of [URE3], a non-mitochondrial, cytoplasmically inherited mutation in yeast.* Mol Gen Genet, 1975. **136**(4): p. 327-35.
86. Masison, D.C. and R.B. Wickner, *Prion-inducing domain of yeast Ure2p and protease resistance of Ure2p in prion-containing cells.* Science, 1995. **270**(5233): p. 93-5.
87. Derkatch, I.L., et al., *Genetic and environmental factors affecting the de novo appearance of the [PSI+] prion in Saccharomyces cerevisiae.* Genetics, 1997. **147**(2): p. 507-19.
88. Osherovich, L.Z. and J.S. Weissman, *Multiple Gln/Asn-rich prion domains confer susceptibility to induction of the yeast [PSI(+)] prion.* Cell, 2001. **106**(2): p. 183-94.
89. Sturtevant, J., R. Cihlar, and R. Calderone, *Disruption studies of a Candida albicans gene, ELF1: a member of the ATP-binding cassette family.* Microbiology, 1998. **144 (Pt 8)**: p. 2311-21.
90. Beisson-Schecroun, J., *[Cellular incompatibility and nucleo-cytoplasmic interactions in the "barrage" phenomena in Podospora anserina.].* Ann Genet, 1962. **4**: p. 4-50.
91. Maddelein, M.L., et al., *Amyloid aggregates of the HET-s prion protein are infectious.* Proc Natl Acad Sci U S A, 2002. **99**(11): p. 7402-7.
92. Malato, L., et al., *Role of Hsp104 in the propagation and inheritance of the [Het-s] prion.* Mol Biol Cell, 2007. **18**(12): p. 4803-12.
93. Sunde, M. and C. Blake, *The structure of amyloid fibrils by electron microscopy and X-ray diffraction.* Adv Protein Chem, 1997. **50**: p. 123-59.
94. Sunde, M., et al., *Common core structure of amyloid fibrils by synchrotron X-ray diffraction.* J Mol Biol, 1997. **273**(3): p. 729-39.
95. Lindquist, S., et al., *Amyloid fibres of Sup35 support a prion-like mechanism of inheritance in yeast.* Biochem Soc Trans, 1998. **26**(3): p. 486-90.
96. Veerhuis, R., R.S. Boshuizen, and A. Familian, *Amyloid associated proteins in Alzheimer's and prion disease.* Curr Drug Targets CNS Neurol Disord, 2005. **4**(3): p. 235-48.
97. Prusiner, S.B., et al., *Scrapie prions aggregate to form amyloid-like birefringent rods.* Cell, 1983. **35**(2 Pt 1): p. 349-58.
98. Westermark, P., et al., *Amyloid: toward terminology clarification. Report from the Nomenclature Committee of the International Society of Amyloidosis.* Amyloid, 2005. **12**(1): p. 1-4.

99. Geddes, A.J., et al., *"Cross-beta" conformation in proteins.* J Mol Biol, 1968. **32**(2): p. 343-58.
100. Balbirnie, M., R. Grothe, and D.S. Eisenberg, *An amyloid-forming peptide from the yeast prion Sup35 reveals a dehydrated beta-sheet structure for amyloid.* Proc Natl Acad Sci U S A, 2001. **98**(5): p. 2375-80.
101. Serpell, L.C., M. Sunde, and C.C. Blake, *The molecular basis of amyloidosis.* Cell Mol Life Sci, 1997. **53**(11-12): p. 871-87.
102. Fraser, H. and A.G. Dickinson, *Scrapie in mice. Agent-strain differences in the distribution and intensity of grey matter vacuolation.* J Comp Pathol, 1973. **83**(1): p. 29-40.
103. Bessen, R.A. and R.F. Marsh, *Distinct PrP properties suggest the molecular basis of strain variation in transmissible mink encephalopathy.* J Virol, 1994. **68**(12): p. 7859-68.
104. Bruce, M., et al., *Transmission of bovine spongiform encephalopathy and scrapie to mice: strain variation and the species barrier.* Philos Trans R Soc Lond B Biol Sci, 1994. **343**(1306): p. 405-11.
105. Wadsworth, J.D., et al., *Human prion protein with valine 129 prevents expression of variant CJD phenotype.* Science, 2004. **306**(5702): p. 1793-6.
106. Doel, S.M., et al., *The dominant PNM2- mutation which eliminates the psi factor of Saccharomyces cerevisiae is the result of a missense mutation in the SUP35 gene.* Genetics, 1994. **137**(3): p. 659-70.
107. Derkatch, I.L., et al., *The PNM2 mutation in the prion protein domain of SUP35 has distinct effects on different variants of the [PSI+] prion in yeast.* Curr Genet, 1999. **35**(2): p. 59-67.
108. Liebman, S.W.a.J.A.A.-R., *A non-Mendelian factor, [eta+] causes lethality of yeast omnipotent suppressor strains.* Curr. Genet., 1984. **8**: p. 567-573.
109. King, C.Y., *Supporting the structural basis of prion strains: induction and identification of [PSI] variants.* J Mol Biol, 2001. **307**(5): p. 1247-60.
110. Krishnan, R. and S.L. Lindquist, *Structural insights into a yeast prion illuminate nucleation and strain diversity.* Nature, 2005. **435**(7043): p. 765-72.
111. Diaz-Avalos, R., et al., *Strain-specific morphologies of yeast prion amyloid fibrils.* Proc Natl Acad Sci U S A, 2005. **102**(29): p. 10165-70.
112. Park, K.W., et al., *De novo appearance and "strain" formation of yeast prion [PSI+] are regulated by the heat-shock transcription factor.* Genetics, 2006. **173**(1): p. 35-47.
113. Shkundina, I.S., et al., *The role of the N-terminal oligopeptide repeats of the yeast Sup35 prion protein in propagation and transmission of prion variants.* Genetics, 2006. **172**(2): p. 827-35.
114. Schlumpberger, M., S.B. Prusiner, and I. Herskowitz, *Induction of distinct [URE3] yeast prion strains.* Mol Cell Biol, 2001. **21**(20): p. 7035-46.
115. Bradley, M.E., et al., *Interactions among prions and prion "strains" in yeast.* Proc Natl Acad Sci U S A, 2002. **99 Suppl 4**: p. 16392-9.
116. Bradley, M.E. and S.W. Liebman, *Destabilizing interactions among [PSI(+)] and [PIN(+)] yeast prion variants.* Genetics, 2003. **165**(4): p. 1675-85.

117. Tanaka, M., et al., *Mechanism of cross-species prion transmission: an infectious conformation compatible with two highly divergent yeast prion proteins.* Cell, 2005. **121**(1): p. 49-62.
118. Hill, A.F., et al., *The same prion strain causes vCJD and BSE.* Nature, 1997. **389**(6650): p. 448-50, 526.
119. Bruce, M.E., et al., *Transmissions to mice indicate that 'new variant' CJD is caused by the BSE agent.* Nature, 1997. **389**(6650): p. 498-501.
120. Collinge, J., et al., *Molecular analysis of prion strain variation and the aetiology of 'new variant' CJD.* Nature, 1996. **383**(6602): p. 685-90.
121. Foster, J.D., et al., *Detection of BSE infectivity in brain and spleen of experimentally infected sheep.* Vet Rec, 1996. **138**(22): p. 546-8.
122. Fraser, H., et al., *Transmission of feline spongiform encephalopathy to mice.* Vet Rec, 1994. **134**(17): p. 449.
123. Santoso, A., et al., *Molecular basis of a yeast prion species barrier.* Cell, 2000. **100**(2): p. 277-88.
124. Chien, P. and J.S. Weissman, *Conformational diversity in a yeast prion dictates its seeding specificity.* Nature, 2001. **410**(6825): p. 223-7.
125. Chien, P., et al., *Generation of prion transmission barriers by mutational control of amyloid conformations.* Nature, 2003. **424**(6951): p. 948-51.
126. Tessier, P.M. and S. Lindquist, *Prion recognition elements govern nucleation, strain specificity and species barriers.* Nature, 2007. **447**(7144): p. 556-61.
127. Chen, B., G.P. Newnam, and Y.O. Chernoff, *Prion species barrier between the closely related yeast proteins is detected despite coaggregation.* Proc Natl Acad Sci U S A, 2007. **104**(8): p. 2791-6.
128. Chernoff, Y.O., et al., *Evolutionary conservation of prion-forming abilities of the yeast Sup35 protein.* Mol Microbiol, 2000. **35**(4): p. 865-76.
129. Dickinson, A.G., et al., *Competition between different scrapie agents in mice.* Nat New Biol, 1972. **237**(77): p. 244-5.
130. Dickenson, A.G., et al., *Extraneural competition between different scrapie agents leading to loss of infectivity.* Nature, 1975. **253**(5492): p. 556.
131. Bartz, J.C., J.M. Aiken, and R.A. Bessen, *Delay in onset of prion disease for the HY strain of transmissible mink encephalopathy as a result of prior peripheral inoculation with the replication-deficient DY strain.* J Gen Virol, 2004. **85**(Pt 1): p. 265-73.
132. Polymenidou, M., et al., *Coexistence of multiple PrPSc types in individuals with Creutzfeldt-Jakob disease.* Lancet Neurol, 2005. **4**(12): p. 805-14.
133. Vitrenko, Y.A., et al., *Visualization of aggregation of the Rnq1 prion domain and cross-seeding interactions with Sup35NM.* J Biol Chem, 2007. **282**(3): p. 1779-87.
134. Derkatch, I.L., et al., *Effects of Q/N-rich, polyQ, and non-polyQ amyloids on the de novo formation of the [PSI+] prion in yeast and aggregation of Sup35 in vitro.* Proc Natl Acad Sci U S A, 2004. **101**(35): p. 12934-9.
135. Schwimmer, C. and D.C. Masison, *Antagonistic interactions between yeast [PSI(+)] and [URE3] prions and curing of [URE3] by Hsp70 protein chaperone Ssa1p but not by Ssa2p.* Mol Cell Biol, 2002. **22**(11): p. 3590-8.

136. Satpute-Krishnan, P., S.X. Langseth, and T.R. Serio, *Hsp104-dependent remodeling of prion complexes mediates protein-only inheritance.* PLoS Biol, 2007. **5**(2): p. e24.
137. Wegrzyn, R.D., et al., *Mechanism of prion loss after Hsp104 inactivation in yeast.* Mol Cell Biol, 2001. **21**(14): p. 4656-69.
138. Sanchez, Y. and S.L. Lindquist, *HSP104 required for induced thermotolerance.* Science, 1990. **248**(4959): p. 1112-5.
139. Jung, G., G. Jones, and D.C. Masison, *Amino acid residue 184 of yeast Hsp104 chaperone is critical for prion-curing by guanidine, prion propagation, and thermotolerance.* Proc Natl Acad Sci U S A, 2002. **99**(15): p. 9936-41.
140. Kimura, Y., et al., *The role of pre-existing aggregates in Hsp104-dependent polyglutamine aggregate formation and epigenetic change of yeast prions.* Genes Cells, 2004. **9**(8): p. 685-96.
141. Chernoff, Y.O., et al., *Evidence for a protein mutator in yeast: role of the Hsp70-related chaperone ssb in formation, stability, and toxicity of the [PSI] prion.* Mol Cell Biol, 1999. **19**(12): p. 8103-12.
142. Jones, G.W., Y. Song, and D.C. Masison, *Deletion of the Hsp70 chaperone gene SSB causes hypersensitivity to guanidine toxicity and curing of the [PSI+] prion by increasing guanidine uptake in yeast.* Mol Genet Genomics, 2003. **269**(3): p. 304-11.
143. Chacinska, A., et al., *Ssb1 chaperone is a [PSI+] prion-curing factor.* Curr Genet, 2001. **39**(2): p. 62-7.
144. Nelson, R.J., et al., *The translation machinery and 70 kd heat shock protein cooperate in protein synthesis.* Cell, 1992. **71**(1): p. 97-105.
145. Geissler, S., K. Siegers, and E. Schiebel, *A novel protein complex promoting formation of functional alpha- and gamma-tubulin.* EMBO J, 1998. **17**(4): p. 952-66.
146. Vainberg, I.E., et al., *Prefoldin, a chaperone that delivers unfolded proteins to cytosolic chaperonin.* Cell, 1998. **93**(5): p. 863-73.
147. Werner-Washburne, M., D.E. Stone, and E.A. Craig, *Complex interactions among members of an essential subfamily of hsp70 genes in Saccharomyces cerevisiae.* Mol Cell Biol, 1987. **7**(7): p. 2568-77.
148. Newnam, G.P., et al., *Antagonistic interactions between yeast chaperones Hsp104 and Hsp70 in prion curing.* Mol Cell Biol, 1999. **19**(2): p. 1325-33.
149. Allen, K.D., et al., *Hsp70 chaperones as modulators of prion life cycle: novel effects of Ssa and Ssb on the Saccharomyces cerevisiae prion [PSI+].* Genetics, 2005. **169**(3): p. 1227-42.
150. Bagriantsev, S.N., et al., *Variant-specific [PSI+] Infection Is Transmitted by Sup35 Polymers within [PSI+] Aggregates with Heterogeneous Protein Composition.* Mol Biol Cell, 2008. **19**(6): p. 2433-43.
151. Jung, G., et al., *A role for cytosolic hsp70 in yeast [PSI(+)] prion propagation and [PSI(+)] as a cellular stress.* Genetics, 2000. **156**(2): p. 559-70.
152. Sharma, D. and D.C. Masison, *Functionally redundant isoforms of a yeast Hsp70 chaperone subfamily have different anti-prion effects.* Genetics, 2008.

153. Roberts, B.T., H. Moriyama, and R.B. Wickner, *[URE3] prion propagation is abolished by a mutation of the primary cytosolic Hsp70 of budding yeast.* Yeast, 2004. **21**(2): p. 107-17.
154. Fan, Q., et al., *The role of Sse1 in the de novo formation and variant determination of the [PSI+] prion.* Genetics, 2007. **177**(3): p. 1583-93.
155. Sadlish, H., et al., *Hsp110 chaperones regulate prion formation and propagation in S. cerevisiae by two discrete activities.* PLoS ONE, 2008. **3**(3): p. e1763.
156. Kryndushkin, D. and R.B. Wickner, *Nucleotide exchange factors for Hsp70s are required for [URE3] prion propagation in Saccharomyces cerevisiae.* Mol Biol Cell, 2007. **18**(6): p. 2149-54.
157. Lu, Z. and D.M. Cyr, *Protein folding activity of Hsp70 is modified differentially by the hsp40 co-chaperones Sis1 and Ydj1.* J Biol Chem, 1998. **273**(43): p. 27824-30.
158. Glover, J.R. and S. Lindquist, *Hsp104, Hsp70, and Hsp40: a novel chaperone system that rescues previously aggregated proteins.* Cell, 1998. **94**(1): p. 73-82.
159. Kurahashi, H., et al., *A regulatory role of the Rnq1 nonprion domain for prion propagation and polyglutamine aggregates.* Mol Cell Biol, 2008. **28**(10): p. 3313-23.
160. Sondheimer, N., et al., *The role of Sis1 in the maintenance of the [RNQ+] prion.* EMBO J, 2001. **20**(10): p. 2435-42.
161. Douglas, P.M., et al., *Chaperone-dependent amyloid assembly protects cells from prion toxicity.* Proc Natl Acad Sci U S A, 2008. **105**(20): p. 7206-11.

Figure Captions

Figure 1. Sup35 function and resultant phenotype in prion ([*PSI*$^+$]) and non-prion ([*psi*$^-$]) cells. A. Protein state. In [*psi*$^-$] cells, Sup35 is found in the supernatant upon centrifugation of cell lysates (left) and analysis of the fractions by SDS-PAGE and anti-Sup35 immunoblotting, and is diffusely distributed throughout the cytoplasm as visualized by a Sup35-GFP fusion (right). In [*PSI*$^+$] cells, Sup35 is found in the pellet fraction (left) and localizes as cytoplasmic foci (right). The centrifugation assay was performed by and the GFP fusion pictures were taken by Tricia Serio. B. Mechanism and function. In the [*psi*$^-$] state, Sup35 is functional and acts as a translation termination factor, recognizing the premature stop codon in the *ade1-14* (UGA) allele (left). Consequently, the Ade1 protein is not made, so there is an accumulation of an adenine metabolic intermediate in cells that causes them to appear red on rich media. In the [*PSI*$^+$] state, Sup 35's function is compromised, leading to read-through of stop codons and allowing the *ade1-14* mutants to express the Ade1 protein and to synthesize adenine, therefore appearing white on rich media (right). This diagram is modeled after Serio and Lindquist, 2000.

Figure 2. Sup35 region structure. Sup35 is composed of three distinct sequence regions, separated by methionines at positions 1, 125, and 254. The glutamine-rich N-terminal domain (N) is known as the prion domain. The middle domain M is highly charged and of unknown function. The essential C-terminal domain (C) encodes the translation termination activity.

Figure 3. [*PSI*$^+$] variants can be distinguished by growth on rich medium (YPD) and by the level of soluble Sup35. A. Indicated strains were struck on rich medium (YPD). Note the difference in color between [*PSI*$^+$] variants ([*PSI*$^+$]^{weak} and [*PSI*$^+$]^{strong}). B. Lysates from indicated [*PSI*$^+$] variants were subjected to differential centrifugation (100,000 x *g*), followed by SDS-PAGE and anti-Sup35 immunoblotting. Note the difference in Sup35 distribution in [*PSI*$^+$] variants. The centrifugation assay was performed by Tricia Serio.

Figure 4. Possible interactions between [*PSI*$^+$] variants and Sup35 prion domain point mutants. Schematic of possible interactions between Sup35 aggregates in the cell (blue) and a plasmid-expressed Sup35 prion domain point mutant (red). The read-through based, colony color phenotype depends on soluble Sup35 levels. The expected colony color phenotypes are shown on the right.

Figure 5. Possible interactions between [*PSI*$^+$] variants. A. Schematic showing that the diploid progeny (symbolized by the clover shape) resulting from a [*PSI*$^+$]^{weak} x [*PSI*$^+$]^{strong} cell cross express the dominant [*PSI*$^+$]^{strong} white colony color phenotype. B. Diagram of possible outcomes of the competition between [*PSI*$^+$]^{weak} and [*PSI*$^+$]^{strong} variants. The variants could continue to co-exist in a mixed cytoplasm (top), the phenotypically dominant [*PSI*$^+$]^{strong} could lead to a loss of the recessive [*PSI*$^+$]^{weak} aggregates (middle), or a novel [*PSI*$^+$] variant can be created as a result of [*PSI*$^+$] variant interaction (bottom). These three possibilities are not mutually exclusive, and it is possible that a combination of two or all three occur during [*PSI*$^+$] variant competition.

Figure 6. The yeast prion cycle depends on several steps. In step one, soluble protein (dark blue rods) is converted into the prion state (dark blue rods with a twist) and

incorporated into prion aggregates (snowflake shape). In step two, prion aggregates are broken up by the action of chaperone proteins in order to generate more surfaces for the conversion of soluble protein into the prion form. Fragmentation of prion aggregates into smaller pieces is also necessary for step three where prion aggregates are transmitted to daughter cells, thereby ensuring stable propagation of the prion phenotype. This diagram was drawn by Tricia Serio and a version of it was published by Pezza and Serio, 2007.

Figure 1.

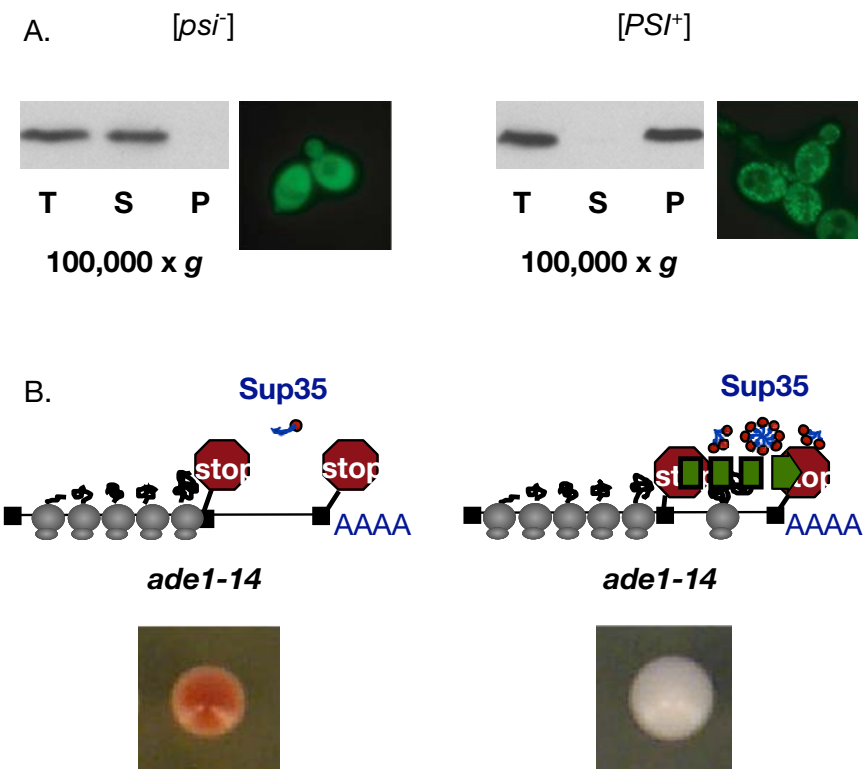
A.
[psi-]
[PSI+]
T S P
100,000 x g
T S P
100,000 x g
B.
Sup35
Sup35
stop
stop
AAAA
AAAA
ade1-14
ade1-14

Figure 2.

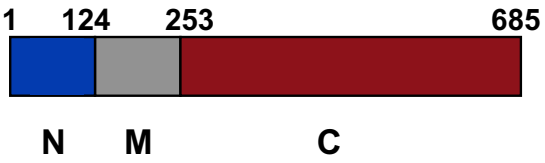

Figure 3.

A.

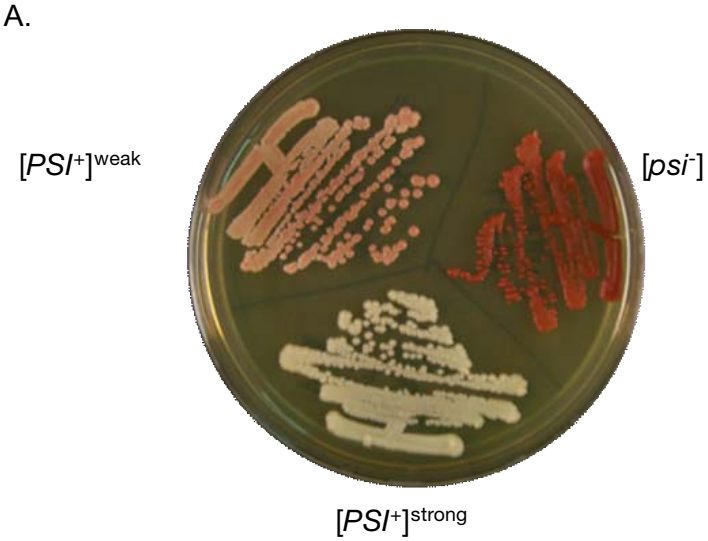

B.

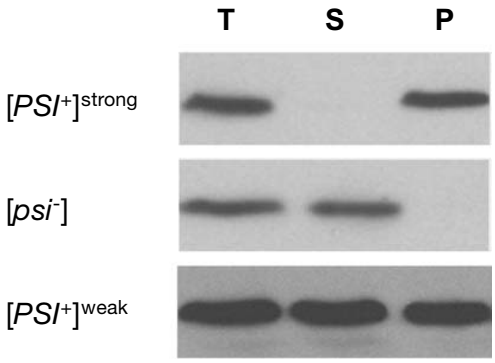

Figure 4.

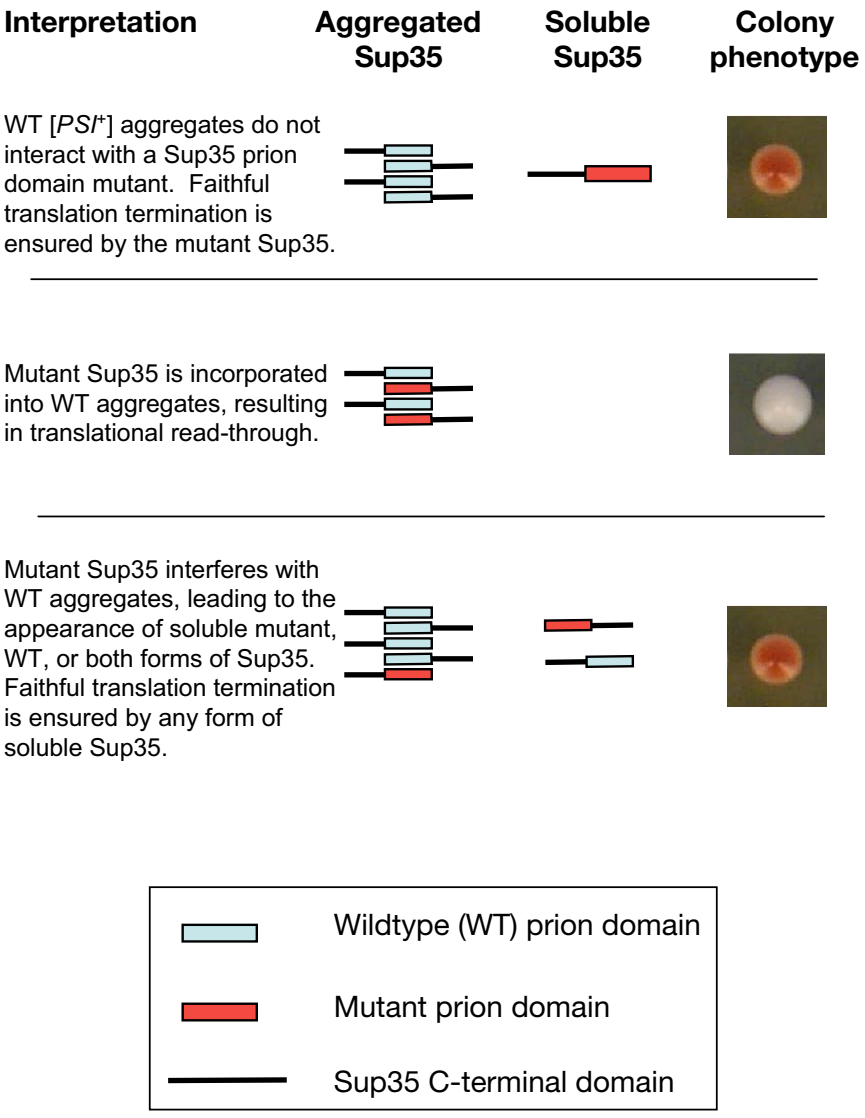
Interpretation
Aggregated Sup35
Soluble Sup35
Colony phenotype
WT [PSI+] aggregates do not interact with a Sup35 prion domain mutant. Faithful translation termination is ensured by the mutant Sup35.
Mutant Sup35 is incorporated into WT aggregates, resulting in translational read-through.
Mutant Sup35 interferes with WT aggregates, leading to the appearance of soluble mutant, WT, or both forms of Sup35. Faithful translation termination is ensured by any form of soluble Sup35.
Wildtype (WT) prion domain
Mutant prion domain
Sup35 C-terminal domain

Figure 5.

A.

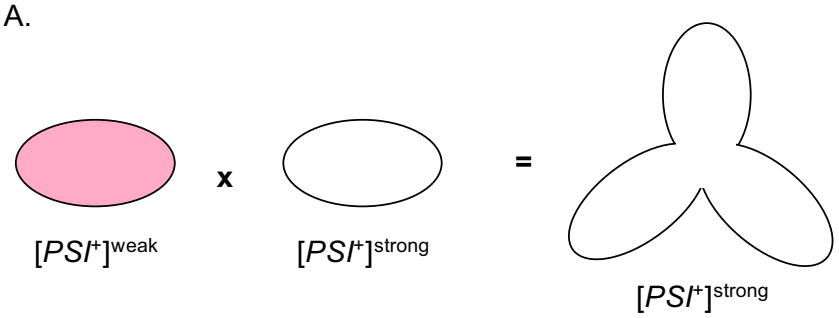

B.

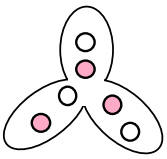

Co-existence of [*PSI*$^{+}$]^{weak} and [*PSI*$^{+}$]^{strong}

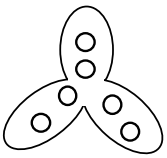

Loss of [*PSI*$^{+}$]^{weak} after competition

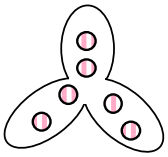

Competition creates a new [*PSI*$^{+}$] variant

Figure 6.

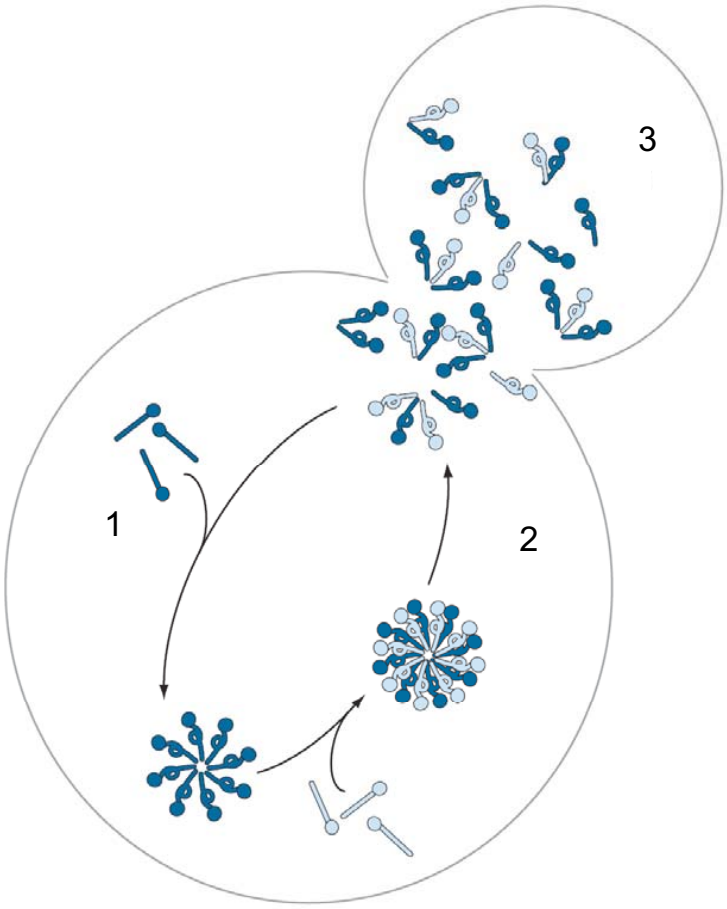

Chapter 2: [PSI^{+}] prion variants co-exist after cytoplasmic mixing

Abstract

Self-propagating prion proteins can exist in a range of heritable forms, or variants, specified by the physical state of the prion protein. Two commonly studied prion variants of the yeast prion protein Sup35 are [*PSI*$^{+}$]^{strong} and [*PSI*$^{+}$]^{weak}. The interaction between these two [*PSI*$^{+}$] variants has been studied previously at the phenotypic level. [*PSI*$^{+}$]^{strong} has been shown to be dominant phenotypically in cell crosses, and the meiotic progeny of a [*PSI*$^{+}$]^{strong} x [*PSI*$^{+}$]^{weak} cross always inherit the dominant [*PSI*$^{+}$]^{strong} phenotype. The proposed mechanism underlying this dominance is a competition for soluble Sup35 substrate [1]. According to this model, the [*PSI*$^{+}$]^{strong} variant more efficiently incorporates newly made Sup35 into the strong prion form, ultimately leading to the loss of the [*PSI*$^{+}$]^{weak} variant. In contrast to this idea, here I report that the [*PSI*$^{+}$]^{strong} and [*PSI*$^{+}$]^{weak} variants can co-exist for many generations after being introduced into the same cytoplasm by cell mating. During this period of co-existence, there is a gradual, increased loss of [*PSI*$^{+}$]^{weak} with each cell generation. These fluctuations in the population, however, cannot be explained by a competition for conversion substrate, as the [*PSI*$^{+}$]^{weak} form constitutes a major fraction of the total protein in some cells. However, modulations in the size of prion complexes by changes in chaperone activity, rates of Sup35 synthesis, and cell division timing, lead to a greater retention of [*PSI*$^{+}$]^{weak} in the population. Together, these observations strongly point to differences in transmission efficiencies between [*PSI*$^{+}$]^{strong} and [*PSI*$^{+}$]^{weak} as a major force impacting the interplay between distinct prion conformers *in vivo*.

Introduction

Prion proteins have the unique ability to exist in multiple physical states that are heritable and that alter cellular phenotype [2-5]. Mammalian prion variants, or distinct conformers of the mammalian prion protein, differ in clinical symptoms such as incubation periods and affected areas of the brain, as well as in their ability to infect multiple species [4, 6-11]. Variants of the yeast prion protein Sup35 also exist, and phenotypic differences between Sup35 conformers can be observed at the colony level by the production of different colored colonies in isogenic yeast [12].

Sup35 is a translation termination factor that can exist in a range of prion forms that compromise its function [5, 13, 14]. Cells that propagate the [*PSI*$^{+}$]^{strong} variant form of Sup35 produce white colonies when grown on rich medium because of high levels of read-through of the *ade1-14* nonsense allele, while the [*PSI*$^{+}$]^{weak} variant produces pink colonies because of intermediate *ade1-14* read-through levels. The white and pink colony color phenotypes result from differences in the amount of soluble, functional Sup35 associated with each [*PSI*$^{+}$] variant. Non-prion [*psi*$^{-}$] cells carrying the *ade1-14* nonsense allele produce red colonies on rich medium because Sup35 is soluble and functional in its non-prion form, resulting in the recognition of the premature stop codon in *ade1-14*, and an accumulation of an adenine biosynthetic intermediate which causes the red colony color [15]. In [*PSI*$^{+}$]^{strong} cells, most Sup35 exists in an aggregated form and its function is compromised [13]. Because of aggregate-associated inactivation of Sup35 in [*PSI*$^{+}$]^{strong} cells, there is read-through of the nonsense *ade1-14* allele, and [*PSI*$^{+}$]^{strong} cells can grow in the absence of adenine and form wildtype-colored white colonies on rich medium. In the [*PSI*$^{+}$]^{weak} variant,

Sup35 is found in both an aggregated and a soluble form resulting in an intermediate level of read-through of *ade1-14*, so [*PSI*$^{+}$]^{weak} cells form pink colonies on rich medium [5, 12].

It is believed that the differences in the amount of soluble Sup35 in [*PSI*$^{+}$]^{strong} and [*PSI*$^{+}$]^{weak} cells are a result of differences between their Sup35 prion aggregates [1, 5, 16-18]. Work from the Weissman lab has shown that *in vitro* polymerization of recombinant Sup35 leads to the formation of fibers, and transformation of yeast with these fibers produces distinct [*PSI*$^{+}$] phenotypes that depend on the conditions under which the fibers were formed [17]. In a parallel study, the King lab showed that [*PSI*$^{+}$] variant aggregates can be purified from cells and used to seed *in vitro* polymerization of recombinant Sup35 fibers [16]. When these recombinant fibers are introduced into yeast, they induce the appearance of the parent [*PSI*$^{+}$] variant that was used to seed *in vitro* recombinant Sup35 polymerization [16]. These two studies have shown that distinct Sup35 conformations produce distinct [*PSI*$^{+}$] variant phenotypes.

In vitro experiments have provided more evidence of the differences in the biophysical properties of [*PSI*$^{+}$] variants. These *in vitro* studies have shown that [*PSI*$^{+}$]^{strong}-like aggregates are slow-growing but extremely brittle, enabling them to be fragmented easily [1]. Frangibility of [*PSI*$^{+}$]^{strong} aggregates leads to efficient generation of new prion aggregate surfaces that can recruit and convert Sup35 to the [*PSI*$^{+}$]^{strong} form, so consequently [*PSI*$^{+}$]^{strong} cells have very little soluble, functional Sup35. In contrast, *in vitro* generated [*PSI*$^{+}$]^{weak}-like aggregates are stable and more resistant to fragmentation, so presumably they cannot generate as many seeding surfaces for the conversion of soluble Sup35 to the [*PSI*$^{+}$]^{weak} state, thereby allowing higher levels of soluble Sup35 in [*PSI*$^{+}$]^{weak} cells [1]. Another

parameter that shows differences between Sup35 aggregates in [*PSI*$^{+}$]^{weak} and [*PSI*$^{+}$]^{strong} cells is aggregate thermodynamic stability [17]. *In vitro* generated [*PSI*$^{+}$]^{weak}-like aggregates require incubation at high temperature before they become denatured and can enter an SDS-PAGE gel [17]. In contrast, *in vitro* generated [*PSI*$^{+}$]^{strong}-like aggregates are less thermodynamically stable and fall apart at lower temperature than [*PSI*$^{+}$]^{weak}-like aggregates. Though these studies were first done with *in vitro* generated Sup35 aggregates, work from the Weissman group and from the Serio lab has confirmed that the thermodynamic stability principle holds true with prion particles from cell lysates: [*PSI*$^{+}$]^{weak} aggregates are more resistant to thermal denaturation than [*PSI*$^{+}$]^{strong} aggregates (Langseth, unpublished) [17].

Differences in frangibility between [*PSI*$^{+}$] variants can have a profound impact on prion phenotype stability. [*PSI*$^{+}$]^{weak} cells with thermodynamically stable Sup35 aggregates tend to lose the prion state much more frequently than [*PSI*$^{+}$]^{strong} cells with frangible, less thermodynamically stable Sup35 aggregates [12]. The connection between Sup35 aggregate frangibility and [*PSI*$^{+}$] phenotype stability is the rate of generation of new prion seeds. Since [*PSI*$^{+}$]^{weak} aggregates are not as efficiently fragmented by Hsp104 as [*PSI*$^{+}$]^{strong} aggregates, [*PSI*$^{+}$]^{weak} cells have fewer prion aggregate seeds that can recruit and convert soluble Sup35 into the prion form [1]. Because of this, the [*PSI*$^{+}$]^{weak} variant is more frequently lost than the [*PSI*$^{+}$]^{strong} variant, leading to the appearance of non-prion [*psi*$^{-}$] cells.

Given the conformational flexibility of prion proteins, different physical forms of the same protein may arise in the same cell and interact with one another. The interplay between prion variants has been studied both in mammals and in yeast. Two well-studied cases of mammalian prion variant interaction examined transmissible mink encephalopathy prion

variants and variants of the sheep disease scrapie. Prion variants of each disease have been shown to affect their variant counterparts adversely: infection with one prion variant somehow blocks subsequent or co-infection by a different conformer of the same prion protein [19-21]. For example, inoculation of mice with the 22A scrapie variant produces a quick onset of disease with characteristic brain lesions (200 day incubation period), while the 22C scrapie variant has a much longer incubation time before disease onset and produces a different pattern of brain lesions (450 day incubation period) [19, 22]. When mice are inoculated with a saline solution control nine weeks before inoculation with the 22A scrapie variant, or with the 22C variant one week prior to injection with 22A, in both cases the 22A agent shows its characteristic quick disease onset and usual pattern of brain lesions [19]. Competition between the two scrapie variants (defined as an increase in incubation time before 22A disease onset) only occurs when the 22C variant is injected five to nine weeks prior to 22A. Competition was manifested as prolonging the onset of 22A disease symptoms by at least 30 days, and the kinetics of incubation period extension caused by scrapie variant competition closely mimic delaying 22A disease onset with decreasing administered doses of 22A in the absence of variant competition [19]. The authors of this study could not deduce whether the delay in disease onset caused by competition between 22C and 22A scrapie agents occurred because of a reduction in scrapie agent titer or because of modification in disease pathogenesis. However, the authors believe that the reason why competition between the 22C and 22A agents only occurs when 22C is given at least a five week head start is because the 22C variant needs more time for replication or processing than the faster-spreading 22A agent. It should also be noted that in all their studies of interaction between scrapie agents, the authors have never found any synergistic interactions between scrapie variants but only competition [19].

A recent study has recapitulated and extended these observations in the model of competition between transmissible mink encephalopathy (TME) variants [23]. This study showed that the competition between TME variants (assayed by extension in disease incubation prior to the onset of symptoms) occurs only when the two competing variants are directed to infect the same population of neurons; if the two variants are targeted to different populations of neurons, there is no extension in disease incubation [23]. When the two variants are directed to infect the same population of neurons, competition between the two is also manifested as a reduction the abundance of variant specific forms of the mammalian prion protein PrP during disease incubation [23]. This reduction in variant-specific forms of PrP does not occur when the two variants are not competing in the same neuronal population.

In addition to showing that TME variants compete only when infecting the same population of cells, this work in the mammalian prion system has demonstrated that the key aspect of mammalian prion variant competition is not whether the two competing variants are administered at the same time (co-infection) or staggered (superinfection). When two mammalian prion variants are administered simultaneously, changing the administered dosage (that is, inoculating a large dose of the slow-replicating variant and a small dose of the fast-replicating variant) will allow the slow variant to establish disease before the fast variant, or even block infection by the fast variant if the two compete for the same replication site in the host [23]. The most important step in the competition between mammalian prion variants appears to be competition for replication in a particular location in the host.

Initial studies of competition between variants of the *S. cerevisiae* prion protein Sup35 reported similar findings in the yeast prion system. The Sup35 [*PSI*$^{+}$]^{strong} variant appears dominant phenotypically over [*PSI*$^{+}$]^{weak} in cell crosses, and the resulting meiotic progeny all inherit the dominant [*PSI*$^{+}$]^{strong} phenotype [24, 25]. This result was interpreted as showing that the competition between [*PSI*$^{+}$] variants leads [*PSI*$^{+}$]^{strong} to eliminate [*PSI*$^{+}$]^{weak}.

The interpretation that [*PSI*$^{+}$]^{strong} is dominant and leads to [*PSI*$^{+}$]^{weak}'s elimination was based on colony color phenotype, which depends on soluble Sup35, but there was no closer examination of Sup35 protein state after competition. It takes about twenty generations for yeast to form a visible colony, so a colony-level assay does not reveal the interplay between [*PSI*$^{+}$] variants in the same cytoplasm.

I suggest that there are at least three possible outcomes to the described competition between [*PSI*$^{+}$] variants. The first outcome is, as suggested above, that competition with [*PSI*$^{+}$]^{strong} leads to the loss or elimination of [*PSI*$^{+}$]^{weak}. The second possibility is that [*PSI*$^{+}$]^{weak} is retained in the cell, but propagated cryptically in the presence of [*PSI*$^{+}$]^{strong}. The third possibility is that the competition between [*PSI*$^{+}$] variants leads to formation of a novel [*PSI*$^{+}$] variant which produces white colonies on rich medium, phenocopying the [*PSI*$^{+}$]^{strong} parent.

The three possibilities outlined above are not mutually exclusive outcomes. It is possible that two or all three mechanisms operate simultaneously when [*PSI*$^{+}$] variants compete. To explore the molecular basis of prion variant competition, I have performed a series of cell

crossing, biochemical and genetic assays to determine the fate of the "recessive" [*PSI*$^{+}$]^{weak} aggregates after competition with [*PSI*$^{+}$]^{strong}.

Results

Sup35 aggregates in [*PSI*$^{+}$]^{weak} x [*PSI*$^{+}$]^{strong} cells differ from parental prion aggregates

To monitor the fate of [*PSI*$^{+}$]^{weak} aggregates after they come into contact with [*PSI*$^{+}$]^{strong} aggregates, I first characterized the physical state of Sup35 aggregates in a cell with a mixed [*PSI*$^{+}$]$^{weak\ x\ strong}$ cytoplasm that was produced by crossing [*PSI*$^{+}$]^{weak} to [*PSI*$^{+}$]^{strong}. One of the most sensitive genetic assays that can distinguish [*PSI*$^{+}$] variants is their interaction with a series of Sup35 prion domain point mutants [26]. In [*PSI*$^{+}$] cells, Sup35 molecules interact through their N-terminal prion domains, and the amino acid sequence of Sup35's prion domain dictates whether a point mutant can join pre-existing Sup35 aggregates (fig. 1) [14, 27]. By introducing a series of plasmid-encoded Sup35 prion domain mutants into a [*PSI*$^{+}$] cell, it is possible to obtain a colony color fingerprint that identifies each [*PSI*$^{+}$] variant uniquely. I decided to test a [*PSI*$^{+}$]$^{weak\ x\ strong}$ cell for its interaction with this series of Sup35 prion domain point mutants to determine if its Sup35 aggregates have changed as a result of variant competition, or whether they consist just of the phenotypically dominant [*PSI*$^{+}$]^{strong} aggregates (fig. 2).

Figure 2 shows that Sup35 aggregates in [*PSI*$^{+}$]$^{weak\ x\ strong}$ cells differ from Sup35 aggregates in the two parents, [*PSI*$^{+}$]^{strong} and [*PSI*$^{+}$]^{weak}, in terms of how each variant interacts with the series of Sup35 mutants. If a Sup35 mutant is unable or has a reduced ability to join one

variant's [*PSI*$^+$] aggregates, red colonies will form on rich medium because the Sup35 mutant will remain soluble and active in translation termination, leading to recognition of the premature stop codon in the *ade1-14* allele and the accumulation of a red adenine biosynthetic intermediate in cells. In contrast, if a Sup35 mutant can join a variant's [*PSI*$^+$] aggregates, the result will be white or pink colonies on rich medium and some degree of growth on medium lacking adenine, as determined by the Sup35 mutant's ability to join [*PSI*$^+$] variant aggregates and thereby dictate the level of soluble Sup35 in the cell. As expected, [*psi*$^-$] control cells remain red on rich medium after interaction with any plasmid-encoded Sup35 molecule (wildtype, N12K, G20D, and G25D) because Sup35 is soluble and functional in [*psi*$^-$] cells, without any Sup35 aggregates to incorporate the Sup35 mutant (fig. 2, row 1). In contrast to [*psi*$^-$], the [*PSI*$^+$]^{weak} variant (fig. 2, row 2) is able to incorporate the G25D mutant into its aggregates, resulting in a pink colony color, but it is unable to incorporate the N12K and G20D mutants, leading to the formation of red colonies on rich medium and no growth on medium lacking adenine. As a control, the [*PSI*$^+$]^{weak} variant incorporates plasmid-encoded wildtype Sup35 molecules into its aggregates (fig. 2, column 1, row 2), producing [*PSI*$^+$]^{weak}'s characteristic pink colonies on rich medium and a very low level of growth on medium lacking adenine. The [*PSI*$^+$]^{strong} variant differs from [*PSI*$^+$]^{weak} in its ability to incorporate Sup35 mutant molecules into its aggregates. For example, [*PSI*$^+$]^{strong} can incorporate the N12K mutant to produce pink colonies on rich medium (fig. 2, row 3, column 2), but the [*PSI*$^+$]^{weak} variant cannot incorporate N12K mutant molecules and therefore produces red colonies on rich medium when exposed to this mutant (fig. 2, row 2, column 2,). Differing abilities between [*PSI*$^+$] variants to incorporate each Sup35 mutant into their respective Sup35 aggregates indicate intrinsic differences between the state of Sup35 aggregates in each [*PSI*$^+$] variant. Comparison of the colony color "fingerprint" of

[*PSI*$^{+}$]^{strong}, [*PSI*$^{+}$]^{weak}, and [*PSI*$^{+}$]$^{weak\ x\ strong}$ reveals that each parent variant and their mixed offspring can be distinguished from the others with this assay. The unique colony color "fingerprint" of [*PSI*$^{+}$]$^{weak\ x\ strong}$ in contrast to each parent indicates that [*PSI*$^{+}$]^{weak} has not simply been lost from the cells upon interaction with [*PSI*$^{+}$]^{strong}. Rather, "recessive" [*PSI*$^{+}$]^{weak} aggregates may persist in competition with [*PSI*$^{+}$]^{strong} aggregates in [*PSI*$^{+}$]$^{weak\ x\ strong}$ cells, with the distinct pattern representing the average of the two forms, or competition between these two variants has produced a novel [*PSI*$^{+}$] variant with a unique colony color fingerprint. It is impossible to distinguish between these possibilities with a genetic colony color assay, and this result does not eliminate the possibility that both outcomes occur during variant competition.

To complement and extend the above approach, I wanted to use a biochemical assay called semi-denaturing detergent agarose gel electrophoresis (SDD-AGE) to determine if I could detect a difference between [*PSI*$^{+}$]$^{weak\ x\ strong}$ and parental Sup35 aggregates. SDD-AGE can distinguish [*PSI*$^{+}$] variants based on the pattern of migration of Sup35 aggregates through an agarose gel and also *via* the level of soluble, monomeric Sup35 associated with each [*PSI*$^{+}$] variant [28]. For example, SDD-AGE resolution of the [*PSI*$^{+}$]^{strong} variant reveals a wide band of high molecular weight Sup35 aggregates and very little or no soluble Sup35 (fig. 3A and 3B, lane 4). In contrast, the [*PSI*$^{+}$]^{weak} variant (fig. 3A and 3B, lane 3) shows an upward shift in the migration of Sup35 aggregates compared to [*PSI*$^{+}$]^{strong}, and a higher level of monomeric Sup35 than in [*PSI*$^{+}$]^{strong}. Lysates from [*psi*$^{-}$] cultures show exclusively monomeric Sup35 (fig. 3A and 3B, lane 2).

Surprisingly, repeated SDD-AGE assays have revealed two distinct outcomes for the Sup35 aggregate profile in [*PSI*$^{+}$]$^{weak\ x\ strong}$ cultures, which were obtained by a cell cross between [*PSI*$^{+}$]^{weak} and [*PSI*$^{+}$]^{strong} (fig. 3A and 3B, lane 1). In one case, the Sup35 aggregate profile in [*PSI*$^{+}$]$^{weak\ x\ strong}$ cells is an intermediate between the two parental Sup35 aggregate profiles because its pattern of Sup35 aggregate migration falls between that of [*PSI*$^{+}$]^{weak} and [*PSI*$^{+}$]^{strong} (fig. 3A). In the second case, Sup35 aggregates from [*PSI*$^{+}$]$^{weak\ x\ strong}$ cultures resemble the dominant [*PSI*$^{+}$]^{strong} profile (fig. 3B). Many repetitions of this experiment have revealed that each outcome occurs in about half of the experiments, despite the highly reproducible pattern observed for either parent. The fact that two distinct results occur with equal chance is consistent with two outcomes to the [*PSI*$^{+}$] variant competition. In the first outcome, [*PSI*$^{+}$]^{weak} aggregates persist in a significant fraction of cells after competition with [*PSI*$^{+}$]^{strong} and cause a change in the Sup35 aggregate profile in [*PSI*$^{+}$]$^{weak\ x\ strong}$ cultures (fig. 3A), or variant competition produces a novel intermediate [*PSI*$^{+}$] variant that changes the Sup35 profile in [*PSI*$^{+}$]$^{weak\ x\ strong}$ cultures. The second SDD-AGE outcome (fig. 3B) shows that [*PSI*$^{+}$]^{weak} aggregates are lost after competition, and that only [*PSI*$^{+}$]^{strong} aggregates remain in [*PSI*$^{+}$]$^{weak\ x\ strong}$ cultures. This inherent fluctuation between two results strongly suggests that a culture of cells arising from a [*PSI*$^{+}$]^{weak} x [*PSI*$^{+}$]^{strong} cell cross is heterogeneous. If this interpretation is correct, distinct [*PSI*$^{+}$] variants should be recoverable from a single culture of this strain.

[*PSI*$^{+}$]^{weak} can be recovered from [*PSI*$^{+}$]$^{weak\ x\ strong}$ cells

To determine whether [*PSI*$^{+}$]^{weak} can be recovered after interaction with [*PSI*$^{+}$]^{strong}, I performed cell crosses between the two variants in order to introduce both types of prion aggregates into the same cell. [*PSI*$^{+}$]^{weak} and [*PSI*$^{+}$]^{strong} cells were crossed on synthetic

complete medium, and nascent diploids were moved to the same medium supplemented with 3mM guanidine hydrochloride (GdnHCl) in order to inhibit Hsp104-dependent fragmentation of Sup35 aggregates. As the nascent zygote divides to form a colony on medium with GdnHCl, pre-existing Sup35 aggregates cannot be fragmented by Hsp104, so they are diluted from mother cells into progeny by cell division, eventually leading to the loss of the prion state and the appearance of [*psi*⁻] cells that do not inherit any [*PSI*⁺] aggregates [29]. I resuspended these zygote-generated colonies in water, and plated them on rich medium (¼ YEPD) where I could score the [*PSI*⁺] phenotype based on colony color. Every cell that does not inherit Sup35 aggregates grows into a single red colony on rich medium, while cells that inherit [*PSI*⁺]^{weak} aggregates form pink colonies and cells that inherit [*PSI*⁺]^{strong} aggregates form white colonies. I counted the number of white [*PSI*⁺]^{strong} colonies and the number of pink [*PSI*⁺]^{weak} colonies recovered from each zygote, and graphed the percent [*PSI*⁺]^{weak} pink colonies recovered out of total [*PSI*⁺] colonies generated by each isolated zygote that was grown on synthetic complete medium with GdnHCl (fig. 4A). To confirm that I had isolated true zygotes and not one of the haploid parents, I verified the ploidy of isolated cells by testing whether they can undergo meiosis and sporulate. In order to verify the [*PSI*⁺] state of scored colonies, I followed a representative sample of isolated white and pink colonies, checking their colony color phenotype against [*PSI*⁺]^{weak} and [*PSI*⁺]^{strong} controls. I also eliminated or cured [*PSI*⁺] in the isolates by overexpression of Hsp104, then reintroduced both [*PSI*⁺]^{weak} and [*PSI*⁺]^{strong} by Sup35 overexpression, and finally cured these isolates again with GdnHCl treatment (fig. 5). All of these manipulations that eliminate and induce [*PSI*⁺] without any alterations in the genetic make-up of the isolated cells show that I did not isolate a mutation that affects colony color, but that I was following the Sup35 protein state-dependent [*PSI*⁺] phenotype.

Each bar in figure 4A represents the percent [*PSI*$^{+}$]^{weak} colonies of total recovered [*PSI*$^{+}$] colonies from a single zygote formed by a cross between [*PSI*$^{+}$]^{weak} and [*PSI*$^{+}$]^{strong} cells. As previously noted, individual cells contain a range of prion complexes, leading to variability in the number of recovered [*PSI*$^{+}$] colonies [1, 30]. Despite this variability, the assay clearly allows the recovery of specific variants from individual starting cells. For example, both [*PSI*$^{+}$]^{strong} and [*PSI*$^{+}$]^{weak} strains give rise to almost exclusively homotypic progeny, with only occasional changes in state (fig. 4A and B). When diploids formed from crosses [*PSI*$^{+}$]^{strong} and [*PSI*$^{+}$]^{weak} strains were subjected to the same analysis, [*PSI*$^{+}$]^{weak} colonies were recovered from a majority of the cells, indicating that this "recessive" variant persists in the presence of the [*PSI*$^{+}$]^{strong} form. For many of these cells, the [*PSI*$^{+}$]^{weak} form constituted >10% of the total prion population. This observation is particularly striking given the fact that the readout of this assay likely under-represents the actual proportion of preserved [*PSI*$^{+}$]^{weak} heritable aggregates from a [*PSI*$^{+}$]^{strong} x [*PSI*$^{+}$]^{weak} cell cross. Specifically, [*PSI*$^{+}$]^{weak} colonies can arise only when a progeny cell inherits just [*PSI*$^{+}$]^{weak} aggregates, whereas those cells that inherited a mixture of the forms will display the [*PSI*$^{+}$]^{strong} phenotype. Thus, in contrast to the rapid conversion of soluble Sup35 to the prion form in [*PSI*$^{+}$] x [*psi*$^{-}$] crosses, a significant portion of the originating [*PSI*$^{+}$]^{weak} form persists upon mixing with [*PSI*$^{+}$]^{strong} [31].

[*PSI*$^{+}$]^{weak} replicates but is lost over time from a mixed population of prion forms

In addition to the population of cells retaining [*PSI*$^{+}$]^{weak} when [*PSI*$^{+}$]^{strong} and [*PSI*$^{+}$]^{weak} parents are mated, a fraction of cells only yield [*PSI*$^{+}$]^{strong} colonies after inhibition of Hsp104 with GdnHCl (fig. 4A). This observation, along with variability in SDD-AGE profiles, suggest that [*PSI*$^{+}$]$^{weak\ x\ strong}$ strains are heterogenous. To explore the fluctuations in prion conformers present in [*PSI*$^{+}$]$^{weak\ x\ strong}$ strains, I varied the period of growth after mating

before inhibiting Hsp104 and allowing existing prion complexes to be diluted by cell division.

Toward this end, I crossed [*PSI*$^{+}$]^{weak} cells to [*PSI*$^{+}$]^{strong} on rich medium (YPD) and allowed the isolated zygotes to grow for either for 14 or more than 80 generations on rich medium. Next, I moved some progeny of these zygotes to synthetic complete medium with 3mM GdnHCl and allowed single isolated cells to grow into colonies, diluting [*PSI*$^{+}$] aggregates from the original cell into daughters by division. These colonies were plated on rich medium where I could score [*PSI*$^{+}$] state by colony color, as described above. As was the case for zygotes moved immediately to media containing GdnHCl, [*PSI*$^{+}$]^{weak} colonies were again recovered from cells many generations after mixing of the variants (fig. 4A). Notably, similar numbers of [*PSI*$^{+}$]^{weak} colonies were isolated from zygotes directly, or from their distant progeny that retain this [*PSI*$^{+}$] variant form.

While those cells retaining [*PSI*$^{+}$]^{weak} did so to similar degrees regardless of generations of growth, the fraction of the population from which this form could no longer be recovered increased with generations. For example, ~27% of isolated zygotes failed to generate [*PSI*$^{+}$]^{weak} colonies, while ~31% and ~65% of zygotes failed to yield [*PSI*$^{+}$]^{weak} colonies after 14 and 80 generations of growth, respectively (fig. 6). These observations suggest that cell division plays an important role in the interplay between distinct prion conformers *in vivo*.

There are several possible reasons for the cell division-dependent loss of [*PSI*$^{+}$]^{weak} that I have observed in the above experiments. One possible explanation for the loss of [*PSI*$^{+}$]^{weak} aggregates is that they cannot compete for the conversion of soluble Sup35 to their prion

variant form in the presence of [*PSI*$^{+}$]^{strong} aggregates. If [*PSI*$^{+}$]^{weak} aggregates cannot replicate in the presence of [*PSI*$^{+}$]^{strong} aggregates, I would expect to see a cell division-dependent loss of [*PSI*$^{+}$]^{weak} as the original [*PSI*$^{+}$]^{weak} aggregates from the parent cell dilute out of the progeny cell population with each generation. This explanation can be ruled out because I see the sustained persistence of [*PSI*$^{+}$]^{weak} aggregates after many cell division cycles (at least 80 cell generations, fig. 4A), and the cells that retain [*PSI*$^{+}$]^{weak} aggregates do so in roughly equal proportions regardless of the number of cell division cycles during which [*PSI*$^{+}$]^{strong} and [*PSI*$^{+}$]^{weak} have been competing (fig. 4A). This retention of similar proportions of [*PSI*$^{+}$]^{weak} aggregates after many generations suggests that [*PSI*$^{+}$]^{weak} aggregates must be able to replicate in the presence of [*PSI*$^{+}$]^{strong}. Therefore, other explanations for the cell division-dependent loss of [*PSI*$^{+}$]^{weak} must be considered. Previous work from the Serio lab has highlighted the role of Hsp104 in [*PSI*$^{+}$] aggregate fragmentation and in the transmission of [*PSI*$^{+}$] aggregates to daughter cells, so I wanted to determine if Hsp104 plays a role in the observed cell division-dependent loss of [*PSI*$^{+}$]^{weak}.

Changes in Hsp104-dependent fragmentation of prion complexes implicate transmission to daughter cells as the key event in variant competition

To explore the role of Hsp104 in variant competition, I repeated the same [*PSI*$^{+}$]^{weak} x [*PSI*$^{+}$]^{strong} cell cross described in the previous section, except that this time cells were mated on synthetic complete medium with 3mM GdnHCl in order to inhibit [*PSI*$^{+}$] aggregate remodeling from the beginning of the mating reaction (fig. 4A). Isolated zygotes were allowed to form colonies on the synthetic complete medium with 3mM GdnHCl, which were resuspended in water and plated on rich medium, then scored for [*PSI*$^{+}$] state as described in the previous section. Under these conditions, there is again variability in the

total proportion of recovered [*PSI*$^{+}$]^{weak} cells, but, in general, the percentage of recovered [*PSI*$^{+}$]^{weak} colonies for each zygote retaining this form is similar in the presence or absence of Hsp104 activity.

However, when the proportion of cells that have lost [*PSI*$^{+}$]^{weak} are compared, I noted that fewer cells lose [*PSI*$^{+}$]^{weak} when Hsp104 is inhibited by GdnHCl and [*PSI*$^{+}$] aggregates are not fragmented (fig. 6, column 2), suggesting that differential [*PSI*$^{+}$] aggregate fragmentation could be at the root of competition between [*PSI*$^{+}$] variants. Consistent with this idea, previous studies from the Weissman group have demonstrated that [*PSI*$^{+}$]^{weak}-like aggregates are more stable and more resistant to fragmentation than [*PSI*$^{+}$]^{strong}-like aggregates *in vitro* [1].

To further explore the relationship between Hsp104-dependent fragmentation of prion complexes and prion variant competition, I developed a strategy to alter the size distribution of prion complexes. At steady-state, the distribution of sizes of prion complexes is dependent on the rate of synthesis of Sup35, the rate of fragmentation of prion complexes by Hsp104, and the cell division rate. I reasoned that by inhibiting new Sup35 synthesis under conditions of cell cycle arrest, Hsp104 would continue to act on the existing complexes, mimicking an increased rate of fragmentation.

Toward this end, I incubated zygotes, auxotrophic for histidine, on minimal media lacking histidine for a period of 24 hours. Under these conditions of amino acid starvation, the cells failed to divide (data not shown), and new protein synthesis was presumably inhibited or greatly reduced, as the steady-state levels of Sup35 did not increase under these conditions (fig. 8). Consistent with the prediction that these conditions would mimick an increased rate

of prion complex fragmentation, the average number of heritable Sup35 aggregates in each zygote compared to zygotes that were never subjected to amino acid starvation increased, as assessed by the number of [*PSI*$^+$] cells recovered after moving the zygotes from media lacking histidine to complete media supplemented with GdnHCl (fig. 7).

When I compare the percent of cells that have lost [*PSI*$^+$]^{weak} aggregates from zygotes that were mated on complete medium and allowed to divide for 24 hours to those that were arrested by amino acid starvation, a greater proportion of cells retain [*PSI*$^+$]^{weak} under the latter condition (fig. 6). These observations again highlight the important role of aggregate fragmentation in prion variant competition.

The [*PSI*$^+$]^{strong} phenotype is not immediately established in [*PSI*$^+$]^{weak} x [*PSI*$^+$]^{strong} zygotes

Though [*PSI*$^+$]^{strong} dominates phenotypically over [*PSI*$^+$]^{weak} at the colony level after 20 generations of growth, it is unknown how quickly this phenotypic dominance is established. The Serio lab has shown previously that [*PSI*$^+$]^{strong} confers an immediate (within a cell cycle) phenotypic switch when crossed to [*psi*$^-$] cells [31], so I wanted to test if [*PSI*$^+$]^{strong} establishes a dominance over [*PSI*$^+$]^{weak} equally quickly. This assay takes advantage of the [*PSI*$^+$]^{strong}-dependent read-through phenotype. Mutant *ade1-14* [*PSI*$^+$]^{strong} cells can grow in the absence of adenine, while [*psi*$^-$] and [*PSI*$^+$]^{weak} cannot grow without adenine due to higher levels of soluble, functional Sup35. Soluble Sup35 is able to fulfill its function as a translation termination factor, so cells with soluble Sup35 ([*psi*$^-$] and [*PSI*$^+$]^{weak} cells) recognize the premature stop codon in the *ade1-14* allele, the Ade1 protein is not made, and [*psi*$^-$] and [*PSI*$^+$]^{weak} cells cannot grow in the absence of adenine. Consequently, zygotes formed by

crossing [*psi*⁻] to [*psi*⁻] cannot grow on media lacking adenine, while zygotes from [*PSI*⁺]^{strong} x [*psi*⁻] grow robustly on the same medium.

To determine the kinetics of [*PSI*⁺]^{strong} phenotypic dominance, I monitored the appearance of adenine prototrophy in [*PSI*⁺]^{weak} x [*PSI*⁺]^{strong} zygotes. If these zygotes can grow in the absence of adenine, then [*PSI*⁺]^{strong} must establish its phenotypic dominance immediately. However, if these zygotes cannot grow in the absence of adenine, then [*PSI*⁺]^{weak} and its associated pool of soluble Sup35 must remain in the zygote at some equilibrium, arguing that [*PSI*⁺]^{strong} establishes its phenotypic dominance after more than one cell division cycle.

I set up a series of cell crosses between wildtype [*psi*⁻] or wildtype [*PSI*⁺]^{weak} with Δ*ade1* [*PSI*⁺]^{strong} or Δ*ade1* [*psi*⁻] (fig. 9). Since the [*PSI*⁺]^{strong} cells in these cell crosses carry the Δ*ade1* deletion, no haploid mating partner in this experiment is able to grow in the absence of adenine. However, I expect that zygotes formed in control cell crosses between Δ*ade1* [*PSI*⁺]^{strong} and wildtype [*psi*⁻] will be able to grow robustly on medium without adenine as was shown previously because the wildtype [*psi*⁻] haploid mating partner will provide an *ade1-14* allele, while [*PSI*⁺]^{strong} aggregates from the other mating partner will read through this allele, allowing synthesis of the Ade1 protein and growth on medium lacking adenine [31]. As a positive control, all cell crosses were grown on complete medium with adenine to show that any cell cross can grow when adenine is available (fig. 9, right column).

Figure 9 shows the results of all four cell crosses. All four types of zygotes can grow on non-selective complete medium with adenine, as expected (fig. 9, right column). [*psi*⁻] x [*psi*⁻] and [*psi*⁻] x [*PSI*⁺]^{weak} zygotes cannot grow in the absence of adenine due to their soluble

Sup35 levels, while [*PSI*$^{+}$]^{strong} x [*psi*$^{-}$] zygotes grow robustly in the absence of adenine, as expected (fig. 9, left column). The surprising result is that [*PSI*$^{+}$]^{strong} x [*PSI*$^{+}$]^{weak} zygotes cannot grow in the absence of adenine, suggesting that [*PSI*$^{+}$]^{strong} does not establish an immediate phenotypic dominance as it does when mixed with a soluble pool of Sup35 in [*psi*$^{-}$] cells (fig. 9, left column). This experiment suggests that the [*PSI*$^{+}$]^{weak}-associated pool of soluble Sup35 can persist in cells with a mix of [*PSI*$^{+}$]^{weak} and [*PSI*$^{+}$]^{strong} aggregates, and that the [*PSI*$^{+}$]^{weak}-derived pool of soluble Sup35 is not immediately inactivated by the presence of [*PSI*$^{+}$]^{strong} aggregates.

Discussion

In this study I have shown that the [*PSI*$^{+}$]^{weak} prion variant persists during competition with [*PSI*$^{+}$]^{strong} and can be re-isolated from cells that are the progeny of a cross between the two [*PSI*$^{+}$] variants. Though [*PSI*$^{+}$]^{weak} is retained by a large fraction of cells during competition with [*PSI*$^{+}$]^{strong}, the proportion of cells that lose [*PSI*$^{+}$]^{weak} increases with cell generations. If [*PSI*$^{+}$]^{weak} persists in some fraction of cells after competition with [*PSI*$^{+}$]^{strong}, why is [*PSI*$^{+}$]^{weak} lost over time with increasing cell division cycles?

One reason why [*PSI*$^{+}$]^{weak} is lost over time is that [*PSI*$^{+}$] aggregate fragmentation by Hsp104 plays a key role in the competition between [*PSI*$^{+}$] variants. I have shown that if Hsp104's fragmentation of [*PSI*$^{+}$] aggregates is blocked when [*PSI*$^{+}$]^{strong} is crossed to [*PSI*$^{+}$]^{weak}, a greater proportion of cells retain [*PSI*$^{+}$]^{weak} than when Hsp104 is allowed to fragment [*PSI*$^{+}$] aggregates for just a single cell cycle (fig. 6).

Why does prion complex fragmentation alter the interplay between prion variants *in vivo*? Previous studies suggest that differences in fragmentation rates of prion variants lead to differences in the number of prion complexes, and it is this parameter that determines whether a given variant will persist under competitive conditions. Those variants with increased rates of fragmentation will produce more prion templates within a given cell cycle, allowing this form to outcompete others for the incorporation of newly made Sup35. Such a scenario implies that the slower replicating form will eventually be diluted out by cell division. However, when $[PSI^+]^{strong\ x\ weak}$ zygotes are isolated in the presence of GdnHCl, $[PSI^+]^{weak}$ is retained in a greater proportion of the zygotes than in those isolated in the absence of GdnHCl (fig. 6). Curiously these two cell mating conditions do not differ in the number of times the nascent zygotes divided before $[PSI^+]^{weak}$ loss was assessed, but rather, only in whether Hsp104 could fragment $[PSI^+]$ aggregates during zygote formation, an observation that is inconsistent with the dilution model.

In addition to generating new templates for prion conversion, fragmentation of $[PSI^+]$ aggregates by Hsp104 is necessary for efficient transmission into daughter cells [29]. Thus, the progressive loss of $[PSI^+]^{weak}$ from cells containing a mixture of prion forms could arise from a differential rate of transfer of exiting prion complexes to daughter cells. Consistent with this idea, work from the Serio lab shows that $[PSI^+]^{weak}$ aggregates do not move into daughter cells efficiently when compared with the movement of $[PSI^+]^{strong}$ aggregates, and $[PSI^+]^{weak}$ mother cells preferentially retain the overwhelming majority of Sup35 aggregates instead of passing them on to daughter cells (Derdowski, unpublished). In this assay, daughter buds of $[PSI^+]$ cells expressing Sup35-GFP were continuously bleached while the

loss of fluorescence from the mother cell was monitored. The length of time it takes to lose fluorescent signal in the mother cell is an indication of how quickly [*PSI*$^{+}$] complexes move from the mother into the daughter. This assay shows that [*PSI*$^{+}$]^{strong} complexes move into daughter cells more rapidly than [*PSI*$^{+}$]^{weak} complexes. Furthermore, [*PSI*$^{+}$]^{weak} mothers retain a higher proportion of Sup35 complexes than [*PSI*$^{+}$]^{strong} mothers instead of transmitting them to daughter cells. This is indicated by the fact that [*PSI*$^{+}$]^{strong} mother cells eventually lose Sup35-GFP signal during the course of the assay, but [*PSI*$^{+}$]^{weak} mothers do not lose the Sup35-GFP signal completely.

Varying the length of time that [*PSI*$^{+}$] complexes were fragmented by Hsp104 increased the rate of [*PSI*$^{+}$]^{weak} retention during competition with [*PSI*$^{+}$]^{strong}. Specifically, both a decrease in the length of time that Hsp104 fragmented prion complexes, and an increase in the length of time that Hsp104 fragmented prion complexes allowed more cells to retain [*PSI*$^{+}$]^{weak}. The decrease in Hsp104 activity time helped [*PSI*$^{+}$]^{weak} compete better because it also blocked [*PSI*$^{+}$]^{strong} complex fragmentation. Because of this, the relative number of [*PSI*$^{+}$]^{strong} complexes in proportion to [*PSI*$^{+}$]^{weak} complexes in the cell was smaller, so a greater number of progeny cells could inherit [*PSI*$^{+}$]^{weak}. An increase in Hsp104 fragmentation of prion complexes also helped [*PSI*$^{+}$]^{weak} to compete better with [*PSI*$^{+}$]^{strong}, but probably through a different mechanism. Allowing Hsp104 to fragment [*PSI*$^{+}$] aggregates in the absence of cell division and in the absence of new Sup35 to join [*PSI*$^{+}$] aggregates causes [*PSI*$^{+}$] aggregates to become smaller and to increase in number. The reduction in [*PSI*$^{+}$]^{weak} aggregate size under these conditions probably improved its mobility into daughter cells, allowing more cells to inherit [*PSI*$^{+}$]^{weak} aggregates. The increased rate of recovery of [*PSI*$^{+}$]^{weak} under these

conditions may also be explained by the fact that the number of [*PSI*$^{+}$]^{weak} aggregates had increased, so more cells could inherit the [*PSI*$^{+}$]^{weak} variant.

The most surprising result in this study is that [*PSI*$^{+}$]^{strong} does not establish immediate phenotypic dominance over [*PSI*$^{+}$]^{weak} when the two variants are introduced into the same cytoplasm by cell crossing. There are at least two possible explanations for this. One possibility is that [*PSI*$^{+}$]^{weak}'s soluble pool of Sup35 is somehow protected from joining [*PSI*$^{+}$]^{strong} aggregates in the zygote formed by crossing the two variants. The second possibility is that there are not enough [*PSI*$^{+}$]^{strong} aggregates in the zygote to recruit and convert soluble Sup35 from [*PSI*$^{+}$]^{weak} into their [*PSI*$^{+}$]^{strong} form, so a soluble pool of Sup35 remains in the zygote.

One possible explanation for the protection of soluble Sup35 from [*PSI*$^{+}$]^{weak} cells from conversion into the [*PSI*$^{+}$]^{strong} form is that soluble Sup35 in [*PSI*$^{+}$]^{weak} cells is composed of monomeric soluble Sup35, but that this soluble Sup35 has assumed a prion domain fold that is more compatible with [*PSI*$^{+}$]^{weak} than with [*PSI*$^{+}$]^{strong}, so that soluble Sup35 from [*PSI*$^{+}$]^{weak} cells cannot readily join [*PSI*$^{+}$]^{strong} aggregates. If this is true, then [*PSI*$^{+}$]^{strong} relies on cell division and the accompanying decrease in the inheritance of [*PSI*$^{+}$]^{weak} aggregates to become phenotypically dominant.

Another possible explanation for the failure of the soluble Sup35 pool from [*PSI*$^{+}$]^{weak} cells to be recruited by [*PSI*$^{+}$]^{strong} aggregates is that there may not be enough [*PSI*$^{+}$]^{strong} aggregate templates to convert all soluble Sup35 into the prion form. It is possible that the establishment of the [*PSI*$^{+}$]^{strong} phenotype when [*PSI*$^{+}$]^{strong} x [*psi*$^{-}$] cells are crossed requires a

few cycles of Hsp104 activity. When [*PSI*$^{+}$]^{strong} x [*psi*$^{-}$] cells are crossed, [*PSI*$^{+}$]^{strong} aggregates grow large because of the influx of soluble Sup35, and once they reach a certain size they are recognized and fragmented by Hsp104, thereby creating more [*PSI*$^{+}$]^{strong} templates that can recruit any remaining soluble Sup35. In contrast, in a [*PSI*$^{+}$]^{strong} x [*PSI*$^{+}$]^{weak} cell cross, there is less soluble Sup35 that can join [*PSI*$^{+}$]^{strong} aggregates. Because of this, [*PSI*$^{+}$]^{strong} aggregates do not become large enough to be recognized and fragmented by Hsp104, so the number of [*PSI*$^{+}$]^{strong} aggregate templates does not increase, and some residual soluble pool of Sup35 may remain in the cell.

Methods

Plasmid construction

Sup35 prion domain point mutant plasmids were kindly provided by Dr. Chih-Yen King, Institute of Molecular Biology, Academia Sinica, Taiwan, R.O.C., but they were modified to include the KanMX4 cassette. The KanMX4 cassette was PCR amplified from the pFA6a-KanMx4 vector, with added BstBI ends (forward primer: ttcgaagatctgtttagcttgcc, reverse primer: ttcgaactggatggcggcgttag), then cloned into the BstBI site in the *URA3* marker in the original plasmids [32].

Strain construction

All strains are derivatives of 74D-694 (*ade 1-14 trp 1-289 his3Δ200, ura3-52 leu2-3,112*) [15]. [*PSI*$^+$] strains were converted to [*psi*$^-$] state by growth on YPD + 3mM guanidine hydrochloride, followed by colony purification on YPD, unless indicated otherwise [33]. [*PSI*$^+$] was also eliminated by overexpression of Hsp104 from P_{GPD} on a 2μ plasmid (p2HG104).

Protein analysis

Sup35 protein aggregates were analyzed by semi-denaturing detergent agarose gel electrophoresis (SDD-AGE) essentially as described, except that the lysis buffer contained 10 mM NaPi (pH 7.5), 100 mM NaCl, 1 mM DTT, 0.48 mg/mL pefabloc, and 0.005 mg/mL pepstatin [28, 34]. Immunoblotting was performed as described previously [13]. Anti-Sup35 western blots were quantitated using ImageJ software from the NIH. SDS-PAGE followed by immunoblotting was done as described previously [13], but cell lysates

were prepared as described in [35]. For SDS-PAGE, cells were grown in YPAD into exponential phase, then washed and kept for 22 hours in synthetic complete medium with 4% dextrose and 2.5 mM adenine, or kept for 22 hours in synthetic medium lacking histidine with 4% dextrose with and without 3mM guanidine hydrochloride (GdnHCl).

Growth conditions for cell crosses

Liquid cultures of *MAT*a and *MAT*α were grown overnight in YPAD so they were in exponential phase for mating (OD_{600} 0.1 – 0.6). Cells were collected by centrifugation, washed once in sterile dH_2O, and then mixed on solid complete medium containing 4% dextrose and 2.5 mM adenine. For the condition where aggregate remodeling was inhibited from the beginning of mating reaction, cells were mixed on solid complete medium containing 4% dextrose, 2.5 mM adenine and 3 mM GdnHCl. In conditions where cell growth was inhibited for 24 hours, cells were mated on synthetic complete medium described above, then zygotes were moved to solid synthetic medium lacking histidine with 4% dextrose. For all conditions, isolated zygotes were then grown into microcolonies on solid complete medium containing 4% dextrose, 2.5 mM adenine and 3 mM GdnHCl for 1-2 days at 30°C. Resulting colonies were punched out of the agar, resuspended in water and plated on ¼ YEPD where propagon counts were scored as described previously [30]. [*PSI*$^+$] status and phenotype was confirmed by comparing the colony color of a representative number of isolates with [*PSI*$^+$]^{weak} and [*PSI*$^+$]^{strong} controls, and by conversion to [*psi*$^-$] state by guanidine hydrochloride treatment. Diploid state after cell crosses was confirmed by sporulation. To test variant zygote growth in the absence of adenine, cells were grown and mated as described in [31].

Imaging and digital processing

Images of zygotes and microcolonies were captured as described previously [31].

Acknowledgements

I would like to thank Dr. C. King for kindly providing Sup35 prion domain point mutant plasmids, all members of the Serio and Laney labs for helpful discussions throughout the course of this project, and Dr. T. Serio for making the Δ*ade1* mutants.

References:

1. Tanaka, M., et al., *The physical basis of how prion conformations determine strain phenotypes.* Nature, 2006. **442**(7102): p. 585-9.
2. Fraser, H. and A.G. Dickinson, *Scrapie in mice. Agent-strain differences in the distribution and intensity of grey matter vacuolation.* J Comp Pathol, 1973. **83**(1): p. 29-40.
3. Bessen, R.A. and R.F. Marsh, *Distinct PrP properties suggest the molecular basis of strain variation in transmissible mink encephalopathy.* J Virol, 1994. **68**(12): p. 7859-68.
4. Bruce, M., et al., *Transmission of bovine spongiform encephalopathy and scrapie to mice: strain variation and the species barrier.* Philos Trans R Soc Lond B Biol Sci, 1994. **343**(1306): p. 405-11.
5. Zhou, P., et al., *The yeast non-Mendelian factor [ETA+] is a variant of [PSI+], a prion-like form of release factor eRF3.* Embo J, 1999. **18**(5): p. 1182-91.
6. Fraser, H., et al., *Transmission of feline spongiform encephalopathy to mice.* Vet Rec, 1994. **134**(17): p. 449.
7. Collinge, J., et al., *Molecular analysis of prion strain variation and the aetiology of 'new variant' CJD.* Nature, 1996. **383**(6602): p. 685-90.
8. Foster, J.D., et al., *Detection of BSE infectivity in brain and spleen of experimentally infected sheep.* Vet Rec, 1996. **138**(22): p. 546-8.
9. Bruce, M.E., et al., *Transmissions to mice indicate that 'new variant' CJD is caused by the BSE agent.* Nature, 1997. **389**(6650): p. 498-501.
10. Hill, A.F., et al., *The same prion strain causes vCJD and BSE.* Nature, 1997. **389**(6650): p. 448-50, 526.
11. Wadsworth, J.D., et al., *Human prion protein with valine 129 prevents expression of variant CJD phenotype.* Science, 2004. **306**(5702): p. 1793-6.
12. Derkatch, I.L., et al., *Genesis and variability of [PSI] prion factors in Saccharomyces cerevisiae.* Genetics, 1996. **144**(4): p. 1375-86.
13. Patino, M.M., et al., *Support for the prion hypothesis for inheritance of a phenotypic trait in yeast.* Science, 1996. **273**(5275): p. 622-6.
14. Paushkin, S.V., et al., *Propagation of the yeast prion-like [psi+] determinant is mediated by oligomerization of the SUP35-encoded polypeptide chain release factor.* Embo J, 1996. **15**(12): p. 3127-34.
15. Chernoff, Y.O., et al., *Role of the chaperone protein Hsp104 in propagation of the yeast prion-like factor [psi+].* Science, 1995. **268**(5212): p. 880-4.
16. King, C.Y. and R. Diaz-Avalos, *Protein-only transmission of three yeast prion strains.* Nature, 2004. **428**(6980): p. 319-23.
17. Tanaka, M., et al., *Conformational variations in an infectious protein determine prion strain differences.* Nature, 2004. **428**(6980): p. 323-8.
18. Toyama, B.H., et al., *The structural basis of yeast prion strain variants.* Nature, 2007. **449**(7159): p. 233-7.
19. Dickinson, A.G., et al., *Competition between different scrapie agents in mice.* Nat New Biol, 1972. **237**(77): p. 244-5.
20. Dickenson, A.G., et al., *Extraneural competition between different scrapie agents leading to loss of infectivity.* Nature, 1975. **253**(5492): p. 556.

21. Bartz, J.C., J.M. Aiken, and R.A. Bessen, *Delay in onset of prion disease for the HY strain of transmissible mink encephalopathy as a result of prior peripheral inoculation with the replication-deficient DY strain.* J Gen Virol, 2004. **85**(Pt 1): p. 265-73.
22. Bruce, M.E., et al., *The disease characteristics of different strains of scrapie in Sinc congenic mouse lines: implications for the nature of the agent and host control of pathogenesis.* J Gen Virol, 1991. **72 (Pt 3)**: p. 595-603.
23. Bartz, J.C., et al., *Prion interference is due to a reduction in strain-specific PrPSc levels.* J Virol, 2007. **81**(2): p. 689-97.
24. Bradley, M.E., et al., *Interactions among prions and prion "strains" in yeast.* Proc Natl Acad Sci U S A, 2002. **99 Suppl 4**: p. 16392-9.
25. Bradley, M.E. and S.W. Liebman, *Destabilizing interactions among [PSI(+)] and [PIN(+)] yeast prion variants.* Genetics, 2003. **165**(4): p. 1675-85.
26. King, C.Y., *Supporting the structural basis of prion strains: induction and identification of [PSI] variants.* J Mol Biol, 2001. **307**(5): p. 1247-60.
27. Derkatch, I.L., et al., *The PNM2 mutation in the prion protein domain of SUP35 has distinct effects on different variants of the [PSI+] prion in yeast.* Curr Genet, 1999. **35**(2): p. 59-67.
28. Kryndushkin, D.S., et al., *Yeast [PSI+] prion aggregates are formed by small Sup35 polymers fragmented by Hsp104.* J Biol Chem, 2003. **278**(49): p. 49636-43.
29. Satpute-Krishnan, P., S.X. Langseth, and T.R. Serio, *Hsp104-dependent remodeling of prion complexes mediates protein-only inheritance.* PLoS Biol, 2007. **5**(2): p. e24.
30. Cox, B., F. Ness, and M. Tuite, *Analysis of the generation and segregation of propagons: entities that propagate the [PSI+] prion in yeast.* Genetics, 2003. **165**(1): p. 23-33.
31. Satpute-Krishnan, P. and T.R. Serio, *Prion protein remodelling confers an immediate phenotypic switch.* Nature, 2005. **437**(7056): p. 262-5.
32. Wach, A., et al., *New heterologous modules for classical or PCR-based gene disruptions in Saccharomyces cerevisiae.* Yeast, 1994. **10**(13): p. 1793-808.
33. Tuite, M.F., C.R. Mundy, and B.S. Cox, *Agents that cause a high frequency of genetic change from [psi+] to [psi-] in Saccharomyces cerevisiae.* Genetics, 1981. **98**(4): p. 691-711.
34. Bagriantsev, S.N., V.V. Kushnirov, and S.W. Liebman, *Analysis of amyloid aggregates using agarose gel electrophoresis.* Methods Enzymol, 2006. **412**: p. 33-48.
35. Kushnirov, V.V., *Rapid and reliable protein extraction from yeast.* Yeast, 2000. **16**(9): p. 857-60.

Figure Captions

Figure 1. Sup35 molecules in [*PSI*$^+$] cells interact through their N-terminal prion regions. The C-terminal region of Sup35 is not necessary for prion function, but it is the region that functions in translation termination.

Figure 2. Interaction between Sup35 prion domain point mutants and [*PSI*$^+$] variants. Colony color on rich medium is determined by the amount of soluble Sup35. Strains were transformed with the indicated Sup35 prion domain point mutant plasmids (amino acid substitutions indicated) or a control wildtype Sup35 (WT), as noted. Exponentially growing cultures were spotted on selective medium. The left panel shows colony color on selective rich medium (1/4 YEPD+G418) after 3 days of growth at 30ºC, and the right panel shows growth on selective minimal medium lacking adenine (SE-ade+G418) after 7 days at 30ºC.

Figure 3. Sup35 aggregates from [*PSI*$^+$]$^{\text{weak x strong}}$ cells generate two distinct migration profiles. A. Sup35 aggregates from [*PSI*$^+$]$^{\text{weak x strong}}$ cells differ from [*PSI*$^+$] aggregates in the two parents, [*PSI*$^+$]$^{\text{weak}}$ and [*PSI*$^+$]$^{\text{strong}}$. The left panel shows semi denaturing detergent agarose gel electrophoresis (SDD-AGE) of lysates from the indicated strains, followed by αSup35 immunoblotting. The right panel shows densitometry of the blot using ImageJ, NIH. Peaks on the left side of the graph correspond to aggregated Sup35, while peaks on the right side represent monomeric Sup35. The blue line represents the Sup35 profile from [*PSI*$^+$]$^{\text{weak x strong}}$ cultures, the red line represents [*psi*], the yellow line represents [*PSI*$^+$]$^{\text{weak}}$, and the green line represents [*PSI*$^+$]$^{\text{strong}}$. B. Sup35 aggregates from [*PSI*$^+$]$^{\text{weak x strong}}$ cells resemble [*PSI*$^+$] aggregates in the phenotypically dominant [*PSI*$^+$]$^{\text{strong}}$ parent. The left panel shows semi denaturing detergent agarose gel electrophoresis

(SDD-AGE) of lysates from the indicated strains, followed by αSup35 immunoblotting. The right panel shows densitometry analysis of the blot (ImageJ, NIH). Peaks on the left side of the graph correspond to aggregated Sup35, while peaks on the right side represent monomeric Sup35. The blue line represents the Sup35 profile from [*PSI*$^{+}$]$^{\text{weak x strong}}$ cultures, the red line represents [*psi*$^{-}$], the yellow line represents [*PSI*$^{+}$]$^{\text{weak}}$, and the green line represents [*PSI*$^{+}$]$^{\text{strong}}$.

Figure 4. [*PSI*$^{+}$]$^{\text{weak}}$ can be re-isolated from [*PSI*$^{+}$]$^{\text{weak x strong}}$ cells. [*PSI*$^{+}$] variants were crossed and exposed to various conditions after mating, as indicated. Zygotes were grown into microcolonies on complete medium with 3mM GdnHCl, the microcolonies were punched out of agar, resuspended in water, and plated on YPD where [*PSI*$^{+}$] state was scored. Each bar represents the percent of [*PSI*$^{+}$]$^{\text{weak}}$ colonies recovered from a single microcolony. A. Percent [*PSI*$^{+}$]$^{\text{weak}}$ of total [*PSI*$^{+}$] colonies recovered in a [*PSI*$^{+}$]$^{\text{weak}}$ x [*PSI*$^{+}$]$^{\text{strong}}$ competition experiment, and in a [*PSI*$^{+}$]$^{\text{strong}}$ x [*PSI*$^{+}$]$^{\text{strong}}$ control experiment. Data set one shows [*PSI*$^{+}$]$^{\text{weak}}$ recovered from the competition experiment when [*PSI*$^{+}$] aggregates are remodeled for just a single cell cycle during zygote formation (18 zygotes, 3,663 total [*PSI*$^{+}$] colonies scored). Data set two shows [*PSI*$^{+}$]$^{\text{weak}}$ recovered from the competition experiment when [*PSI*$^{+}$] aggregates are prevented from remodeling from the beginning of the mating reaction (13 zygotes, 4,277 total [*PSI*$^{+}$] colonies scored). Data set three shows [*PSI*$^{+}$]$^{\text{weak}}$ recovered from progeny of [*PSI*$^{+}$]$^{\text{weak}}$ x [*PSI*$^{+}$]$^{\text{strong}}$ zygotes that divided for 24 hours with aggregate remodeling (11 zygotes, 33 microcolonies, and 7,882 [*PSI*$^{+}$] colonies scored). Data set four shows [*PSI*$^{+}$]$^{\text{weak}}$ recovered from a [*PSI*$^{+}$]$^{\text{weak}}$ x [*PSI*$^{+}$]$^{\text{strong}}$ diploid that had been propagated for many generations before the analysis (14 microcolonies, 2,805

total [*PSI*$^+$] colonies scored). Data set five shows [*PSI*$^+$]^{weak} recovered from a control [*PSI*$^+$]^{strong} x [*PSI*$^+$]^{strong} cross where [*PSI*$^+$] aggregates are remodeled for just a single cell cycle during zygote formation (33 zygotes, 5,279 total [*PSI*$^+$] colonies scored). Data set six shows [*PSI*$^+$]^{weak} recovered from a control [*PSI*$^+$]^{strong} x [*PSI*$^+$]^{strong} cross where [*PSI*$^+$] aggregates are prevented from remodeling from the beginning of the mating reaction (17 zygotes, 1,287 total [*PSI*$^+$] colonies scored). B. Percent [*PSI*$^+$]^{weak} of total [*PSI*$^+$] colonies recovered in a [*PSI*$^+$]^{weak} x [*PSI*$^+$]^{weak} control experiment. Data set one shows [*PSI*$^+$]^{weak} recovered when [*PSI*$^+$] aggregates are remodeled for just a single cell cycle during zygote formation (15 zygotes, 4,769 total [*PSI*$^+$] colonies scored). Data set two shows [*PSI*$^+$]^{weak} recovered when [*PSI*$^+$] aggregates are prevented from remodeling from the beginning of the mating reaction (16 zygotes, 2,186 total [*PSI*$^+$] colonies scored).

Figure 5. [*PSI*$^+$] variants isolated from competition experiments are epigenetic. Exponentially growing cultures were spotted on rich medium (1/4 YEPD) and minimal medium lacking adenine (SD-ade). [*PSI*$^+$]^{weak} and [*PSI*$^+$]^{strong} strains isolated from competition experiments are shown in column one (original). Column two shows these isolates after prion elimination by Hsp104 overexpression (Hsp104), columns three and four (Sup35) show that both [*PSI*$^+$]^{weak} (3) and [*PSI*$^+$]^{strong} (4) can be induced in the Hsp104-cured isolates after Sup35 overproduction. Column five shows that the newly induced [*PSI*$^+$]^{weak} from column three can be cured by 3mM GdnHCl (GdnHCl), while column six shows that the newly induced [*PSI*$^+$]^{strong} from column four can be cured by 3mM GdnHCl (GdnHCl).

Figure 6. Loss of $[PSI^+]^{weak}$ increases with cell division cycles in the progeny of zygotes isolated from $[PSI^+]^{weak}$ x $[PSI^+]^{strong}$ cell crosses. $[PSI^+]$ variants were crossed and exposed to various conditions after mating, as indicated. Zygotes were grown into microcolonies on complete medium with 3mM GdnHCl, the microcolonies were punched out of agar, resuspended in water, and plated on YPD where $[PSI^+]$ state was scored. Column one shows the percent of zygotes that have completely lost $[PSI^+]^{weak}$ from the $[PSI^+]^{weak}$ x $[PSI^+]^{strong}$ competition experiment condition where aggregates were remodeled for just one cell cycle during zygote formation (18 zygotes). Column two shows the percent of zygotes that have completely lost $[PSI^+]^{weak}$ from the $[PSI^+]^{weak}$ x $[PSI^+]^{strong}$ competition experiment condition where aggregates were prevented from remodeling from the beginning of the mating reaction (13 zygotes). Column three shows the percent of cells that have completely lost $[PSI^+]^{weak}$ from the $[PSI^+]^{weak}$ x $[PSI^+]^{strong}$ competition experiment condition where aggregates were remodeled for 24 hours (14 generations) after zygote formation (33 microcolonies). Column four shows the percent of cells that have completely lost $[PSI^+]^{weak}$ in the progeny of a $[PSI^+]^{weak}$ x $[PSI^+]^{strong}$ diploid that had been propagated for many generations (>80) before the analysis (14 microcolonies). Column five shows the percent of zygotes that have completely lost $[PSI^+]^{weak}$ from the $[PSI^+]^{weak}$ x $[PSI^+]^{strong}$ competition experiment condition where cell division was inhibited for 24 hours by incubation of minimal media lacking histidine, but aggregate remodeling continued (2/15 zygotes).

Figure 7. The number of propagons in zygotes increases after amino acid starvation compared to normal growth conditions. $[PSI^+]^{weak}$ and $[PSI^+]^{strong}$ cells were

crossed on synthetic complete medium, nascent zygotes were incubated on medium lacking histidine for 24 hours (amino acid starvation for 24 hours), and then moved to complete medium with 3mM GdnHCl and allowed to grow into a microcolony. Alternatively, [*PSI*$^+$]^{weak} and [*PSI*$^+$]^{strong} cells were crossed on synthetic complete medium (normal growth), then nascent zygotes were moved to complete medium with 3mM GdnHCl and allowed to grow into a microcolony. Microcolonies were punched out of agar, resuspended in water, and plated on rich medium where colonies were scored for [*PSI*$^+$] by color. The distribution of the numbers of total [*PSI*$^+$] colonies recovered from single zygotes for each growth condition (normal or amino acid starvation) is shown in the two graphs. Numbers of total [*PSI*$^+$] colonies per zygote (propagons) were binned in increments of 50. Each binned category (legend, right side of the graph) shows the percent of zygotes that contained the indicated range of propagons out of the total number of bin categories for each growth condition (normal growth or amino acid starvation).

Figure 8. Sup35 levels do not significantly change after 22 hours of amino acid starvation. SDS-PAGE followed by immunoblotting as indicated. αPGK is a loading control. Lane 1 is [*PSI*$^+$]^{weak} grown in synthetic complete medium. Lane 2 is [*PSI*$^+$]^{strong} grown in synthetic complete medium. Lanes 3 and 4 are [*PSI*$^+$]^{weak} and [*PSI*$^+$]^{strong} after 22 hours in media lacking histidine, respectively.

Figure 9. The [*PSI*$^+$]^{strong} phenotype is not immediately established in [*PSI*$^+$]^{strong} x [*PSI*$^+$]^{weak} zygotes. [*PSI*$^+$]^{strong}, [*PSI*$^+$]^{weak} or [*psi*$^-$] cells were crossed in indicated combinations on synthetic complete medium with adenine and cytosine, and then moved to synthetic medium lacking adenine (-adenine) or to synthetic

complete medium (+adenine). All zygotes grow on synthetic complete medium, while medium without adenine requires the [*PSI*$^{+}$]^{strong}-dependent translational read-through of the *ade1-14* allele. DIC images. Zygotes from cell crosses indicated on the left are shown growing on medium lacking adenine (-adenine) or on complete medium (+adenine). The left-side mating partner is carrying an Δ*ade1* deletion, while the partner indicated on the right side is carrying the wildtype *ade1-14* allele. The two mating partners are isogenic, except for their *ade1* alleles.

Figure 1.

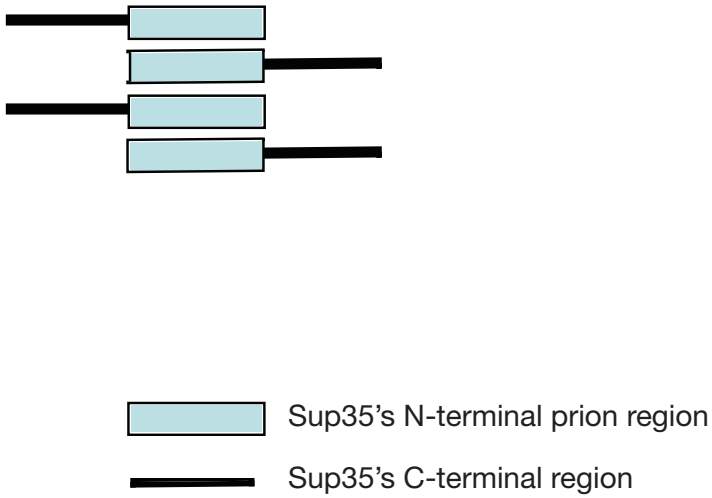

Figure 2.

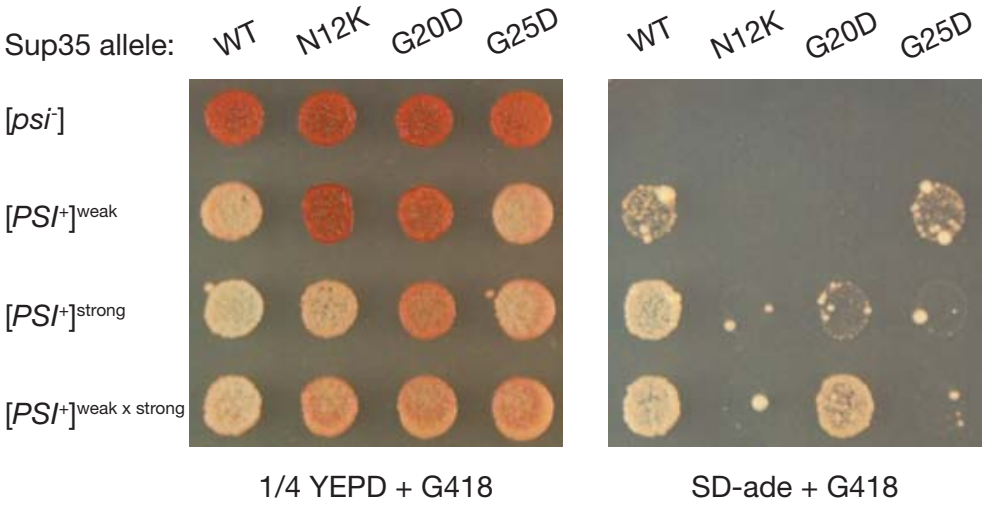
Sup35 allele:
WT
N12K
G20D
G25D
WT
N12K
G20D
G25D
[psi-]
[PSI+]weak
[PSI+]strong
[PSI+]weak x strong
1/4 YEPD + G418
SD-ade + G418

Figure 3.

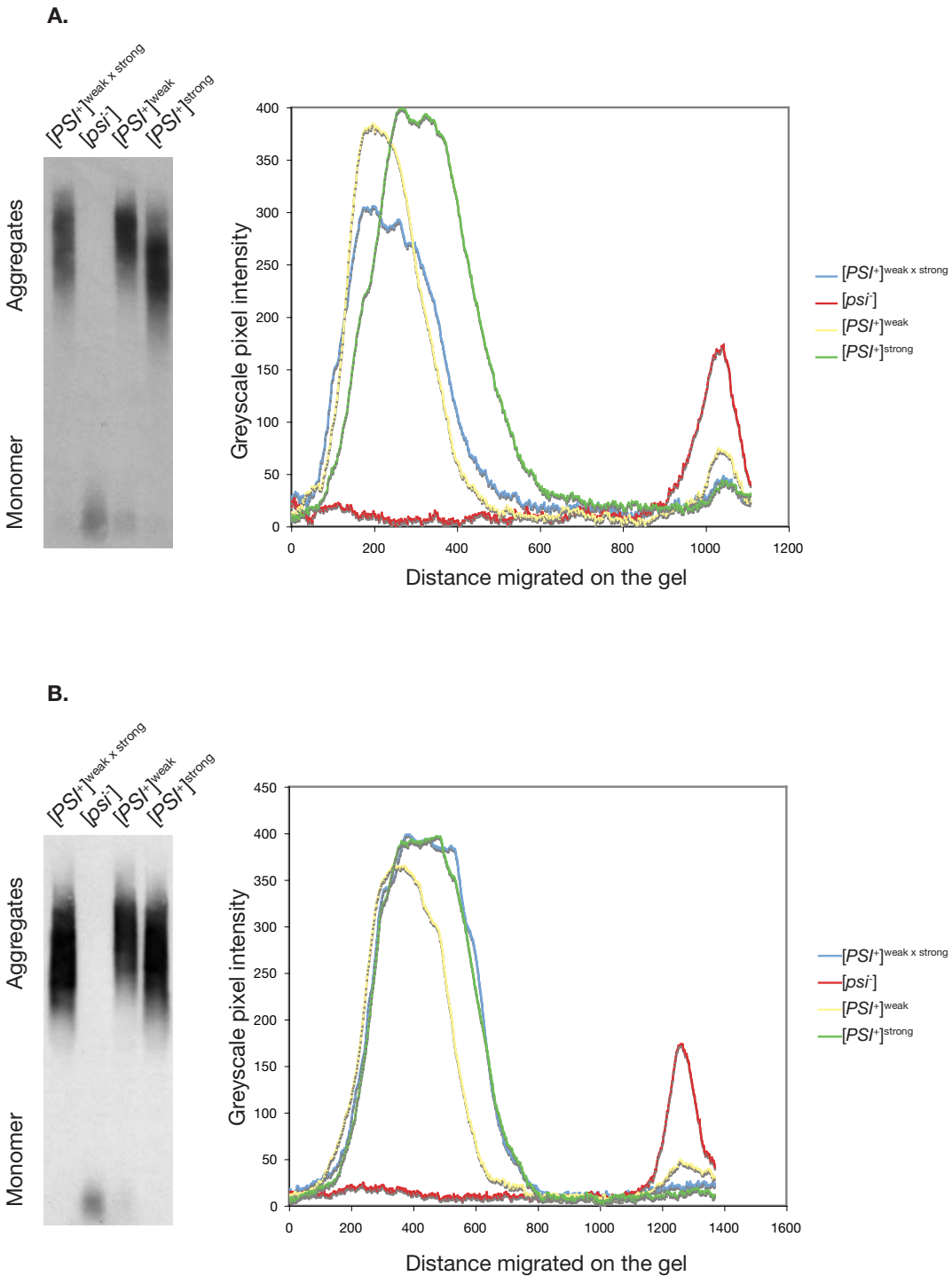
A.
[PSI+]weak x strong
[psi-]
[PSI+]weak
[PSI+]strong
Aggregates
Monomer
Greyscale pixel intensity
Distance migrated on the gel
[PSI+]weak x strong
[psi-]
[PSI+]weak
[PSI+]strong
B.
[PSI+]weak x strong
[psi-]
[PSI+]weak
[PSI+]strong
Aggregates
Monomer
Greyscale pixel intensity
Distance migrated on the gel
[PSI+]weak x strong
[psi-]
[PSI+]weak
[PSI+]strong

Figure 4.

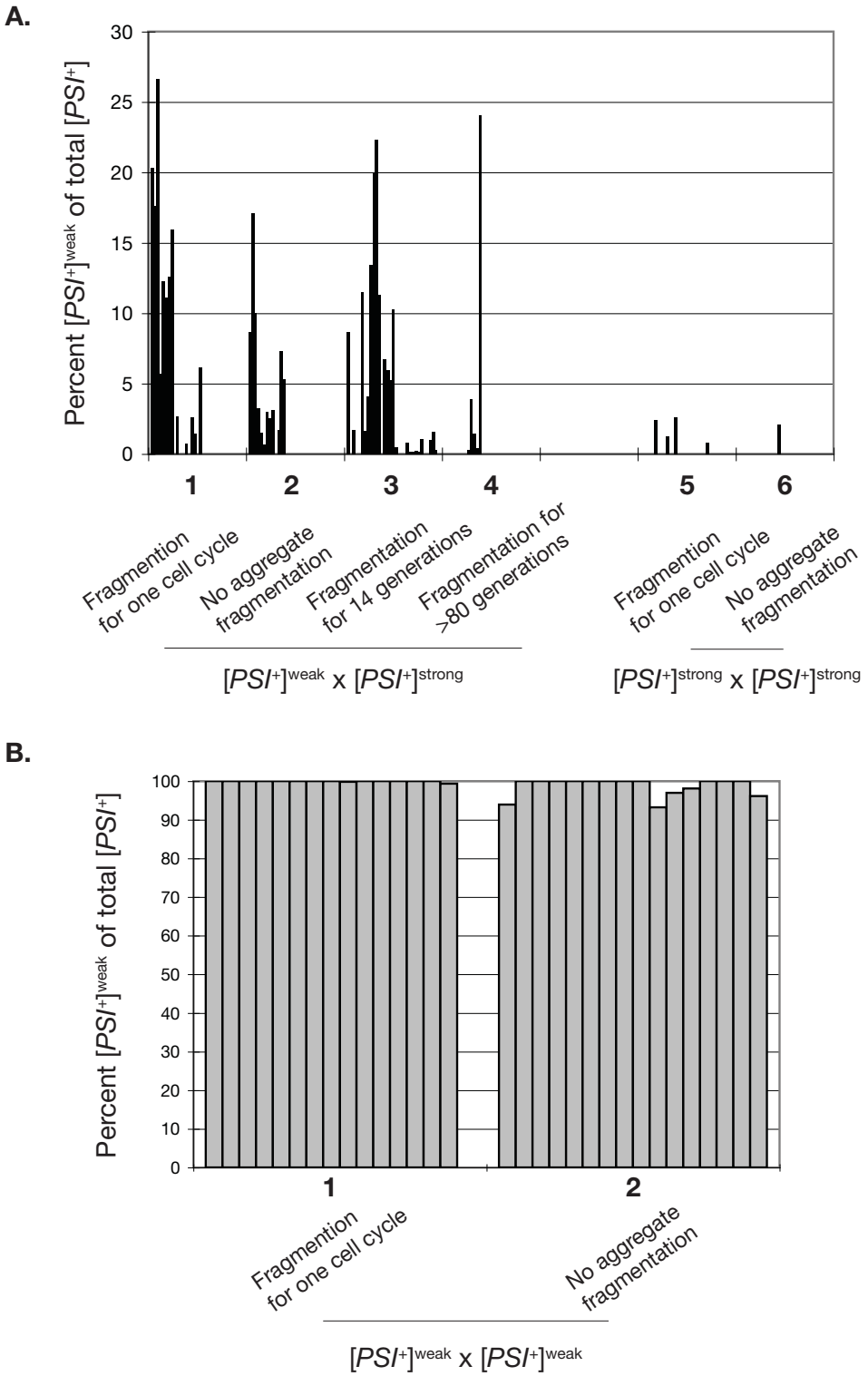
A.
Percent [PSI+]weak of total [PSI+]
30
25
20
15
10
5
0
1
2
3
4
5
6
Fragmention for one cell cycle
No aggregate fragmentation
Fragmentation for 14 generations
Fragmentation for >80 generations
Fragmention for one cell cycle
No aggregate fragmentation
[PSI+]weak x [PSI+]strong
[PSI+]strong x [PSI+]strong
B.
Percent [PSI+]weak of total [PSI+]
100
90
80
70
60
50
40
30
20
10
0
1
2
Fragmention for one cell cycle
No aggregate fragmentation
[PSI+]weak x [PSI+]weak

Figure 5.

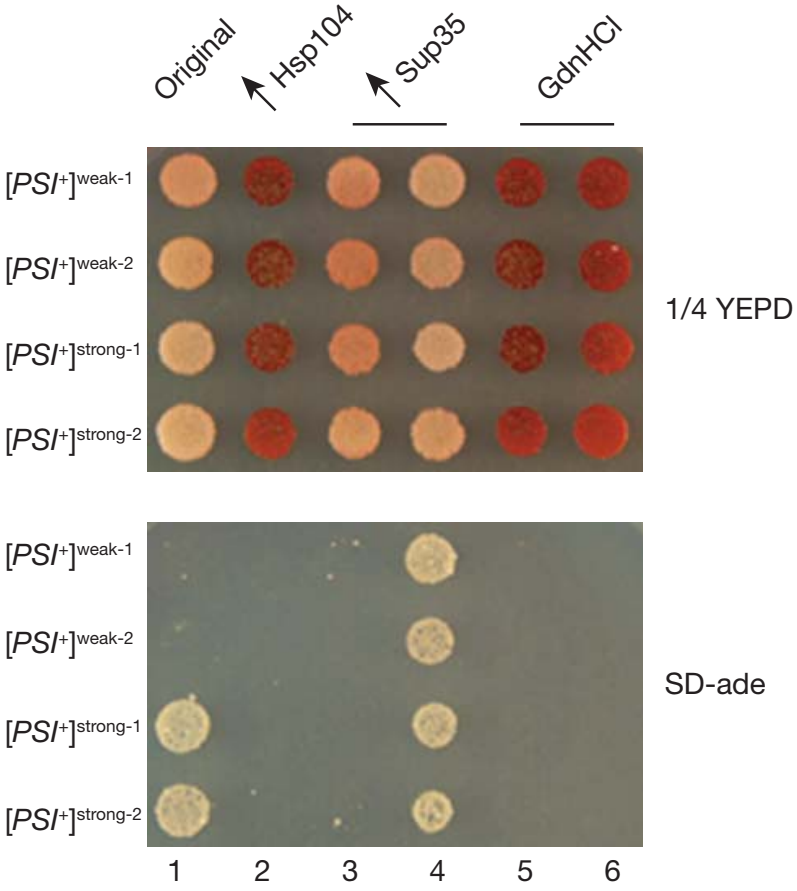
Original
Hsp104
Sup35
GdnHCl
[PSI+]weak-1
[PSI+]weak-2
[PSI+]strong-1
[PSI+]strong-2
1/4 YEPD
[PSI+]weak-1
[PSI+]weak-2
[PSI+]strong-1
[PSI+]strong-2
SD-ade
1
2
3
4
5
6

Figure 6.

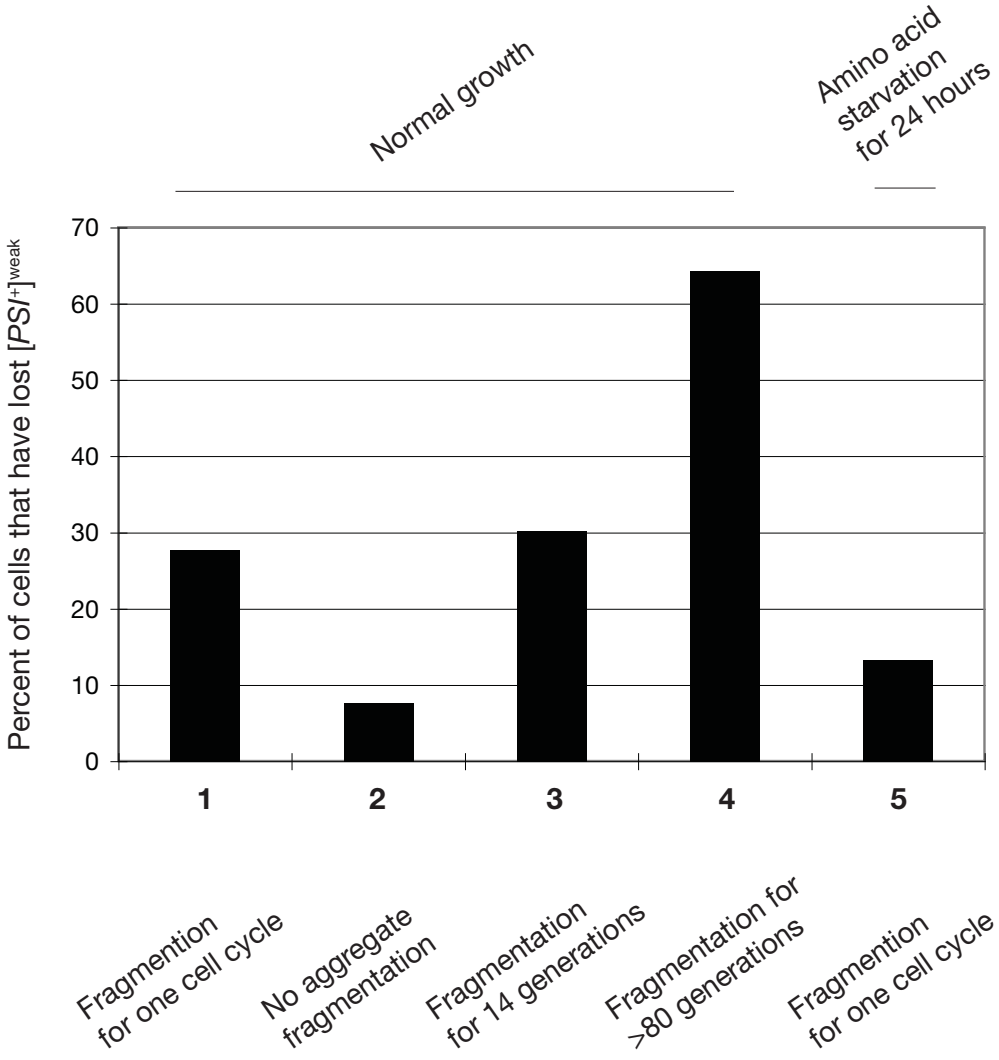
Normal growth
Amino acid starvation for 24 hours
Percent of cells that have lost [PSI+]weak
70
60
50
40
30
20
10
0
1
2
3
4
5
Fragmention for one cell cycle
No aggregate fragmentation
Fragmentation for 14 generations
Fragmentation for >80 generations
Fragmention for one cell cycle

Figure 7.

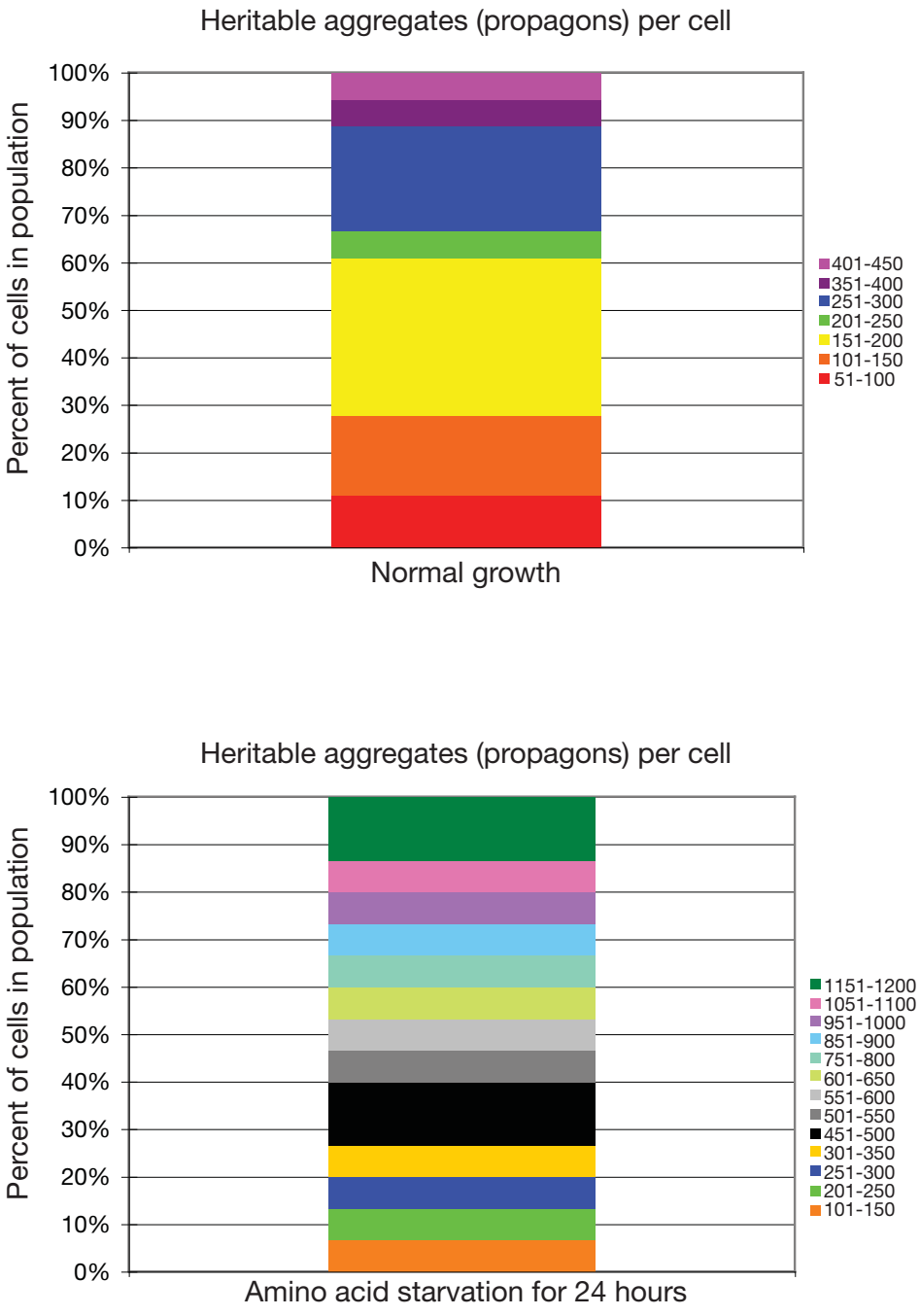
Heritable aggregates (propagons) per cell
Percent of cells in population
100%
90%
80%
70%
60%
50%
40%
30%
20%
10%
0%
Normal growth
401-450
351-400
251-300
201-250
151-200
101-150
51-100
Heritable aggregates (propagons) per cell
Percent of cells in population
100%
90%
80%
70%
60%
50%
40%
30%
20%
10%
0%
Amino acid starvation for 24 hours
1151-1200
1051-1100
951-1000
851-900
751-800
601-650
551-600
501-550
451-500
301-350
251-300
201-250
101-150

Figure 8.

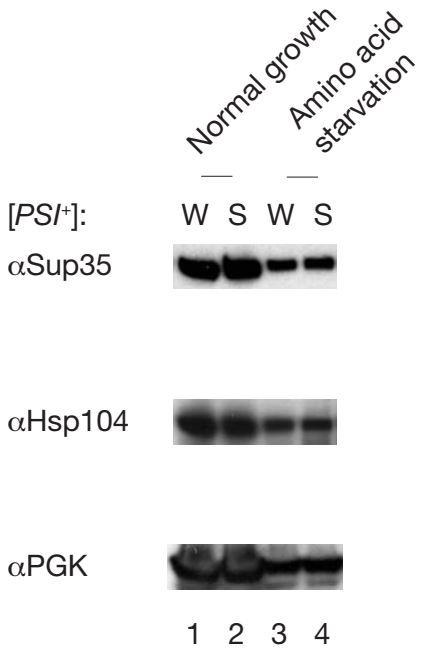
Normal growth
Amino acid starvation
[PSI+]:
W S W S
αSup35
αHsp104
αPGK
1 2 3 4

Figure 9.

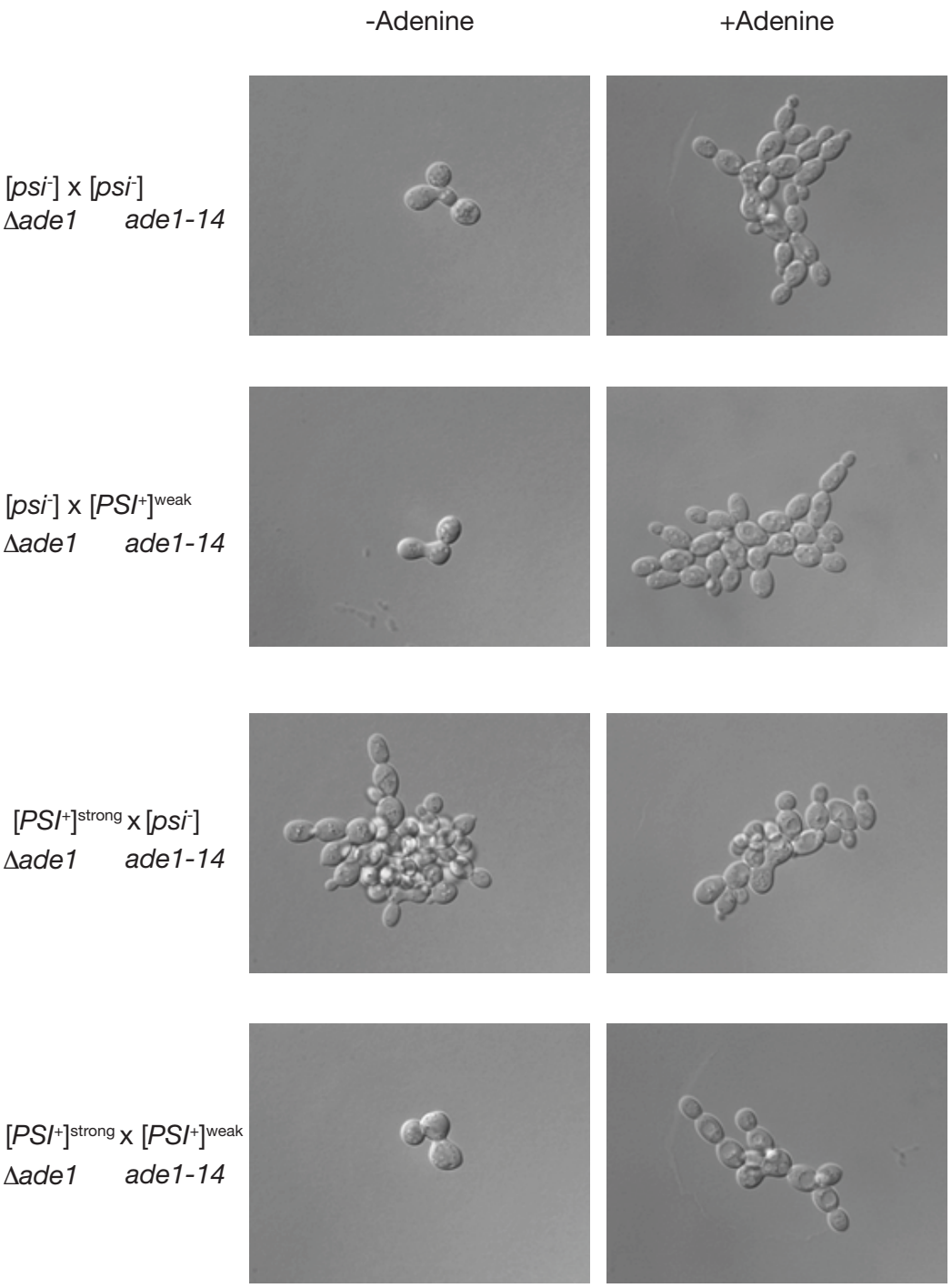
-Adenine
+Adenine
[psi-] x [psi-]
Δade1 ade1-14
[psi-] x [PSI+]weak
Δade1 ade1-14
[PSI+]strong x [psi-]
Δade1 ade1-14
[PSI+]strong x [PSI+]weak
Δade1 ade1-14

Chapter 3: The prefoldin chaperone is an indirect regulator of [PSI^+]

Abstract

Much evidence suggests that maintenance of the [*PSI*$^+$] and [*psi*$^-$] states is regulated by post-translationally acting quality control pathways, including Hsp70 (Ssa's) and Hsp104; however the effects of co-translationally acting chaperones on prion propagation have only recently begun to be addressed [1, 2]. In eukaryotes, two chaperone families have been implicated in the folding of nascent polypeptides: Ssb1 and Ssb2 (Hsp70) and Prefoldin (Pfd) [3, 4]. Genetic studies have already linked Ssb1 and Ssb2 to the Sup35 cycle [5-7]. Here, I report the characterization of [*PSI*$^+$] strains isolated from prefoldin single subunit deletion mutants. When any one of the six prefoldin subunits is deleted in a [*PSI*$^+$] strain, colonies with a range of translation termination efficiencies are recovered. While these distinct phenotypes have some characteristics of epigenetic traits (*i.e.* dominant in crosses and specified by novel physical states of the Sup35 protein), my subsequent analyses indicate that they arise from single genetic lesions falling into five linkage groups that are unlinked to the original *pfd* deletions. In an effort to molecularly characterize these prion modifiers, I have performed linkage analysis to two previously identified genes known to exert dominant effects on [*PSI*$^+$] propagation when mutated: *HSP104*, encoding a molecular chaperone, and *SUP35* itself [1, 8-10]. All of the characterized mutants segregate independently of Hsp104, and two of the mutants are linked to Sup35, although none are associated with mutations in the prion domain of the protein. My studies indicate that the absence of a functional co-translationally acting chaperone prefoldin is mutagenic to the cell, and point to the existence of novel dominant genetic modulators of [*PSI*$^+$].

Introduction

Post-translationally acting chaperones of the Hsp70 family, Ssb1 and Ssb2, have been implicated in [*PSI*$^{+}$] maintenance [5-7]. Cells lacking these two Hsp70 proteins spontaneously acquire the prion state at higher levels and are more sensitive to loss of the prion by Hsp104 inactivation. When this project was started, it had been reported that Ssb1 and Ssb2 functionally overlap with the prefoldin (Pfd) chaperone, and that loss of all six Pfd subunits in yeast, combined with loss of Ssb1 and Ssb2, results in a synthetic lethal defect [11]. Based on this observation, I thought it possible that the functional redundancy between Ssbs and Pfd extends to regulation of the [*PSI*$^{+}$] prion, so this project was initiated. However, the original study that reported the synthetic lethal interaction between Ssbs and Pfd has recently been retracted [12]. The retraction states that most of the general conclusions of the study, including the synthetic lethal interaction between *ssb* and *pfd* deletion mutants, still hold true, but further work is needed to clarify which conclusions from the retracted study can be verified independently.

Prefoldin is a hexameric complex composed of two α and four β subunits [13]. In archaea, one α and one β gene encode all of the subunits, while in yeast, there are two α and four β genes [14]. Though it is thought that eukaryotic prefoldin complexes are composed of six unique subunits, complexes of differing composition remain possible given the high sequence similarity between the two α subunits and between the four β subunits [15]. The assembled archaeal prefoldin complex resembles a jellyfish with a large central cavity, and the tips of the six individual subunits form coiled coils that look like tentacles [16]. The coiled coil prefoldin tentacles are two intertwined alpha helices, and there are six such coils

that form the peripheral tentacles of the chaperone complex. The tips of the coiled coil tentacles contain hydrophobic patches that are important for multivalent binding of non-native proteins [16]. When the tips of the coiled coil regions are truncated, prefoldin loses its ability to prevent the aggregation of bovine rhodanese and firefly luciferase [16]. The crystal structure of archaeal prefoldin indicates that the coiled coil tentacles are quite flexible, which may allow prefoldin to interact with a broad spectrum of substrates [16].

Prefoldin plays a vital role in the folding of actin and tubulin [4, 15, 17]. In eukaryotes, prefoldin binds to denatured, but not native, actin and delivers it to the CCT chaperonin for folding [4]. Experiments employing competitive inhibitors of folding (*i.e.* chaperone traps) indicate that prefoldin does not release its substrate into the cytosol after action, but delivers it directly to CCT for folding [4]. The importance of prefoldin in actin and tubulin folding is underscored by the extreme sensitivity of prefoldin mutants to the mictrotubule depolymerizing drug benomyl, and by the 40-50% reduction in the amount of folded actin in prefoldin mutants [4, 15, 17]. Though prefoldin has been described as playing a crucial role in the folding of actin and tubulin, there are several observations that suggest it may play a more general role in protein folding. First, a prefoldin homologue is present in archaea, which do not possess actin nor tubulin [14]. Archaea do not have Hsp70 co-translational chaperones, so the absence of Hsp70 co-translational chaperones opens the possibility that the archaeal prefoldin homologue fulfills a co-translational chaperone function [14]. Second, archaeal prefoldin can form complexes with a wide range of non-native substrates *in vitro*, preventing the aggregation of guanidine- or heat- denatured hen lysozyme and bovine mitochondrial rhodanese [14]. Actin and tubulin exist in high abundance in cells, which makes it easy to identify their interaction with prefoldin in comparison to the potential

interaction between prefoldin and less highly expressed proteins. It is possible that prefoldin interacts with less abundant targets that have not yet been identified.

Prefoldin interacts directly with the CCT chaperonin, probably handing off its target substrates upon forming a complex with CCT, where the substrates can complete folding with the assistance of CCT [4, 15, 18]. *In vitro* evidence of prefoldin's interaction with CCT is that purified prefoldin can bind to CCT complexed with ATP-agarose on a column, but it does not bind to a control column with the prokaryotic chaperone GroEL [15]. This result is complemented by the observation that in yeast about 10% of cytosolic prefoldin complexes can be co-immunoprecipitated with CCT [4]. Prefoldin-CCT complexes can also be isolated using gel filtration, and three-dimensional reconstruction of these complexes has revealed that outer regions of prefoldin's tentacles can interact with the apical domain of the CCT chaperonin [18].

When this project was initiated, prefoldin and the co-translational chaperones Ssb1 and Ssb2 showed some functional overlap in genetic tests, though this study has since been retracted [11, 12]. Based on this genetic interaction between prefoldin and the Ssb proteins, and because Ssbs have been shown to affect [*PSI*$^+$], I believed that prefoldin is a candidate chaperone that may be involved in regulation of the Sup35 prion [2, 5, 7]. Co-translational chaperones like prefoldin and Ssbs ensure that nascent polypeptides fold properly. Since prions are unique proteins that are able to adopt more than one physical state, I believe it is likely that co-translational chaperones play a key role in stabilizing nascent prion proteins and thereby limit their range of accessible folds. Here, I report that disruptions in prefoldin but not in Ssb1/Ssb2 destabilize [*PSI*$^+$] propagation, producing a spectrum of [*PSI*$^+$]

phenotypes. These novel [*PSI*$^{+}$]^{pfd} phenotypes were transferred into a prefoldin wildtype background, where genetic and biochemical analysis showed that the novel [*PSI*$^{+}$]^{pfd} phenotypes are linked to distinct Sup35 physical states. Finally, I show that the disruptions in prefoldin function are mutagenic to the cell, and that I have isolated novel dominant genetic modulators of [*PSI*$^{+}$] state that are responsible for creating the observed [*PSI*$^{+}$]^{pfd} phenotypes.

Results

Generation of *pfd* and *ssb* deletion mutants and their characterization

In order to study how the co-translational chaperones prefoldin and Hsp70 family members Ssb1 and Ssb2 affect the [*PSI*$^{+}$] prion, I have made *pfd1, pfd3, pfd4, pfd6, ssb1,* and *ssb2* deletion mutants, individually knocking out each gene of interest in diploid [*PSI*$^{+}$]^{strong} strains. Deletions were confirmed by PCR and by 2:2 segregation of the gene replacement selectable marker (data not shown, see tables 1 and 2 for a list of primers used to make and verify deletion mutants). Δ*pfd2* and Δ*pfd5* mutants were already available in the lab. These two mutants were generated by deletion of the corresponding genes in a haploid [*PSI*$^{+}$]^{strong} strain, and they were verified by PCR for correct integration using the same approach as when Δ*pfd* and Δ*ssb* mutants were generated in [*PSI*$^{+}$]^{strong} diploids. After *ssb* and *pfd* knockout confirmation, single deletion mutants were recovered in haploids by sporulating and dissecting out meiotic progeny (tetrads) from the parent heterozygous knockout. Deletion mutants were followed by the presence of antibiotic resistance or auxotrophy markers used to generate them. Double deletion mutant combinations were created by crossing two single

deletion mutants to create a double heterozygous deletion mutant, which was sporulated and dissected, allowing the recovery of a double deletion mutant in the meiotic progeny. In order to create triple or quadruple mutants, the cell crossing procedure was repeated, followed by sporulation and recovery of desired mutant combinations in meiotic progeny. [*PSI*$^+$] was eliminated or cured from the deletion mutants by plasmid-driven overexpression of Hsp104 or by treating cells with guanidine hydrochloride (see table 3 for a list of all deletion mutants and how they were cured). Cells cured of [*PSI*$^+$] by Hsp104 overexpression retain the ability to reacquire the prion, either spontaneously or by Sup35 overexpression, while curing with guanidine hydrochloride often eliminates the ability to reacquire the [*PSI*$^+$] prion [19]. Elimination of [*PSI*$^+$] in *pfd* and *ssb* mutants by these two methods that do not affect nucleic acids confirms that [*PSI*$^+$] is an epigenetic trait.

To characterize the genetic interaction between prefoldin and Ssbs, I determined the exponential growth rates for various combinations of *ssb* and *pfd* deletion mutants in rich medium (YPAD) (table 4). Δ*ssb1*Δ*ssb2* and Δ*pfd* mutants grow more slowly than their wildtype parent, and the mutants also show an interesting [*PSI*$^+$]-specific growth effect. Δ*ssb1*Δ*ssb2* [*PSI*$^+$] cells divide much more slowly than Δ*ssb1*Δ*ssb2* [*psi*$^-$] cells (table 4), and this [*PSI*$^+$]-specific growth defect can also be observed in triple mutants where Δ*ssb1*Δ*ssb2* is combined with Δ*pfd2* or Δ*pfd5*. Growth in YPAD supplemented with 3mM guanidine hydrochloride (GdnHCl) slows down the doubling times of both wildtype cells and Δ*pfd* mutants, but Δ*pfd* cells are more sensitive to GdnHCl than wildtype cells. The combination of Δ*ssb1*Δ*ssb2* and Δ*pfd* mutants did not have a cumulative effect on the growth of [*psi*$^-$] cells, indicating that a genetic interaction between Ssbs and prefoldin that affects cell growth is

specific to the [*PSI*$^+$] state. After characterizing the doubling times of *ssb* and *pfd* deletion mutants, I wanted to determine their effects on [*PSI*$^+$].

Although [*PSI*$^+$]^{strong} propagation continues in strains deleted for each of the prefoldin subunits, I compared the stability of the prion state in these deletion mutants to a wildtype strain by plating exponentially growing cells on rich medium and analyzing colony phenotype. In these experiments, I observed that Δ*pfd* destabilizes the [*PSI*$^+$]^{strong} phenotype, leading to both loss of [*PSI*$^+$], as indicated by growth of red colonies, and to the appearance of pink colonies that resemble another form of [*PSI*$^+$] that is known as [*PSI*$^+$]^{weak} (fig. 1) [20]. I wanted to verify that loss of prefoldin affects all forms of [*PSI*$^+$], and not just [*PSI*$^+$]^{strong}, so I made a Δ*pfd3* mutant in a [*PSI*$^+$]^{weak} haploid strain as described above, and I analyzed [*PSI*$^+$]^{weak} propagation in Δ*pfd3* by plating exponentially growing cells on rich medium and analyzing the colony color phenotype as described above (fig. 2). Loss of prefoldin function has an even greater destabilizing effect on [*PSI*$^+$]^{weak} than on [*PSI*$^+$]^{strong}, and [*PSI*$^+$]^{weak} Δ*pfd3* mutants produce a spectrum of colony colors on rich medium (fig. 2). These observations suggest that in wildtype cells prefoldin ensures the stable propagation of [*PSI*$^+$].

Since the Ssb Hsp70 proteins and the prefoldin complex both interact with nascent proteins, I wanted to determine if the combined effect of Δ*ssb1*Δ*ssb2* with a Δ*pfd* mutant could exacerbate destabilization of the [*PSI*$^+$] phenotype (fig. 3) [3, 15]. I plated exponentially growing [*PSI*$^+$] cultures of Δ*ssb1*Δ*ssb2* alone and in combination with Δ*pfd* on rich medium, scoring for [*PSI*$^+$] as described above (fig. 3). I did not observe any loss or change in [*PSI*$^+$] in Δ*ssb1*Δ*ssb2* cells. Combining Δ*ssb1*Δ*ssb2* with Δ*pfd* does not have a cumulative destabilizing effect on [*PSI*$^+$], and since destabilization of [*PSI*$^+$] is only observed in Δ*pfd*

mutants regardless of Ssb function, it appears that loss of prefoldin is responsible for the observed destabilizing effect on [*PSI*$^+$] propagation in Δ*pfd* mutants. However, the combination of two *pfd* deletion mutants with Δ*ssb* (Δ*ssb1/2*Δ*pfd2*Δ*pfd5)* does appear to have a cumulative destabilization effect, and disrupts faithful [*PSI*$^+$] propagation to a greater degree than either *pfd* mutant alone (fig. 3). This observation suggests that the hexameric prefoldin complex is partially functional when a single subunit is deleted, but that prefoldin function is further impaired when two subunits are deleted. Stable [*PSI*$^+$] propagation is dependent on prefoldin function, so [*PSI*$^+$] is further destabilized when multiple rather than single prefoldin subunits are deleted.

Since prefoldin interacts with nascent polypeptides as they emerge from the ribosome, and given the instability of [*PSI*$^+$] in Δ*pfd*, I expected that disruptions to the prefoldin complex would increase the likelihood of misfolding of nascent Sup35, thereby leading to an increase in the rate of spontaneous [*PSI*$^+$] appearance [15]. I plated exponentially growing [*psi*$^-$] Δ*pfd* and wildtype cells on synthetic medium lacking adenine that only allows for the growth of newly induced [*PSI*$^+$] cells, or spontaneous ADE+ revertants (fig. 4). The [*psi*$^-$] cells used in this experiment were cured of [*PSI*$^+$] by Hsp104 overexpression, which preserves the cells' ability to reacquire the [*PSI*$^+$] prion [21]. In order to distinguish between true [*PSI*$^+$] inductants and ADE+ revertants, all recovered ADE+ colonies were cured by GdnHCl. GdnHCl treatment allowed me to eliminate ADE+ revertants, which remain white after GdnHCl treatment, and only score true [*PSI*$^+$] colonies, which turn red after GdnHCl treatment. Contrary to my expectation that potential increased rates of Sup35 misfolding in Δ*pfd* cells would increase the rate of spontaneous [*PSI*$^+$] appearance, Δ*pfd* does not lead to an

increase in spontaneous [*PSI*$^+$] induction (fig. 4). Thus, the partial loss of prefoldin function alone does not stimulate an increased frequency of spontaneous prion induction.

Transmission of Δ*pfd* [*PSI*$^+$] phenotype to [*psi*$^-$] cells

To begin to determine the molecular basis of [*PSI*$^+$] destabilization in Δ*pfd* strains, I first performed genetic analyses. I crossed pink colonies recovered from Δ*pfd* [*PSI*$^+$]^{strong} strains to wildtype [*psi*$^-$] cells, thereby complementing the loss of prefoldin (fig. 5a). The [*PSI*$^+$] phenotypes recovered from these cell crosses between Δ*pfd* and wildtype [*psi*$^-$] cells will be referred to as [*PSI*$^+$]^{pfd} from now on, with [*PSI*$^+$]^{pfd1} meaning a [*PSI*$^+$] phenotype recovered from a Δ*pfd1* mutant, and so on for each of the six Δ*pfd* mutants. Upon complementation by cell crossing, [*PSI*$^+$]^{pfd} phenotypes from Δ*pfd* mutant strains were always dominant in crosses to [*psi*$^-$] cells. Some Δ*pfd* [*PSI*$^+$]^{pfd} pink isolates are particularly unstable, and they transmit a mix of [*PSI*$^+$]^{pfd} phenotypes to [*psi*$^-$] cells in genetic crosses (fig. 5b). Next, I sporulated Δ*pfd* / *PFD* [*PSI*$^+$]^{pfd} strains and tried to recover and stabilize the [*PSI*$^+$]^{pfd} phenotype in meiotic progeny with a wildtype *PFD* background. Two progeny of these meiotic tetrads always inherit the Δ*pfd* mutation, which will continue to destabilize [*PSI*$^+$] and cause variability in the colony colors produced by Δ*pfd* meiotic progeny. However, I expected that the two wildtype *PFD* meiotic progeny will stably propagate the isolated [*PSI*$^+$]^{pfd} phenotype. Because of [*PSI*$^+$] destabilization caused by Δ*pfd* in two out of four meiotic progeny, many meiotic tetrads produced different colony colors when grown on rich medium, making it difficult to monitor colony color phenotypes. Figure 5c shows the variability in colony colors produced by spores from meiotic tetrads from Δ*pfd* / *PFD* [*PSI*$^+$]^{pfd} strains. I recovered some meiotic tetrads where all four spores inherited the pink [*PSI*$^+$]^{pfd} phenotype, but I also recovered many tetrads with 2:2, 3:1, and 1:3 pink:white colony color segregation. This instability in

colony colors produced by meiotic progeny from Δ*pfd* / *PFD* [*PSI*$^{+}$]^{pfd} strains was not surprising because of the destabilizing effect of Δ*pfd* on [*PSI*$^{+}$]. I saved wildtype *PFD* [*PSI*$^{+}$]^{pfd} strains where [*PSI*$^{+}$]^{pfd} was stably propagated, and used these strains for subsequent analysis of Sup35 state. I confirmed the [*PSI*$^{+}$] state of these [*PSI*$^{+}$]^{pfd} isolates by curing with guanidine hydrochloride treatment (fig. 6). The names of all [*PSI*$^{+}$]^{pfd} isolates used in these experiments are listed in table 5.

To circumvent the difficulties of characterizing [*PSI*$^{+}$] in the unstable Δ*pfd* background, I performed additional genetic characterizations of the wildtype meiotic segregants I recovered from Δ*pfd* / *PFD* [*PSI*$^{+}$]^{pfd} strains described above. Unlike [*PSI*$^{+}$]^{weak} strains, which have the same pink colony color phenotype, [*PSI*$^{+}$]^{pfd} strains 1, 4 and 5 are dominant in genetic crosses with [*PSI*$^{+}$]^{strong} (fig. 7). The [*PSI*$^{+}$]^{pfd6} isolate is a non-mater, possibly because of a mutation that it is carrying, so I could not further analyze the [*PSI*$^{+}$]^{pfd6} isolate in any experiments where cell crosses were necessary. To determine if the dominance of [*PSI*$^{+}$]^{pfd} strains 1, 4 and 5 in cell crosses with [*PSI*$^{+}$]^{strong} was based on an epigenetic or genetic trait, I cured these [*PSI*$^{+}$]^{pfd} strains both by GdnHCl treatment and Hsp104 overexpression (data not shown) and crossed the resulting [*psi*]^{pfd} strains to [*PSI*$^{+}$]^{strong} (data not shown). Instead of recovering [*PSI*$^{+}$]^{strong} progeny as I would expect from a cross between wildtype [*psi*] and wildtype [*PSI*$^{+}$]^{strong}, surprisingly, I recovered progeny with the [*PSI*$^{+}$]^{pfd} phenotype (fig. 8). These observations together indicate that Δ*pfd* strains have induced a change in the [*PSI*$^{+}$] phenotype through some genetic alteration that is independent of the *PFD* loci.

To begin to characterize these genetic lesions, I determined the meiotic segregation patterns of the [*PSI*$^{+}$]-altering gene(s) by sporulating and dissecting progeny from several

combinations of cell crosses between [*PSI*]^{pfd} isolates and wildtype [*PSI*$^+$]^{strong} or [*psi*$^-$] cells. I crossed [*PSI*$^+$]^{pfd} isolates 1, 4 and 5 to both [*PSI*$^+$]^{strong} and [*psi*$^-$] cells, and I also crossed cured [*psi*$^-$]^{pfd} isolates 1, 4, and 5 to [*PSI*$^+$]^{strong} cells. In each case, meiotic progeny showed that the altered phenotype segregated 2:2, consistent with a single [*PSI*$^+$]-altering mutation (or multiple closely linked mutations) (tbl. 6).

The recovery of 2:2 meiotic segregation patterns from diploids created by cell crosses between wildtype cells and three independently isolated [*PSI*$^+$]^{pfd} strains leads me to conclude that the loss of prefoldin function is mutagenic to cells. The molecular basis for the change in [*PSI*$^+$] phenotype observed in [*PSI*$^+$]^{pfd} strains is a dominant, Mendelian mutation that is independent of the *PFD* loci.

Tubulin cytoskeletal defects may phenocopy Δ*pfd*'s destabilization of [*PSI*$^+$]

When this study was initiated, it was unknown that the loss of prefoldin function is mutagenic, so this was a surprising result. I reasoned that one possible explanation for the mutagenic effect of Δ*pfd* is an effect on the tubulin cytoskeleton, which could indirectly lead to mutations because of improper chromosome segregation. It has been shown that one of the major targets of prefoldin-assisted folding is tubulin [15, 17]. Prefoldin mutants have an altered ratio of α to β tubulin. Specifically, Δ*pfd* mutants have higher relative levels of β tubulin, and this imbalance causes prefoldin mutants to be sensitive to the microtubule depolymerizing drug benomyl [17, 22]. One way to phenocopy Δ*pfd* tubulin defects is to delete the minor α tubulin gene *tub3* or to delete the gene for Rbl2, a protein that binds β tubulin [22]. To determine whether Δ*pfd* destabilizes [*PSI*$^+$] through its cytoskeletal effects, I constructed Δ*tub3* and Δ*rbl2* mutants in [*PSI*$^+$] cells in the same manner as described for Δ*pfd*

mutants. I plated cells from exponentially growing cultures of Δ*tub3* and Δ*rbl2* on rich medium, and then scored [*PSI*] state as described for Δ*pfd* mutants (fig. 9). This analysis revealed that Δ*rbl2* does not affect [*PSI*$^+$] because Δ*rbl2* cells faithfully propagate [*PSI*$^+$], but that Δ*tub3* does lead to the alteration and loss of [*PSI*$^+$] as described for Δ*pfd* mutants. The isolated [*PSI*$^+$]^{tub3} strains can be cured by GdnHCl and are dominant in cell crosses with [*psi*$^-$] cells (data not shown), indicating that although Δ*tub3* alters the [*PSI*$^+$] phenotype, it can still propagate the prion. These results suggest that it is possible that the tubulin cytoskeleton plays a role in the regulation of the [*PSI*$^+$] prion, or that alterations in the tubulin cytoskeleton caused by Δ*tub3* lead to similar chromosome segregation problems as in Δ*pfd* mutants, resulting in mutations that can dominantly affect the [*PSI*$^+$] phenotype.

[*PSI*$^+$]^{pfd} isolates fall into five distinct linkage groups

Whatever the mechanism of their generation, disruption of PFD subunits has led to a mutagenic state that has allowed the isolation of prion modifiers. In order to begin characterizing the mutations carried by [*PSI*$^+$]^{pfd} strains, the lesions were first placed into linkage groups (fig. 10). I crossed each of the 5 [*PSI*$^+$]^{pfd} variants to each other in all combinations, and then analyzed the colony color phenotype of their meiotic progeny (tetrads). If the pink colony color phenotype segregates 4:0 in the resultant progeny, the two [*PSI*$^+$]^{pfd} parents likely carry mutations in the same locus or at two tightly linked loci. In contrast, any deviation from 4:0 segregation indicates that the mutations carried by parental [*PSI*$^+$]^{pfd} strains map to unlinked loci. The results of complementation analysis are shown in figure 10b, and they show that each of the 5 analyzed [*PSI*$^+$]^{pfd} isolates forms a unique linkage group, but there is linkage between [*PSI*$^+$]^{pfd} isolates 2 and 5, and between isolates 1, 3, and 4. Since crosses between all combinations of [*PSI*$^+$]^{pfd} isolates produced some tetrads

with non 4:0 pink colony color segregation, this indicates that mutations carried by all 5 [*PSI*$^{+}$]^{pfd} isolates fall into 5 independent loci. If the mutations carried by any two [*PSI*$^{+}$]^{pfd} isolates were tightly linked or mapped to the same locus, I would expect that all meiotic progeny from their cross would show 4:0 pink colony color segregation because all meiotic progeny would inherit the underlying mutation. There is some linkage between [*PSI*$^{+}$]^{pfd} isolates 2 and 5, and between isolates 1, 3, and 4 because cell crosses between 2 and 5, or between 1, 3 and 4 produced some meiotic progeny with 4:0 inheritance of the pink colony color phenotype, indicting that the mutations carried in these groups are linked because they are not always inherited independently of each other.

[*PSI*$^{+}$]^{pfd} mutations are not genetically linked to *HSP104*

The isolated [*PSI*$^{+}$]^{pfd} strains dominantly increase translation termination fidelity, which is referred to as an antisuppressor phenotype. Previously described mutations in Hsp104 also have a dominant antisuppressor phenotype [1, 10], so the mutations in the [*PSI*$^{+}$]^{pfd} strains were tested for linkage to the *HSP104* locus. The experimental strategy for this genetic analysis is outlined in figure 11. Briefly, each [*PSI*$^{+}$]^{pfd} variant was crossed to a Δ*hsp104* strain, which cannot propagate [*PSI*$^{+}$] and therefore forms red colonies on rich medium [1]. Next, meiotic progeny were isolated from these diploids, and segregation of the colony color phenotypes was analyzed. If the mutation in the [*PSI*$^{+}$]^{pfd} strain is linked to *HSP104*, 2 pink : 2 red colony color segregation is expected. Deviation from 2 pink : 2 red segregation suggests that the [*PSI*$^{+}$]^{pfd} mutation is not linked to *HSP104*. Each of the 5 [*PSI*$^{+}$]^{pfd} mutants showed deviation from the 2 pink : 2 red deviation (fig. 11b); thus, none of the isolated [*PSI*$^{+}$]^{pfd} strains carry a mutation with genetic linkage to *HSP104*.

The [*PSI*$^+$]^{pfd5} strain carries a mutation tightly linked to *SUP35*

In addition to *HSP104*, mutations within the Sup35 ORF itself have been described previously to have a dominant antisuppressor phenotype in [*PSI*$^+$] strains [8, 9]. To determine if the genetic lesions within the [*PSI*$^+$]^{pfd} strains map to the *SUP35* locus, the prion determining domain (150 nucleotides upstream of amino acid 1 to amino acid 310) was amplified from genomic DNA by PCR and sequenced. In each of the [*PSI*$^+$]^{pfd} strains, the sequence of the *SUP35* prion domain is wildtype (data not shown). However, mutations outside of the prion domain, such as mutations in the C-terminal region of Sup35 that impair its activity in translation termination, may also produce a dominant antisuppressor phenotype [23, 24]. To determine if any of the [*PSI*$^+$]^{pfd} mutations fell into this category, they were genetically analyzed for linkage to the *SUP35* locus (fig. 12). First, the isolated [*PSI*$^+$]^{pfd} variants were crossed to a strain that carries a *SUP35*::GFP allele. Next, meiotic progeny were isolated from these diploids, and segregation of the colony color phenotype and the *SUP35*::GFP allele were analyzed. The results are summarized in figure 12b. If the *SUP35*::GFP allele always gives rise to white colonies in meiotic progeny, while the [*PSI*$^+$]^{pfd} *SUP35* allele always gives rise to pink colonies, such co-segregation of the pink colony color phenotype and [*PSI*$^+$]^{pfd} *SUP35* allele indicates that the [*PSI*$^+$]^{pfd} *SUP35* allele is linked to the mutation that causes pink colonies. However, if the [*PSI*$^+$]^{pfd} *SUP35* allele sometimes gives rise to wildtype white colonies, this shows that the two traits can be inherited independently, indicating that there is no linkage the between [*PSI*$^+$]^{pfd} *SUP35* allele and the mutation. The *SUP35* allele from [*PSI*$^+$]^{pfd} isolates 2 and 5 always gave rise to pink colonies in all recovered meiotic progeny, and this co-segregation indicates linkage between the isolated mutations and [*PSI*$^+$]^{pfd} 2 and 5 *SUP35* alleles. [*PSI*$^+$]^{pfd} isolates 1, 3 and 4 do not carry mutations with

linkage to *SUP35* because they produced meiotic progeny where the pink colony color and the [*PSI*$^{+}$]^{pfd} allele were inherited independently.

To determine if [*PSI*$^{+}$]^{pfd} isolates 2 and 5 carry mutations that map to the Sup35 ORF, I crossed [*PSI*$^{+}$]^{pfd} 2 to itself, and [*PSI*$^{+}$]^{pfd} 5 to itself to create diploids that are homozygous for strain 2 and strain 5 mutations. In these homozygous mutant diploids, one of the *SUP35* loci was ablated by PCR-mediated disruption, and then a wildtype copy of *SUP35* was integrated at the *URA3* locus (fig. 13a). Segregation of the [*PSI*$^{+}$]^{pfd} antisuppressor phenotype and the endogenous *SUP35* locus was then analyzed in the meiotic progeny. I analyzed the inheritance of the endogenous *SUP35* locus and the antisuppressor pink colony color phenotype. If the endogenous *SUP35* locus always co-segregates with the antisuppressor [*PSI*$^{+}$]^{pfd} phenotype, this indicates that the isolated dominant antisuppressor mutation is located in *SUP35*. The wildtype copy of *SUP35* integrated at the *URA3* locus will always give rise to wildtype white colonies. Some meiotic progeny carrying the endogenous *SUP35* locus and the wildtype [*PSI*$^{+}$]^{strong} white colony color phenotype were isolated from the [*PSI*$^{+}$]^{pfd} strain 2 (fig. 13b), indicating that this strain does not carry a mutation within *SUP35* . However, all recovered meiotic progeny from the [*PSI*$^{+}$]^{pfd} strain 5 that carry the endogenous *SUP35* locus have the antisuppressor pink colony color phenotype, indicating that [*PSI*$^{+}$]^{pfd} isolate 5 carries a mutation in *SUP35*, or a mutation with very tight linkage to *SUP35*. Since the Sup35 prion domain in strain 5 has been shown to be wildtype by sequencing, the isolated mutation may lie in the Sup35 promoter, or the M or C-terminal domains.

Genetic evidence that the ratio between soluble and aggregated Sup35 is altered in [*PSI*$^+$]^{pfd} isolates

In addition to characterizing the genetic determinants of the changes in prion phenotype observed in [*PSI*$^+$]^{pfd} strains, I also began to characterize their molecular effects on prion propagation. In [*PSI*$^+$] cells, aggregated Sup35 molecules interact and direct the conversion of non-aggregated Sup35 into the prion state [25]. In the prion form, Sup35 molecules interact through their N-termini (*i.e.* the prion domain), and this region alone is sufficient to transmit [*PSI*$^+$] [26] [20]. The King lab has taken advantage of this prion domain interaction and created a series of full-length Sup35 clones containing single point mutations in the prion domain [27]. Each of these mutants is compromised in its interaction with Sup35 aggregates, and therefore the read-through phenotype is affected (fig. 14). If a Sup35 prion domain mutant cannot join pre-existing Sup35 aggregates, it will remain soluble and increase translation fidelity, leading to redder colonies on rich medium. Every [*PSI*$^+$] variant is able to incorporate Sup35 mutants into its prion aggregates to a different degree, because each Sup35 mutant can fold into a limited number of conformations specified by its primary structure, which dictate whether or not it can join wildtype Sup35 [*PSI*$^+$] aggregates. The inability to incorporate mutant Sup35 into aggregates leads to an accumulation of soluble and functional Sup35, detected as a lower level of read-through and a redder colony on rich media. The interaction between each [*PSI*$^+$] variant and a prion domain mutant is unique and produces a characteristic colony color. It is possible to distinguish [*PSI*$^+$] conformational variants of the same colony color through their unique interaction with this series of point mutants [27].

I transformed wildtype controls and [*PSI*$^+$]^{pfd} strains with plasmids expressing Sup35 point mutants, and then plated the transformants on selective media side-by-side, allowing for direct comparison of the colony color read-out resulting from the interaction between mutant Sup35 pre-existing [*PSI*$^+$] aggregates (fig. 14). The interaction between each isolated [*PSI*$^+$]^{pfd} variant and the series of Sup35 prion domain mutants reveals a unique colony-color fingerprint. The six [*PSI*$^+$]^{pfd} variants differ from each other and from their [*PSI*$^+$]^{strong} parent, but once the [*PSI*$^+$]^{pfd} mutation is segregated away by crosses with wildtype cells as described above, the parental [*PSI*$^+$]^{strong} phenotype is recovered. This indicates that Sup35 aggregates in [*PSI*$^+$]^{pfd} remain unchanged, but that their phenotype is masked by the isolated dominant antisuppressor mutation. Differences detected by this assay between the [*PSI*$^+$]^{strong} parent and the [*PSI*$^+$]^{pfd} isolates suggest that perhaps the independent dominant antisuppressor mutations are affecting translation fidelity independently of [*PSI*$^+$], or that the dominant antisuppressors are affecting the interaction between [*PSI*$^+$] aggregates and other aggregate-associated factors, which may influence how well Sup35 prion domain mutant can add on to pre-existing [*PSI*$^+$] aggregates. It is also possible that the antisuppressor mutations are affecting the adenine metabolic pathway, and thereby they influence the colony color phenotype.

Biochemical evidence that Sup35 aggregates are altered in [*PSI*$^+$]^{pfd} isolates

The altered phenotype of [*PSI*$^+$]^{pfd} strains suggests that functional Sup35 is accumulating under these conditions. To directly assay the physical state of Sup35 in wildtype and mutant strains, I used a biochemical assay called semi-denaturing detergent agarose gel electrophoresis (SDD-AGE) [28]. In this assay, cell lysates are prepared in buffer with a very low SDS concentration to preserve Sup35 aggregates, and then these complexes are

separated by agarose gel electrophoresis. It has been demonstrated that this assay can distinguish [*PSI*$^+$] variants based on the pattern of migration of Sup35 aggregates, in combination with the amount of soluble, monomeric Sup35 associated with each [*PSI*$^+$] variant [28].

Consistent with the phenotypic observations, SDD-AGE analysis reveals that each [*PSI*$^+$]^{pfd} isolate is associated with a unique Sup35 profile that differs from the Sup35 profile of its [*PSI*$^+$]^{strong} parent (fig. 15). For example, Sup35 aggregates in [*PSI*$^+$]^{pfd4} migrate faster than Sup35 aggregates in the [*PSI*$^+$]^{strong} parent. Also, the combination of monomeric Sup35 levels and Sup35 aggregates is unique for each [*PSI*$^+$]^{pfd} isolate. Since the [*PSI*$^+$]^{strong} phenotype re-emerges in a wildtype background upon backcrosses and isolation of meiotic progeny, these changes in Sup35 physical state most likely do not represent conformational changes in the protein but rather an alteration in prion propagation leading to the accumulation of both soluble and aggregated pools of Sup35 within the same cell or within individual cells in the population.

Analyzing the number of [*PSI*$^+$] aggregate seeds in Δ*pfd* cells

One possible explanation for the increased rates of [*PSI*$^+$] instability and antisuppression in [*PSI*$^+$]^{pfd} strains is a reduction in [*PSI*$^+$] aggregate seeds compared to wildtype cells. One way to measure the number of heritable [*PSI*$^+$] units, termed propagons, is to add GdnHCl to a culture of exponentially growing cells, plate aliquots of this culture over time on rich medium where [*PSI*] state can be scored, and monitor the loss of [*PSI*$^+$] from the population of cells as a function of cell generations in rich medium with GdnHCl [29, 30]. Since GdnHCl inhibits the molecular chaperone Hsp104 and therefore blocks fragmentation of

Sup35 complexes, existing prion complexes are essentially frozen by this treatment and can be subsequently partitioned to daughter cells. Work from Brian Cox and Mick Tuite has shown that this treatment causes [*PSI*$^+$] aggregates to become larger and be retained in the mother cell, so that continued cell division generates cells that have not inherited any [*PSI*$^+$] aggregates and are therefore [*psi*$^-$] [29, 31]. While such an assay does not evoke a linear and random dilution of [*PSI*$^+$] aggregates into daughters, exposure to GdnHCl and subsequent cell growth does provide a parameter that describes Sup35 physical state in the cell by determining the relative number of transmissible prion complexes (propagons), indicated by the number of recovered [*PSI*$^+$] colonies.

To determine the relative propagon numbers in wildtype and Δ*pfd* strains, I performed GdnHCl curing experiments in wildtype, Δ*pfd2* and Δ*pfd5* cells (fig. 16). The kinetics of curing show that [*PSI*$^+$] is most rapidly lost in Δ*pfd5* cells, followed by Δ*pfd2* and finally by wildtype cells. These results indicate that Δ*pfd2* and Δ*pfd5* cells on average contain less heritable aggregates than the wildtype [*PSI*$^+$]^{strong} parent. Parallel to this, [*PSI*$^+$]^{pfd} isolates 2 and 5 do show some increase in the level of soluble Sup35 as compared to the [*PSI*$^+$]^{strong} parent when assayed by SDD-AGE (fig. 15), so it is possible that this higher level of soluble Sup35 is related to the more rapid loss of [*PSI*$^+$] in Δ*pfd2* and Δ*pfd5* cells. A decrease in the number of [*PSI*$^+$] complexes in Δ*pfd2* and Δ*pfd5* cells could lead to the observed accumulation of soluble Sup35 because in that case, Δ*pfd* cells would have less [*PSI*$^+$] aggregates to recruit soluble Sup35 and convert it into the aggregated prion form, and any increase in soluble Sup35 will result in an antisuppressor phenotype, which is observed in [*PSI*$^+$]^{pfd} isolates.

Expression levels of Sup35 and other chaperone proteins are not altered in Δ*pfd* mutants

It is possible that Δ*pfd* mutants destabilize [*PSI*$^+$] indirectly, through the action of another factor, and possibly through another cellular chaperone. The molecular chaperone network in eukaryotic cells functions so that when one chaperone protein is disabled, oftentimes the expression level of another chaperone will be affected to compensate for the loss of function [13]. To test whether loss of any prefoldin subunit affects the expression of other chaperones, I analyzed the expression levels of Hsp70 proteins Ssb1, Ssb2, Ssa1, Ssa3, Ssa4 and Hsp104 by SDS-PAGE of cell lysates, followed by immunoblotting (fig. 17). The gels show that the levels of Ssb1, Ssb2, Ssa1, Ssa3, Ssa4 and Hsp104 remained unchanged in Δ*pfd* mutants regardless of their [*PSI*] state compared to wildtype cells. These experiments reveal that the loss of any one prefoldin subunit in both [*PSI*$^+$] and [*psi*$^-$] cells does not alter the expression levels of major Hsp70 proteins, nor of the molecular disaggregase Hsp104. This result indicates that none of the major Hsp70 proteins, nor Hsp104, are responsible for the destabilization of [*PSI*$^+$] observed in Δ*pfd* cells.

It is also possible that Δ*pfd* mutants affect [*PSI*$^+$] because of an alteration in Sup35 levels. Altering Sup35 levels could change the balance between soluble and aggregated Sup35 in [*PSI*$^+$] cells, and result in an accumulation of soluble Sup35 which would lead to an antisuppressor phenotype. However, SDS-PAGE followed by immunoblotting reveals that the loss of any prefoldin subunit does not affect the expression of Sup35 (fig. 17). Therefore, the destabilization of [*PSI*$^+$] observed in Δ*pfd* mutants is not likely to be the result of a change in the expression levels of Sup35.

Discussion

This study has revealed that loss of prefoldin function can be mutagenic to cells. This has allowed me to isolate dominant mutations that affect prion propagation. These dominant mutations fall into five distinct linkage groups. None of the five isolated dominant antisuppressor mutations are linked to *HSP104*, but isolates 2 and 5 show genetic linkage to the *SUP35* locus, with isolate 5 showing tight genetic linkage to the Sup35 ORF. In addition to this, loss of any single prefoldin subunit destabilizes [*PSI*$^+$] propagation.

In this study, I have also shown that Δ*ssb1*Δ*ssb2* mutants exhibit a [*PSI*$^+$]-specific growth defect, and I envision at least two possible explanations for this observation. First, [*PSI*$^+$] prion aggregates may be toxic to the cell, but wildtype cells can mediate that toxicity with the help of the chaperone network, including the Ssb co-translational chaperones. In that situation, the toxic effect of [*PSI*$^+$] aggregates would only be observed in Δ*ssb1*Δ*ssb2* cells where the chaperone network is impaired. To test whether prion aggregates in general are toxic to yeast, the growth rates of Δ*ssb1*Δ*ssb2* mutants in combination with other yeast prions, such as [*URE3*], can be analyzed. Another possibility is that the combination of [*PSI*$^+$] and Δ*ssb1*Δ*ssb2* has a detrimental effect on translation, resulting in a slow cell growth defect. [*PSI*$^+$] impairs translation termination and results in translational read-through, while Δ*ssb1*Δ*ssb2* cells contain few translating ribosomes [3]. To test whether [*PSI*$^+$] and Δ*ssb1*Δ*ssb2* together overwhelm the translational machinery, translation termination can be restored by introducing Sup35's C-terminal functional domain. If Sup35-C restores cell growth rate, then Δ*ssb1*Δ*ssb2* [*PSI*$^+$] cells show a growth defect because of translational problems. However, if Sup35-C does not restore cell growth rate, this result implies that

something other than translation is impaired in Δ*ssb1*Δ*ssb2* [*PSI*$^+$] cells, and it may lend credibility to the idea that [*PSI*$^+$] prion aggregates have some toxic effect on the cell.

This study has shown that disruptions in the prefoldin complex are mutagenic to the cell, which has allowed me to isolate novel dominant modulators of Sup35 state. The mechanism of mutagenesis in prefoldin mutants is unclear. The only proven native prefoldin substrates are actin and tubulin, but it is possible that prefoldin may assist in the folding of many substrates since it is found in archaea, which do not possess actin or tubulin [14, 15, 17]. If one of prefoldin's targets is involved in, for example, the DNA damage response, then loss of prefoldin may affect the DNA damage response pathway and in turn lead to an accumulation of mutations in the cell. However, disruptions in prefoldin function have recently been shown to lead to defects in the tubulin cytoskeleton, and these defects increase the rate of mini-chromosome loss, so it is possible that the dominant antisuppressor mutations that I have isolated arose as a result of improper chromosome segregation in Δ*pfd* mutants [32].

Genetic data show that [*PSI*$^+$]^{pfd5} is carrying a mutation in Sup35, but outside of the prion domain. It is possible that the [*PSI*$^+$]^{pfd5}'s mutation lies in Sup35's M region. The M region of Sup35 has been shown to be necessary for the faithful propagation of [*PSI*$^+$] variants, so this type of mutation might alter Sup35 aggregate kinetics, leading to an increase in soluble Sup35 and producing the dominant antisuppressor phenotype [33]. It is also possible that isolate 5's mutation lies in Sup35's C region. This would be a surprising result because so far no Sup35 C region mutations have been shown to alter [*PSI*$^+$] aggregates.

Deletion of *tub3* phenocopies prefoldin mutant cytoskeletal defects, and destabilizes [*PSI*$^+$] similarly to *pfd* mutants. It is possible that the cytoskeleton plays a role in [*PSI*$^+$] regulation, as alterations in the actin cytoskeleton can disrupt the propagation of [*PSI*$^+$]^{weak} [34, 35]. However, the destabilization of [*PSI*$^+$] in Δ*tub3* did not lead to as broad of a spectrum of [*PSI*$^+$] colony color phenotypes as was observed in Δ*pfd* mutants, so Tub3 and prefoldin may affect [*PSI*$^+$] through different pathways.

In summary, this work has shown that [*PSI*$^+$] propagation is unstable in Δ*pfd* mutants, and that loss of prefoldin function is mutagenic to cells. The mutagenic effect of Δ*pfd* has allowed me to isolate mutants that affect the link between [*PSI*$^+$] phenotype and Sup35 state dominantly. One possible explanation for the observed loss of correlation between Sup35 state and [*PSI*$^+$] phenotype in Δ*pfd* mutants is that they propagate a lower number of [*PSI*$^+$] complexes, which may allow for the accumulation of soluble Sup35 in cells. Loss of prefoldin function in Δ*pfd* mutants does not affect the expression levels of Sup35 and of major chaperones in the cell, so the observed unstable propagation of [*PSI*$^+$] in Δ*pfd* mutants probably occurs through a pathway that is unrelated to Sup35 and to major chaperone proteins.

Methods

Plasmid construction

Sup35 prion domain point mutant plasmids were kindly provided by Dr. Chih-Yen King, Institute of Molecular Biology, Academia Sinica, Taiwan, R.O.C., but they were modified to include the KanMX4 cassette. The KanMX4 cassette was PCR amplified from the pFA6a-KanMx4 vector, with added BstBI ends (forward primer: ttcgaagatctgtttagcttgcc, reverse primer: ttcgaactggatggcggcgttag), then cloned into the BstBI site in the *URA3* marker in the original plasmids [36]. The klTRP1MX cassette used for creating Δ*pfd4* was constructed from a pFA6a-KanMX4 backbone by PCR amplification of klTRP1 from the pYM3 vector with a PCR-introduced NcoI 5' overhang, and a SacI 3' overhang (forward primer: ccatggatgctcgttaaagtgtgtgg, reverse primer: gagctcctattgagaggcctgctggat) [37]. The klTRP1 PCR fragment was cloned into the NcoI and SacI digested pFA6a-KanMX4 backbone. NcoI/SacI digestion of pFA6a-KanMX4 removes the KanR gene and T_{tef} terminator, so the T_{tef} terminator was cloned back into the EcoRI digested pFA6a-klTRP1 plasmid by PCR amplification of T_{tef} from the parent pFA6a-KanMX4 plasmid with added EcoRI sites at the 5' and 3' ends (forward primer: gaattcactgacaataaaaagattctt, reverse primer: gaattcctggatggcggcgttagtatc). Proper orientation of T_{tef} after cloning was confirmed by PCR verification (forward primer: ccgttgatgatgtccttcaac, reverse primer: cagatgatgtcgaggcgaaa). The constructed pFA6a-klTRP1 cassette was successfully used to generate Δ*pfd4*::klTRP1 mutants that could grow in the absence of tryptophan, confirming that the klTRP1 sequence can confer tryptophan autotrophy.

Strain construction

All strains are derivatives of 74D-694 (*ade 1-14 trp 1-289 his3Δ200, ura3-52 leu2-3,112*) [1]. The accession numbers of all deletion mutants and [*PSI*$^{+}$]^{pfd} isolates are listed in tables 3 and 5, respectively. [*PSI*$^{+}$]^{strong} deletion mutants Δ*ssb1,* Δ*ssb2,* Δ*pfd1,* Δ*pfd3,* Δ*pfd4,* Δ*pfd6,* Δ*rbl2,* and Δ*tub3* were generated by PCR amplification of various selectable markers in MX cassettes, followed by transformation into diploid [*PSI*$^{+}$] yeast strain SLL 3071 (see table 1 for a list of MX cassettes and primers used for creating the deletion mutants) [36, 38]. Gene disruption was confirmed by PCR amplification of genomic DNA isolated from diploids (see table 2 for a list of primers used to verify gene disruption). The confirmed diploids were sporulated; 2:2 segregation of selectable markers and mating types was confirmed by replica plating to selective medium, and deletion mutants were recovered from the meiotic progeny. Δ*pfd2* [*PSI*$^{+}$]^{strong} and Δ*pfd5* [*PSI*$^{+}$]^{strong} were made by Andrew Kusmierczyk by PCR amplification of the hphMX4 cassette from the pFA6a-hphMX4 plasmid, transformation of the PCR product into the wildtype [*PSI*$^{+}$]^{strong} strain SLL 2606, selection of transformants on YPD+Hyg, and PCR verification of correct cassette integration (see tables 1 and 2 for primer sequences) [39]. Δ*pfd3* [*PSI*$^{+}$]^{weak} was made by PCR amplification of the KanMX cassette, and transformation of the PCR product into the haploid [*PSI*$^{+}$]^{weak} parent strain SLL 2600. Δ*pfd3* [*PSI*$^{+}$]^{weak} transformants were plated on selective medium, and correct integration of the knockout cassette was confirmed by PCR.

Δ*sup35* deletion in the diploids [*PSI*$^{+}$]^{pfd2} and [*PSI*$^{+}$]^{pfd5} was created by PCR amplification of the pFA6a-KanMX4 cassette, transformation of the PCR product into yeast, selection of transformants on YPD+G418, and PCR verification of correct integration [36]. The resultant Δ*sup35*/*SUP35* diploids were transformed with pRS306-35$_{p}$Sup35 linearized by

PpuMI and targeted to the *URA3* locus. Transformants were selected by growth on medium lacking uracil. All deletion mutants were cured by treatment with 3mM GdnHCl and/or Hsp104 overexpression, as indicated in each experiment. Hsp104 was overexpressed by transforming yeast with the URA3 p2UD104 plasmid where Hsp104 overexpression is driven by the GPD promoter. [PSI^+] yeast were transformed with the p2UD104 plasmid, and transformants were selected by uracil prototrophy. Uracil prototrophs were grown overnight in YPD to allow for the loss of the p2UD104 plasmid, and then plated on YPD where [*psi*$^-$] state could be scored by the appearance of red colonies. Red [*psi*$^-$] colonies were grown on medium containing 5-FOA, which counterselects against uracil prototrophs. Colonies that can grow on medium containing 5-FOA have lost the p2UD104 plasmid. After growth on 5-FOA, cells were struck on YPD to confirm [*psi*$^-$] state by the growth of red colonies, and these [*psi*$^-$] strains were used in experiments as indicated. Double, triple, and quadruple combinations of deletion mutants were created by mixing two deletion mutants on YPD and incubating overnight at 30°C to allow zygote formation. The next morning, mating medium was replica plated to double selective medium that only allows for the growth of newly formed diploids, but not of the haploid parents. Resulting diploids were sporulated and dissected, 2:2 segregation of mating types and parental deletion markers was confirmed by replica plating to selective media, and the desired double deletion haploid mutant was recovered from meiotic progeny based on the presence of both parental deletion markers. The process was repeated as described to generate triple and quadruple mutants.

Spontaneous [PSI^+] induction

Exponentially growing cells were plated on synthetic defined medium lacking adenine (csm-ade) and incubated at 30°C until colonies were visible. To calculate the total number of cells

plated on csm-ade plates, cells were also plated on rich medium (YPD). The percentage of cells spontaneously acquiring [*PSI*$^+$] was calculated as the ratio of colonies on csm-ade to that on YPD. To confirm that adenine prototrophs were indeed [*PSI*$^+$], colonies from csm-ade plates were replica plated to ¼ YEPD + 3mM GdnHCl and restruck to YPD. Strains reverting to adenine auxotrophs by this treatment were confirmed to be [*PSI*$^+$].

Quantitative curing of [*PSI*$^+$]

Quantitative curing was performed as described previously [29]. Exponentially growing [*PSI*$^+$] wildtype and Δ*pfd* cultures were maintained in YPD + 3mM GdnHCl. Culture growth and generation number were monitored by OD_{600}, and cultures were diluted as necessary for maintenance of exponential growth. During growth in YPD + 3mM GdnHCl, cell culture aliquots were taken, washed three times in water, then plated on YPD where [*PSI*] state was scored by colony color. Gradual loss of white [*PSI*$^+$] colonies and the appearance of red [*psi*$^-$] colonies during growth in YPD + 3mM GdnHCl indicates that the [*PSI*$^+$] Δ*pfd* mutants analyzed by this method are true [*PSI*$^+$], and not adenine revertants.

Protein analysis

Sup35 protein aggregates were analyzed by semi-denaturing detergent agarose gel electrophoresis (SDD-AGE) essentially as described, except that the lysis buffer contained 10 mM NaPi (pH 7.5), 100 mM NaCl, 1 mM DTT, 0.48 mg/mL pefabloc, and 0.005 mg/mL pepstatin [28, 40]. Immunoblotting was performed as described previously [41]. SDS-PAGE followed by immunoblotting was done as described previously [41], but cell lysates were prepared as described in [42]. Cells from log phase cultures OD_{600} 0.4-0.6 were collected by centrifugation, washed once in water, then resuspended in 0.05M NaOH for 5

minutes at room temperature. After incubation in NaOH, cells were collected by centrifugation, the NaOH supernatant was discarded, cell pellets were boiled in SDS sample buffer and then loaded on an SDS-PAGE gel.

[*PSI*$^+$]^{pfd} typing with a series of Sup35 prion domain mutants

[*PSI*$^+$]^{pfd} isolates and [*PSI*$^+$]^{strong} and [*PSI*$^+$]^{weak} controls were transformed with a series of KanR Sup35 prion domain point mutant or wildtype Sup35 plasmids donated by Dr. C. King and described above. Transformants were selected on YPD + G418. G418-resistant colonies were inoculated into liquid YPD + G418, and grown overnight so they were in exponential phase for spotting on ¼ YEPD + G418 (OD_{600} 0.3 – 0.6). The exponentially growing cultures were diluted into water in a 5-fold serial dilution, and then spotted on ¼ YEPD + G418 and incubated at 30^o for 3-5 days to allow growth. The resulting colonies on ¼ YEPD + G418 were photographed, and analyzed for the colony color that is produced by the interaction of each [*PSI*$^+$] isolate and a plasmid-encoded Sup35 wildtype or mutant molecule.

Yeast doubling time calculations

Exponentially growing yeast cultures were diluted from YPD into either YPAD or YPAD + 3mM GdnHCl so that the starting OD_{600} was 0.1. Cultures were grown at 30^{o}C with shaking, and over time aliquots were taken and their OD_{600} was determined. OD_{600} readings were followed until cultures reached OD_{600} 1.2, when they began to enter stationary phase. The OD_{600} readings were graphed in Excel, and doubling times during exponential growth were determined from the slope of the line representing the exponential phase of growth

(OD_{600} 0.1-0.6). The indicated doubling times for each sample are the result of three independent experiments.

Determination of Δ*pfd* effects on [*PSI*$^+$] propagation

Exponentially growing YPAD cultures of wildtype [*PSI*$^+$]^{strong}, wildtype [*PSI*$^+$]^{weak}, and [*PSI*$^+$] Δ*pfd*, Δ*ssb*, and Δ*pfd*Δ*ssb* mutants were plated on ¼ YEPD and incubated for 3-4 days at 30°C to allow colony growth. Resultant colonies were scored by color for [*PSI*] state. To determine the effect of Δ*pfd* and Δ*ssb* mutants on [*PSI*$^+$]^{strong} propagation, any change from the white colony [*PSI*$^+$]^{strong} parental phenotype in [*PSI*$^+$]^{strong} wildtype and Δ*pfd* and Δ*ssb* colonies, such as the appearance pink or red colonies, was scored as a change in [*PSI*] state. To determine the effect of Δ*pfd3* on [*PSI*$^+$]^{weak} propagation, any change from the pink colony [*PSI*$^+$]^{weak} parental phenotype in wildtype and [*PSI*$^+$]^{weak} Δ*pfd3* colonies, such as the appearance white or red colonies, was scored as a change in [*PSI*] state. The percent of colonies with a change in [*PSI*] state out of total plated colonies for each sample was determined. The ratio of the rates of [*PSI*] state change in Δ*pfd* and Δ*ssb* cells compared to wildtype parent [*PSI*$^+$]^{strong} or [*PSI*$^+$]^{weak} cells was calculated, and this ratio value is referred to as the fold difference in the change in [*PSI*] state in Δ*pfd* and Δ*ssb* compared to wildtype cells. [*PSI*$^+$] state of the spontaneously occurring pink and white colonies that differ from the corresponding [*PSI*$^+$] parent was confirmed by curing on YPD + 3mM GdnHCl. Results represent at least three independent experiments for each wildtype, Δ*pfd* and Δ*ssb* [*PSI*$^+$] strain.

Sequencing the NM region of Sup35

The Sup35 NM region (150 nucleotides upstream of amino acid 1 – amino acid 310) in [*PSI*$^+$]^{pfd} isolates 1-6 was sequenced by PCR amplification of the indicated region with primers TTTTTCACTCGACCAAAGCTCC and AAGTACCAACCTTGTCTGCCTG. Triplicate PCR products for each [*PSI*$^+$]^{pfd} were sequenced, ensuring that there were no PCR-introduced mutations in the coding sequence.

Transferring Δ*pfd* [*PSI*$^+$] phenotypes into a wildtype background

Δ*pfd1*, Δ*pfd2,* Δ*pfd3,* Δ*pfd5,* and Δ*pfd6* [*PSI*$^+$]^{strong} cells were mated to the wildtype [*psi*$^-$] yeast strain SY 457 (*ade 1-14 TRP1 his3Δ200, ura3-52 leu2-3,112*) by mixing the two cells types on solid rich medium (YPD), and incubating overnight at 30°C to allow zygote formation. The next morning, the mating medium was replica plated to double selective medium (synthetic medium –trp to select for the SY 457 parental genome, and also selecting for the Δ*pfd* deletion marker listed for each mutant in table 1) that allows only for the growth of newly formed diploids, but not for the growth of either parent. Δ*pfd4* [*PSI*$^+$]^{strong} was crossed to wildtype [*psi*$^-$] strain SLL 3251 by mixing parent cells on YPD and incubating at 30°C for 4-5 hours to allow zygote formation. Zygotes were isolated by micromanipulation. All six combinations of Δ*pfd*/wildtype diploids were sporulated and dissected. 2:2 Δ*pfd* deletion marker segregation was confirmed in the meiotic progeny by replica plating to selective medium, and haploid state was confirmed by 2:2 segregation of each mating type. The spontaneously occurring pink colony [*PSI*$^+$]^{pfd} phenotype was recovered in wildtype meiotic progeny from above dissections that did not contain the Δ*pfd* deletion marker, and these wildtype [*PSI*$^+$]^{pfd} isolates were used in subsequent SDD-AGE, Sup35 prion domain mutant interaction, and genetic analyses as indicated.

Cell crosses between [*PSI*$^+$]^{pfd} isolates and wildtype [*psi*$^-$], [*PSI*$^+$]^{strong}, Δ*hsp104*, *SUP35*::GFP

The pink isolates [*PSI*$^+$]^{pfd1} (MSY 207), [*PSI*$^+$]^{pfd4} (MSY 196), and [*PSI*$^+$]^{pfd5} (MSY 203) were crossed to wildtype [*psi*$^-$] strain SLL 3252 by mixing each mating partner on YPD, incubating at 30°C to allow zygote formation, then isolating zygotes by micromanipulation. Diploid state was confirmed by sporulation, and transfer of the [*PSI*$^+$]^{pfd} pink colony phenotype to diploid progeny was confirmed by growth on YPD in comparison with parent [*PSI*$^+$]^{pfd} and [*psi*$^-$] controls. The resulting diploids were used to analyze segregation of [*PSI*$^+$]^{pfd} pink colony color phenotype in meiotic progeny. 2:2 segregation of mating type phenotypes was confirmed by replica plating dissections onto selective medium. If the [*PSI*$^+$]^{pfd} pink colony color phenotype is inherited by all four meiotic progeny, this indicates dominant cytoplasmic inheritance that is a characteristic of [*PSI*$^+$]. 2 pink : 2 white colony color segregation indicates that the [*PSI*$^+$]^{pfd} parent is carrying a dominant anti-suppressor that leads to an increase in translation fidelity, and thereby in the presence of [*PSI*$^+$] aggregates leads to pink rather than white colonies on rich medium.

The pink isolates [*PSI*$^+$]^{pfd1} (MSY 207), [*PSI*$^+$]^{pfd4} (MSY 196), and [*PSI*$^+$]^{pfd5} (MSY 203) were crossed to wildtype [*PSI*$^+$]^{strong} strain SLL 3250 by mixing each mating partner on YPD, incubating at 30°C to allow zygote formation, then isolating zygotes by micromanipulation. Diploid state was confirmed by sporulation, and transfer of the dominant [*PSI*$^+$]^{pfd} pink colony phenotype to diploid progeny was confirmed by growth on YPD next to parent [*PSI*$^+$]^{pfd} and [*PSI*$^+$]^{strong} controls. The resulting diploids were used to analyze segregation of [*PSI*$^+$]^{pfd} pink colony color phenotype in meiotic progeny. 2:2 segregation of mating type phenotypes was confirmed by replica plating dissections onto selective medium. If the

[*PSI*$^{+}$]^{pfd} pink colony color phenotype is inherited by all four meiotic progeny, this indicates dominant cytoplasmic inheritance that is a characteristic of [*PSI*$^{+}$]. 2 pink : 2 white colony color segregation indicates that the [*PSI*$^{+}$]^{pfd} parent is carrying a dominant anti-suppressor that leads to an increase in translation fidelity, and thereby in the presence of [*PSI*$^{+}$] aggregates leads to pink rather than white colonies on rich medium.

Hsp104-overexpression cured isolates of [*psi*$^{-}$]^{pfd1} (MSY 233), [*psi*$^{-}$]^{pfd4} (MSY 222), and [*psi*$^{-}$]^{pfd5} (MSY 229) were crossed to wildtype [*PSI*$^{+}$]^{strong} strain SLL 3250 by mixing each mating partner on YPD, incubating at 30°C to allow zygote formation, then isolating zygotes by micromanipulation. Diploid state was confirmed by sporulation, and transfer of the dominant [*PSI*$^{+}$]^{pfd} pink colony phenotype to diploid progeny was confirmed by growth on YPD next to parent [*psi*$^{-}$]^{pfd} and [*PSI*$^{+}$]^{strong} controls. The resulting diploids were used to analyze segregation of [*PSI*$^{+}$]^{pfd} pink colony color phenotype in meiotic progeny. 2:2 segregation of mating type phenotypes was confirmed by replica plating dissections onto selective medium. If the [*PSI*$^{+}$]^{pfd} pink colony color phenotype is inherited by all four meiotic progeny, this indicates dominant cytoplasmic inheritance that is a characteristic of [*PSI*$^{+}$]. 2 pink : 2 white colony color segregation indicates that the [*PSI*$^{+}$]^{pfd} parent is carrying a dominant anti-suppressor that leads to an increase in translation fidelity, and thereby in the presence of [*PSI*$^{+}$] aggregates leads to pink rather than white colonies on rich medium.

[*PSI*$^{+}$]^{pfd} isolates 1-5 were crossed to Δ*hsp104::LEU2* obligate [*psi*$^{-}$] strains SLL 3058 a or SY 420 α, according to their mating types. [*PSI*$^{+}$]^{pfd6} is not able to mate with cells of the opposite mating type, so it was not analyzed in cell crosses. The dominant anti-suppressor mutation in [*PSI*$^{+}$]^{pfd6} may cause the observed mating defect, but this was not analyzed. The

two mating partners [*PSI*$^{+}$]^{pfd} and Δ*hsp104::LEU2* were mixed on YPD, incubated at 30^{o}C to allow zygote formation, and zygotes were isolated by micromanipulation. Resulting diploids were sporulated and dissected. 2:2 segregation of mating types and *LEU2* was confirmed by replica plating to selective medium. The two Δ*hsp104::LEU2* meiotic progeny from each tetrad will always give rise to red [*psi*] colonies, so linkage between the [*PSI*$^{+}$]^{pfd} *HSP104* allele and the [*PSI*$^{+}$]^{pfd} pink colony color phenotype was analyzed. Recovery of leu- meiotic progeny that carry the [*PSI*$^{+}$]^{pfd} *HSP104* allele and produce white colonies on rich medium indicates there is no linkage between [*PSI*$^{+}$]^{pfd} *HSP104* and the isolated unknown dominant mutation that causes the pink colony color phenotype.

[*PSI*$^{+}$]^{pfd} isolates 1-5 were crossed to *SUP35*::GFP strains SY 80 α or SY 81 a, according to their mating types, to analyze linkage between the unmarked [*PSI*$^{+}$]^{pfd} *SUP35* allele and the pink colony color phenotype. Mating partners were mixed on YPD, incubated at 30^{o}C to allow zygote formation, and zygotes were isolated by micromanipulation. The isolated zygotes were sporulated and dissected. 2:2 segregation of mating types was confirmed by replica plating to selective medium, and 2:2 segregation of unmarked [*PSI*$^{+}$]^{pfd} *SUP35* : *SUP35*::GFP was analyzed by PCR (forward primer: TTTGTATAGTTCATCCATGCCAT, reverse primer: ATGGCTAGCAAAGGAGAA). If the two [*PSI*$^{+}$]^{pfd} *SUP35* meiotic progeny always give rise to pink colonies while the two *SUP35*::GFP alleles are always found with white colonies, this suggests linkage between [*PSI*$^{+}$]^{pfd} *SUP35* and the pink colony phenotype, indicating that perhaps a mutation in [*PSI*$^{+}$]^{pfd} *SUP35* is responsible for the pink colony color phenotype.

To determine if [*PSI*$^+$]^{pfd2} and [*PSI*$^+$]^{pfd5} carry a mutation in or very tightly linked to their *SUP35* alleles that causes the pink colony color phenotype, [*PSI*$^+$]^{pfd2} / [*PSI*$^+$]^{pfd2} and [*PSI*$^+$]^{pfd5} / [*PSI*$^+$]^{pfd5} diploids were made by crossing the original [*PSI*$^+$]^{pfd2} and [*PSI*$^+$]^{pfd5} isolates (MSY 148 and MSY 203, respectively) to otherwise isogenic yeast of the opposite mating type ([*PSI*$^+$]^{pfd2} = MSY 303, and [*PSI*$^+$]^{pfd5} = MSY 305). The opposite mating types were recovered from dissections of Hsp104 overexpression cured [*psi*$^-$]^{pfd2} and [*psi*$^-$]^{pfd5} to [*PSI*$^+$]^{strong} (described above), where the [*PSI*$^+$]^{pfd} mutations produced 2 white : 2 pink colony color segregants. The 2 pink colony color segregants carry the unknown [*PSI*$^+$]^{pfd} mutation, and these were crossed with the parental original isolates [*PSI*$^+$]^{pfd2} and [*PSI*$^+$]^{pfd5} of the opposite mating type. Mating partners were mixed on YPD and incubated at 30ºC to allow zygote formation. Zygotes were isolated by micromanipulation, and diploid state was confirmed by sporulation. Next, one *SUP35* allele was deleted in each diploid by PCR amplification of the pFA6a-KanMX4 cassette and primers listed in table 1, followed by transformation of the PCR product into yeast. Transformants were selected on YPD + G418, and Δ*sup35* was confirmed by PCR with primers listed in table 2. A second wildtype copy of *SUP35* was integrated into the *URA3* locus with PpuMI digested pRS306-35$_p$Sup35. Transformants were selected by uracil prototrophy, sporulated, and dissected. 2:2 segregation of mating types and [*PSI*$^+$]^{pfd} *SUP35* : wildtype *SUP35::URA3* was confirmed by replica plating to selective medium, though in this case many incomplete tetrads were recovered because Sup35 is essential, so any meitotic progeny that did not inherit either *SUP35* allele were inviable. G418-sensitive ura- spores carry only the [*PSI*$^+$]^{pfd} *SUP35* allele, so the linkage between the pink colony phenotype and the [*PSI*$^+$]^{pfd} *SUP35* allele was analyzed. If the G418-sensitive ura- meiotic progeny always produce pink colonies, this indicates that the unknown dominant anti-suppressor mutation is located in *SUP35*. Recovery of G418-

sensitive ura- meiotic progeny that give rise to white colonies on rich medium indicates that the [*PSI*$^{+}$]^{pfd} *SUP35* allele is not carrying the unknown dominant anti-suppressor mutation.

Acknowledgements

I would like to thank Andrew Kusmierczyk for starting the prefoldin project, Chris Wells for his work with prefoldin mutants, and all the members of the Serio and Laney labs for their suggestions and support during the course of this project.

References:

1. Chernoff, Y.O., et al., *Role of the chaperone protein Hsp104 in propagation of the yeast prion-like factor [psi+].* Science, 1995. **268**(5212): p. 880-4.
2. Jung, G., et al., *A role for cytosolic hsp70 in yeast [PSI(+)] prion propagation and [PSI(+)] as a cellular stress.* Genetics, 2000. **156**(2): p. 559-70.
3. Nelson, R.J., et al., *The translation machinery and 70 kd heat shock protein cooperate in protein synthesis.* Cell, 1992. **71**(1): p. 97-105.
4. Siegers, K., et al., *Compartmentation of protein folding in vivo: sequestration of non-native polypeptide by the chaperonin-GimC system.* EMBO J, 1999. **18**(1): p. 75-84.
5. Chernoff, Y.O., et al., *Evidence for a protein mutator in yeast: role of the Hsp70-related chaperone ssb in formation, stability, and toxicity of the [PSI] prion.* Mol Cell Biol, 1999. **19**(12): p. 8103-12.
6. Jones, G.W., Y. Song, and D.C. Masison, *Deletion of the Hsp70 chaperone gene SSB causes hypersensitivity to guanidine toxicity and curing of the [PSI+] prion by increasing guanidine uptake in yeast.* Mol Genet Genomics, 2003. **269**(3): p. 304-11.
7. Chacinska, A., et al., *Ssb1 chaperone is a [PSI+] prion-curing factor.* Curr Genet, 2001. **39**(2): p. 62-7.
8. McCready, S.J., B.S. Cox, and C.S. McLaughlin, *The extrachromosomal control of nonsense suppression in yeast: an analysis of the elimination of [psi+] in the presence of a nuclear gene PNM.* Mol Gen Genet, 1977. **150**(3): p. 265-70.
9. Doel, S.M., et al., *The dominant PNM2- mutation which eliminates the psi factor of Saccharomyces cerevisiae is the result of a missense mutation in the SUP35 gene.* Genetics, 1994. **137**(3): p. 659-70.
10. Wegrzyn, R.D., et al., *Mechanism of prion loss after Hsp104 inactivation in yeast.* Mol Cell Biol, 2001. **21**(14): p. 4656-69.
11. Siegers, K., et al., *TRiC/CCT cooperates with different upstream chaperones in the folding of distinct protein classes.* Embo J, 2003. **22**(19): p. 5230-40.
12. Siegers, K., et al., *TRiC/CCT cooperates with different upstream chaperones in the folding of distinct protein classes.* EMBO J, 2008. **27**(1): p. 301.
13. Young, J.C., et al., *Pathways of chaperone-mediated protein folding in the cytosol.* Nat Rev Mol Cell Biol, 2004. **5**(10): p. 781-91.
14. Leroux, M.R., et al., *MtGimC, a novel archaeal chaperone related to the eukaryotic chaperonin cofactor GimC/prefoldin.* EMBO J, 1999. **18**(23): p. 6730-43.
15. Vainberg, I.E., et al., *Prefoldin, a chaperone that delivers unfolded proteins to cytosolic chaperonin.* Cell, 1998. **93**(5): p. 863-73.
16. Siegert, R., et al., *Structure of the molecular chaperone prefoldin: unique interaction of multiple coiled coil tentacles with unfolded proteins.* Cell, 2000. **103**(4): p. 621-32.
17. Geissler, S., K. Siegers, and E. Schiebel, *A novel protein complex promoting formation of functional alpha- and gamma-tubulin.* Embo J, 1998. **17**(4): p. 952-66.

18. Martin-Benito, J., et al., *Structure of eukaryotic prefoldin and of its complexes with unfolded actin and the cytosolic chaperonin CCT.* EMBO J, 2002. **21**(23): p. 6377-86.
19. Derkatch, I.L., et al., *Genetic and environmental factors affecting the de novo appearance of the [PSI+] prion in Saccharomyces cerevisiae.* Genetics, 1997. **147**(2): p. 507-19.
20. Derkatch, I.L., et al., *Genesis and variability of [PSI] prion factors in Saccharomyces cerevisiae.* Genetics, 1996. **144**(4): p. 1375-86.
21. Derkatch, I.L., et al., *Dependence and independence of [PSI(+)] and [PIN(+)]: a two-prion system in yeast?* Embo J, 2000. **19**(9): p. 1942-52.
22. Alvarez, P., et al., *Modulation of tubulin polypeptide ratios by the yeast protein Pac10p.* Genetics, 1998. **149**(2): p. 857-64.
23. Liebman, S.W. and M. Cavenagh, *An antisuppressor that acts on omnipotent suppressors in yeast.* Genetics, 1980. **95**(1): p. 49-61.
24. All-Robyn, J.A., et al., *Isolation of omnipotent suppressors in an [eta+] yeast strain.* Genetics, 1990. **124**(3): p. 505-14.
25. Satpute-Krishnan, P. and T.R. Serio, *Prion protein remodelling confers an immediate phenotypic switch.* Nature, 2005. **437**(7056): p. 262-5.
26. Paushkin, S.V., et al., *Propagation of the yeast prion-like [psi+] determinant is mediated by oligomerization of the SUP35-encoded polypeptide chain release factor.* Embo J, 1996. **15**(12): p. 3127-34.
27. King, C.Y., *Supporting the structural basis of prion strains: induction and identification of [PSI] variants.* J Mol Biol, 2001. **307**(5): p. 1247-60.
28. Kryndushkin, D.S., et al., *Yeast [PSI+] prion aggregates are formed by small Sup35 polymers fragmented by Hsp104.* J Biol Chem, 2003. **278**(49): p. 49636-43.
29. Eaglestone, S.S., et al., *Guanidine hydrochloride blocks a critical step in the propagation of the prion-like determinant [PSI(+)] of Saccharomyces cerevisiae.* Proc Natl Acad Sci U S A, 2000. **97**(1): p. 240-4.
30. Cox, B., F. Ness, and M. Tuite, *Analysis of the generation and segregation of propagons: entities that propagate the [PSI+] prion in yeast.* Genetics, 2003. **165**(1): p. 23-33.
31. Satpute-Krishnan, P., S.X. Langseth, and T.R. Serio, *Hsp104-dependent remodeling of prion complexes mediates protein-only inheritance.* PLoS Biol, 2007. **5**(2): p. e24.
32. Lacefield, S., M. Magendantz, and F. Solomon, *Consequences of defective tubulin folding on heterodimer levels, mitosis and spindle morphology in Saccharomyces cerevisiae.* Genetics, 2006. **173**(2): p. 635-46.
33. Bradley, M.E. and S.W. Liebman, *The Sup35 domains required for maintenance of weak, strong or undifferentiated yeast [PSI+] prions.* Mol Microbiol, 2004. **51**(6): p. 1649-59.
34. Bailleul-Winslett, P.A., et al., *An antiprion effect of the anticytoskeletal drug latrunculin A in yeast.* Gene Expr, 2000. **9**(3): p. 145-56.
35. Ganusova, E.E., et al., *Modulation of prion formation, aggregation, and toxicity by the actin cytoskeleton in yeast.* Mol Cell Biol, 2006. **26**(2): p. 617-29.

36. Wach, A., et al., *New heterologous modules for classical or PCR-based gene disruptions in Saccharomyces cerevisiae.* Yeast, 1994. **10**(13): p. 1793-808.
37. Knop, M., et al., *Epitope tagging of yeast genes using a PCR-based strategy: more tags and improved practical routines.* Yeast, 1999. **15**(10B): p. 963-72.
38. Goldstein, A.L., X. Pan, and J.H. McCusker, *Heterologous URA3MX cassettes for gene replacement in Saccharomyces cerevisiae.* Yeast, 1999. **15**(6): p. 507-11.
39. Goldstein, A.L. and J.H. McCusker, *Three new dominant drug resistance cassettes for gene disruption in Saccharomyces cerevisiae.* Yeast, 1999. **15**(14): p. 1541-53.
40. Bagriantsev, S.N., V.V. Kushnirov, and S.W. Liebman, *Analysis of amyloid aggregates using agarose gel electrophoresis.* Methods Enzymol, 2006. **412**: p. 33-48.
41. Patino, M.M., et al., *Support for the prion hypothesis for inheritance of a phenotypic trait in yeast.* Science, 1996. **273**(5275): p. 622-6.
42. Kushnirov, V.V., *Rapid and reliable protein extraction from yeast.* Yeast, 2000. **16**(9): p. 857-60.

Figure Captions

Figure 1. Δ*pfd* mutants destabilize the [*PSI*$^{+}$]^{strong} phenotype. A. Exponentially growing cultures of wildtype [*PSI*$^{+}$]^{strong}, wildtype [*psi*$^{-}$], and Δ*pfd3* [*PSI*$^{+}$]^{strong} cells were plated on rich medium (1/4 YEPD). Note the variety of colors of Δ*pfd3* colonies. Δ*pfd3* mutants produce a slight variability in colony size (right panel), compared with wildtype yeast shown in the left and middle panels. Δ*pfd3* [*PSI*$^{+}$]^{strong} was chosen as a representative of [*PSI*$^{+}$]^{strong} destabilization observed in Δ*pfd* mutants because it shows the greatest [*PSI*$^{+}$]^{strong} destabilization phenotype. B. Fold difference in the rate of spontaneous change in the [*PSI*$^{+}$]^{strong} phenotype in Δ*pfd* mutants compared to wildtype cells. Exponentially growing cultures were scored for change in the [*PSI*$^{+}$]^{strong} phenotype following plating on rich medium as indicated by colony color. Change in [*PSI*$^{+}$]^{strong} phenotype is defined as the appearance of pink or red colonies, since wildtype [*PSI*$^{+}$]^{strong} cells grow into uniform white colonies on rich medium with rare 1 in 10^{6} spontaneous change in the white colony color phenotype (compare panels in 1A). [*PSI*] state was confirmed by curing with GdnHCl and by mating to wildtype [*psi*$^{-}$] (data not shown). Error bars represent standard deviation. N = 4902 wildtype [*PSI*$^{+}$]^{strong} colonies were scored from 4 independent experiments, 4007 Δ*pfd1* colonies from 3 experiments, 3748 Δ*pfd2* colonies from 3 experiments, 2454 Δ*pfd3* colonies from 3 experiments, 5178 Δ*pfd4* colonies from 4 experiments, 3321 Δ*pfd5* colonies from 3 experiments, and 5715 Δ*pfd6* colonies from 3 experiments.

Figure 2. Destabilization of [*PSI*$^{+}$] by Δ*pfd* is exacerbated in cells with the [*PSI*$^{+}$]^{weak} phenotype. A. Exponentially growing cultures of wildtype [*PSI*$^{+}$]^{weak}, wildtype [*psi*$^{-}$], and Δ*pfd3* [*PSI*$^{+}$]^{weak} cells were plated on rich medium (1/4 YEPD). Note

the variety of colors of Δ*pfd3* colonies. Δ*pfd3* mutants produce a slight variability in colony size (right panel), compared with wildtype yeast shown in the left and middle panels. Δ*pfd3* [*PSI*$^{+}$]^{weak} was created to determine the destabilizing effect of Δ*pfd* on [*PSI*$^{+}$]^{weak} because Δ*pfd3* had a great destabilizing effect on [*PSI*$^{+}$]^{strong} (see figure 1). B. Fold difference in the rate of spontaneous change in the [*PSI*$^{+}$]^{weak} phenotype in Δ*pfd3* mutants compared to wildtype cells. Exponentially growing cultures were plated on rich medium and scored for change in [*PSI*$^{+}$] phenotype as indicated by colony color. Change in [*PSI*$^{+}$]^{weak} phenotype is defined as the appearance of white or red colonies, since wildtype [*PSI*$^{+}$]^{weak} cells grow into uniform pink colonies on rich medium with rare spontaneous change in the pink colony color phenotype. [*PSI*] state was confirmed by curing with GdnHCl and by mating to wildtype [*psi*$^{-}$] (data not shown). Error bars represent standard deviation. N = 3417 wildtype [*PSI*$^{+}$]^{weak} colonies were scored from 3 independent experiments, and 3037 Δ*pfd3* colonies were scored from 3 independent experiments.

Figure 3. Δ*ssb* mutants do not destabilize the [*PSI*$^{+}$]^{strong} phenotype. Fold difference in the rate of spontaneous change in the [*PSI*$^{+}$]^{strong} phenotype in Δ*ssb*, Δ*pfd* and combination Δ*ssb*Δ*pfd* mutants compared to wildtype cells. Change in [*PSI*$^{+}$]^{strong} phenotype is defined as the appearance of pink or red colonies, since wildtype [*PSI*$^{+}$]^{strong} cells grow into uniform white colonies on rich medium with rare 1 in 10^{6} spontaneous change in the white colony color phenotype. Exponentially growing cultures were plated on rich medium and scored for change in [*PSI*$^{+}$] phenotype as indicated by colony color. [*PSI*] state was confirmed by curing with GdnHCl and by mating to wildtype [*psi*$^{-}$] (data not shown). Error bars

represent standard deviation. N = 4800 Δ*ssb* colonies were scored from 4 independent experiments, 4800 Δ*ssb*Δ*pfd2* colonies were scored from 4 independent experiments, 2664 Δ*ssb*Δ*pfd5* colonies from 3 experiments, and 1393 Δ*ssb*Δ*pfd2*Δ*pfd5* colonies from 3 experiments.

Figure 4. Rates of spontaneous [*PSI*$^+$] induction in Δ*pfd* cells are equivalent to wildtype. Exponentially growing cells were plated on synthetic medium lacking adenine (CSM-ade) to score *de novo* [*PSI*$^+$] appearance, and on rich medium (YPD) to determine the total number of colonies plated. Once colonies were visible on CSM-ade, they were replica plated to ¼ YEPD + 3mM guanidine hydrochloride, and restruck on ¼ YEPD to confirm [*PSI*$^+$] state by curing. Error bars represent standard deviation. Spontaneous [*PSI*$^+$] induction rates in wildtype and Δ*pfd* cells represent data from 3 independent experiments. Spontaneous [*PSI*$^+$] induction was analyzed in approximately 2.4 million wildtype cells, 7.6 million Δ*pfd1* cells, 11.1 million Δ*pfd2* cells, 9.6 million Δ*pfd3* cells, 6.9 million Δ*pfd4* cells, 9.7 million Δ*pfd5* cells, and 12.2 million Δ*pfd6* cells.

Figure 5. Δ*pfd* pink colony color phenotype transmits in cell crosses with wildtype [*psi*$^-$], and is stabilized in a *PFD* wildtype background. A. Schematic diagram showing how the [*PSI*$^+$]^{pfd} phenotype was transferred to wildtype cells by mating. Single Δ*pfd* pink colonies (pink oval) were mixed with wildtype TRP+ [*psi*$^-$] cells (red oval) on YPD and incubated at 30°C to allow zygote formation. Mating medium was replica plated to double selective medium that only allows for the growth of zygotes formed by mating wildtype TRP+ [*psi*$^-$] cells and Δ*pfd* ::selectable marker (indicated for each Δ*pfd* in table 1). The resultant diploids inherit the Δ*pfd* pink colony color phenotype, referred to as [*PSI*$^+$]^{pfd}, and these diploids are

represented by a pink clover shape. The resulting diploids were sporulated and dissected, and the [*PSI*$^{+}$]^{pfd} pink colony color phenotype was recovered in *PFD* wildtype cells, as determined by 2:2 segregation of *PFD*:Δ*pfd-selectable marker* phenotype by replica plating to selective medium. Sup35 physical state was subsequently analyzed in these [*PSI*$^{+}$]^{pfd} *PFD* wildtype cells. B. Indicated strains were plated from exponentially growing cultures onto YPD. 5-fold serial dilution, L to R. Row one shows the parent [*PSI*$^{+}$]^{strong} haploid cells that grow as white colonies on rich medium, and in which Δ*pfd* mutants were created. Row two shows wildtype haploid [*psi*$^{-}$] cells. Row three shows the variability of the [*PSI*$^{+}$]^{pfd} phenotype in a Δ*pfd1* haploid mutant. Notice the range of colony colors in Δ*pfd1*. Row four shows the Δ*pfd1*/*PFD* diploids created by crossing Δ*pfd1* to [*psi*$^{-}$] as explained in A. Notice the range of colony color phenotypes that were transmitted in this cell cross. Row five shows [*PSI*$^{+}$]^{weak} haploid cells which form pink colonies on rich medium. C. Segregation of colony color phenotypes in the meiotic progeny of Δ*pfd1*/*PFD* diploids. The diploids were created by cell crossing as described in A, then sporulated and dissected. The table indicates how many meiotic tetrads inherited each combination of colony color phenotypes (4:0 pink, 3 white:1 pink, 3 pink:1 white, 2 pink:2 white). Notice the variability in the inheritance of colony colors. This variability was at first believed to be due to Δ*pfd*'s destabilization of [*PSI*$^{+}$], but it might also be due to Δ*pfd*'s mutagenic effect on cells. Widltype *PFD* cells with the [*PSI*$^{+}$]^{pfd} pink colony color phenotype from these dissections were subsequently used for the analysis of Sup35 physical state.

Figure 6. [*PSI*$^{+}$]^{pfd} pink isolates can be cured by treatment with guanidine hydrochloride. Indicated strains were struck on ¼ YEPD plates to show that [*PSI*$^{+}$]^{pfd} pink isolates can be cured after treatment with guanidine hydrochloride (GdnHCl). Wildtype (WT) [*PSI*$^{+}$]^{strong} and [*psi*$^{-}$] strains are shown next to [*PSI*$^{+}$]^{pfd} pink isolates and cured [*psi*$^{-}$]^{pfd} strains for color comparison. Plates were incubated for four days at 30°C, and photographed.

Figure 7. [*PSI*$^{+}$]^{pfd} pink isolates 1, 4, and 5 are dominant in cell crosses with [*PSI*$^{+}$]^{strong}. Indicated strains were struck on ¼ YEPD to show that [*PSI*$^{+}$]^{pfd} pink isolates 1, 4, and 5 ([*PSI*$^{+}$]^{pfd1}, [*PSI*$^{+}$]^{pfd4}, [*PSI*$^{+}$]^{pfd5}) transmit their pink colony color phenotype when crossed to wildtype [*PSI*$^{+}$]^{strong} (WT [*PSI*$^{+}$]^{strong} N) cells. Wildtype [*PSI*$^{+}$]^{strong} diploids (WT [*PSI*$^{+}$]^{strong} 2N) are shown next to diploids recovered from crosses between [*PSI*$^{+}$]^{pfd} and [*PSI*$^{+}$]^{strong} ([*PSI*$^{+}$]^{pfd} x [*PSI*$^{+}$]^{strong}). Plates were incubated for four days at 30°C before being photographed.

Figure 8. [*PSI*$^{+}$]^{pfd} variants are a dominant antisuppressor rather than an epigenetic trait. Summary of the [*PSI*$^{+}$]^{pfd} inheritance data. The data is shown in table 6. Both [*PSI*$^{+}$]^{pfd} and [*psi*$^{-}$]^{pfd} cells (pink and red ovals on the left side) produce pink colony-forming diploids (pink clover shape) when crossed to wildtype [*psi*$^{-}$] (red oval) and wildtype [*PSI*$^{+}$] (white oval) cells, indicating that [*PSI*$^{+}$]^{pfd} isolates are carrying a dominant antisuppressor that increases translation fidelity independently of [*PSI*$^{+}$]. The meiotic progeny of the resultant pink diploids always showed 2 pink: 2 white colony color segregation, indicating that [*PSI*$^{+}$]^{pfd} isolates are carrying an antisuppressor mutation with Mendelian inheritance. Shown is a picture of four meiotic progeny on rich medium, representative of 2

pink: 2 white colony color inheritance recovered in meiotic tetrads from the pink colony forming [*PSI*$^{+}$]^{pfd} / wildtype diploids.

Figure 9. Δ*tub3* phenocopies the destabilization of [*PSI*$^{+}$]^{strong} seen in Δ*pfd* mutants, but Δ*rbl2* does not. A. Exponentially growing cultures of wildtype [*PSI*$^{+}$]^{strong}, Δ*rbl2* [*PSI*$^{+}$]^{strong}, and Δ*tub3* [*PSI*$^{+}$]^{strong} cells were plated on rich medium (1/4 YEPD). Note the variety of colors of Δ*tub3* colonies. The Δ*tub3* mutant produces a range of colony sizes. B. Fold difference in the rate of spontaneous change in the [*PSI*$^{+}$]^{strong} phenotype in Δ*tub3* mutants compared to wildtype cells. Exponentially growing cultures were scored for change in the [*PSI*$^{+}$]^{strong} phenotype following plating on rich medium as indicated by colony color. Change in [*PSI*$^{+}$]^{strong} phenotype is defined as the appearance of pink or red colonies, since wildtype [*PSI*$^{+}$]^{strong} cells grow into uniform white colonies on rich medium with rare 1 in 10^{6} spontaneous change in the white colony color phenotype (compare panels in A). [*PSI*] state was confirmed by curing with GdnHCl and by mating to wildtype [*psi*$^{-}$] (data not shown). Error bars represent standard deviation. Destabilization of [*PSI*$^{+}$]^{strong} in Δ*tub3* mutants was analyzed in 3 independent experiments, and a total of 2024 colonies was scored. Destabilization of [*PSI*$^{+}$]^{strong} in wildtype cells was analyzed in 4 independent experiments, and a total of 4902 colonies was scored.

Figure 10. [*PSI*$^{+}$]^{pfd} isolates map to five distinct linkage groups. A. Diagram explaining the cell crossing approach used to place [*PSI*$^{+}$]^{pfd} isolates (pink ovals) into linkage groups. [*PSI*$^{+}$]^{pfd} isolates were crossed to each other in all combinations by mixing both mating partners on YPD and incubating at 30^{o}C to allow zygote formation (pink clover shape). Zygotes were isolated by micromanipulation, and

diploid state was confirmed by sporulation. Meiotic progeny (pink ovals labeled x and y) were recovered by dissection of spores, and 2:2 segregation of mating types was confirmed by replica plating to selective medium. If all meiotic progeny recovered from the cross between [*PSI*$^{+}$]^{pfd} isolates x and y inherit the pink colony color phenotype, this indicates that the dominant antisuppressor mutations carried in [*PSI*$^{+}$]^{pfd} isolates x and y are genetically linked. If meiotic progeny from the cross between [*PSI*$^{+}$]^{pfd} isolates x and y show any deviation from 4:0 pink colony color inheritance, this indicates that [*PSI*$^{+}$]^{pfd} isolates x and y carry genetically unlinked dominant suppressor mutations. In this case, white colonies will arise in meiotic progeny that do not inherit mutation x nor mutation y, producing wildtype white colonies on rich medium. B. Results of the linkage group testing. Each isolate forms an independent linkage group, because each shows deviations from 4:0 pink colony color inheritance in meiotic progeny, as described in A. Note that there is linkage between isolates 2 and 5, and between isolates 1, 3, and 4. Isolates 2 and 5, and isolates 1, 3 and 4 show genetic linkage because cell crosses between 2 and 5, and between 1, 3 and 4 did produce some meiotic tetrads with 4:0 pink colony color segregation.

Figure 11. The mutations carried by [*PSI*$^{+}$]^{pfd} isolates are not linked to *HSP104*. A. Diagram explaining the approach used to test if there is linkage between [*PSI*$^{+}$]^{pfd} isolate mutations and *HSP104*. [*PSI*$^{+}$]^{pfd} isolates (pink oval) were crossed to Δ*hsp104::LEU2* cells (red oval) which cannot propagate [*PSI*$^{+}$]. Both mating partners were mixed on YPD and incubated at 30°C to allow zygote formation. Resultant zygotes (pink clover shape) were isolated by micromanipulation, sporulated, and dissected. Meoitic tetrads always gave rise to two red colonies,

corresponding to Δ*hsp104::LEU2* cells, which cannot propagate [*PSI*$^+$]. 2:2 segregation of mating types and LEU+:leu- was confirmed by replica plating to selective medium. If the [*PSI*$^+$]^{pfd} leu- meiotic progeny always give rise to pink colonies, this indicates the [*PSI*$^+$]^{pfd} isolates carry a mutation linked to *HSP104*. If any [*PSI*$^+$]^{pfd} leu- meiotic progeny give rise to white colonies, this indicates that the parent [*PSI*$^+$]^{pfd} isolate does not carry a mutation linked to *HSP104*, because the white colony color phenotype can be recovered even in the presence of the [*PSI*$^+$]^{pfd} *HSP104* allele. B. Results of the analysis described in A. None of the five [*PSI*$^+$]^{pfd} isolates show genetic linkage to *HSP104*, because they all give rise to some meiotic progeny where the [*PSI*$^+$]^{pfd} *HSP104* allele co-segregates with the white colony color phenotype. Shown is the number of meiotic tetrads from each [*PSI*$^+$]^{pfd} x Δ*hsp104::LEU2* diploid that showed 2:2 pink:red colony color inheritance, suggesting linkage between the [*PSI*$^+$]^{pfd} antisuppressor and *hsp104*, and the number of meiotic tetrads that showed deviation from 2:2 pink:red colony color segregation, indicating there is no linkage between the [*PSI*$^+$]^{pfd} antisuppressor and *HSP104*.

Figure 12. [*PSI*$^+$]^{pfd} isolates 2 and 5 are genetically linked to the *SUP35* locus. A. Diagram explaining the approach used to test if [*PSI*$^+$]^{pfd} isolate mutations are linked to the *sup35* locus. [*PSI*$^+$]^{pfd} isolates (pink oval) were crossed to wildtype [*PSI*$^+$] *sup35*::GFP cells (white oval) by mixing both mating partners on YPD, and incubating at 30^{o}C to allow zygote formation. Resultant zygotes (pink clover shape) were isolated by micromanipulation, sporulated and dissected. 2:2 segregation of mating types in meiotic tetrads was confirmed by replica plating to selective medium, and 2:2 segregation of *sup35* : *sup35*::GFP was determined by

PCR analysis of meiotic progeny. If the [*PSI*$^+$]^{pfd} isolate *sup35* allele always produces meiotic progeny that give rise to pink colonies, this indicates linkage between [*PSI*$^+$]^{pfd} isolate *sup35* and the dominant antisuppressor mutation. If the [*PSI*$^+$]^{pfd} isolate *sup35* allele sometimes gives rise to white colonies, this indicates that there is no linkage between [*PSI*$^+$]^{pfd} isolate *sup35* and the dominant antisuppressor mutation because they can be inherited independently. B. Results of the analysis explained in A. Shown is the number of meiotic tetrads for each indicated cell cross that always show linkage between the pink colony antisuppressor phenotype and the [*PSI*$^+$]^{pfd} isolate *sup35* allele, and the number of meiotic tetrads where the [*PSI*$^+$]^{pfd} isolate *sup35* allele gave rise to white colonies, indicating there is no linkage between the [*PSI*$^+$]^{pfd} *sup35* and the antisuppressor mutation. Notice that the [*PSI*$^+$]^{pfd} isolates 2 and 5 show genetic linkage between their *sup35* alleles and the antisuppressor mutation.

Figure 13. The mutation in [*PSI*$^+$]^{pfd} isolate 5 is tightly linked to the *SUP35* locus. A. Diagram explaining the experimental approach used to determine if *sup35* is mutated in [*PSI*$^+$]^{pfd} isolates 2 and 5. [*PSI*$^+$]^{pfd} isolates 2 and 5 were crossed to themselves (2x2, 5x5) to create isogenic diploids. Mating partners were mixed on YPD, and incubated at 30ºC to allow zygote formation. Resultant zygotes were isolated by micromanipulation, and diploid state was confirmed by sporulation. Next, one *sup35* allele was deleted from the diploids by PCR amplification of the KanMX4 cassette and targeting of the *SUP35* locus as described in methods, followed by transformation of the PCR product into yeast, and selection of transformants on YPD+G418. Correct intergration of the KanMX4 cassette into the *sup35* locus was confirmed by PCR, as described in methods. Next,

another copy of *sup35* was integrated into the *URA3* locus by transformation with PpuMI linearized pRS306-35$_p$Sup35. Integrants were selected for uracil prototrophy. These manipulations resulted in cells represented by the white oval, which carry one [*PSI*$^+$]^{pfd} *sup35* allele, and one wildtype *sup35* allele at the *URA3* locus on a different chromosome. These diploids were sporulated and dissected, and linkage between the [*PSI*$^+$]^{pfd} *sup35* allele and the pink colony antisuppressor phenotype was analyzed. 2:2 segregation of mating types, *sup35*:*ura3-sup35*, and G418 resistance: G418 sensitivity was confirmed by replica plating to selective media. If the [*PSI*$^+$]^{pfd} *sup35* allele always gives rise to pink colonies, this indicates tight linkage between [*PSI*$^+$]^{pfd} *sup35* and the antisuppressor mutation. If the [*PSI*$^+$]^{pfd} *sup35* allele sometimes gives rise white colonies, this indicates there is no tight linkage between [*PSI*$^+$]^{pfd} *sup35* and the antisuppressor mutation because they can be inherited independently. B. Results of the analysis explained in A. Shown is number G418-sensitive, ura- meiotic progeny that carry only the [*PSI*$^+$]^{pfd} *sup35* allele and that give rise to white or pink colonies, as indicated. Notice that all G418-sensitive, ura- meiotic progeny from [*PSI*$^+$]^{pfd} isolate 5 always give rise to pink colonies, indicating tight linkage between [*PSI*$^+$]^{pfd} isolate 5 *sup35* and the antisuppressor mutation.

Figure 14. Interaction between [*PSI*$^+$]^{pfd} isolates and Sup35 prion domain point mutants. Strains were transformed with Sup35 prion domain wildtype or point mutant plasmids, as noted. Exponentially growing cultures were spotted on selective medium and incubated for 3 days at 30^{o}C to allow colony growth, then photographed.

Figure 15. Sup35 physical state is altered in [*PSI*$^{+}$]^{pfd} variants. Semi denaturing detergent agarose gel electrophoresis (SDD-AGE) of lysates from the indicated strains, followed by αSup35 immunoblotting.

Figure 16. Quantitative curing of [*PSI*$^{+}$] in wildtype and Δ*pfd* cells. A. Schematic explaining the output of the quantitative curing experiment. The rate of curing is represented by the exponential part of the curve, while the lag phase is representative of the number of transmissible prion complexes in each cell. B. Quantitative curing. Cells were maintained in exponential phase in YPD + 3mM GdnHCl. At various timepoints, cells were plated on rich medium and scored for loss of [*PSI*$^{+}$] by colony color. [*PSI*] status of representative white colonies was confirmed by curing on GdnHCl and by mating to [*psi*$^{-}$]. Data is compiled from 2 independent experiments, which are plotted together in the graph. Each experiment consists of 7 timepoints during which cells were scored for percent cured to [*psi*$^{-}$] state. For every timepoint, 700-1000 colonies were scored each of wildtype and Δ*pfd*. A total of 0.05 % spontaneous ADE+ revertants, 0.02% petite colonies with loss of mitochondrial function, and 0.07% pink [*PSI*$^{+}$] colonies that are curable and transferred their pink colony color phenotype in crosses with wildtype [*psi*$^{-}$] were recovered from the two experiments.

Figure 17. Chaperone and Sup35 expression profiles are not altered in Δ*pfd* mutant strains. SDS-PAGE of indicated cell lysates, followed by immunoblotting with the indicated antisera. αPGK1 is the loading control.

Table Captions

Table 1. Cassettes and primers used to create deletion mutants for this study. Each deletion mutant (left column) was created by replacing the indicated gene with a selectable marker from the knockout cassette listed in the middle column, using the primers indicated in the right column.

Table 2. Primers used to verify deletion mutants that were created for this study. Each deletion mutant (left column) was verified by PCR for the correct integration of the knockout cassette at the 5' and 3' ends of the integration construct using the primers indicated in the middle and right columns.

Table 3. Accession numbers of deletion mutants used in this study. The accession numbers of indicated deletion mutants (left column) are listed. The second column shows the accession number of the [*PSI*$^+$] deletion mutants, the third column shows the guanidine hydrochloride (GdnHCl) cured [*psi*$^-$] version of each deletion mutant, and the fourth column shows that Hsp104 overexpression cured [*psi*$^-$] version of each deletion mutant, as applicable. Not all deletion mutants were cured by Hsp104 overexpression or by GdnHCl, so in instances when such a [*psi*$^-$] version of the mutant was not used in this study, this is indicated as N/A.

Table 4. Doubling times of Δ*ssb* and Δ*pfd* mutants. Doubling times of wildtype, Δ*ssb*, and Δ*pfd* mutants in liquid rich medium (YPAD) and in liquid rich medium supplemented with 3mM guanidine hydrochloride (YPAD + 3mM GdnHCl). Cell doubling times were calculated from the rates of change in optical density (OD_{600}) while cells were in exponential growth.

Table 5. Accession numbers of [*PSI*$^+$]^{pfd} anti-suppressor mutants analyzed in this study. Each [*PSI*$^+$]^{pfd} anti-suppressor mutant was isolated from a single Δ*pfd* mutant and

transferred into a wildtype *PFD* background by cell crossing as described in the text and in the methods section. The second column show the accession numbers of the original [*PSI*$^{+}$]^{pfd} isolates, the third column shows the names of the guanidine hydrochloride cured [*psi*$^{-}$]^{pfd} version of each isolate, and the fourth column shows the names of the Hsp104 overexpression cured [*psi*$^{-}$]^{pfd} versions of each isolate.

Table 6. Segregation of colony colors in meiotic tetrads recovered from cell crosses between [*PSI*$^{+}$]^{pfd1}, [*PSI*$^{+}$]^{pfd4}, [*PSI*$^{+}$]^{pfd5} and wildtype [*psi*$^{-}$] or wildtype [*PSI*$^{+}$]^{strong}, and [*psi*$^{-}$]^{pfd1}, [*psi*$^{-}$]^{pfd4}, [*psi*$^{-}$]^{pfd5} and wildtype [*PSI*$^{+}$]^{strong}, as indicated. Notice that the meiotic progeny from all combinations of cell crosses always show 2 pink : 2 white colony color inheritance, indicating that [*PSI*]^{pfd} isolates are carrying a dominant antisuppressor mutation.

Figure 1.

A.

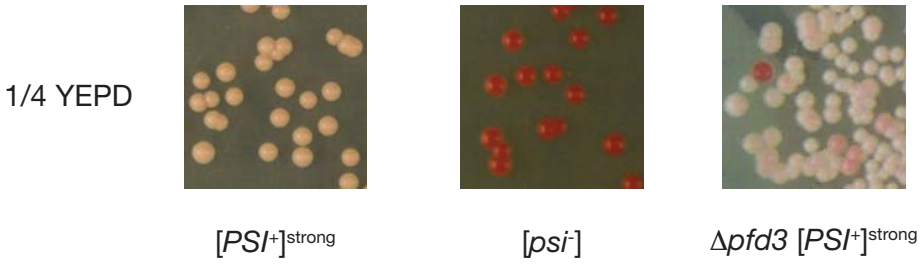
1/4 YEPD
[PSI+]strong
[psi-]
Δpfd3 [PSI+]strong

B.

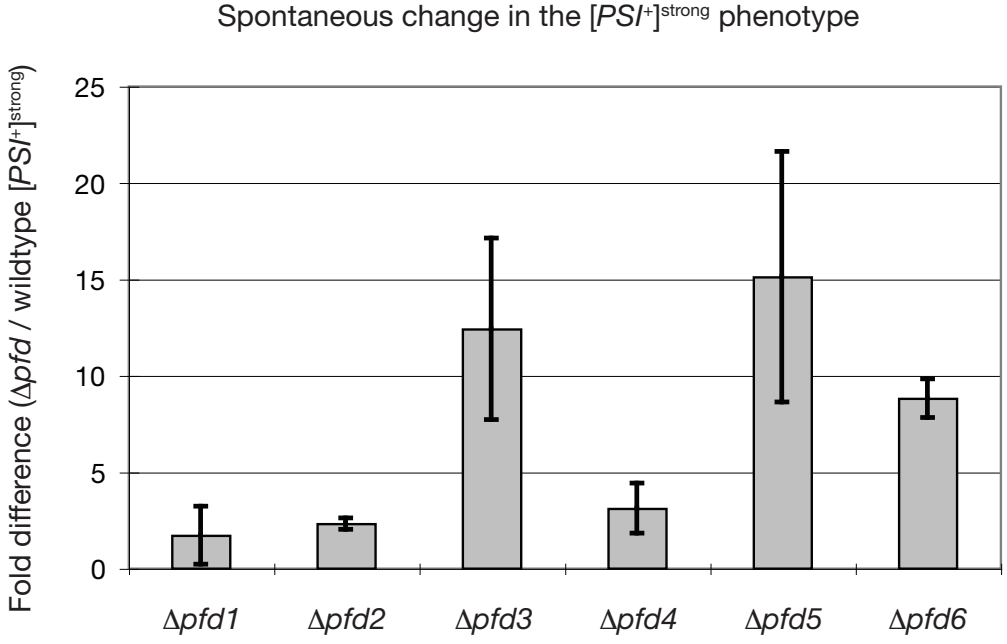
Spontaneous change in the [PSI+]strong phenotype
Fold difference (Δpfd / wildtype [PSI+]strong)
25
20
15
10
5
0
Δpfd1
Δpfd2
Δpfd3
Δpfd4
Δpfd5
Δpfd6

Figure 2.

A.

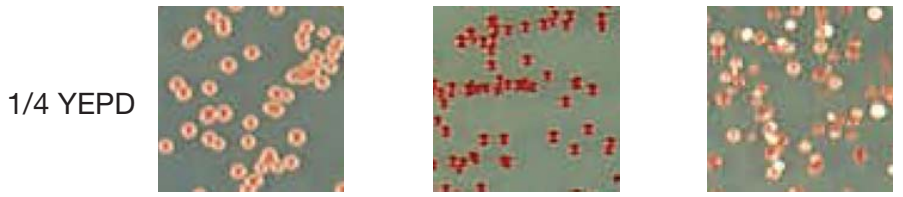

B.

Spontaneous change in the prion phenotype of the Δ*pfd3* [*PSI*$^{+}$]^{weak} mutant

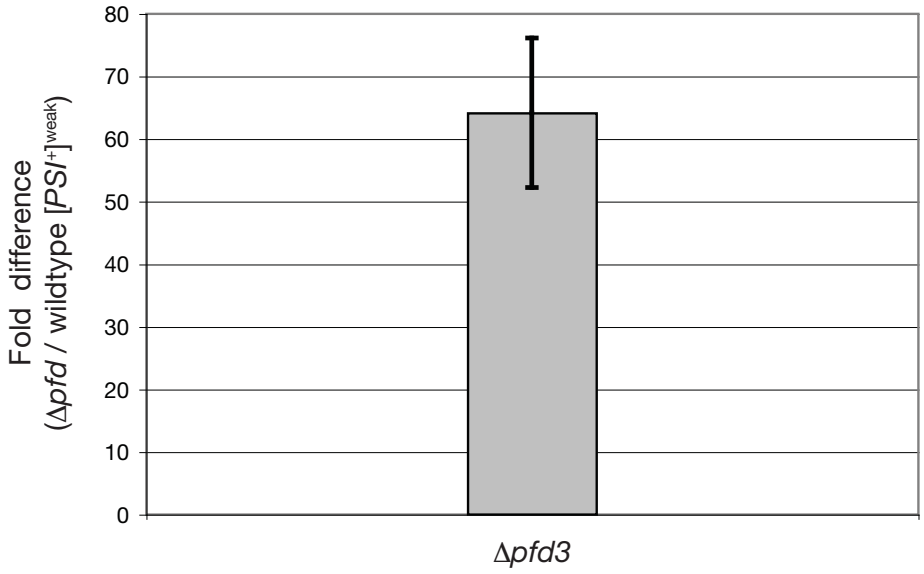

Figure 3.

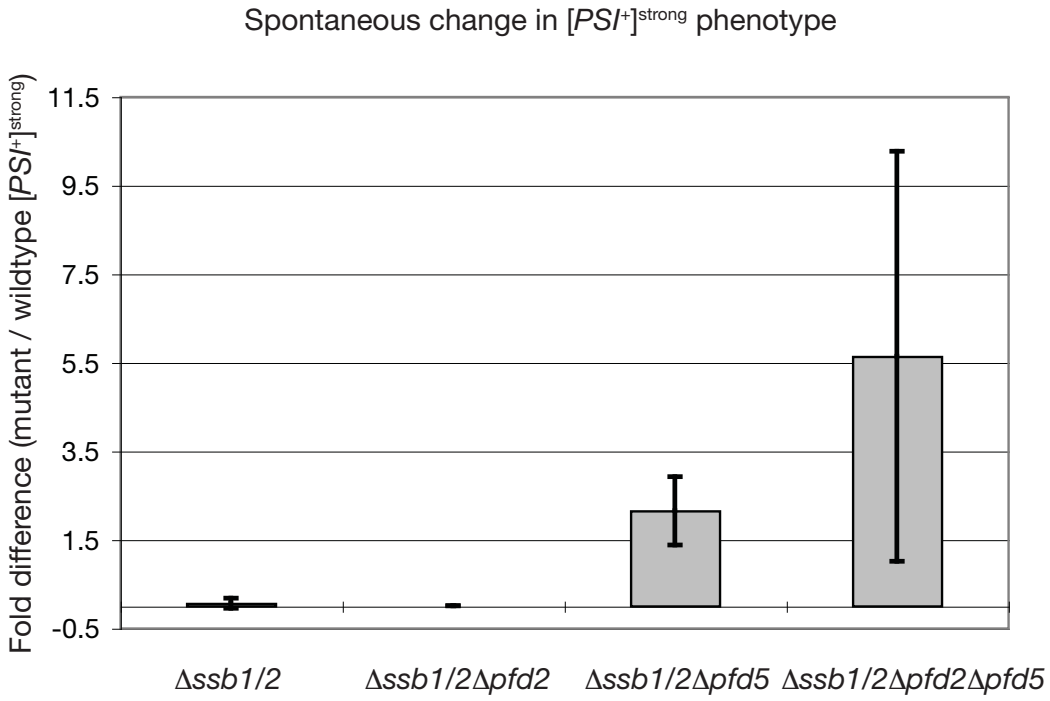
Spontaneous change in [PSI+]strong phenotype
Fold difference (mutant / wildtype [PSI+]strong)
11.5
9.5
7.5
5.5
3.5
1.5
-0.5
Δssb1/2
Δssb1/2Δpfd2
Δssb1/2Δpfd5
Δssb1/2Δpfd2Δpfd5

Figure 4.

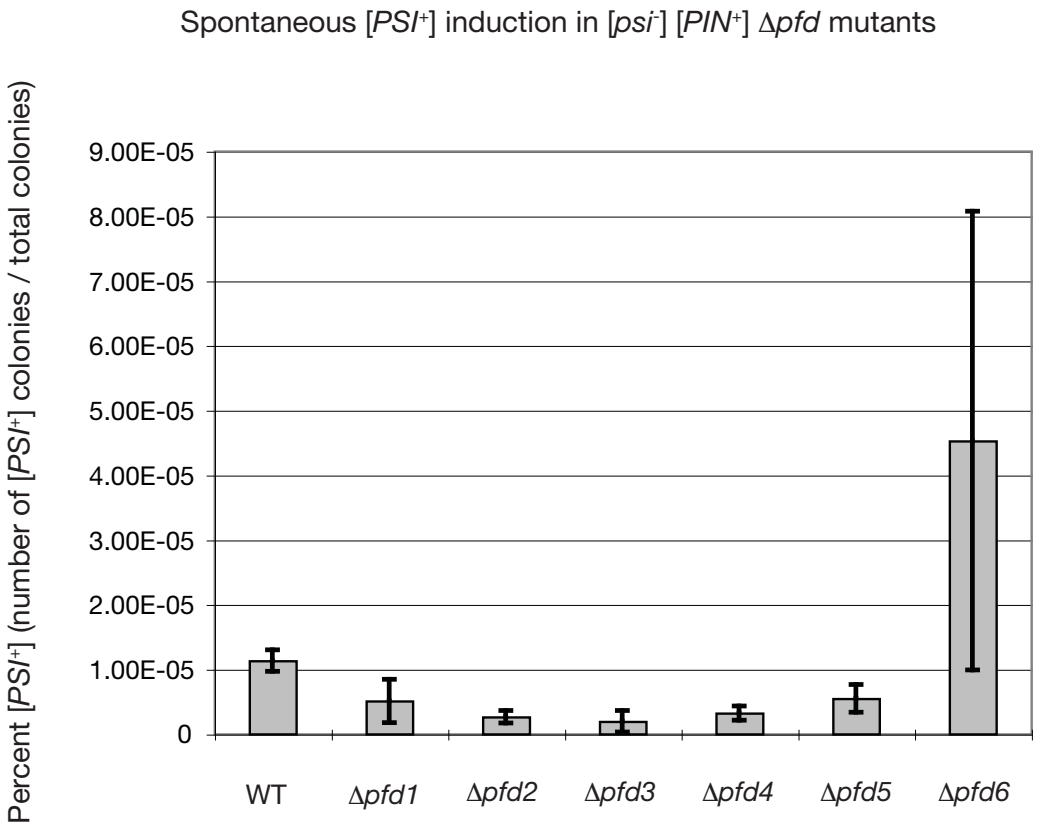
Spontaneous [PSI+] induction in [psi-] [PIN+] Δpfd mutants
Percent [PSI+] (number of [PSI+] colonies / total colonies)
9.00E-05
8.00E-05
7.00E-05
6.00E-05
5.00E-05
4.00E-05
3.00E-05
2.00E-05
1.00E-05
0
WT
Δpfd1
Δpfd2
Δpfd3
Δpfd4
Δpfd5
Δpfd6

Figure 5.

A.

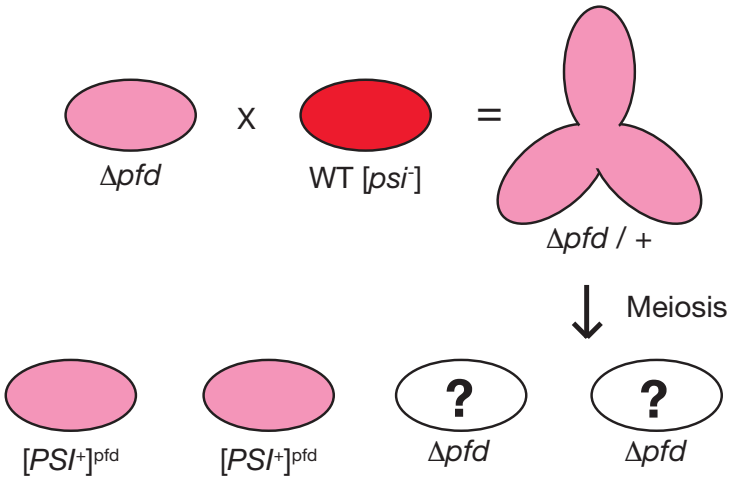

B.

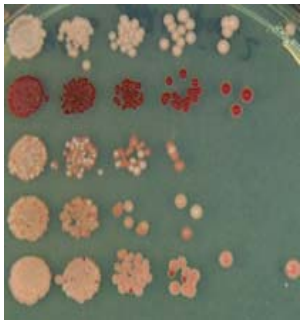

[*PSI*$^{+}$]^{strong}

[*psi*$^{-}$]

Δ*pfd1* [*PSI*$^{+}$]^{strong}

Δ*pfd1* / + [*PSI*$^{+}$]^{strong}

[*PSI*$^{+}$]^{weak}

C.

Δ*pfd* / + diploid	**Number of tetrads with 4:0 pink colony color segregation**	**Number of tetrads with 3 white : 1 pink colony color segregation**	**Number of tetrads with 3 pink : 1 white colony color segregation**	**Number of tetrads with 2 white : 2 pink colony color segregation**
Δ*pfd1* / +	21/30	5/30	0/30	4/30
Δ*pfd2* / +	9/14	3/14	1/14	1/14
Δ*pfd3* / +	15/30	3/30	3/30	9/30
Δ*pfd4* / +	2/25	5/25	8/25	10/25
Δ*pfd5* / +	7/21	6/21	1/21	7/21
Δ*pfd6* / +	1/10	5/10	1/10	3/10

Figure 6.

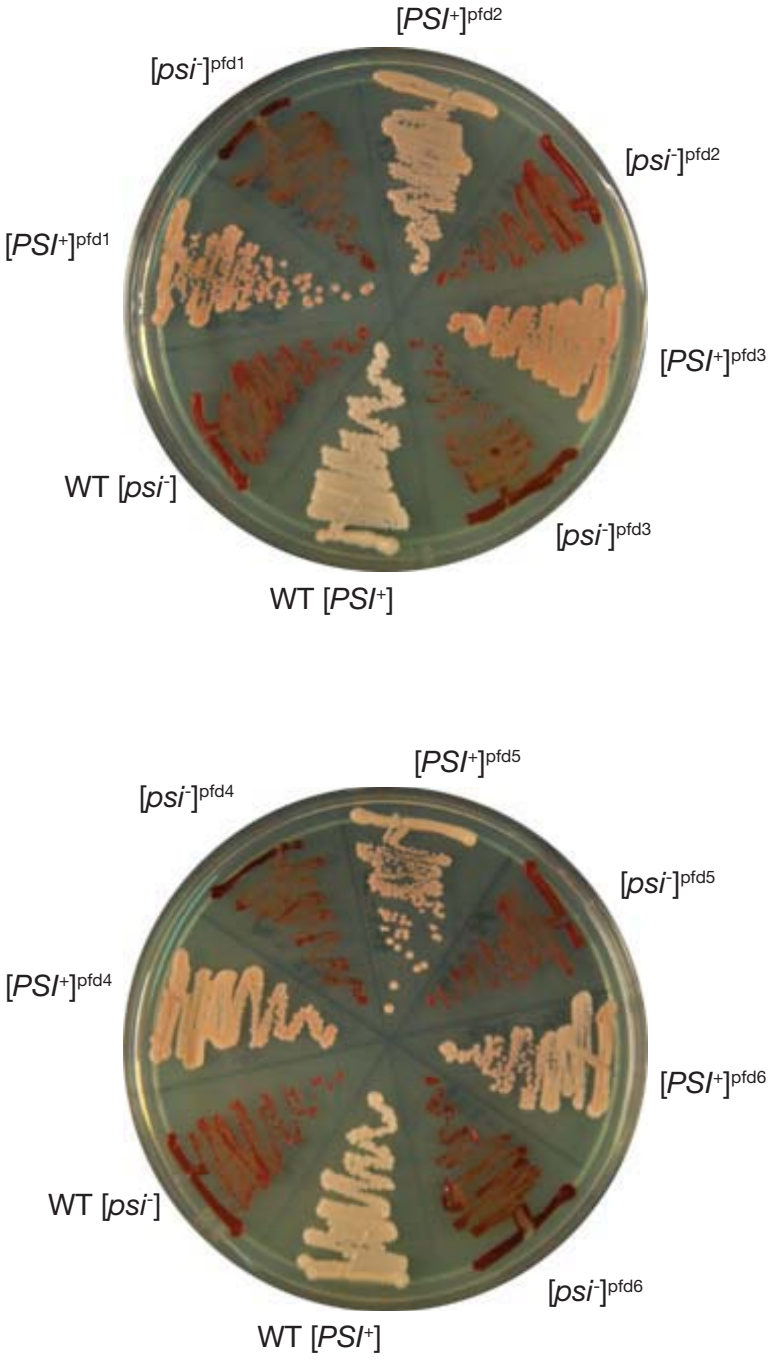
[PSI+]pfd2
[psi-]pfd1
[psi-]pfd2
[PSI+]pfd1
[PSI+]pfd3
WT [psi-]
[psi-]pfd3
WT [PSI+]
[PSI+]pfd5
[psi-]pfd4
[psi-]pfd5
[PSI+]pfd4
[PSI+]pfd6
WT [psi-]
[psi-]pfd6
WT [PSI+]

Figure 7.


WT [PSI+]strong 2N
[PSI+]pfd1 x [PSI+]strong
WT [PSI+]strong N
[PSI+]pfd1
WT [PSI+]strong 2N
[PSI+]pfd4 x [PSI+]strong
WT [PSI+]strong N
[PSI+]pfd4
WT [PSI+]strong 2N
[PSI+]pfd5 x [PSI+]strong
WT [PSI+]strong N
[PSI+]pfd5

Figure 8.

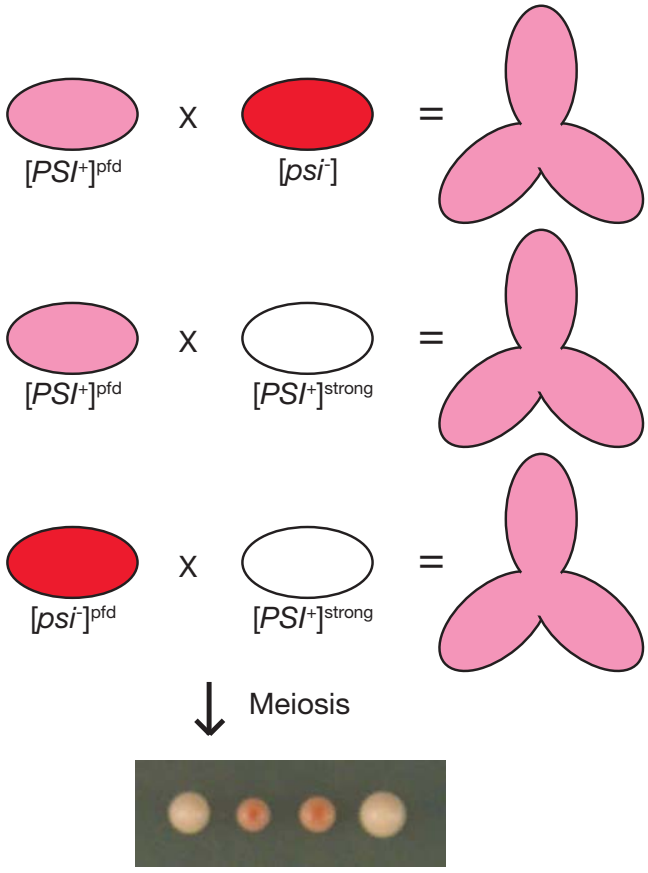

Figure 9.

A.

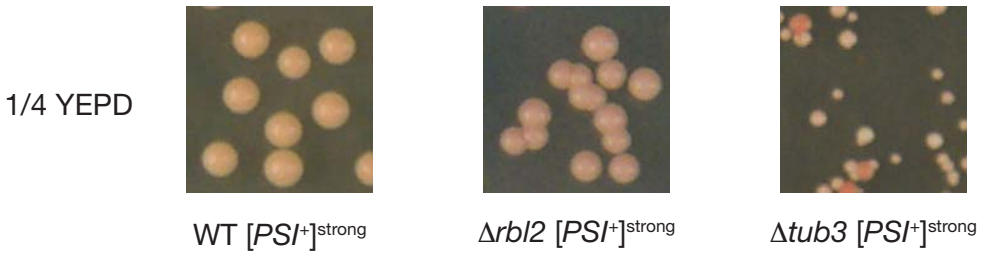
1/4 YEPD
WT [PSI+]strong
Δrbl2 [PSI+]strong
Δtub3 [PSI+]strong

B.

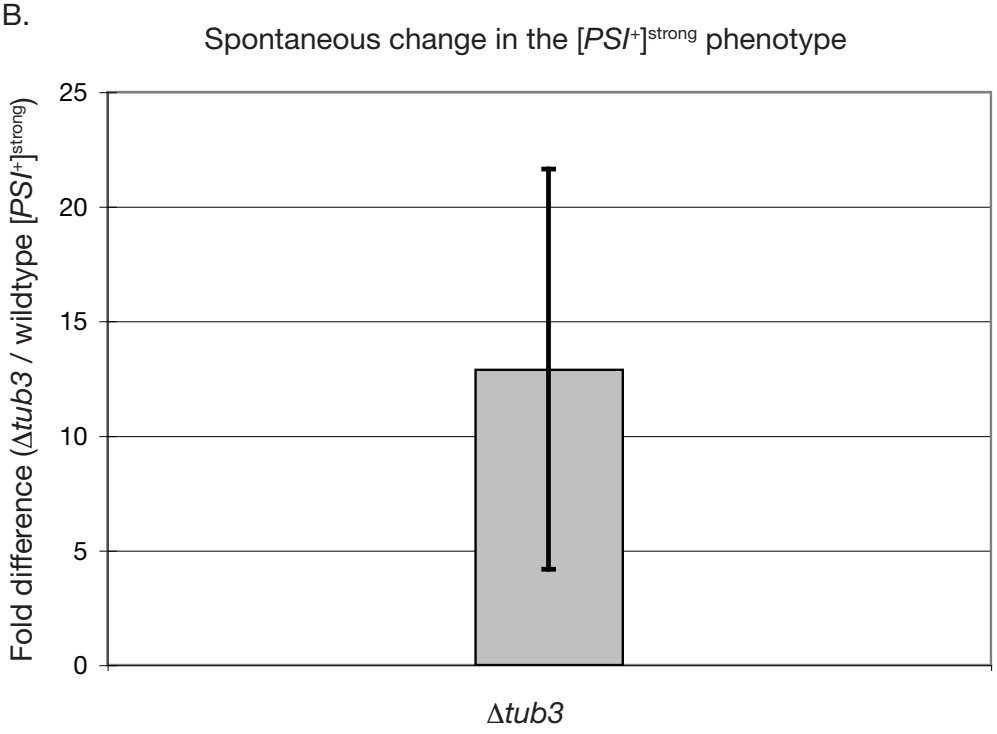
Spontaneous change in the [PSI+]strong phenotype
Fold difference (Δtub3 / wildtype [PSI+]strong)
25
20
15
10
5
0
Δtub3

Figure 10.

A.

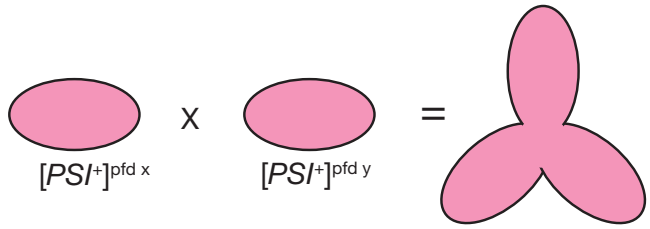

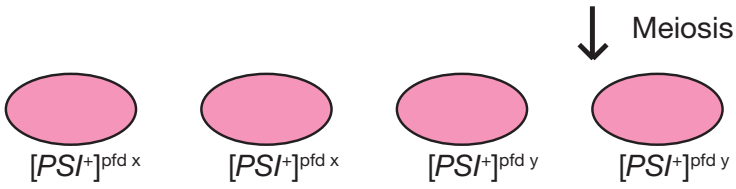

4:0 colony color segregation suggests that [*PSI*$^{+}$]$^{pfd\ x}$ and [*PSI*$^{+}$]$^{pfd\ y}$ carry a mutation in the same locus, or in two tightly linked loci.

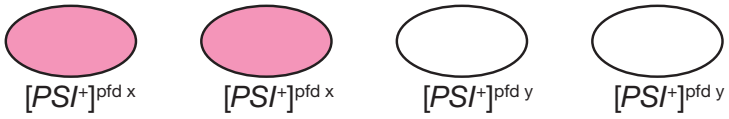

Deviation from 4:0 segregation suggests that mutations carried by [*PSI*$^{+}$]$^{pfd\ x}$ and [*PSI*$^{+}$]$^{pfd\ y}$ are in different loci.

B.

[*PSI*$^{+}$]^{pfd} x [*PSI*$^{+}$]^{pfd}	Number of tetrads with 4:0 segregation	Number of tetrads with non-4:0 segregation
2 x 5	7/10	3/10
1 x 3	25/29	4/29
1 x 4	26/28	2/28
3 x 4	22/25	3/25
1 x 2	0/8	8/8
1 x 5	0/8	8/8
2 x 3	0/10	10/10
2 x 4	0/15	15/15
3 x 5	0/7	7/7
4 x 5	0/2	2/2

Figure 11.

A.

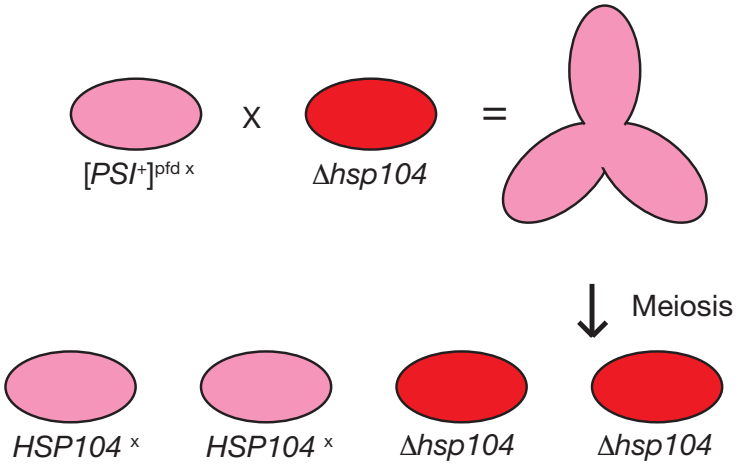

2 pink : 2 red colony color segregation suggests a mutation with linkage to [*PSI*$^{+}$]$^{pfd\ x}$'s *HSP104.*

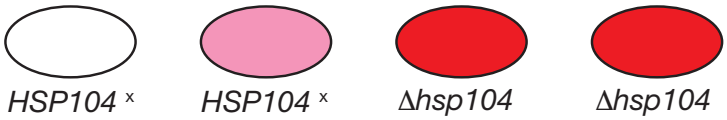

Colony color variability in the progeny of the two [*PSI*$^{+}$]$^{pfd\ x}$ spores indicates that the mutation is not linked to *HSP104* ^{x}.

B.

Cells crossed	**Number of tetrads with 2 red : 2 pink colony color segregation**	**Number of tetrads with deviation from 2 red : 2 pink colony color segregation**
[*PSI*$^{+}$]^{pfd1} x Δ*hsp104*	1/7	6/7
[*PSI*$^{+}$]^{pfd2} x Δ*hsp104*	4/9	5/9
[*PSI*$^{+}$]^{pfd3} x Δ*hsp104*	2/9	7/9
[*PSI*$^{+}$]^{pfd4} x Δ*hsp104*	0/6	6/6
[*PSI*$^{+}$]^{pfd5} x Δ*hsp104*	0/5	5/5

Figure 12.

A.

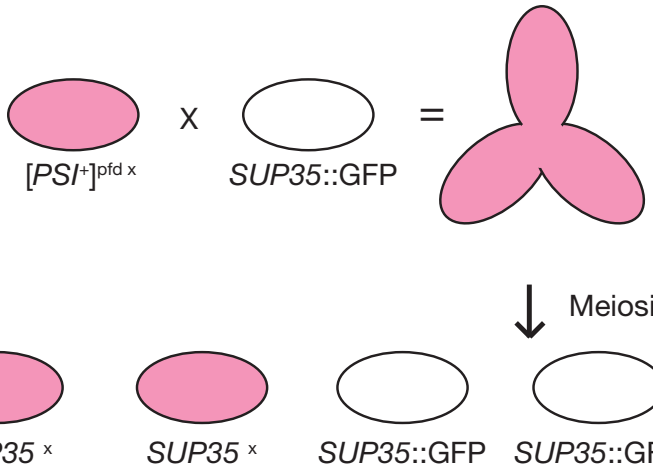

Co-segregation of [*PSI*$^{+}$]$^{pfd\ x}$ *SUP35* and pink colony color suggests the mutation is linked to [*PSI*$^{+}$]$^{pfd\ x}$ *SUP35.*

Co-segregation of *SUP35*::GFP and pink colony color suggests the there is no linkage between the mutation and [*PSI*$^{+}$]$^{pfd\ x}$ *SUP35.*

B.

Cells crossed	**Number of tetrads where pink colony color co-segregates with [*PSI*$^{+}$]^{pfd} *sup35***	**Number of tetrads where pink colony color does not co-segregate with [*PSI*$^{+}$]^{pfd} *sup35***
[*PSI*$^{+}$]^{pfd1} x *sup35*::GFP	0/8	8/8
[*PSI*$^{+}$]^{pfd2} x *sup35*::GFP	9/9	0/9
[*PSI*$^{+}$]^{pfd3} x *sup35*::GFP	0/10	10/10
[*PSI*$^{+}$]^{pfd4} x *sup35*::GFP	0/9	9/9
[*PSI*$^{+}$]^{pfd5} x *sup35*::GFP	10/10	0/10

Figure 13.

A.

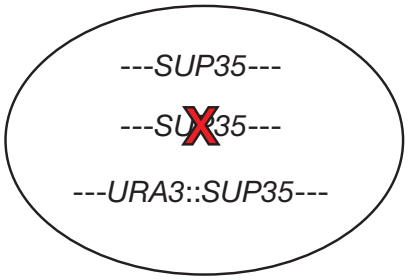

[*PSI*+]pfd *SUP35* [*PSI*+]pfd *SUP35* *URA3*::*SUP35* *URA3*::*SUP35*

The mutation is tightly linked to the *SUP35* locus.

URA3::*SUP35* [*PSI*+]pfd *SUP35* [*PSI*+]pfd *SUP35* *URA3*::*SUP35*

The mutation is not tightly linked to the *SUP35* locus.

B.

[*PSI*+]pfd isolate analyzed	**Number of [*PSI*+]pfd *sup35* meiotic progeny that always give rise to pink colonies**	**Number of [*PSI*+]pfd *sup35* meiotic progeny that give rise to white colonies**
2	0/9	9/9
5	26/26	0/26

Figure 14.

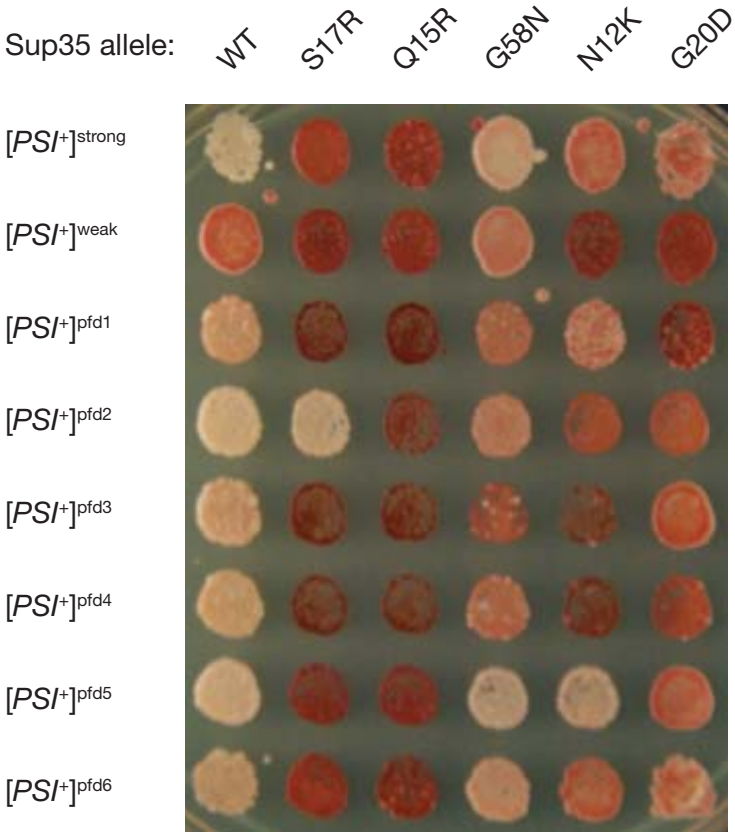
Sup35 allele:
WT
S17R
Q15R
G58N
N12K
G20D
[PSI+]strong
[PSI+]weak
[PSI+]pfd1
[PSI+]pfd2
[PSI+]pfd3
[PSI+]pfd4
[PSI+]pfd5
[PSI+]pfd6
1/4 YEPD + G418

Figure 15.

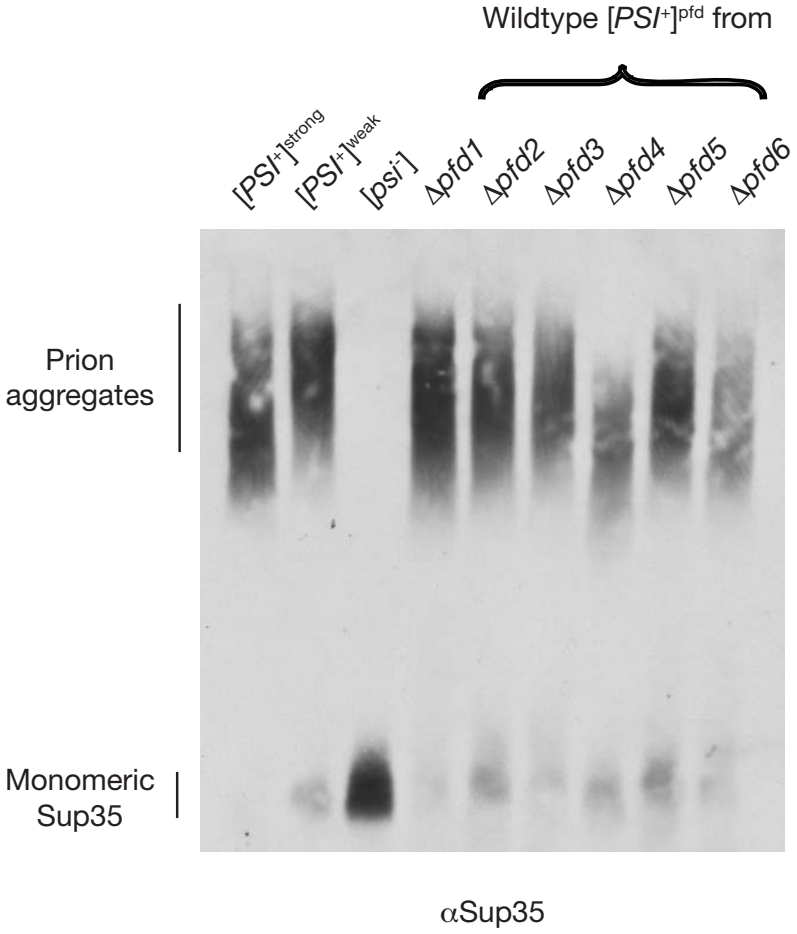
Wildtype [PSI+]pfd from
[PSI+]strong
[PSI+]weak
[psi-]
Δpfd1
Δpfd2
Δpfd3
Δpfd4
Δpfd5
Δpfd6
Prion aggregates
Monomeric Sup35
αSup35

Figure 16.

A.

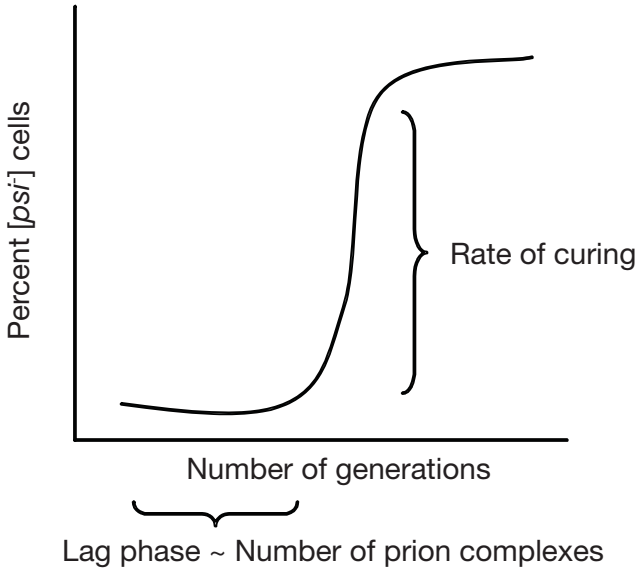
Percent [psi-] cells
Rate of curing
Number of generations
Lag phase ~ Number of prion complexes

B.

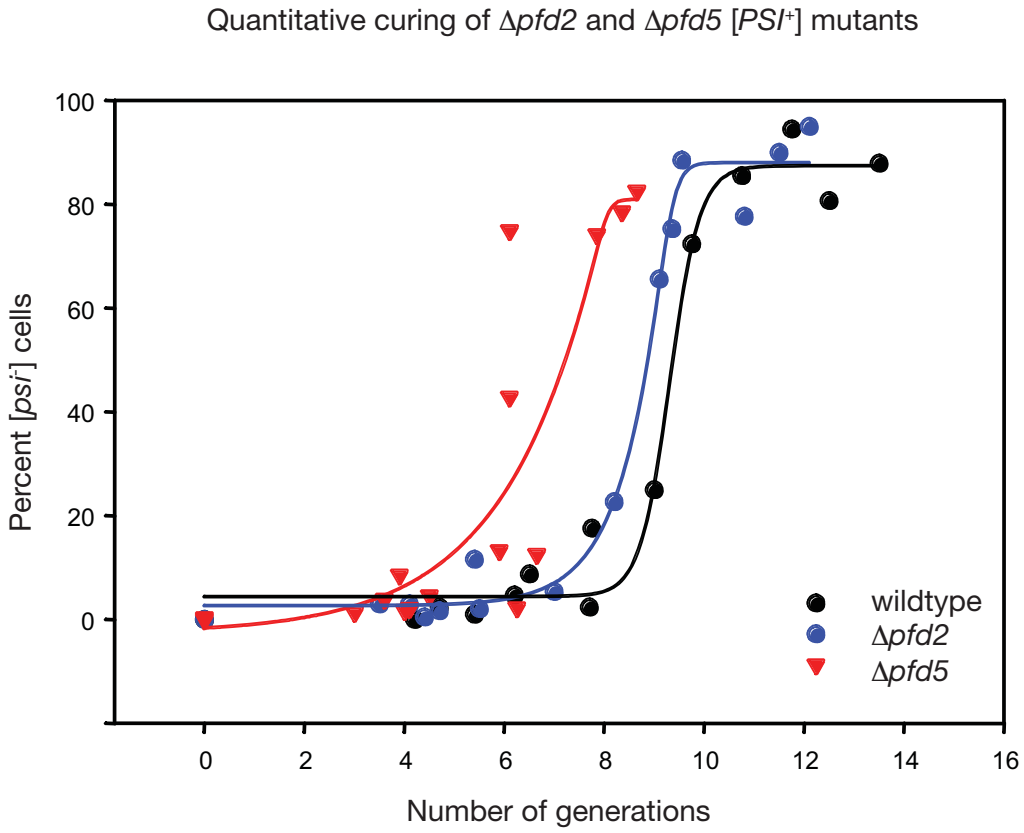
Quantitative curing of Δpfd2 and Δpfd5 [PSI+] mutants
Percent [psi-] cells
100
80
60
40
20
0
0
2
4
6
8
10
12
14
16
Number of generations
wildtype
Δpfd2
Δpfd5

Figure 17.

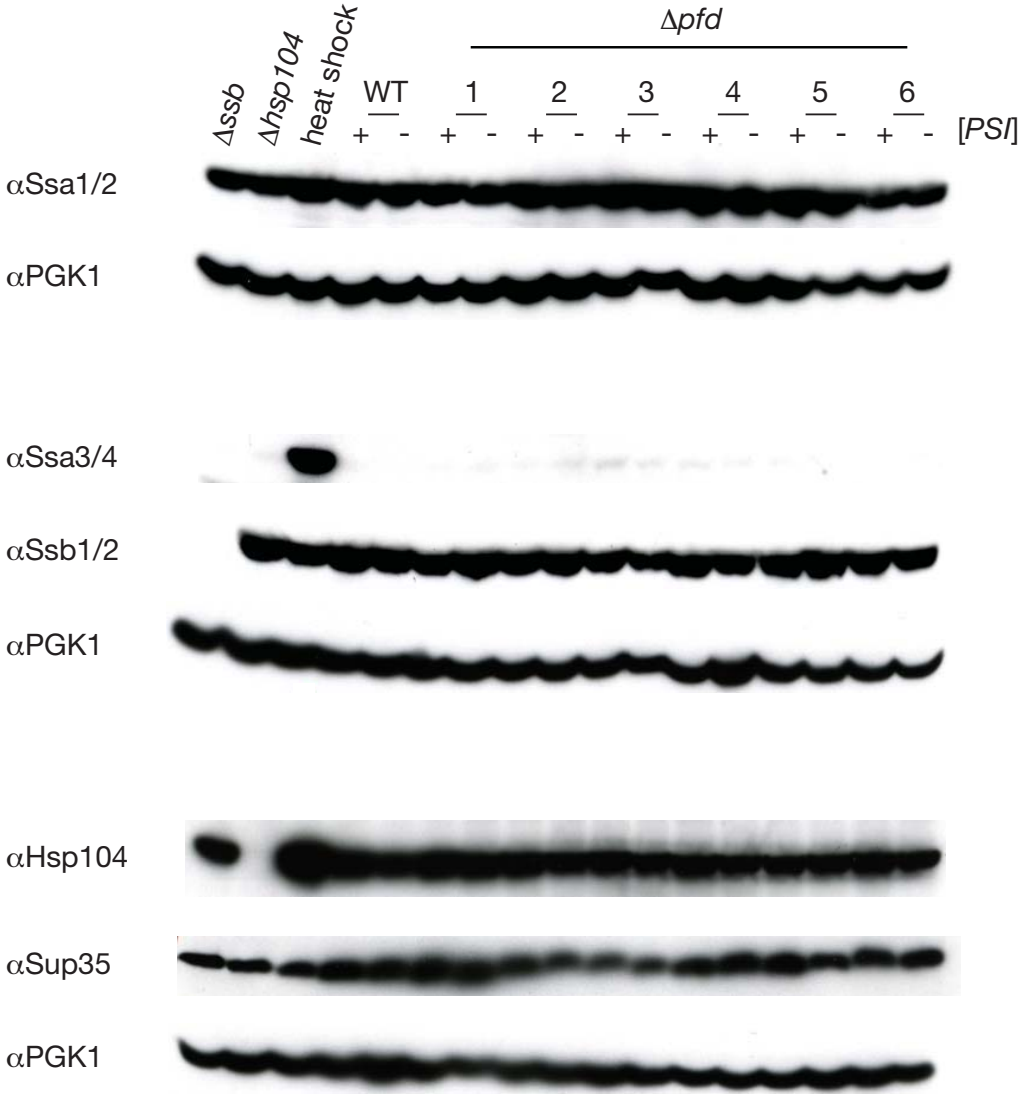
Δpfd
Δssb
Δhsp104
heat shock
WT
1
2
3
4
5
6
+ - + - + - + - + - + - + -
[PSI]
αSsa1/2
αPGK1
αSsa3/4
αSsb1/2
αPGK1
αHsp104
αSup35
αPGK1

Table 1.

Deletion mutant	Cassette used for deletion	Primers used for cassette amplification and gene targeting
Δ*ssb1* [*PSI*$^{+}$]^{strong}	pFA6a-KanMx4	Fwd: CAG ATG TCC CAA GAT CAT TAC AGT ATT TTA ATT GAA CAA ACG GAT CCC CGG GTT AAT TAA Rev: CAA TAT AAG TAA TAT TCA TAT ATA TGT GAT GAA TGC AGT CGA ATT CGA GCT CGT TTA AAC
Δ*ssb2* [*PSI*$^{+}$]^{strong}	pFA6a-His3Mx6	Fwd: TCG TTT TTT CTT TCA AGA AAC CAA GAA CCA ATA TCC TCA TTA ACA CGG ATCCCCGGGTTAATTAA Rev: AAA ATA TAT ATA TGT GTA TAA CCT TAA CCA GAA TGA CAT CGA ATT CGA GCT CGT TTA AAC
Δ*pfd1* [*PSI*$^{+}$]^{strong}	pFA6a-His3Mx6	Fwd: GCT CTT TAC TAA ATT GAA TCA ATA ATA CAT ACT TAC AAA CCG GAT CCC CGG GTT AAT TAA Rev: TAA GTT TTC CGG CTA AGA AAG GAA AGG CTA TTG CCG CTT TCT TGA ATT CGA GCT CGT TTA AAC
Δ*pfd2* [*PSI*$^{+}$]^{strong}	pFA6a-HphMx4	Fwd: GAA CAA CGG TAT GCA AAA TTT CGA TCT CTG GGT TTT AAT AA CAG CTG AAG CTT CGT ACG CT Rev: TTT TGC CAA ACT AAG TAC TGC AAT AGA TTT TAT ATA TGG TGC ATA GGC CAC TAG TGG AAC
Δ*pfd3* [*PSI*$^{+}$]^{strong}	pFA6a-KanMx4	Fwd: GAA AAC TGT ACG CAC ATA TAT AAC AGA TAC TAC GGT TAT TCG GAT CCC CGG GTT AAT TAA Rev: GTG CCC TTT ATT TTT CTT TGG ATT TAA ATT TAC AGA CAC ACG CAC TTA ACT TCG CAT CTG
Δ*pfd4* [*PSI*$^{+}$]^{strong}	pFA6a-klTRP1MX4	Fwd: ACC AGA ATA CAC AAC GCC AAG AAA CTA ACA GAG GAC CAT TCG GAT CCC CGG GTT AAT TAA Rev: TCA TTT TGT GGA GAC ACC CAC AGC CCA CAC TTT AAT GAG TGT TGA ATT CGA GCT CGT TTA AAC
Δ*pfd5* [*PSI*$^{+}$]^{strong}	pFA6a-HphMx4	Fwd: CTG TGA CCC AAA CAA GAA AGA GCA CTG TAA AAA TCA AGC CCG GAT CCC CGG GTT AAT Rev: AAT GAG ATA TGA AAA ATC GTA GGA AAA GCA AAA GAG TTA CGA ATT CGA GCT CGT TTA
Δ*pfd6* [*PSI*$^{+}$]^{strong}	pFA6a-NatMx4	Fwd: TTG AAA AAG ACT ACA TTT GAG TGG AGG AAC AAA AGC AAA ACG GAT CCC CGG GTT AAT TAA Rev: TGT GCG CTT TCT TGT CTT TCC GAG GAC CTG TGA GTT TGT T CGC ACT TAA CTT CGC ATC TG
Δ*pfd3* [*PSI*$^{+}$]^{weak}	pFA6a-KanMx4	Fwd: GAA AAC TGT ACG CAC ATA TAT AAC AGA TAC TAC GGT TAT TCG GAT CCC CGG GTT AAT TAA Rev: GTG CCC TTT ATT TTT CTT TGG ATT TAA ATT TAC AGA CAC ACG CAC TTA ACT TCG CAT CTG
Δ*tub3* [*PSI*$^{+}$]^{strong}	pFA6a-KanMx4	Fwd: TTG CAC ATC TAA AAG AAA TAT AAA CAC AGA TCA GGT ATC TCA GCT GAA GCT TCG TAC GC Rev: TGT GAT AAG TTT GGG TGG CAA CGA GAT GAG CTC AAA ACT CGC ATA GGC CACTAG TGG ATC TG
Δ*rbl2* [*PSI*$^{+}$]^{strong}	pFA6a-HphMx4	Fwd: CAC AAC AGG TTG AAC TCA AGA AAA CTA CAT TTC ACT ATC ACA GCT GAA GCT TCG TAC GC Rev: AAA ATA AAT GCG AAA AGG TAA GAA AAA GGT TAT CTA TAG AGC ATA GGC CAC TAG TGG ATC TG
Δ*sup35*	pFA6a-KanMx4	Fwd: ACTTGCTCGG AATAACATCT ATATCTGCCC ACTAGCAACA CAG CTG AAG CTT CGT ACG C Rev: GGTATTATTGTGTTTGCATTTACTTATGTTTGCAAGAAAT GCA TAG GCC ACT AGT GGA TCT G

Table 2.

Deletion mutant	Primers used for 5' end PCR verification of the deletion mutant	Primers used for 3' end PCR verification of the deletion mutant
Δ*ssb1* [*PSI*$^{+}$]^{strong}	Fwd: GGA CTT GAT CGA ACA GAT CG Rev: GCACGTCAAGACTGTCAAGG	Fwd: CCC GAA GGT TTG CCA GTT AA Rev: TGCCCAGATGCGAAGTTAAGTG
Δ*ssb2* [*PSI*$^{+}$]^{strong}	Fwd: GAG AAT TGA AAG CTT GAG GG Rev: GCACGTCAAGACTGTCAAGG	Fwd: GGC CAC TTG AGT AGA ATT CG Rev: TGCCCAGATGCGAAGTTAAGTG
Δ*pfd1* [*PSI*$^{+}$]^{strong}	Fwd: AAT TCC ATT TCC TAG AGG AG Rev: GCACGTCAAGACTGTCAAGG	Fwd: TGG CGA CGG CGA TAA TGG TA Rev: TGCCCAGATGCGAAGTTAAGTG
Δ*pfd2* [*PSI*$^{+}$]^{strong}	Fwd: GTC CCG CGA GAA GAA ACT CT Rev: GCACGTCAAGACTGTCAAGG	Fwd: AGT GTG CAT GCG GTT CAT TCA C Rev: TGCCCAGATGCGAAGTTAAGTG
Δ*pfd3* [*PSI*$^{+}$]^{strong}	Fwd: TGA ACG CTC GTC GAG GGA AT Rev: GCACGTCAAGACTGTCAAGG	Fwd: TGG ACA ATG AAC TGC GAT CG Rev: TGCCCAGATGCGAAGTTAAGTG
Δ*pfd4* [*PSI*$^{+}$]^{strong}	Fwd: AAC AGA CAT ACT CCA AGC TG Rev: TTT GAC CTG CTC GAT GTA GA	Fwd: TAA GCG GAG GTG TGG AGA CA Rev: AAG GAT GGG GGT AAA GTA CC
Δ*pfd5* [*PSI*$^{+}$]^{strong}	Fwd: GCG TGG CTG TCT CAT AAG Rev: GCACGTCAAGACTGTCAAGG	Fwd: GGA AAA CTA CAA AGT GAC G Rev: TGCCCAGATGCGAAGTTAAGTG
Δ*pfd6* [*PSI*$^{+}$]^{strong}	Fwd: ACT CAA CTT TTG GAA CCG GG Rev: GCACGTCAAGACTGTCAAGG	Fwd: CCT GAA CTA CAC AGA TTG TC Rev: TGCCCAGATGCGAAGTTAAGTG
Δ*pfd3* [*PSI*$^{+}$]^{weak}	Fwd: TGA ACG CTC GTC GAG GGA AT Rev: GCACGTCAAGACTGTCAAGG	Fwd: TGG ACA ATG AAC TGC GAT CG Rev: TGCCCAGATGCGAAGTTAAGTG
Δ*tub3* [*PSI*$^{+}$]^{strong}	Fwd: GAG ACG GTA AGC CAA CCA AC Rev: GCACGTCAAGACTGTCAAGG	Fwd: TGG AAC GCG TAC AGC AAC ATG A Rev: TGCCCAGATGCGAAGTTAAGTG
Δ*rbl2* [*PSI*$^{+}$]^{strong}	Fwd: GCC CAG AAT ACA CCA CGT CT Rev: GCACGTCAAGACTGTCAAGG	Fwd: CGG ATG GTG TTG TCT TCG CAT T Rev: TGCCCAGATGCGAAGTTAAGTG
Δ*sup35*	Fwd: ACGCGTCACAG TGTTCGAGT Rev: GCACGTCAAGACTGTCAAGG	Fwd: TATTTACGAAGGAGACCCGGAG Rev: TGCCCAGATGCGAAGTTAAGTG

Table 3.

Deletion mutant	Accession number of the [*PSI*$^+$] strain	Accession number of the GdnHCl-cured [*psi*$^-$] strain	Accession number of the Hsp104-overexpression cured [*psi*$^-$] strain
Δ*pfd1* [*PSI*$^+$]^{strong}	SY 656	SY 675	SY 689
Δ*pfd2* [*PSI*$^+$]^{strong}	SY 363	SY 438	SY 691
Δ*pfd3* [*PSI*$^+$]^{strong}	SY 657	SY 677	SY 693
Δ*pfd4* [*PSI*$^+$]^{strong}	SY 717	SY 719	SY 735
Δ*pfd5* [*PSI*$^+$]^{strong}	SY 365	SY 439	SY 696
Δ*pfd6* [*PSI*$^+$]^{strong}	SY 660	SY 679	SY 699
Δ*ssb1*Δ*ssb2* [*PSI*$^+$]^{strong}	SY 393	SY 440	N/A
Δ*ssb1*Δ*ssb2*Δ*pfd2* [*PSI*$^+$]^{strong}	SY 427	SY 452	N/A
Δ*ssb1*Δ*ssb2*Δ*pfd5* [*PSI*$^+$]^{strong}	SY 419	SY 451	N/A
Δ*ssb1*Δ*ssb2*Δ*pfd2* Δ*pfd5* [*PSI*$^+$]^{strong}	SY 653	SY 674	N/A
Δ*rbl2* [*PSI*$^+$]^{strong}	SY 956	SY 965	N/A
Δ*tub3* [*PSI*$^+$]^{strong}	SY 971	SY 974	N/A
			N/A
Δ*pfd3* [*PSI*$^+$]^{weak}	MSY 116	N/A	N/A

Table 4.

Yeast strain	**Doubling time in YPAD (hours ± standard deviation)**	**Doubling time in YPAD + 3mM GdnHCl (hours ± standard deviation)**
Wildtype [*PSI*$^+$]	1.8 ± 0.1	2.4 ± 0.4
Wildtype [*psi*$^-$]	1.9 ± 0.1	2.5 ± 0.5
Δ*ssb1* [*PSI*$^+$]	1.9 ± 0.1	n/a
Δ*ssb1* [*psi*$^-$]	1.9 ± 0.05	n/a
Δ*ssb2* [*PSI*$^+$]	1.9 ± 0	n/a
Δ*ssb2* [*psi*$^-$]	2.4 ± 0.2	n/a
Δ*ssb1* Δ*ssb2* [*PSI*$^+$]	4 ± 0.8	n/a
Δ*ssb1* Δ*ssb2* [*psi*$^-$]	2.4 ± 0.3	n/a
Δ*ssb1* Δ*ssb2* Δ*pfd2* [*PSI*$^+$]	4.5 ± 0.5	n/a
Δ*ssb1* Δ*ssb2* Δ*pfd2* [*psi*$^-$]	2.7 ± 0.2	n/a
Δ*ssb1* Δ*ssb2* Δ*pfd5* [*PSI*$^+$]	4.7 ± 1.1	n/a
Δ*ssb1* Δ*ssb2* Δ*pfd5* [*psi*$^-$]	2.2 ± 0.4	n/a
Δ*pfd1* [*PSI*$^+$]	2.2 ± 0.1	2.6 ± 0.3
Δ*pfd1* [*psi*$^-$]	1.9 ± 0.1	2.3 ± 0.2
Δ*pfd2* [*PSI*$^+$]	2 ± 0.2	2.7 ± 0.5
Δ*pfd2* [*psi*$^-$]	2 ± 0.2	2.7 ± 0.1
Δ*pfd3* [*PSI*$^+$]	3.1 ± 0.5	3.8 ± 1.2
Δ*pfd3* [*psi*$^-$]	2.9 ± 0.2	3.7 ± 0.4
Δ*pfd4* [*PSI*$^+$]	2.4 ± 0.1	n/a
Δ*pfd4* [*psi*$^-$]	2.6 ± 0.2	n/a
Δ*pfd5* [*PSI*$^+$]	2.2 ± 0.2	3.7 ± 1.3
Δ*pfd5* [*psi*$^-$]	2.2 ± 0.2	4.5 ± 1
Δ*pfd6* [*PSI*$^+$]	2.3 ± 0.1	2.8 ± 0.2
Δ*pfd6* [*psi*$^-$]	2.9 ± 0.7	3.8 ± 0.6

Table 5.

[*PSI*$^{+}$]^{pfd} isolates	**Accession number of the original pink isolate from Δ*pfd*/wildtype dissections and its mating type**	**Accession number of the GdnHCl-cured [*psi*$^{-}$] version of the isolate**	**Accession number of the Hsp104 overexpression-cured [*psi*$^{-}$] version of the isolate**
[*PSI*$^{+}$]^{pfd1}	MSY 207 a	MSY 233	MSY 281
[*PSI*$^{+}$]^{pfd2}	MSY 148 α	MSY 184	MSY 282
[*PSI*$^{+}$]^{pfd3}	MSY 190 a	MSY 216	MSY 283
[*PSI*$^{+}$]^{pfd4}	MSY 196 a	MSY 222	MSY 284
[*PSI*$^{+}$]^{pfd5}	MSY 203 a	MSY 229	MSY 285
[*PSI*$^{+}$]^{pfd6}	MSY 151 a	MSY 187	MSY 286

Table 6.

Cells crossed	Number of tetrads with 4:0 pink colony color segregation	Number of tetrads with 2 pink : 2 white colony color segregation
[*PSI*$^{+}$]^{pfd1} x [*psi*$^{-}$]	0/20	20/20
[*PSI*$^{+}$]^{pfd4} x [*psi*$^{-}$]	2/28	26/28
[*PSI*$^{+}$]^{pfd5} x [*psi*$^{-}$]	2/23	21/23
[*PSI*$^{+}$]^{pfd1} x [*PSI*$^{+}$]^{strong}	2/19	17/19
[*PSI*$^{+}$]^{pfd4} x [*PSI*$^{+}$]^{strong}	0/10	10/10
[*PSI*$^{+}$]^{pfd5} x [*PSI*$^{+}$]^{strong}	0/8	8/8
[*psi*$^{-}$]^{pfd1} x [*PSI*$^{+}$]^{strong}	0/15	15/15
[*psi*$^{-}$]^{pfd4} x [*PSI*$^{+}$]^{strong}	13/27	14/27
[*psi*$^{-}$]^{pfd5} x [*PSI*$^{+}$]^{strong}	0/20	20/20

Chapter 4: Conclusions

The prion hypothesis

The prion hypothesis states that prion proteins are able to adopt a unique, self-propagating form that enables them to convert like molecules into the self-replicating prion state. This self-propagating quality allows prions to act both as infectious agents, and a novel repository of genetic information that alters cellular phenotype. The ability of prion proteins to adopt alternate forms has phenotypic consequences for the cell: the prion form can mimic a loss-of function mutation in the determinant protein, as is the case for the yeast prions [*PSI*$^{+}$] and [*URE3*], or the prion form can act as a gain-of-function mutation, as seen with the prions [*PIN*$^{+}$] and [Het-S] [1-4].

Prion variants arise from differences in the physical state of the prion protein

Prion variants are analogous to bacterial and viral strains, and they have been documented in both the yeast and mammalian prion systems [5-10]. The difference between prion variants when compared to bacterial and viral strains is that bacterial and viral strains arise as a result of genomic mutations, while prion variants occur in the absence of changes in nucleic acids, and they are determined by different states of the prion protein [8, 9, 11-13]. Studies in the yeast prion system have shown that prion variants are determined solely by differences in prion protein state. Work from J. Weissman's lab has shown that recombinant Sup35 can form fibrils *in vitro* with different stabilities and conformations, and that transforming yeast with these recombinant Sup35 fibrils produces distinct [*PSI*$^{+}$] variants that depend on the conditions under which Sup35 fibrils were formed [13]. In a parallel publication, C. King and R. Diaz-Avalos showed that three [*PSI*$^{+}$] variants are transmitted solely through protein. King *et al.* purified fibrous Sup35 aggregates from three [*PSI*$^{+}$] variant yeast strains and used them to nucleate *in vitro* fiber-forming reactions with recombinant Sup35 [12]. When these

in vitro formed fibrils were transformed into non-infected [*psi*⁻] yeast, they produced [*PSI*⁺] phenotypes identical to those of the parent [*PSI*⁺] variants, indicating that all the information necessary for specifying prion variants can be transmitted through protein [12].

Experimental approaches used to distinguish prion variants

One of the earliest indications that [*PSI*⁺] prion variants are dependent upon the Sup35 prion protein was that multiple [*PSI*⁺] variants that differ in mitotic stabilities, as well as in levels of translational suppression, can be recovered in isogenic yeast after Sup35 overexpression [11]. A follow up study showed that [*PSI*⁺] variants differ in their interaction with a Sup35 prion domain point mutant known as *PNM2* [14]. Transforming yeast with a plasmid-encoded copy of *PNM2* caused an increase in the level of translational read-through in [*PSI*⁺]^{weak}, but it had the opposite effect on [*PSI*⁺]^{strong} where translational read-through was lowered [14]. The King lab took advantage of this observation and created a series of Sup35 prion domain point mutants which can distinguish [*PSI*⁺] variants [15]. The concept behind this assay is that each Sup35 prion domain mutant can access a limited range of states that are specified by its primary structure. This limited range of states determines whether a Sup35 molecule can join a particular [*PSI*⁺] variant's aggregates: if the Sup35 molecule cannot assume a form that allows it to be incorporated into variant [*PSI*⁺] aggregates, it will remain soluble and increase translational fidelity, thereby leading to redder colonies on rich medium. By challenging a [*PSI*⁺] variant with a series of Sup35 prion domain point mutants, a unique colony color fingerprint is produced that specifically identifies each [*PSI*⁺] variant. Another assay that can distinguish [*PSI*⁺] variants is semi-denaturing agarose gel electrophoresis (SDD-AGE) [16]. In this assay, cell lysates are incubated in buffer with a low concentration of detergent that enables prion aggregates to migrate through an agarose

gel, but it does not completely disrupt them. [*PSI*$^{+}$] variants analyzed by SDD-AGE show differences in the migration of Sup35 aggregates and in the levels of soluble Sup35. The combination of these two qualities can distinguish many [*PSI*$^{+}$] variants, but it may not be as sensitive as the colony color fingerprint generated by the interaction of a [*PSI*$^{+}$] variant with a series of Sup35 prion domain point mutants [16]. Differences in the thermal stability of Sup35 aggregates between [*PSI*$^{+}$] variants can also be detected by incubating cell lysates in a buffer with low detergent concentration, heating the samples at different temperatures, and determining at which temperature Sup35 aggregates become denatured by assaying if they can enter an SDS-PAGE gel [13].

Differences between mammalian prion variants are more difficult to determine than differences between yeast prion variants because they depend in part on clinical symptoms, such as the speed of disease onset, and specific neurodegenerative symptoms, such as whether a prion variant causes lethargy or hyperactivity after infection [6]. Such clinical symptoms can be correlated with variations in the distribution of brain lesions, and with the patterns of partial PrP digestion by proteases [5, 6]. However, these measurements can be subjective (for example, scoring changes in behavior after infection) or extremely difficult to carry out. For instance, distinguishing PrP patterns after partial protease digestion depends on several factors: the length of treatment, and the concentration of PrP and protease. Variations in any of these parameters can affect the degree of proteolytic digestion, change the pattern of PrP migration in an SDS-PAGE gel, and produce misleading results when typing prion variants.

Connections between prion variants and the species barrier to infection

Prion variants can be distinguished by genetic and biochemical assays, as well as by clinical symptoms, and they have been linked to interspecies transmission. Some bovine spongiform encephalopathy (BSE) variants are able to cross the species barrier and infect humans, mice, and sheep, while a single amino acid change in the prion domain sequence of the yeast protein Sup35 can render it capable or incapable of crossing a species barrier [7, 17-19]. The amino acid sequence of each prion protein dictates its range of accessible folds, which in turn directly affects its ability to adopt a form that is compatible with a particular prion variant.

Extensive work from the Weissman lab has shown that the degree of similarity in the sequence of prion proteins is the limiting factor in crossing the species barrier [17-20]. There is a robust species barrier between [*PSI*$^+$] prions formed by *S. cerevisiae* and *C. albicans* [20]. The Sup35 prion domain from *C. albicans* can form aggregates on its own, but when *C. albicans* Sup35 and *S. cerevisiae* Sup35 form aggregates in the same cell, the two types of aggregates do not co-localize and one species' [*PSI*$^+$] aggregates cannot recruit the other species' Sup35 [20]. Though there is a species barrier to [*PSI*$^+$] infection between *S. cerevisiae* and *C. albicans*, a chimeric Sup35 construct with resides 1-39 of the *S. cerevisiae* prion domain and residues 40-140 of the *C. albicans* prion domain can be induced to form [*PSI*$^+$] *in vivo* after transient overexpression of either species' Sup35 [19, 20]. The chimeric construct forms distinct [*PSI*$^+$] variants that depend on which species' Sup35 is used to induce chimeric [*PSI*$^+$] [19]. The chimeric Sup35 molecule can also form fibers *in vitro* when seeded with either species' Sup35 fibers, but chimera fibers that were seeded by *S. cerevisiae* can only catalyze the formation of *S. cerevisiae* but not *C. albicans* fibers in subsequent reactions, and *vice*

versa [19]. This suggests that the chimeric Sup35 molecule can form multiple heritable self-propagating prion conformations. Subsequent work demonstrated that a single point mutation in this chimeric Sup35 construct can generate a new prion transmission barrier that prevents the chimeric construct from forming fibers *in vitro* when seeded with *S. cerevisiae* fibers, but is still compatible with *C. albicans* fibers [17]. This species barrier to infection is also recapitulated *in vivo,* where the chimera point mutant construct can only be converted into the [*PSI*$^{+}$] state by transient overexpression of *C. albicans* but not *S. cerevisiae* Sup35 [17]. The explanation for these observations is that a single point mutation can change the spectrum of states that is accessible to a prion protein, and this limited range of states determines whether a prion protein is able interact with prion proteins from other species and cause infection.

Two models have been proposed to explain the connection between prion variants and interspecies prion state transmission: variant conversion and variant selection (fig. 1) [21]. The variant conversion model suggests that during crossing of a species barrier, the host-encoded heterologous prion protein adopts a new conformation that is seeded by the invading prions, but with different qualities than the invading species prion because of limitations in the range of states accessible to the host-encoded prion protein. In contrast, the variant selection model postulates that each prion variant is actually a mix of several different prion states, and that when this mix is introduced into a new host, some subsets of the invading prion variant forms are compatible with the host protein and therefore become amplified and dominant phenotypically, while incompatible forms of the original variant cannot propagate and therefore become stagnant or are otherwise lost. These two models propose alternate explanations for the observation that crossing of the species barrier is

usually accompanied by a change in prion form, which can be assayed by clinical symptoms, timing of disease onset, and conformational stability in the presence of the denaturant guanidine hydrochloride (GdnHCl) [22].

Competition can occur between two variants of the same prion protein

In addition to crossing of the species barrier, another scenario that examines the interaction between prion variants is competition between prion variants composed of identical prion proteins. In this case, two conformational variants of the same protein are introduced into one host. To date, these types of variant competition interactions have been shown to result in the phenotypic dominance of one variant at the expense of the other [10, 23, 24]. Specifically, interactions between the [*PSI*$^{+}$]^{weak} and [*PSI*$^{+}$]^{strong} yeast prion variants have been shown to result in the phenotypic dominance of [*PSI*$^{+}$]^{strong} in both the mitotic and meiotic progeny of cell crosses between the two variants [10]. The molecular basis of this phenotypic dominance was unclear, so experiments outlined in chapter two were designed to provide a better understanding of what happens when [*PSI*$^{+}$]^{weak} and [*PSI*$^{+}$]^{strong} are introduced into the same cytoplasm by a cell cross.

Mathematical modeling of [*PSI*$^{+}$] variant competition

One mathematical model has attempted to provide a better understanding of the interaction between [*PSI*$^{+}$] variants [25]. The model proposes that the prion variant with the lowest level of soluble protein ([*PSI*$^{+}$]^{strong}) will win the competition [25]. According to the model, the two key parameters in the competition between [*PSI*$^{+}$]^{weak} and [*PSI*$^{+}$]^{strong} are the rate of prion fiber growth (β), and the rate of fiber division (γ), both of which are specific to each [*PSI*$^{+}$] variant. *In vitro* experimental measurements show that [*PSI*$^{+}$]^{strong}-like fibers are the

slowest growing but easiest to fragment, so the [*PSI*$^{+}$]^{strong} variant generates a great number of small aggregates that can act as templates for the recruitment and conversion of soluble Sup35 into the [*PSI*$^{+}$]^{strong} form, and it is very efficient at *in vitro* seeding of Sup35 fibers [25]. In contrast, [*PSI*$^{+}$]^{weak}-like fibers are fast growing but very resistant to fragmentation, so [*PSI*$^{+}$]^{weak} generates a very small number of prion aggregate templates for the conversion of soluble Sup35, and it is not as efficient as [*PSI*$^{+}$]^{strong} at seeding Sup35 fiber formation [25]. These *in vitro* parameters do correlate to some observed differences between [*PSI*$^{+}$] variants *in vivo*. For example, [*PSI*$^{+}$]^{weak} contains higher levels of soluble Sup35 than [*PSI*$^{+}$]^{strong} [8], presumably because it generates less prion aggregate complexes for the conversion of soluble Sup35. Also, experimental measurements of the number of heritable aggregates have shown that [*PSI*$^{+}$]^{strong} cells contain more heritable prion complexes than [*PSI*$^{+}$]^{weak} cells, complementing the *in vitro* data that shows [*PSI*$^{+}$]^{strong} generates more seeds for Sup35 fiber formation than [*PSI*$^{+}$]^{weak} [25].

The proposed mathematical model makes several assumptions that overlook important steps in prion biogenesis. First of all, the mathematical model does not take into account cell division, and work from the Serio lab has shown that [*PSI*$^{+}$]^{weak} aggregates move more slowly than [*PSI*$^{+}$]^{strong} into daughter cells, with a greater bias for the retention of [*PSI*$^{+}$]^{weak} than [*PSI*$^{+}$]^{strong} aggregates in the mother cell (Derdowski, unpublished). Also, the mathematical model assumes that the competition between [*PSI*$^{+}$] variants does not depend upon the concentration of each type of aggregate. Work from the Weissman lab has shown that [*PSI*$^{+}$]^{strong} has a greater average number of heritable aggregates or propagons than [*PSI*$^{+}$]^{weak} [25]. When the two variants are introduced into the same cytoplasm by cell mating, [*PSI*$^{+}$]^{strong} has more surfaces than [*PSI*$^{+}$]^{weak} for the conversion of soluble Sup35 into the

prion form, which favors it over [*PSI*$^{+}$]^{weak} in the competition for inheritance. The prion variant interaction model proposed by the Weissman lab is a steady-state solution model which best predicts a population average, so it is very possible that such a model will miss the retention of [*PSI*$^{+}$]^{weak} aggregates in a fraction of cells after competition. A better way to model [*PSI*$^{+}$] variant interaction may be to use a stochastic or probability-based mathematical model that accounts for unequal segregation of prions during cell division [26].

Another factor that may influence the outcome of competition between [*PSI*$^{+}$] variants is competition for the substrate of conversion, Sup35. [*PSI*$^{+}$] variants are believed to result from alternate folds or forms of Sup35. Differences in tertiary or quaternary structure between [*PSI*$^{+}$] variants have been shown by the Weissman lab with hydrogen/deuterium exchange experiments, where [*PSI*$^{+}$]^{weak} and [*PSI*$^{+}$]^{strong} aggregates show differences in areas of protection from H/D exchange [27]. It is possible that Sup35 more easily folds into a form that is compatible with addition to [*PSI*$^{+}$]^{strong} aggregates, and that the form required to join [*PSI*$^{+}$]^{weak} aggregates is less preferred. This difference in the folding preferences of Sup35 monomers may tip the scales in favor of [*PSI*$^{+}$]^{strong} both in terms of its greater mitotic and meiotic stability compared to [*PSI*$^{+}$]^{weak} and in terms of [*PSI*$^{+}$] variant competition favoring [*PSI*$^{+}$]^{strong}.

The mechanism of prion variant competition *in vivo*

[*PSI*$^+$]^{weak} can be re-isolated after a cell cross with [*PSI*$^+$]^{strong}

Experiments outlined in chapter two have shed light on the mechanisms of interaction and competition between [*PSI*$^+$] variants. I took advantage of the yeast cell mating system that allowed me to introduce the [*PSI*$^+$]^{weak} and [*PSI*$^+$]^{strong} prion variants into the same cell by a cell cross. Growing these crossed cells in the presence of guanidine hydrochloride (GdnHCl) inhibits prion aggregate fragmentation by Hsp104, the molecular disaggregase that is responsible for fragmentation of [*PSI*$^+$] aggregates, and allows pre-existing prion aggregates to dilute into progeny cells through cell division, eventually leading to a loss of the prion state in progeny [28, 29]. If a colony produced by the growth of a single [*PSI*$^+$] cell on GdnHCl is resuspended in water and plated on rich medium, it will produce a mix of [*PSI*$^+$] and [*psi*$^-$] colonies. Each resultant [*PSI*$^+$] colony is believed to arise from a single cell that inherited a single prion aggregate complex, or propagon, so this assay can give an estimate of the number of heritable prion complexes generated by a [*PSI*$^+$] variant [30].

I applied this assay to study the inheritance of [*PSI*$^+$]^{weak} and [*PSI*$^+$]^{strong} aggregates from a single cell that was generated by a cross between [*PSI*$^+$]^{strong} and [*PSI*$^+$]^{weak}. Surprisingly, I recovered progeny cells that inherited the recessive [*PSI*$^+$]^{weak} aggregates, suggesting that [*PSI*$^+$]^{strong} and [*PSI*$^+$]^{weak} aggregates can co-exist after cytoplasmic mixing in a cell cross. One possible explanation for why I recovered some cells that inherited [*PSI*$^+$]^{weak} aggregates is that these [*PSI*$^+$]^{weak} colonies arose from a spontaneous change into the [*PSI*$^+$]^{weak} phenotype, rather than from the inheritance of [*PSI*$^+$]^{weak} aggregates from the original cell cross with [*PSI*$^+$]^{strong}. To test this possibility, I have performed control experiments where I crossed

[*PSI*$^+$]^{strong} to itself and [*PSI*$^+$]^{weak} to itself, grew the newly formed zygotes into colonies on GdnHCl, and then assayed what types of [*PSI*$^+$] colonies can be recovered from the progeny cells, as described above. Control [*PSI*$^+$]^{weak} x [*PSI*$^+$]^{weak} crosses generated only [*PSI*$^+$]^{weak} colonies, and control [*PSI*$^+$]^{strong} x [*PSI*$^+$]^{strong} crosses generated almost 100% [*PSI*$^+$]^{strong} colonies with very few spontaneous occurrences of [*PSI*$^+$]^{weak} colonies. In comparison to these control cell crosses, the cell cross between [*PSI*$^+$]^{weak} and [*PSI*$^+$]^{strong} generated a significant number of colonies that inherited the [*PSI*$^+$]^{weak} phenotype, supporting the idea that [*PSI*$^+$]^{strong} and [*PSI*$^+$]^{weak} aggregates can co-exist after mixing in a cell cross.

[*PSI*$^+$]^{weak} is lost progressively over time during competition with [*PSI*$^+$]^{strong}

Next, I observed that the number of cells that inherited the [*PSI*$^+$]^{weak} phenotype decreased over time. The longer [*PSI*$^+$]^{weak} and [*PSI*$^+$]^{strong} aggregates co-existed after a cell cross and before prion aggregate fragmentation was inhibited by the addition of GdnHCl, the smaller the number of recovered cells that inherited the [*PSI*$^+$]^{weak} phenotype. I propose that the most likely reason why [*PSI*$^+$]^{weak} is lost progressively over time is due to differences in transmission of [*PSI*$^+$]^{weak} versus [*PSI*$^+$]^{strong} into daughter cells. Unpublished work from the Serio lab has shown that [*PSI*$^+$]^{weak} aggregates move much more slowly than [*PSI*$^+$]^{strong} into daughter cells, and that [*PSI*$^+$]^{weak} aggregates tend to be retained in mother cells to a greater extent than [*PSI*$^+$]^{strong} aggregates (Derdowski, unpublished). This decreased efficiency of [*PSI*$^+$]^{weak} inheritance due to the lesser mobility of its Sup35 aggregates fits with my observation that [*PSI*$^+$]^{weak} is lost progressively from the progeny of [*PSI*$^+$]^{weak} x [*PSI*$^+$]^{strong} cells. For example, if 20% of progeny in each cell generation fail to inherit [*PSI*$^+$]^{weak} aggregates because [*PSI*$^+$]^{weak} aggregates were not transmitted to them, then this 20% loss of [*PSI*$^+$]^{weak} after each generation will become more pronounced over time because it will lead

to an accumulation of cells that did not inherit [*PSI*$^{+}$]^{weak}. Another observation that supports this idea is that [*PSI*$^{+}$]^{weak} is less mitotically stable than [*PSI*$^{+}$]^{strong}, so perhaps this greater rate of spontaneous [*PSI*$^{+}$]^{weak} loss is a result of its decreased ability to be transmitted into daughter cells [8]. The stable inheritance of [*PSI*$^{+}$] depends upon the ability of [*PSI*$^{+}$] aggregates to recruit soluble Sup35 and be fragmented (fig. 2). Sup35 aggregates must continue to grow by incorporating new Sup35 molecules, and they must also be fragmented in order to create new surfaces for the conversion of Sup35 into the prion form. Fragmentation of Sup35 aggregates is crucial for the inheritance of [*PSI*$^{+}$] by daughter cells. If [*PSI*$^{+}$] aggregates are not fragmented by Hsp104, they become large and immobile, and cannot be transmitted into daughter cells [29]. *In vitro* work from the Weissman lab discussed above has shown that [*PSI*$^{+}$]^{weak}-like aggregates are more resistant to fragmentation than [*PSI*$^{+}$]^{strong}-like aggregates, providing additional support for the idea that [*PSI*$^{+}$]^{weak} aggregates are lost after competition with [*PSI*$^{+}$]^{strong} because [*PSI*$^{+}$]^{weak} aggregates are not fragmented as easily as [*PSI*$^{+}$]^{strong}, which causes [*PSI*$^{+}$]^{weak} aggregates to be retained in mother cells rather than be transmitted into daughters.

Inhibition of [*PSI*$^{+}$] aggregate fragmentation by Hsp104 allows [*PSI*$^{+}$]^{weak} to compete better with [*PSI*$^{+}$]^{strong}

I tested the idea that the inhibition of [*PSI*$^{+}$] aggregate fragmentation by Hsp104 will take away [*PSI*$^{+}$]^{strong}'s advantage and allow more [*PSI*$^{+}$]^{weak} to be inherited by progeny cells. In the original set of cell crosses between [*PSI*$^{+}$]^{weak} and [*PSI*$^{+}$]^{strong}, I mated cells on rich medium and then moved them to medium with GdnHCl to inhibit Hsp104 immediately after zygote formation. These zygotes spent just a single cycle on rich medium, where Hsp104 could fragment [*PSI*$^{+}$] aggregates. In the next set of experiments, I crossed [*PSI*$^{+}$]^{weak} x [*PSI*$^{+}$]^{strong}

directly on medium with GdnHCl, so that Hsp104 could not fragment [*PSI*$^+$] aggregates during zygote formation. The only difference between the zygotes from the two experiments is the presence or absence of Hsp104 fragmentation for a single cell cycle; there is no difference in the number of cell divisions before I assayed how much [*PSI*$^+$]^{weak} is inherited by progeny, so comparing these two sets of conditions allowed me to analyze the role of Hsp104's fragmentation of prion aggregates in the competition between [*PSI*$^+$]^{weak} and [*PSI*$^+$]^{strong}. I reasoned that if [*PSI*$^+$]^{weak} aggregates are lost after competition with [*PSI*$^+$]^{strong} largely because they are not as efficiently fragmented by Hsp104 and therefore are not efficiently transmitted into daughters, then inhibition of Hsp104 activity will take away some of [*PSI*$^+$]^{strong}'s advantage and more cells will inherit [*PSI*$^+$]^{weak}. Data in chapter 2 shows that this idea holds true: inhibition of prion aggregate fragmentation by Hsp104 allows [*PSI*$^+$]^{weak} to compete better with [*PSI*$^+$]^{strong} and be inherited by more progeny cells. This observation is in agreement with work from the Weissman lab showing that [*PSI*$^+$]^{strong}-like fibers fragment more easily than [*PSI*$^+$]^{weak}-like fibers [25]. In the absence of prion aggregate fragmentation *in vivo*, the less easily fragmented [*PSI*$^+$]^{weak} variant gains an advantage compared to when aggregate fragmentation is allowed to occur, because during *in vivo* fragmentation the more easily fragmented [*PSI*$^+$]^{strong} aggregates will outnumber the less easily fragmented [*PSI*$^+$]^{weak} aggregates, thereby reducing the overall proportion of [*PSI*$^+$] cells that inherit [*PSI*$^+$]^{weak} just because there will be so much more [*PSI*$^+$]^{strong} that can be transmitted into progeny cells.

Another [*PSI*$^+$]^{weak} characteristic that may put it at a disadvantage when it comes to competition with [*PSI*$^+$]^{strong} is that [*PSI*$^+$]^{weak} is much more sensitive than [*PSI*$^+$]^{strong} to changes in the expression level of Hsp104. [*PSI*$^+$]^{weak} is more readily lost than [*PSI*$^+$]^{strong} both

when Hsp104 is overexpressed and when it is inactivated with guanidine hydrochloride (T. Serio, unpublished) [11, 31]. Perhaps [*PSI*$^{+}$]^{weak}'s sensitivity with respect to Hsp104 activity is what causes it to be lost gradually when competing with [*PSI*$^{+}$]^{strong}. [*PSI*$^{+}$]^{strong} is more resistant to alterations in the expression level of Hsp104, perhaps because [*PSI*$^{+}$]^{strong} aggregates recruit Hsp104 efficiently, enabling them to be fragmented and passed on to daughter cells easily. In comparison with [*PSI*$^{+}$]^{strong}, [*PSI*$^{+}$]^{weak} aggregates may not recruit Hsp104 as efficiently. This possibility is supported indirectly by several observations. Firstly, [*PSI*$^{+}$]^{weak} aggregates appear to be larger than [*PSI*$^{+}$]^{strong} by SDD-AGE, and the larger average size of [*PSI*$^{+}$]^{weak} aggregates can be explained by them not being fragmented efficiently by Hsp104 (chapters 2 and 3) [16]. Also, [*PSI*$^{+}$]^{weak} variants contain more soluble Sup35 than [*PSI*$^{+}$]^{strong}, again suggesting that Hsp104 does not fragment [*PSI*$^{+}$]^{weak} aggregates efficiently, resulting in less surfaces for conversion to prion form, and, consequently, more soluble Sup35 [8]. Larger [*PSI*$^{+}$]^{weak} aggregates also result in fewer heritable [*PSI*$^{+}$]^{weak} aggregates or propagons per cell in comparison with [*PSI*$^{+}$]^{strong} (Strbuncelj, unpublished) [25]. All these observations suggest that [*PSI*$^{+}$]^{weak} is not as readily fragmented by Hsp104 as [*PSI*$^{+}$]^{strong}, resulting in [*PSI*$^{+}$]^{weak}'s increased mitotic instability [8]. Perhaps inhibition of Hsp104 activity during the cell cross between [*PSI*$^{+}$]^{weak} and [*PSI*$^{+}$]^{strong} took away some of [*PSI*$^{+}$]^{strong}'s advantage in the variant competition, so that when [*PSI*$^{+}$]^{strong} aggregates are not fragmented by Hsp104 they become larger, more difficult to transmit to daughter cells, and therefore more similar to [*PSI*$^{+}$]^{weak}. This set of conditions could be the reason why more [*PSI*$^{+}$]^{weak} aggregates are inherited by progeny cells when prion aggregate fragmentation is blocked during a cell cross between [*PSI*$^{+}$]^{weak} and [*PSI*$^{+}$]^{strong}, because when aggregate fragmentation is blocked, there are fewer [*PSI*$^{+}$]^{strong} aggregates that can be passed on to daughter cells, so a greater proportion of total [*PSI*$^{+}$] cells will inherit [*PSI*$^{+}$]^{weak}. In support

of this idea, an increase in Sup35 aggregate size after treating cells with guanidine hydrochloride to inhibit Hsp104 has been documented [16].

Increased fragmentation of [PSI^+]^{weak} aggregates allows them to compete better with [PSI^+]^{strong}

Next, I wanted to determine if allowing Hsp104 more time to fragment [*PSI*$^+$] aggregates before cell division and before [*PSI*$^+$] transmission to daughters will increase the proportion of cells that inherit [*PSI*$^+$]^{weak}. I inhibited cell division by incubating [*PSI*$^+$]^{weak} x [*PSI*$^+$]^{strong} zygotes on media lacking histidine for 24 hours. The cells used in this experiment cannot divide in the absence of histidine, but Hsp104 remains active and fragments pre-existing [*PSI*$^+$] aggregates. Hsp104 fragmentation of [*PSI*$^+$] aggregates in the absence of cell division during incubation on medium lacking histidine should increase the number of heritable [*PSI*$^+$] complexes. This prediction is validated by the observation that there is an increase in the number of heritable [*PSI*$^+$] aggregates (propagons) after 24 hours of histidine starvation, compared to the number of propagons in normally growing cells (chapter 2). Besides inhibiting cell division, histidine starvation does not allow the synthesis of new Sup35 molecules. The levels of Sup35 expression in actively growing cells compared to cells that were histidine starved for 24 hours are not significantly different (chapter 2). The combination of increased [*PSI*$^+$] aggregate fragmentation and an inhibition of new Sup35 synthesis for 24 hours before cell division is resumed (by moving zygotes to complete medium with GdnHCl) allows [*PSI*$^+$]^{weak} to compete better with [*PSI*$^+$]^{strong}, and a greater proportion of progeny cells inherit [*PSI*$^+$]^{weak} after these conditions (chapter 2).

Several key steps of the prion cycle may be behind the observed link between loss of [*PSI*$^{+}$]^{weak} and cell division. In order for each [*PSI*$^{+}$] variant to be inherited by daughter cells, prion aggregates must migrate through a cell's bud neck into the new daughter cell. Work from the Serio lab has shown that [*PSI*$^{+}$]^{weak} aggregates move more slowly through the bud neck and have a greater tendency to be retained in mother cells, while [*PSI*$^{+}$]^{strong} aggregates move more efficiently into daughter cells (Derdowski, unpublished). This difference in prion transport efficiency into daughter cells may account for the observed gradual loss of [*PSI*$^{+}$]^{weak}. Since incubating cells on medium lacking histidine increases the number of heritable [*PSI*$^{+}$] aggregates in the absence of new Sup35 synthesis, this means that the heritable [*PSI*$^{+}$] aggregates must become smaller and hence more mobile after 24 hours of histidine starvation. An increase in [*PSI*$^{+}$]^{weak} mobility after histidine starvation should make [*PSI*$^{+}$]^{weak} more transmissible, and this increase in [*PSI*$^{+}$]^{weak} transmissibility can be detected because I recover more progeny cells that inherit [*PSI*$^{+}$]^{weak} after histidine starvation (chapter 2). Clearly, the transmissibility of [*PSI*$^{+}$] aggregates is crucial for their inheritance. SDD-AGE shows that [*PSI*$^{+}$]^{weak} aggregates are larger than [*PSI*$^{+}$]^{strong}, and unpublished work from the Serio lab has shown that the larger [*PSI*$^{+}$]^{weak} aggregates move more slowly than [*PSI*$^{+}$]^{strong} into daughter cells, and that a smaller proportion of [*PSI*$^{+}$]^{weak} aggregates moves into daughter cells when compared with [*PSI*$^{+}$]^{strong} (Derdowski, unpublished). This implies that there may be a size limit that determines which size [*PSI*$^{+}$] complexes can move into daughter cells, with a bias for better transmission of smaller aggregates. In support of this idea, incubating cells on medium lacking histidine probably decreases the average size of [*PSI*$^{+}$] complexes, making smaller [*PSI*$^{+}$]^{weak} complexes (smaller after histidine starvation for 24 hours) more transmissible and more heritable than larger [*PSI*$^{+}$]^{weak} aggregates (chapter 2).

The discovery that [*PSI*$^{+}$] aggregate size is crucial for transmission to daughter cells and for inheritance offers one explanation for why larger [*PSI*$^{+}$]^{weak} aggregates are lost with increasing cycles of cell division when competing with the smaller and more mobile [*PSI*$^{+}$]^{strong} aggregates (chapter 2 and Derdowski, unpublished). In contrast to this result, the proposed mathematical model of [*PSI*$^{+}$] variant competition predicts that the competition between [*PSI*$^{+}$]^{weak} and [*PSI*$^{+}$]^{strong} does not occur at the level of transmission into daughter cells, but it depends on the number of [*PSI*$^{+}$] aggregate templates that convert soluble Sup35 into the prion form [25]. Experimental data that supports the mathematical model shows that *in vitro* generated [*PSI*$^{+}$]^{weak}-like aggregates are not efficiently fragmented, so a cell contains fewer [*PSI*$^{+}$]^{weak} aggregates that can recruit soluble Sup35 in comparison to the readily fragmented, more numerous [*PSI*$^{+}$]^{strong} aggregates [25]. The mathematical model proposes that [*PSI*$^{+}$]^{weak} cannot efficiently compete with [*PSI*$^{+}$]^{strong} for recruitment of soluble Sup35, so that [*PSI*$^{+}$]^{weak} aggregates are diluted and lost by cell division. In contrast to this prediction, I recovered some cells from the [*PSI*$^{+}$]^{weak} x [*PSI*$^{+}$]^{strong} cross that retain high levels of heritable [*PSI*$^{+}$]^{weak} aggregates even after many rounds (at least 80 generations) of cell division (chapter 2). These data argue that [*PSI*$^{+}$]^{weak} aggregates are not as deficient at recruiting soluble Sup35 as is predicted by the mathematical model, because if [*PSI*$^{+}$]^{weak} could not readily recruit soluble Sup35, then it would not be retained in a high proportion of cells after many cycles of cell division. This observation is also in agreement with work published alongside the mathematical model that shows that [*PSI*$^{+}$]^{weak}-like fibers grow more quickly than [*PSI*$^{+}$]^{strong}-like fibers, suggesting that [*PSI*$^{+}$]^{weak} is not deficient at recruiting soluble Sup35 molecules into its aggregates [25].

The transport of mammalian prions through the body is not well understood, but clearly some transport mechanism must exist because ingestion of tainted meat can cause people to fall sick with a form of bovine spongiform encephalopathy (BSE) called variant Creutzfeldt-Jakob disease (vCJD) [32, 33]. It is unknown how mammalians prions travel from the digestive system and into neurons. However, transport through the host body must be a key step for establishment of infection, because work with transmissible mink encephalopathy (TME) variants has shown that they compete somewhere in the body before infecting the brain [24]. The competition between TME variants at this unknown location is crucial because it can extend the incubation time before disease onset caused by the dominant TME variant, and it is possible that antagonism between TME variants may occur at the level of competition for transport factors that enable the prions to travel to and infect the brain. The importance of mammalian prion aggregate size for infectivity was demonstrated by work from the Caughey lab [34]. The Caughey lab showed that the most infectious prion aggregates are small in size and fall in the range of 300-600 KDa, which corresponds to about 14-28 PrP molecules. These small PrP aggregates are most infectious because they shorten the time before disease onset when they are inoculated intracerebrally into hamsters [34]. Inoculation with larger PrP fibrils or with PrP complexes that contain fewer than 5 PrP molecules produced virtually no infectivity [34]. This is another parallel between the yeast and mammalian prion systems, because in chapter 2 I have shown that decreasing the size of $[PSI^{+}]^{weak}$ aggregates by histidine starvation makes these smaller $[PSI^{+}]^{weak}$ aggregates more transmissible and more infectious. Mathematical modeling of the spread of mammalian prion diseases in a host has also shown that prion infectivity is specified both by the number of prion aggregates and by their size [35]. Studies of mammalian prions have shown that they do not replicate uniformly in all locations in a host, but that they must be transported to

some site of replication in order to be infectious [24]. Because of this need for transport inside the host, the mathematical model predicts that a small aggregate may be transported more quickly than a large aggregate, so small prion aggregates are more likely to cause disease than large aggregates [35]. This mathematical prediction has been shown to hold true both in the mammalian and yeast prion systems. Small PrP aggregates of 14-28 molecules are the most infectious, and decreasing the size of $[PSI^{+}]^{weak}$ aggregates makes them more heritable and transmissible (chapter 2) [34].

Implications for prion biology

Experimental work in chapter 2 and unpublished data from the Serio lab examining $[PSI^{+}]^{weak}$ and $[PSI^{+}]^{strong}$ transmission rates into daughter cells show that the efficiency of prion aggregate transmission into daughter cells plays a key role in the inheritance of $[PSI^{+}]$ variants (Derdowski, unpublished). This work (chapter 2) shows it is possible for "recessive" prion variants to propagate cryptically after exposure to a dominant variant, and that their presence can be masked by the dominant prion variant phenotype. The same principle of cryptic prion propagation may apply in the mammalian system. It is particularly difficult to "type" mammalian prion variants because typing relies on clinical symptoms that may be somewhat subjective in nature, and on partial proteolytic digests that look at the average proteolytic profile of PrP^{sc} (the disease-associated form of PrP) in cell lysates. Proteolytic profiling of lysates may not be sensitive enough to detect low levels of a prion variant if it is mixed with another higher abundance variant, and clinical symptoms that are characteristic of one prion variant infection do not exclude the masked presence of another variant in the diseased animal.

This raises the question, are individual prion strains/variants distinct and unique states of the prion protein? Or are prion variants actually a mix of prion protein states, whose phenotypic appearance depends on the ratios and interplay between different forms of the same prion protein that are simultaneously present in one host? Both options are possible explanations of the prion strain phenomenon. If prion strains are not actually caused by single distinct forms of the prion protein, but are a mix of several prion protein forms, then the phenomenon of the species barrier to infection is well explained by the variant selection model (fig. 1). According to the variant selection model, when a mix of prion protein forms that we think of as a prion variant is introduced into a heterologous host, the species barrier can be crossed and infection can be established if one of the original inoculate prion forms is compatible with recruiting and converting the prion protein molecules of the new host. If this happens, all the other prion protein forms from the original inoculate will be lost because they will be unable to grow and divide. One result of the loss of certain prion forms in the new host may be that the prion phenotype will change after crossing the species barrier. Such a change or adaptation in the prion phenotype and in the prion protein state has been documented during crossing of the species barrier [22]. Another possibility opened by the idea that prion variants may be composed of a mix of prion forms is that the host's environment may change prion phenotypes. For example, a host may be particularly resistant to infection with one prion variant out of a mix, but susceptible to infection with others. In this way the host may select for the amplification of certain prion forms out of a mixed pool.

Remaining questions and possible experimental approaches

While my observations indicate that under specific conditions [*PSI*$^{+}$]^{weak} can be recovered from [*PSI*$^{+}$]^{strong} x [*PSI*$^{+}$]^{weak} crosses, the possibility remains that the interaction between prion variants also leads to the generation of novel conformational states. A major challenge in addressing this issue experimentally is the sensitivity of the available assays. SDD-AGE and variant typing *via* interaction with Sup35 prion domain mutants report the average aggregate profile in a population of cells. They are very useful for typing cultures consisting of one type of variant, and they are sensitive enough to detect a mixture of [*PSI*$^{+}$]^{weak} and [*PSI*$^{+}$]^{strong} variants in a population of cells (chapter 2). However, when these assays detect a mixture or a change in [*PSI*$^{+}$] aggregates in a population, the assay outputs cannot distinguish how many [*PSI*$^{+}$] variants are propagated in the population, and they only show a change in the average [*PSI*$^{+}$] profile.

Previous studies have revealed that distinct conformational variants of the [*PSI*$^{+}$] prion often cannot be distinguished by their phenotypes [12, 15]. One strategy to determine if new conformational variants have emerged from a mixed population is to selectively amplify that subpopulation or alternately to eliminate its competitors. For example, the *PNM2* Sup35 mutant has differential effects on [*PSI*$^{+}$]^{weak} and [*PSI*$^{+}$]^{strong}. PNM2 expression increases translational read-through in [*PSI*$^{+}$]^{weak}, but decreases it in [*PSI*$^{+}$]^{strong} [14]. If *PNM2* could specifically eliminate or cure [*PSI*$^{+}$]^{strong} without adversely affecting [*PSI*$^{+}$]^{weak}, it would be possible to selectively amplify [*PSI*$^{+}$]^{weak} with PNM2 expression after [*PSI*$^{+}$] variant competition. While *PNM2*, or any other reported Sup35 prion domain point mutant, does not have this desirable [*PSI*$^{+}$] variant-specific curing effect (S. DiSalvo, unpublished) [15], other *cis* or *trans* modulators of [*PSI*$^{+}$] propagation could be tested for these effects. For

example, work from the Ter-Avanesyan lab has shown that [*PSI*$^{+}$]^{strong} is resistant to curing by overexpression of the chaperones Ssa1, Ssb1, and Ydj1, but that [*PSI*$^{+}$]^{weak} can be cured by the overexpression of these proteins [36]. Modulating the expression levels of such [*PSI*$^{+}$] regulators could selectively amplify one [*PSI*$^{+}$] variant out of a mixed population.

Another possible way to selectively amplify a particular [*PSI*$^{+}$] variant after competition would be to exploit potential differences in sensitivity to Hsp104 expression levels between the variants. For example, if [*PSI*$^{+}$]^{strong} were more sensitive to Hsp104 overexpression than [*PSI*$^{+}$]^{weak}, then modulation of Hsp104 levels could lead to the loss of the dominant [*PSI*$^{+}$]^{strong} variant and reveal the presence of [*PSI*$^{+}$]^{weak} after variant competition. Unfortunately, the "recessive" [*PSI*$^{+}$]^{weak} variant is more sensitive to modulation of Hsp104 levels so this approach cannot be used to select for the [*PSI*$^{+}$]^{weak} variant (Serio, unpublished) [13, 31]. However, in theory it is possible that modulation of Hsp104 levels can be used to select for other [*PSI*$^{+}$] variants.

My studies support a model of prion variant competition in which distinct conformational forms fluctuate in the population primarily due to differences in their transmissibility to daughter cells. While this parameter is likely influenced by the rate of action of Hsp104 on [*PSI*$^{+}$] complexes as well as cell division timing and rate of Sup35 synthesis, the model predicts essentially no interaction between the two prion forms. Distinct variants, however, could interact directly to impact the outcome of the competition. One way to explore this possibility would be to use fluorescence resonance energy transfer, FRET. The [*PSI*$^{+}$] variant competition experiment could be set up so that each variant mating cell would express Sup35 fused to one FRET partner under the control of a haploid-specific promoter

that would be shut off in the diploid upon cell crossing of the two variants. One problem with this approach is that [*PSI*$^{+}$]^{weak} has a pool of soluble Sup35 that should readily join [*PSI*$^{+}$]^{strong} aggregates, so FRET would detect the interaction of soluble Sup35 from [*PSI*$^{+}$]^{weak} with [*PSI*$^{+}$]^{strong} aggregates, rather than just detecting the interaction between each variant's aggregates. This could be controlled for by comparing FRET signal after crossing [*PSI*$^{+}$]^{weak} and [*PSI*$^{+}$]^{strong} variants in the presence of GdnHCl, which will inhibit aggregate fragmentation and should report the baseline signal generated by the interaction of soluble Sup35 from [*PSI*$^{+}$]^{weak} with [*PSI*$^{+}$]^{strong} aggregates. Additional baselines and controls that the [*PSI*$^{+}$]^{weak} x [*PSI*$^{+}$]^{strong} cross should be compared to include the cell cross [*psi*$^{-}$] x [*psi*$^{-}$], where Sup35 is soluble and there should be minimal, if any, FRET signal. [*PSI*$^{+}$]^{weak} x [*psi*$^{-}$] and [*PSI*$^{+}$]^{strong} x [*psi*$^{-}$] should both give a more intense FRET signal than the [*PSI*$^{+}$]^{weak} x [*PSI*$^{+}$]^{strong} cell cross, because the soluble pool of Sup35 from [*psi*$^{-}$] cells should readily add on to any [*PSI*$^{+}$] variant aggregates. If [*PSI*$^{+}$]^{weak} and [*PSI*$^{+}$]^{strong} aggregates truly do interact, then their cell cross should generate a stronger FRET signal when cells are kept in complete medium than when cells are crossed in the presence of GdnHCl. GdnHCl will block aggregate fragmentation by Hsp104 but not the addition of soluble Sup35 to pre-existing aggregates, so if [*PSI*$^{+}$] variants truly interact, I expect less interaction between [*PSI*$^{+}$] variants and less FRET signal in the absence of [*PSI*$^{+}$] aggregate fragmentation [29]. However, if [*PSI*$^{+}$]^{weak} and [*PSI*$^{+}$]^{strong} aggregates do not interact, then crossing these cells in the absence or presence of GdnHCl should generate the same FRET signal because in both cases only the soluble Sup35 pool from [*PSI*$^{+}$]^{weak} will join [*PSI*$^{+}$]^{strong} aggregates to generate FRET, and this process of conversion of soluble Sup35 into the prion form is not affected by the presence of GdnHCl [29].

While [*PSI*$^{+}$]^{strong} is phenotypically dominant over [*PSI*$^{+}$]^{weak} at the colony level, the [*PSI*$^{+}$]^{weak} phenotype appears to be dominant in the nascent zygotes as assessed by growth on media lacking adenine (chapter 2). This surprising observation contrasts with the immediate phenotypic dominance of [*PSI*$^{+}$]^{strong} over [*psi*$^{-}$] in similar crosses, previously observed [37]. As the adenine prototrophy monitored in this assay is dependent on the level of soluble Sup35, the inability of [*PSI*$^{+}$]^{weak} x [*PSI*$^{+}$]^{strong} zygotes to grow in the absence of adenine suggests that the soluble Sup35 present in the [*PSI*$^{+}$]^{weak} cytoplasm did not join [*PSI*$^{+}$]^{strong} aggregates upon cell fusion (chapter 2) [8]. What prevents soluble Sup35 in [*PSI*$^{+}$]^{weak} cells from converting to [*PSI*$^{+}$]^{strong} in this mating? There are several possibilities. Soluble Sup35 in [*PSI*$^{+}$]^{weak} cells could exist in a form that is not readily able to join [*PSI*$^{+}$]^{strong} aggregates if, for example, a portion of the soluble pool is generated by exchange with [*PSI*$^{+}$]^{weak} complexes. Another possibility is that the inactivation of soluble Sup35 from [*psi*$^{-}$] cells by assimilation into [*PSI*$^{+}$]^{strong} complexes in [*PSI*$^{+}$] x [*psi*$^{-}$] crosses may be dependent upon a substantial increase in the size of prion complexes and their subsequent fragmentation. In this way, the number of prion templates would quickly amplify. Since [*PSI*$^{+}$]^{weak} strains contain a far less abundant soluble pool of Sup35 than [*psi*$^{-}$] strains, this process of template amplification could be severely compromised leading to the persistence of soluble, functional Sup35 as has been previously observed in crosses performed under conditions of Hsp104 inhibition [29]. Allowing [*PSI*$^{+}$]^{weak} x [*PSI*$^{+}$]^{strong} zygotes more time for aggregate remodeling by keeping them longer on mating medium containing cytosine before moving them to medium lacking adenine, however, did not improve their growth in the absence of adenine, suggesting that the soluble pool of Sup35 remained, preventing growth in the absence of adenine (Strbuncelj, unpublished).

Since cell division plays an important role in the loss of [*PSI*$^{+}$]^{weak}, a third possibility is that some cycles of cell division are necessary to alter the balance between [*PSI*$^{+}$]^{weak} and [*PSI*$^{+}$]^{strong} aggregates after mixing, allowing progeny cells to inherit a greater proportion of the more efficiently inherited [*PSI*$^{+}$]^{strong} aggregates which can then assert their phenotypic dominance in such a mixed cytoplasm. Inheriting a larger number of [*PSI*$^{+}$]^{strong} complexes in proportion to [*PSI*$^{+}$]^{weak} complexes will enable the more numerous [*PSI*$^{+}$]^{strong} aggregates to recruit the soluble Sup35 pool that is associated with [*PSI*$^{+}$]^{weak}. Perhaps in a [*PSI*$^{+}$]^{strong} x [*PSI*$^{+}$]^{weak} zygote there are not enough [*PSI*$^{+}$]^{strong} complexes to recruit all the soluble Sup35 from [*PSI*$^{+}$]^{weak}, so the remaining soluble Sup35 prevents zygote growth on medium lacking adenine. This idea could be tested by lowering the number of heritable [*PSI*$^{+}$]^{weak} aggregates before variant competition by mating. One way to do this would be to briefly expose the [*PSI*$^{+}$]^{weak} mating partner to guanidine hydrochloride before mating, just enough to increase aggregate size, but not enough to cause loss of [*PSI*$^{+}$]^{weak} aggregates. Zygotes from such a cross could then be challenged for their ability to grow without adenine, and if the [*PSI*$^{+}$]^{strong} phenotype is immediately established and allows for growth without adenine, this would suggest that the ratio between the number of [*PSI*$^{+}$]^{strong} and [*PSI*$^{+}$]^{weak} aggregates is key for [*PSI*$^{+}$]^{strong}'s ability to assert phenotypic dominance.

Work from the Liebman lab has shown that [*PSI*$^{+}$]^{strong} asserts its phenotypic dominance after about 20 generations, so it remains to be determined when exactly, if not in the zygote, this phenotypic dominance is established [10]. A possible way to answer this question would be allow [*PSI*$^{+}$]^{strong} x [*PSI*$^{+}$]^{weak} zygotes to form several daughter buds, isolate these daughters on medium lacking adenine, and determine how many cell divisions and how many daughter generations are necessary before the [*PSI*$^{+}$]^{strong} phenotype is established and daughters can

grow in the absence of adenine. Another way to measure the level of soluble Sup35 is with a fluorescent translational read-through UGA-dsRed reporter [37]. If this reporter were integrated into [*PSI*$^+$]^{weak} cells, these cells should remain dark because of faithful translation termination function provided by the soluble pool of Sup35. When UGA-dsRed [*PSI*$^+$]^{weak} cells are crossed to [*PSI*$^+$]^{strong}, the zygote should remain dark because Sup35 from [*PSI*$^+$]^{weak} remains soluble, as was shown by the absence of growth of [*PSI*$^+$]^{strong} x [*PSI*$^+$]^{weak} zygotes on adenine. However, if these zygotes are allowed to grow on rich medium, fluorescent dsRed signal should appear after several rounds of cell division during which [*PSI*$^+$]^{weak} aggregates will be diluted out of some progeny cells. The timing of the appearance of the dsRed signal would give an estimate for how long it takes [*PSI*$^+$]^{strong} to assert phenotypic dominance over [*PSI*$^+$]^{weak}.

Effects of the co-translational chaperone prefoldin on [*PSI*$^+$] prion propagation

In chapter 3, I have shown that single subunit deletion mutants of the prefoldin chaperone destabilize the [*PSI*$^+$] phenotype, leading to an increased rate of [*PSI*$^+$] loss and to the emergence of new [*PSI*$^+$] phenotypes. Surprisingly, the loss of prefoldin function was also found to be mutagenic to cells. The mutagenic effect of Δ*pfd* has allowed me isolate mutants that dominantly alter the link between [*PSI*$^+$] complexes and [*PSI*$^+$] phenotypes independently of prefoldin.

Why is [*PSI*$^+$] destabilized in Δ*pfd* mutants? Genetic analysis has shown that [*PSI*$^+$] aggregate conformation is not altered by mutations in prefoldin, nor by the isolated dominant mutations that arose as a result of loss of prefoldin function. [*PSI*$^+$] aggregate conformation appears to be unaffected by these mutations, because once the mutations are segregated

away by a series of cell crosses with wildtype cells followed by the recovery of wildtype meiotic progeny, the original parental [*PSI*$^{+}$]^{strong} phenotype re-emerges in wildtype meiotic segregants (chapter 3, meiotic tetrad analyses). This result suggests that [*PSI*$^{+}$] propagation is disrupted in prefoldin mutants.

The possibility that Δ*pfd* mutants have a defect in [*PSI*$^{+}$] propagation is supported by the observation that Δ*pfd* mutants have a decreased number of heritable [*PSI*$^{+}$] complexes called propagons (quantitative curing, chapter 3). Cells with fewer heritable aggregates may be prone to losing [*PSI*$^{+}$] more readily than cells with higher number of heritable aggregates because when there are fewer [*PSI*$^{+}$] aggregates that can be inherited by daughter cells, the chances of [*PSI*$^{+}$] transmission into daughters are reduced. Such a reduction in the proportion of daughter cells that inherit [*PSI*$^{+}$] aggregates would result in the increased rate of [*PSI*$^{+}$] loss, which was observed in Δ*pfd* mutants. In some ways, the reduction in the number of [*PSI*$^{+}$] aggregates in Δ*pfd* mutants that is accompanied by higher rate of [*PSI*$^{+}$] loss in Δ*pfd* mutants parallels the situation with [*PSI*$^{+}$]^{weak} aggregates: [*PSI*$^{+}$]^{weak} cells contain fewer heritable Sup35 aggregates than [*PSI*$^{+}$]^{strong}, so [*PSI*$^{+}$]^{weak} cells show a higher rate of mitotic loss than [*PSI*$^{+}$]^{strong} cells [8, 25].

SDD-AGE analysis of [*PSI*$^{+}$]^{pfd} phenotypes isolated from Δ*pfd* mutants shows that [*PSI*$^{+}$]^{pfd} isolates contain higher levels of soluble Sup35 than the parent [*PSI*$^{+}$]^{strong} cells. This increase in the soluble pool of Sup35 in [*PSI*$^{+}$]^{pfd} isolates correlates with the observation that Δ*pfd* mutants contain fewer heritable [*PSI*$^{+}$] aggregates. Since Δ*pfd* mutants contain fewer [*PSI*$^{+}$] aggregates, this means that there are less surfaces for the conversion of soluble Sup35 into

prion aggregates in Δ*pfd* cells, which would lead to the observed increase in the soluble pool of Sup35.

The isolated dominant mutations that affect the [*PSI*$^+$] phenotype in Δ*pfd* cells resemble the dominant Hsp70 Ssa1-21 mutant characterized by the Masison lab [38]. Just like the dominant [*PSI*$^+$]^{pfd} mutants that I have isolated, Ssa1-21 also has an antisuppressor phenotype that produces pink colonies in a [*PSI*$^+$] background [38]. The Ssa1-21 mutant decreases [*PSI*$^+$] mitotic stability, again mimicking the increased rates of [*PSI*$^+$] loss that I have observed in the isolated [*PSI*$^+$]^{pfd} mutants. Another parallel between Ssa1-21 and Δ*pfd* mutants is that they both have a reduced number of heritable [*PSI*$^+$] aggregates [38]. The proposed model of Ssa1-21 action is that it interferes with the formation of Sup35 aggregates, and it is possible that the dominant mutants that I have isolated have a similar mode of action [38].

Remaining questions and future directions

One surprising result revealed in my work with prefoldin mutants is that loss of prefoldin is somehow mutagenic to the cell. Recent work from the Solomon lab has shown that loss of one prefoldin subunit can lead to higher rates of mini-chromosome loss due to an imbalance in the α/β tubulin heterodimer ratio, offering an explanation for the mutagenic effect I observed in prefoldin deletion mutants [39]. While I did not assess chromosomal abnormalities in the prefoldin mutants that I constructed, the prefoldin mutant strains grew at wildtype rates, mated normally, underwent meiosis, and exhibited high spore viability following dissection, suggesting the absence of gross genomic defects. Rather, the sole observable phenotype of these strains, instability of the red/pink/white colony color prion

phenotype (chapter 3), segregated as a single genetic trait, consistent with mechanism of accumulating mutations distinct from chromosome loss.

The dominant modifiers of [*PSI*$^+$] that I have isolated from Δ*pfd* mutants can be isolated and characterized with a genetic screen. Since the isolated mutations are dominant, cDNA libraries would have to be made from each mutant. The mutant cDNA libraries can be transformed into [*PSI*$^+$] cells, and plated on rich medium where the appearance of the dominant antisuppressor pink colony color phenotype would be looked for. This genetic screen would allow for the isolation of the dominant mutants, which could then be sequenced and further characterized for their effects on [*PSI*$^+$].

Summary of thesis work

The experiments presented in this work show that multiple prion variants can co-exist in one host for many generations. When two yeast prion [*PSI*$^+$] variants co-exist, one variant is phenotypically dominant and masks the presence of the other variant. It is possible that similar prion variant co-existence occurs in other systems. Two basic steps of the prion biogenesis cycle appear important in the competition between [*PSI*$^+$] variants: segregation of heritable prion particles into daughter cells, and aggregate fragmentation that increases the number of heritable prion particles. Prion variants that intrinsically perform one of these two processes less efficiently tend to be gradually reduced in numbers during competition with more "efficient" variants.

Additional experiments presented here show that the co-translational chaperone prefoldin regulates the [*PSI*$^+$] prion, but that it does so through an indirect effect. Mutations in the prefoldin complex are linked to defects in the microtubule cytoskeleton, so it is possible that a functional microtubule cytoskeleton is necessary for faithful [*PSI*$^+$] propagation. However, loss of prefoldin function was shown to be mutagenic to the cell, so it is more likely that underlying mutations generated in Δ*pfd* cells produced the observed destabilization of [*PSI*$^+$] propagation. This unexpected mutagenic effect in the absence of prefoldin function has allowed for the isolation of novel dominant antisuppressors that affect Sup35 state in [*PSI*$^+$] cells. None of the isolated mutants show genetic linkage to Hsp104, a known dominant modulator of [*PSI*$^+$] [40]. One mutant shows genetic linkage to the *SUP35* locus, another known dominant modulator of [*PSI*$^+$], and another mutant shows tight linkage to the Sup35 ORF [41].

References:

1. Wickner, R.B., *[URE3] as an altered URE2 protein: evidence for a prion analog in Saccharomyces cerevisiae.* Science, 1994. **264**(5158): p. 566-9.
2. Paushkin, S.V., et al., *Propagation of the yeast prion-like [psi+] determinant is mediated by oligomerization of the SUP35-encoded polypeptide chain release factor.* Embo J, 1996. **15**(12): p. 3127-34.
3. Coustou, V., et al., *The protein product of the het-s heterokaryon incompatibility gene of the fungus Podospora anserina behaves as a prion analog.* Proc Natl Acad Sci U S A, 1997. **94**(18): p. 9773-8.
4. Derkatch, I.L., et al., *Genetic and environmental factors affecting the de novo appearance of the [PSI+] prion in Saccharomyces cerevisiae.* Genetics, 1997. **147**(2): p. 507-19.
5. Fraser, H. and A.G. Dickinson, *Scrapie in mice. Agent-strain differences in the distribution and intensity of grey matter vacuolation.* J Comp Pathol, 1973. **83**(1): p. 29-40.
6. Bessen, R.A. and R.F. Marsh, *Distinct PrP properties suggest the molecular basis of strain variation in transmissible mink encephalopathy.* J Virol, 1994. **68**(12): p. 7859-68.
7. Bruce, M., et al., *Transmission of bovine spongiform encephalopathy and scrapie to mice: strain variation and the species barrier.* Philos Trans R Soc Lond B Biol Sci, 1994. **343**(1306): p. 405-11.
8. Zhou, P., et al., *The yeast non-Mendelian factor [ETA+] is a variant of [PSI+], a prion-like form of release factor eRF3.* Embo J, 1999. **18**(5): p. 1182-91.
9. Schlumpberger, M., S.B. Prusiner, and I. Herskowitz, *Induction of distinct [URE3] yeast prion strains.* Mol Cell Biol, 2001. **21**(20): p. 7035-46.
10. Bradley, M.E., et al., *Interactions among prions and prion "strains" in yeast.* Proc Natl Acad Sci U S A, 2002. **99 Suppl 4**: p. 16392-9.
11. Derkatch, I.L., et al., *Genesis and variability of [PSI] prion factors in Saccharomyces cerevisiae.* Genetics, 1996. **144**(4): p. 1375-86.
12. King, C.Y. and R. Diaz-Avalos, *Protein-only transmission of three yeast prion strains.* Nature, 2004. **428**(6980): p. 319-23.
13. Tanaka, M., et al., *Conformational variations in an infectious protein determine prion strain differences.* Nature, 2004. **428**(6980): p. 323-8.
14. Derkatch, I.L., et al., *The PNM2 mutation in the prion protein domain of SUP35 has distinct effects on different variants of the [PSI+] prion in yeast.* Curr Genet, 1999. **35**(2): p. 59-67.
15. King, C.Y., *Supporting the structural basis of prion strains: induction and identification of [PSI] variants.* J Mol Biol, 2001. **307**(5): p. 1247-60.
16. Kryndushkin, D.S., et al., *Yeast [PSI+] prion aggregates are formed by small Sup35 polymers fragmented by Hsp104.* J Biol Chem, 2003. **278**(49): p. 49636-43.
17. Chien, P., et al., *Generation of prion transmission barriers by mutational control of amyloid conformations.* Nature, 2003. **424**(6951): p. 948-51.
18. Tanaka, M., et al., *Mechanism of cross-species prion transmission: an infectious conformation compatible with two highly divergent yeast prion proteins.* Cell, 2005. **121**(1): p. 49-62.

19. Chien, P. and J.S. Weissman, *Conformational diversity in a yeast prion dictates its seeding specificity.* Nature, 2001. **410**(6825): p. 223-7.
20. Santoso, A., et al., *Molecular basis of a yeast prion species barrier.* Cell, 2000. **100**(2): p. 277-88.
21. Chien, P., J.S. Weissman, and A.H. DePace, *Emerging principles of conformation-based prion inheritance.* Annu Rev Biochem, 2004. **73**: p. 617-56.
22. Peretz, D., et al., *A change in the conformation of prions accompanies the emergence of a new prion strain.* Neuron, 2002. **34**(6): p. 921-32.
23. Dickenson, A.G., et al., *Extraneural competition between different scrapie agents leading to loss of infectivity.* Nature, 1975. **253**(5492): p. 556.
24. Bartz, J.C., J.M. Aiken, and R.A. Bessen, *Delay in onset of prion disease for the HY strain of transmissible mink encephalopathy as a result of prior peripheral inoculation with the replication-deficient DY strain.* J Gen Virol, 2004. **85**(Pt 1): p. 265-73.
25. Tanaka, M., et al., *The physical basis of how prion conformations determine strain phenotypes.* Nature, 2006. **442**(7102): p. 585-9.
26. Cole, D.J., et al., *Estimating the number of prions in yeast cells.* Math Med Biol, 2004. **21**(4): p. 369-95.
27. Toyama, B.H., et al., *The structural basis of yeast prion strain variants.* Nature, 2007. **449**(7159): p. 233-7.
28. Eaglestone, S.S., et al., *Guanidine hydrochloride blocks a critical step in the propagation of the prion-like determinant [PSI(+)] of Saccharomyces cerevisiae.* Proc Natl Acad Sci U S A, 2000. **97**(1): p. 240-4.
29. Satpute-Krishnan, P., S.X. Langseth, and T.R. Serio, *Hsp104-dependent remodeling of prion complexes mediates protein-only inheritance.* PLoS Biol, 2007. **5**(2): p. e24.
30. Cox, B., F. Ness, and M. Tuite, *Analysis of the generation and segregation of propagons: entities that propagate the [PSI+] prion in yeast.* Genetics, 2003. **165**(1): p. 23-33.
31. Sadlish, H., et al., *Hsp110 chaperones regulate prion formation and propagation in S. cerevisiae by two discrete activities.* PLoS ONE, 2008. **3**(3): p. e1763.
32. Bruce, M.E., et al., *Transmissions to mice indicate that 'new variant' CJD is caused by the BSE agent.* Nature, 1997. **389**(6650): p. 498-501.
33. Hill, A.F., et al., *The same prion strain causes vCJD and BSE.* Nature, 1997. **389**(6650): p. 448-50, 526.
34. Silveira, J.R., et al., *The most infectious prion protein particles.* Nature, 2005. **437**(7056): p. 257-61.
35. Masel, J. and V.A. Jansen, *The measured level of prion infectivity varies in a predictable way according to the aggregation state of the infectious agent.* Biochim Biophys Acta, 2001. **1535**(2): p. 164-73.
36. Kushnirov, V.V., et al., *Chaperones that cure yeast artificial [PSI+] and their prion-specific effects.* Curr Biol, 2000. **10**(22): p. 1443-6.
37. Satpute-Krishnan, P. and T.R. Serio, *Prion protein remodelling confers an immediate phenotypic switch.* Nature, 2005. **437**(7056): p. 262-5.
38. Jung, G., et al., *A role for cytosolic hsp70 in yeast [PSI(+)] prion propagation and [PSI(+)] as a cellular stress.* Genetics, 2000. **156**(2): p. 559-70.

39. Lacefield, S., M. Magendantz, and F. Solomon, *Consequences of defective tubulin folding on heterodimer levels, mitosis and spindle morphology in Saccharomyces cerevisiae.* Genetics, 2006. **173**(2): p. 635-46.
40. Chernoff, Y.O., et al., *Role of the chaperone protein Hsp104 in propagation of the yeast prion-like factor [psi+].* Science, 1995. **268**(5212): p. 880-4.
41. Doel, S.M., et al., *The dominant PNM2- mutation which eliminates the psi factor of Saccharomyces cerevisiae is the result of a missense mutation in the SUP35 gene.* Genetics, 1994. **137**(3): p. 659-70.

Figure Captions

Figure 1. Two proposed models that explain the change in prion form that occurs during crossing of the interspecies transmission barrier. A. The variant conversion model postulates that when the invading prion variant (blue snowflake shape) comes into contact with the heterologous host-encoded prion protein (yellow), the host-encoded protein assumes a different prion form (yellow shape incorporated into blue snowflake) that is compatible with but differs from the invading prion form, eventually leading to the appearance of a new prion form (yellow snowflake shape). B. The variant selection model proposes that each prion variant is actually a mix of protein states (represented by blue snowflake shapes). When this mix of protein states comes into contact with the host-encoded prion protein (yellow), the host-encoded protein can assume a new prion form (yellow shape incorporated into blue snowflake) that is compatible with a subset of invading prion forms. After several rounds of replication, the most compatible prion form will dominate the mixture (yellow snowflake), and the incompatible forms of the original invading prion variant will be lost or become undetectable due to low abundance. This figure is modeled after one published by Chien, Weissman, and DePace, 2004, and after a figure drawn by T. Serio.

Figure 2. The yeast prion cycle depends on several steps. In step one, soluble protein (dark blue rods) is converted into the prion state (dark blue rods with a twist) and incorporated into prion aggregates (snowflake shape). In step two, prion aggregates are broken up by the action of chaperone proteins in order to generate more surfaces for the conversion of soluble protein into the prion form.

Fragmentation of prion aggregates into smaller pieces is also necessary for step three where prion aggregates are transmitted to daughter cells, thereby ensuring stable propagation of the prion phenotype. This diagram was drawn by Tricia Serio and a version of it was published by Pezza and Serio, 2007.

Figure 1.

A. The variant conversion model

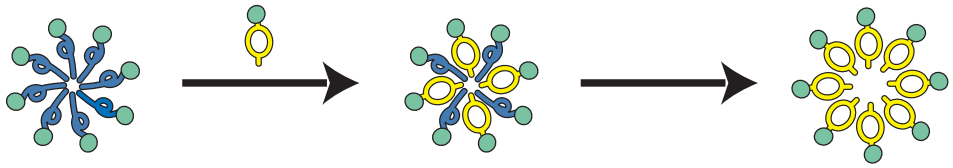

B. The variant selection model

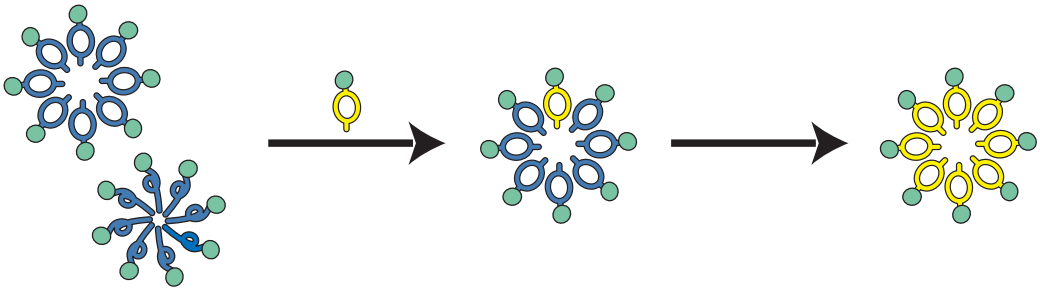

Figure 2.